Antiretroviral drug loaded Lactoferrin nanoparticle formulation for oral delivery: Improved Efficacy, Bioavailability and Safety

DOCTOR OF PHILOSOPHY

By

PRASHANT KUMAR

Department of Biotechnology and Bioinformatics
School of Life Sciences
University of Hyderabad
PO Central University, Gachibowli
Hyderabad – 500046, Telangana, India

September 2016

सर्वतीर्थमयी माता सर्वदेवमयः पिता |
मातरं पितरं तस्मात् सर्वयत्नेन पूजयेत् ||

यह शोध प्रबंध मैं अपने सर्वाधिक प्रिय व् आदरणीय माता-पिता, भाइयों और स्नेहिल भाभी को समर्पित कर रहा हूँ जिनका निश्छल प्रेम और अबाधित सहयोग मुझे संपूर्ण जीवन के सपनों, लक्ष्यों और खुशियों के लिए सतत प्राप्त है |

This Thesis is dedicated to my dear parents, brothers and my sweet bhabhi for their incessant love and unwavering support to my lifelong pursuit of dreams and happiness.

This page is intentionally left blank.

Antiretroviral drug loaded Lactoferrin nanoparticle formulation for oral delivery: Improved Efficacy, Bioavailability and Safety

A thesis submitted to University of Hyderabad
for the award of a Ph.D. Degree in Biotechnology

By

PRASHANT KUMAR

Department of Biotechnology and Bioinformatics
School of Life Sciences
University of Hyderabad
PO Central University, Gachibowli
Hyderabad – 500046, Telangana, India

Enrollment No: – 10LTPM01
September 2016

UNIVERSITY OF HYDERABAD
(A central university established in 1974 by an act of Parliament)
Department of Biotechnology and Bioinformatics
School of Life Sciences
University of Hyderabad, Hyderabad 500 046, India

CERTIFICATE

This is to certify that thesis entitled "Antiretroviral drug loaded Lactoferrin nanoparticle formulation for oral delivery: Improved Efficacy, Bioavailability and Safety" is a record of bonafide work done by Mr. Prashant Kumar, a research scholar for Ph.D. programme in department of biotechnology and bioinformatics, university of Hyderabad under my guidance and supervision. The thesis has not been submitted previously in part or full to this or any other university or institution for the award of any degree or diploma. I recommend his thesis for submission towards the partial fulfillment of Doctor of Philosophy degree in Biotechnology.

(Signature of supervisor)

(Head of the Department)

(Dean of the School)

UNIVERSITY OF HYDERABAD
(A central university established in 1974 by an act of Parliament)
Department of Biotechnology and Bioinformatics
School of Life Sciences
University of Hyderabad, Hyderabad 500 046, India

DECLARATION

I, Prashant Kumar, hereby declare that the work presented in this thesis, entitled as "Antiretroviral drug loaded Lactoferrin nanoparticle formulation for oral delivery: Improved Efficacy, Bioavailability and Safety" has been carried out by me under the supervision of Prof. Anand K. Kondapi, Department of Biotechnology and Bioinformatics. To the best of my knowledge this work has not been submitted for the award of any degree or diploma at any other university or institution. I hereby agree that my thesis can be deposited in Shodganga/INFLIBNET. A report on plagiarism statistics from the University Librarian is enclosed.

Place: Hyderabad

Prashant Kumar
10LTPM01

Date:

Acknowledgements

Although I am indeed the sole author of this thesis, I am by no means the sole contributor! So many people have contributed to my thesis, my education, and to my life and it is now my opportunity to thank them.

First of all, I offer my genuine gratitude to my supervisor, ***Prof Anand K. Kondapi****, who has supported me throughout my work in all the possible way with his patience and guidance. I must say that Prof. Kondapi is a very wise personality by whom I have learnt various important aspects of life.*

I would like to express my sincere thanks to present Dean School of Life Sciences, ***Prof. P. Reddanna*** *and former Dean* ***Prof. Aparna Dutta Gupta****,* ***Prof. R.P. Sharma****,* ***Prof. A. S. Raghavendra*** *and* ***Prof M. Ramanadham*** *for giving me the opportunity to use necessary facilities to carry out my work. I would also like to express my sincere regards to the present Head, Department of Biotechnology and Bioinformatics,* ***Dr. Niyaz Ahmed*** *and former Head of the department* ***Prof. P. Prakash Babu****. I offer my sincere gratitude to my doctoral committee members* ***Dr. S Bhattacharya and Dr. N. Prakash Prabhu*** *for their valuable suggestions and guidance throughout my study period. I sincerely thank to all the faculty members of Department of Biotechnology and Bioinformatics. They are my teachers during my M.Sc.*

I thank ***Dr. Insaf Ahmed Qureshi*** *for recommendation for summer project during my M.Sc. I thank all the* ***faculty*** *members of Life Sciences for cooperation and their extended help during my work. I thank the Department of Biotechnology and Bioinformatics office staffs for the support during this tenure.*

I thank ***Prof. N. Madhusudhana Rao****, Chief Scientist CCMB (Centre for Cellular and Molecular Biology), Hyderabad and Nikhil Sharma (PhD student at CCMB) for DLS facility.*

For financial support, again I want to thank sincerely to my supervisor for providing me project manpower support during my study period.

I thank my lab mates Dr. Bhaskar, Dr. Kishore, Dr. Preethi, Dr. Anil, Dr. Balakrishna, Dr. Upendhar, Dr. Sarada, Dr. Satish, Dr. Farhan, Dr. venkanna, Kurumurthy, Harikiran, Sonali, Srujana (Late), Jagadeesh, Kiran, Akhila, Suresh, Godan, Ajay, Reena, Neha, Satyajeet, Priya and Chuku for their co-operation, support and cheerful nature all through my research.

I want to thank Dr. Bhaskar and Dr. Sarada through whom I have learnt the cell culture and virus culture work.

I thank to Dr. Golla Kishore for teaching me animal handling and data representation using various software.

I thank to Miss. Bommakanti Akhila for helping me in writing this acknowledgement section and for critical revision of thesis and manuscripts and she only insisted me to highlight her name. She is very a very good person and she keeps her surroundings very joyful.

I specially thank to Miss. Y. Samrajya Lakshmi, my colleague who worked with me hand to hand and shoulder to shoulder throughout my study period.

I want to acknowledge the one and only original chemist of our lab Mr. K. kurumurthy, a brave heart shy person. I thank for the forest trip in your village and your warm hospitality.

I present my greetings to the pseudo chemist of lab, Mr. Senapathi Jagadeesh. I thank for the regular laughter therapy in lab.

I want to say a warm thanks to Mr. Harikiran for maintaining the good laboratory practices which has helped me a lot during my PhD.

I also want to acknowledge Sonali Dey/Kumari, the visiting research scientist of lab for creating transient cheerful environment in the lab.

I shall not forget to say thanks to my part time room-mate cum full time lab mate Mr. D A Kiran Kumar, he has helped me in culture work and other routine lab work.

My acknowledgement will not complete until I acknowledge Mr. Suresh and Mr. Godan, these both guys helped me in lab work and outside lab work too.

I thank my roommate Mr. Amit Ranjan for his unwavering support during my stay in hostel.

I want to say a sincere thanks to my friends Mr. Praveen, Pandey ji, Deepak babu from Prof. Prakash Babu lab for seamless support throughout my study tenure.

I specially thank to ***Mr. PankaZ Singh*** *for the moral and emotional and support during this tenure. I remember him as a good preacher rather than a researcher. I have learnt various significant aspects of life from him.*

I Thank to Nidhi, Tanvi, Deepak Babu, Prateek, Angamba, Deepak singh and Sanjay sharma for making my stay pleasant in the campus. I thank all my friends in the school and university for making my stay pleasant.

I thank animal house staff members for their co-operation.

I want to say a special thanks to CNF (Campus Network Facility) University of Hyderabad for providing the seamless internet connectivity throughout my study tenure.

I thank Mr. Sreenivas, Mr. Bhanu, Mr. Chandra, and Mr. B H Sreenivas Murthy for their cooperation.

I want to say a special thanks to A. Bramhini and Virat (Chinnu) for the constant emotional, moral and financial support during my study tenure at University of Hyderabad.

I wish to express my deepest gratitude to all my family members. The "Thank" word is not appropriate to thank them. I just can say that my mother, father, younger brother (moon), elder brother (chunchun bhaiya) and my Bhabhi is one of few best of best person on the planet, by whom I have learnt the way to live life.

Lastly, I offer my regards to all of those who supported me in any aspect during my work.

Last but not least I thank almighty for giving me good health.

Prashant Kumar

ABBREVIATIONS

3TC or LMV	: Lamivudine
AIDS	: Acquired Immuno-Deficiency Syndrome
ALT	: Alanine transaminase
ARV	: Antiretroviral
AST	: Aspartate transaminase
ATV	: Atazanavir
AZT	: Azidothymidine (Zidovudine)
Blank NP	: Blank nanoparticles
BSA	: Bovine serum albumin
CD4	: Cluster of differentiation 4
C_{max}	: Maximum (or peak) serum concentration
DL%	: Drug loading percent
EE%	: Encapsulation efficiency percent
EFV	: Efavirenz
FBS	: Fetal Bovine Serum
FDA	: Food and Drug Administration
HAART	: Highly Active Anti-Retroviral Therapy
HIV	: Human Immunodeficiency Virus
HR	: Hemolysis rate
GI_{50}	: 50% Growth Inhibitory Concentration
IC_{50}	: 50% Inhibitory Concentration
kDa	: Kilo Dalton
Lacto-nano	: lactoferrin nanoparticles
LDH	: Lactose Dehydrogenase
Lf	: Lactoferrin
mM	: Millimolar
MTT	: 3-(4,5-dimethylthiazol-2-yl)-2,5-diphenyltetrazolium
mV	: Millivolts
NP	: Nanoparticles

PBMC	: Peripheral Blood Mononuclear Cell
PBS	: Phosphate Buffer Saline
RTV or r	: Ritonavir
$T_{1/2}$	: Half Life
TNF	: Tenofovir
µg	: Microgram
µl	: Microliter
µM	: Micromolar

CONTENTS

Chapter 1

Introduction

There are many disputes about the timing of origin of life on the earth. The first life on earth was originated approximately 3.8 billion years ago from now i.e. after 750 million years of formation of earth [1]. According to Oparin and Haldane theory of evolution of life, the life has been evolved from the carbon containing molecules "primordial soup" [2]. After origin of the first species on earth i.e. bacteria, many other species were evolved [3]. The first humans were evolved around 6 to 8 million years ago [4]. After the evolution of human, various disease causative agents were also discovered such as, bacteria, fungus, nematode, protozoa, virus and many more [5]. Among all, viruses are type of obligatory agent which leads to world's catastrophic diseases, such as chickenpox, small pox, influenza, polio, AIDS, Rabies, Ebola, Hepatitis, Dengue fever etc. [6]. The focus of current study is AIDS (Acquired Immune Deficiency Syndrome).

HIV structure: HIV is a type of lentivirus; contain two copies of single strand of RNA as a genetic material [7]. The genetic materials of human immunodeficiency virus (HIV) encode a total of nine genes. Further, the genome is composed of three key structural genes namely, gag, pol, and env. The central viral core which is surrounded by p24 capsid protein contains two single strands of RNA and three types of enzymes (reverse transcriptase, integrase and protease). The virus outer envelope contains two different types of spiked glycoproteins (gp), such as gp41 and gp120.

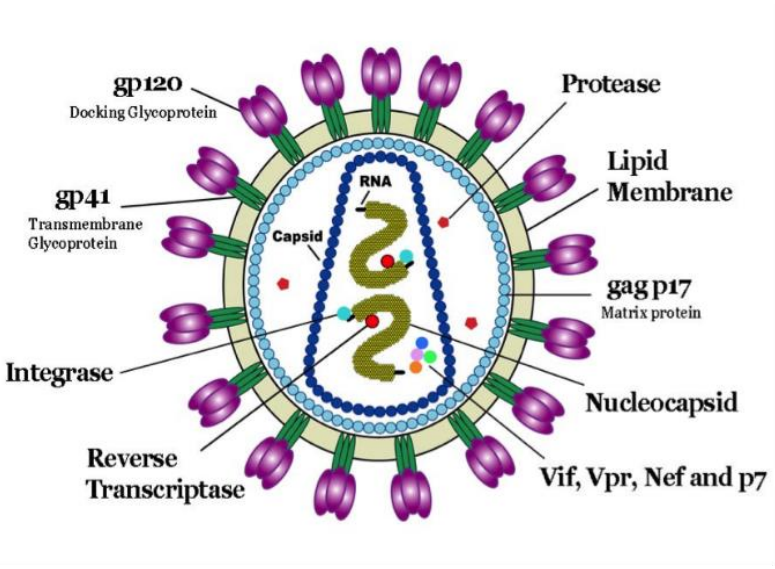

Figure 1.1 Schematic structure of human immunodeficiency virus.

HIV biology: The HIV infection initiated when the enveloped glycoprotein, gp120 binds to the CD4 receptor with the help of CCR5 membrane spanning chemokine receptor type 5 (step one). This leads to the fusion of virus outer membrane to the cell surface (step two). It is followed by uncoating of virus particles and release of genetic materials inside the cell (step three). Further the reverse transcriptase facilitates the reverse transcription (step four), that leads to the formation of PIC (Pre-integration complexes). The PIC is then transported inside the nucleus (step five). Then with the help of integrase, proviral DNA is integrated to the host genome (step six). After integration with the host genome, the provirus transcription occurs (step seven). The viral DNA transcription is facilitates by host transcription elongation factor b (P-TEFb) and RNA polymerase II. The newly formed RNA strands are then transported (step eight) outside the nucleus to the cytoplasm for translation (step nine). The new viral RNA molecules and viral proteins are then assembles to form new progeny virus particles (step ten). Then after budding (step eleven), release (step twelve) and maturation (step thirteen) the new virus particle are now ready for the next round of infection [8].

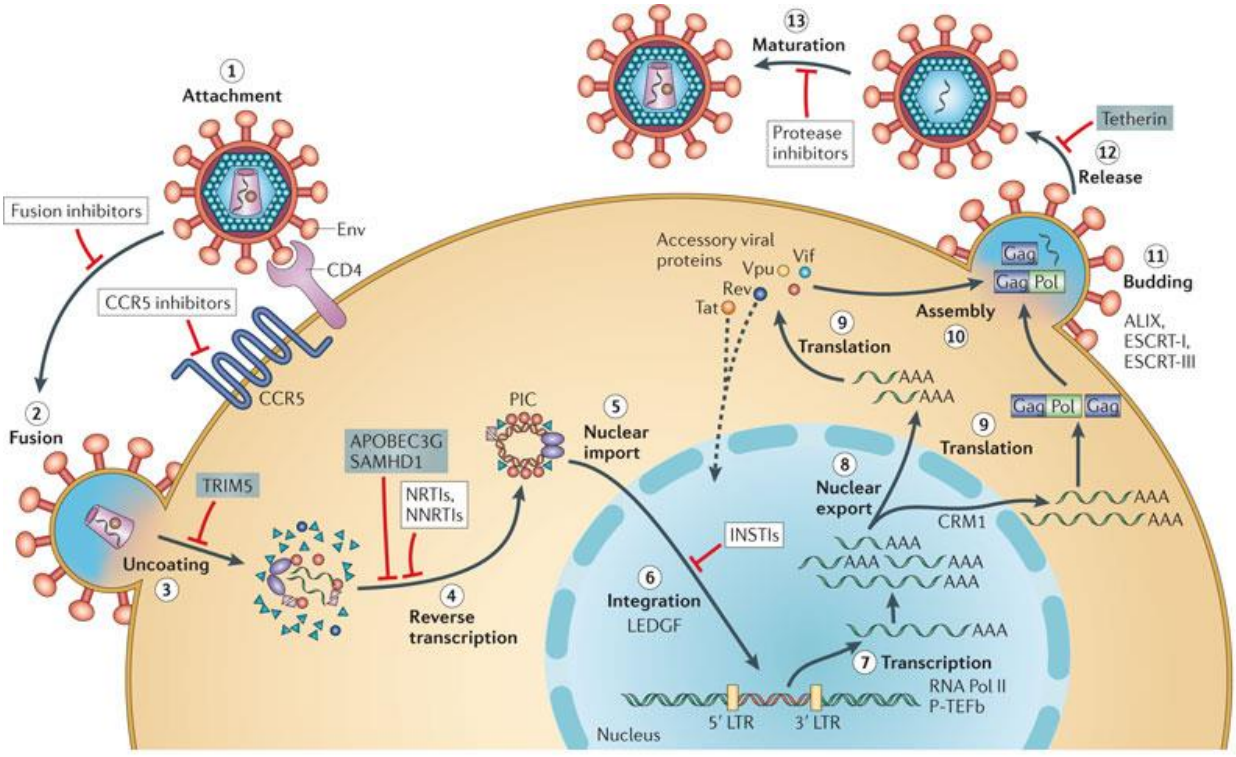

Figure 1.2 The brief life cycle of HIV **[8].**

Epidemiology of HIV/AIDS

The HIV/AIDS is considered as a biggest threat to the human kind [9]. According to UNAIDS fact sheet 2015, 36.9 million people are living with HIV/AIDS globally, whereas only 15.8 million Infected population are getting access to antiretroviral based therapy. A population of 17.1 million is unaware of their HIV infection [10]. Sub-Saharan locale of Africa is the most extremely influenced territory on the planet, where around 14000 new infections are emerging day by day and roughly 11000 are passing on because of HIV/AIDS and its related ailment [11]. The UNAIDS has committed to end this epidemic disease by the end of 2030 [12].

Antiretroviral therapy for HIV/AIDS treatment

Soon after the onset of HIV/AIDS, the various treatment strategies has been introduced and antiretroviral (ARV) based drug therapy is one of them. The antiretroviral therapy is the most trusted therapy till now. There are total 6 class of ARV approved by FDA for its clinical use. It include (I) non–nucleoside reverse transcriptase inhibitors (NNRTIs, E.g. – EFV), (II) nucleoside/nucleoside analog reverse transcriptase inhibitors (NRTIs, E.g. – AZT, 3TC), (III) integrase inhibitors, (IV) protease inhibitors (PIs, E.g. – ATV, RTV or r), (V) fusion inhibitors, and (VI) co-receptor antagonists [13].

The details of antiretroviral therapy is provided in Table 1.1

Types	Target	Drugs
1. Nucleoside/ nucleotide reverse transcriptase inhibitors **(NRTI)**.	Reverse transcriptase (NRTI mimic nucleotide)	Emtricitabine, **Lamivudine (3TC)**, **Tenofovir (TNF)**, Abacavir, Stavudine, **Zidovudine (AZT)**, Didanosine, Zalcitabine
2. Non-nucleoside reverse transcriptase inhibitors **(NNRTI)**.	Reverse transcriptase (NNRTI bind to Rtase, terminate DNA polymerization)	**Efavirenz (EFV)**, Nevirapine, Rilpivirine, Etravirine Delavirdine.

3. Protease inhibitors **(PI)**.	Protease	**Atazanavir (ATA)**, Darunavir, Indinavir, Amprenavir, Fosamprenavir, Lopinavir, Nelfinavir, Tipranavir, **Ritonavir (r)**, Saquinavir
4. Fusion inhibitors	Six-helix bundle formation	Enfuvirtide
5. CCR5 inhibitors.	Entry inhibitors	Maraviroc
6. Integrase inhibitors (INI)	Integrase	Raltegravir

In early period during late nineties the treatment was started as mono-drug therapy. Zidovudine (ZDV), also known as azidothymidine (AZT), was the first drug approved by FDA for its clinical use [14]. But after few years of mono-drug treatment the therapy has been discontinued [15] due to side effects (long term side effect and short term side effects)[16, 17]. The short term side effect includes severe skin rashes, vomiting, headache, dizziness, fatigue, weakness and muscle pain etc. This side effect will disappear soon after the stoppage of therapy. The long term side effect includes **Lipodystrophy** (abnormal redistribution of fat in the body, there is devoid of fat from extremities. Limbs and face become thin and there is more accumulation of fat in the shoulder and stomach), **Insulin Resistance** (leads to the development of type2 diabetes), **Lipid abnormalities** and **Decrease in bone density** (leads to osteoporosis that causes the bone to be fragile). The other reasons to discontinue the monotherapy are, I) **Drug resistance:** HIV is known for its drug resistance property. The progeny virus will have the capability to reproduce and mutate itself in presence of antiretroviral treatment that finally leads to the ARV drugs resistance towards HIV [18]. This may leads to the treatment failure. II) High cost of treatment: according to CDC (Centers for Disease Control and Prevention) in 2010 the life time treatment cost for HIV was approximately $379,668 [19].

When to start antiretroviral treatment?

According to WHO guidelines, the CD4 cell count must be tested before starting of antiretroviral based therapy following by evaluation of viral load is also recommended for confirmation of the entire suspected individual. The mono-drug therapy was discontinued after few years of treatment and HAART (Highly Active Anti-Retroviral Therapy) started. The HAART was started in the year 1996, despite of its various side effects and toxic effect to the body, HAART is still considered as standard therapy for HIV. HAART is the combination of three or more different types of drugs and often called as "three drugs cocktail" therapy. The benefits of combination therapy over single drug therapies are, 1) it is more efficacious than mono-drug therapy as it can target the HIV at multiple stages of its life cycle, as the drugs present in the combination have different mode of action on HIV and its life cycle. 2) The dose frequency has been reduced, in mono-drug therapy patient used to take 12-15 pills in a day which reduced to 1 pills a day in HAART treatment. The death rate due to HIV has been reduced by 50-80% after the introduction of HAART. WHO/FDA recommend two type of HAART regimen often called as first line regimen and second line regimen. First line and second line regimen consist of 2NRTI+1NNRTI and 2NRTI+PI/r respectively. According to WHO (world health organization), First-line ART regimen should comprise of two NRTI (nucleoside reverse-transcriptase inhibitors) plus one NNRTI (non-nucleoside reverse-transcriptase inhibitor). The recommended FL-HAART regimen generally contain TDF + 3TC + EFV as a fixed dose. In some cases if TDF is not available the other recommended FL-HAART regimens are AZT + EFV +3TC or AZT + 3TC + NVP. The level of viral load is recommenced for switching in therapy as directed by WHO. If the viral load is >5000copies/ml, it is considered as treatment failure and this is the time for switching of regimen [20]. First line regimen is switches to second line regimen which contain two NRTI plus one ritonavir boosted PI (ATV/r). The recommended second line regimen is a combination of 3TC + TDF + ATV/r. The HAART is the standard treatment for HIV treatment, even though it is observed that approximately 25% of patients stop HAART within first year of the treatment. The reason behind this are drug resistance development, poor bioavailability of drugs, short half-life of drug and other drug related toxicity.

Nanoparticles mediated drug delivery: an alternate formulation therapy

These limitations led to the development of novel formulations of existing drug regimen, which reduces its side effects and improve its efficacy; Nano formulation is one of emerging form of the drug. Nanotechnology, as the name itself suggest, it is the branch of science which deals with the materials in nanometer range. These nanometer range materials have several applications in the various branches of science, such as food industry, medicine, pharmacology, energy, biomedical application and other industrial applications. The nanotechnology was also being used in ancient times. The main aim of our study is nano-medicine, i.e. Nanoparticles mediated drug delivery. Even in case of medicine, the Nano based therapy are being used since centuries [21]. In Indian medicine system, in Ayurveda the *"Bhasma"* is considered a kind of Nano therapy [22].

Nanoparticles: Nanoparticles (NP, size <400nm) are defined as a small objects that behaves as a whole unit with respect to its transport and properties. NP is considered as smart drug delivery system [23]**.** NP has brought significant changes in the treatment and diagnosis of disease.

Advantages of nanoparticles mediated drug delivery system.

NP is found as specific and more advanced drug delivery system (DDS) as compared to other delivery system. The main advantage of NP mediated DDS are as follows.

I. Large surface to mass ratio: The NP shows high surface to mass ratios. So it is easy to accommodate more than one ligand at a time together. This will enhance the loading efficiency of NP [24].
II. Target-specific delivery of drug [25].
III. Reduction of drug-related toxicity while maintaining therapeutic effects [24].
IV. Greater safety and biocompatibility [26].
V. Improved bioavailability of poor bioavailable drugs [27].
VI. Enhanced stability of rapid metabolizing drugs [28].
VII. Minimized first pass metabolism and reduced renal clearance [29] [30].
VIII. Nanoparticles provide a slow and sustained delivery system [31].

IX. Nanoparticles greatly improves the pharmacokinetics behavior of poor bioavailable drugs [32, 33].

Limitations of nanoparticles mediated drug delivery system.

Despite of having so much of beneficial activities of nanoparticles mediated DDS, it also has some limitations, and few of them are listed below.

I. The complexity of biological system: Absence of legitimate information about the impact of nanoparticles on biochemical pathways and procedures of human body. It happens often, a certain type of nanoparticles shows tremendous positive effect in an in-vitro system but when it comes to the biological system *in-vivo* it fails.

II. Currently researchers are essentially worried about the toxic quality, portrayal and presentation pathways connected with NP DDS that may represent a genuine danger to the individuals and environment.

Types of nanoparticles

NP shows a various type depending on their composition. Some of the major types of NP are discussed below.

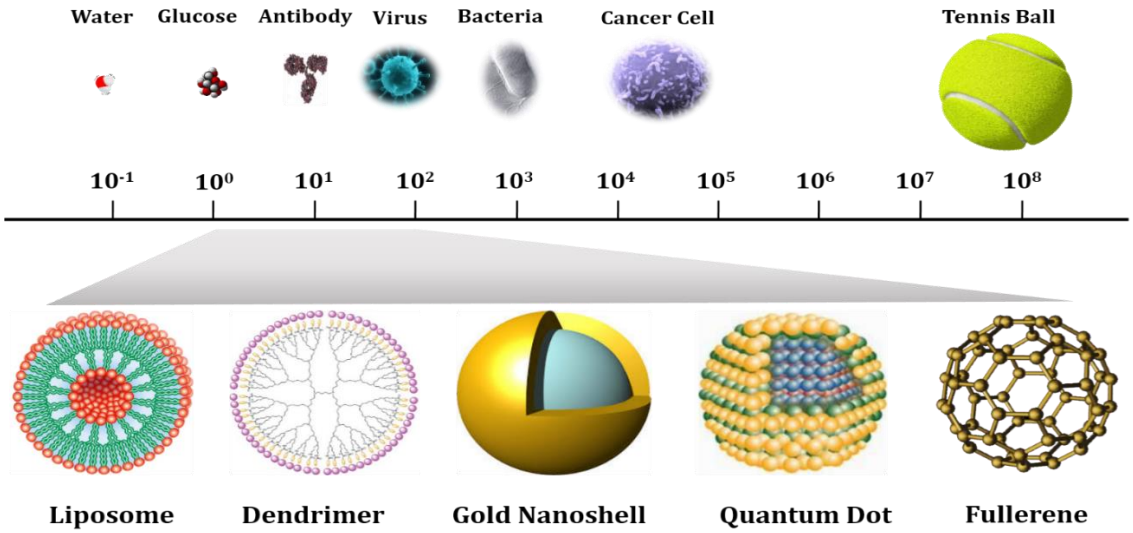

Figure 1.3: The size scale for various sorts of nanoparticles. The span of nanoparticles are contrasted with different materials.

Solid Lipid NP: SLN is a type of organic NP established in early nineties [34]. SLN is composed of lipid core which is designed to internalize the lipophilic molecules easily. The core of SLN is stabilized by the presence of emulsifier [35]. They are generally spherical in shape. The lipid used in the preparation of SLN is often a mixture of monoglycerides, diglycerides and triglycerides, wax and fatty acids [35]. SLN is considered as substitute delivery system to Liposome and polymeric NP [36]. This colloidal delivery system is very efficient in gene and drug delivery. SLN has proven its usefulness in ocular and as well as other type of cancer drug delivery [37, 38]. SLN has developed for dermal and pulmonal and parenteral routes.

Metal NP (Au, Ag, and Fe): Metal NP is inorganic type of NP. The important characteristics about metal NP is that, it could be conjugated with various type of bits such as peptide, antibodies, ligands, drugs, etc. Further the metal NP are found to be very useful in biomedical imaging techniques, such as CT scan, PET and MRI. Mainly three type of metal NP are in practice, which include silver NP, gold NP and iron oxide NP [39].

Quantum dots: Quantum dots are very tiny particles, their size ranges in nanometer (15-35nm). Quantum dots generally composed of materials that belongs to semiconductor properties like germanium and silicon. Quantum dot color depend on their size. Further the fluorescent quantum dots are very useful in immunohistochemistry [40, 41].

Dendrimer: Dendrimer are tree like structure macromolecules (1.5 to 10 nm). It contains a center core (stem) around which a series of braches are present. The branches are made up of two chemical forms and that are present in same order though out its structure. Dendrimer has shown its efficacy in oral drug delivery, antimicrobial agent, [42].

Liposomes: Liposomes are spherical shape vesicles made up of lipid bilayer [24]. Liposome composition are same as of plasma membrane. Liposome are generally prepared by physical disruption (sonication) of biological membrane. These are composed of naturally derived phospholipid. Liposomes can be loaded with anticancer drugs to deliver

to the target cell through passive targeting. Liposome are found to be very effective against cancer drug delivery [43].

Protein nanoparticles: Protein NP are biodegradable and easily surface manipulated materials. Recent study has shown that protein NP have found to be more effective in cancer and HIV therapy [44, 45].

Type of Protein NP and their advantages

Gelatin: gelatin protein is widely used as a Nano vehicle for delivery of varieties of molecules. Gelatin can be obtained by controlled hydrolysis of collagen protein. Gelatin NP can be sterilized very easily, it is biodegradable, non-toxic [46]. Gelatin NP has been found to successfully encapsulate drugs, gene and peptide [47-49].

Albumin: albumin is the most versatile protein found in human body. It is often present in many sources such as bovine serum albumin, human serum albumin and ovalbumin. Bovine serum albumin nanoparticles are found to provide a sustained release in local environment. [50].

Elastin: elastin is a highly elastic connective tissue which provides elasticity to the internal organs and skin. Elastin nanoparticles has successfully encapsulates and deliver the anticancer drugs doxorubicin [51]. Previous report has shown that elastin based nanoparticles has greatly enhanced the growth of bone by delivering the Bone morphogenetic proteins (BMPs) [52].

Zein: Zein is a storage protein of prolmaine class is found in maize and it comprises approximately 45 to 50% of whole protein content [53]. In one report zein NP are found to be encapsulating and delivering an anti-inflammatory agent i.e. 6,7-dihydroxycoumarin (DHC)[54].

Soy Proteins: soy protein is present in soybean and have various nutritional and medicinal benefits [55]. Curcumin loaded soy proteins are already in study and found that soy protein NP has improved the release of Curcumin over time in vitro [56].

Whey Proteins: whey is a milk protein present in milk [57]. It is also available commercially and used as nutritional support. It is a water soluble protein. Aroma loaded whey protein nanoparticles was found to be release slowly with a higher improvement in retention from 7% to 24% [58].

Apo-transferrin nanoparticles: The previous research groups from our laboratory has developed Apo-transferrin based nanoparticles. Apo-transferrin is a protein belongs to transferrin family. Transferrin is the primary molecule for iron transport and its delivery through transferrin receptor present on the cell surface. Previously we have developed Curcumin loaded apotransferrin nanoparticles, which efficiently inhibits the HIV-1 *in vitro* [59]. Further, doxorubicin loaded apotransferrin nanoparticles was found to be more efficacious towards hepatocellular carcinoma [60]. In addition to this, apotransferrin loaded carboplatin nanoparticles were found to be improve the anti-proliferative activity in retinoblastoma cells [61].

Lactoferrin nanoparticles: Our study involve the development of lactoferrin (Lf) based protein NP drug delivery system. Lf is a protein (80kDa) [62] of transferrin family which is found is many body secretions such as milk, tears, saliva etc. In addition to the iron transport, Lf also shows multifunctional properties such as, anti-HIV [63], anti-inflammatory [64], anti-carcinogenic [65] and immune modulator [66]. Earlier some ARV drugs loaded nanoformulation have been developed such as Chitosan NP [67], Polymeric NP [68] and Lipid NP [69] but their use is limited due to some drawbacks.

Nanoparticles and pharmacokinetics

The nano range size of particles greatly affects the pharmacokinetics (PK) of the drug. There are many differences in the pharmacokinetics profile of free drug and drugs encapsulated in the nanoparticles. So it is very crucial to define the PK as well as bio tissue

distribution of free drugs and nanoparticles encapsulated with drug. Pharmacokinetics study helps us to understand the therapeutic index, efficacy, toxicities, and side effects of normal and nanoparticles loaded drugs.

The PK is simply defined as what body does with the drugs. It is study of time course movement of drugs in the body. PK study tells about the ADME (absorption, distribution, metabolism, and excretion). PK study involves measuring drug concentration in every single significant tissue after medication over a timeframe until complete elimination of drug. Generally the PK study is performed on the basis of half-life of a drug, for any study the time point is chosen approximately three times of drug's half-life. The PK parameters are evaluated on the basis of drug's concentration in the blood over a period of time. PK study includes many important parameters, namely AUC, AUMC, Cmax, tmax, t1/2, MRT, Cl.

AUC (area under the curve): mathematically the AUC is defined as the area under the curve in a graph of concentration of drug in blood verses time. Normally the area is calculated from the start time of drug administration till the elimination of drug from blood. The quantity of drugs available to the body is referred as bioavailability. The bioavailability of the drug is generally evaluated using the AUC.

AUMC (area under the first moment curve): It is a curve plotted between drug concentrations in plasma multiplied by the time on the Y-axis verses time on the X-axis.

C_{max}: In compartmental pharmacokinetics analysis, C_{max} is the maximum plasma concentration of the drug achieved at particular time point after administration of single dose.

T_{max}: T_{max} is the time at which the drug's peak plasma concentration is achieved.
MRT (mean resident time): this is the average time that a drug or molecule stays in the body. Some molecule last for very short time and some molecule last for very longer time.

Generally based on the above mentioned various parameters, the PK analysis will be carried out. If any drug or drug formulations shows extended systemic blood circulation, it

corresponds to the increase in the half life on drugs or formulation. The other parameters such as C_{max}, AUC and MRT are found to be increased and the clearance (cl) is decreased in this case. Further, if any drug or formulations shows fast elimination from the body, it result in to the decreased AUC, t1/2, and MRT; simultaneously an increase in the clearance (cl) was observed. Pharmacokinetics profile reflects the behavior of nanoparticles towards the body. PK data suggest the therapeutic index, efficacy and toxicity effect of drug in nanoparticles. The concentration of drug or nanoformulation in tissues or blood greatly defines the toxicity effect. PK study also helps in determining the optimum doses of any formulation. In case of targeted drug delivery, a higher accumulation of formulation is found in targeted tissue, thus leads to the more therapeutic index; on the other hand if more accumulation of formulations is accumulated in the non-targeted tissues, it may leads to the unwanted side effect and toxicity.

Rationale of the study

The clinical use of anti-retroviral drugs is limited due to their low solubility, low stability, low bioavailability and high toxicity, this can be overcome by encapsulating the drug in nanoparticle. This is expected to improve solubility, stability, safety and bioavailability of drug. Thus provide longer monotherapy and line of HAART option for treatment. In addition, the vehicle, lactoferrin, due to its intrinsic anti-HIV potential would provide a synergistic prophylactic action.

The present study addresses this hypothesis through development of lactoferrin based nano formulation for oral delivery of single drug as well as combination anti-HIV-1 drugs (as per HAART), and demonstrate that this nanoformulation provide a sustained optimum release of drug along with reduced toxicity, improved pharmacological properties and anti-HIV activity profile.

Chapter 2

Materials and Methods

Materials: All antiretroviral drugs (Zidovudine, Efavirenz, Lamivudine, Atazanavir, Tenofovir and Ritonavir) were purchased from Sigma Aldrich. Bovine lactoferrin was purchased from Symbiotics USA, Olive oil was purchased from Leonardo.

Cell lines: SupT1, PBMC, U-937.

Virus strain: HIV_{NL4-3}

Instrumentation: During the preparation of nanoparticle, the mixture was sonicated using narrow titanium probe of an ultrasonic homogenizer (model 300V/T, Biologics Inc. Virginia, USA). The centrifuge used for pelleting down of nanoparticles from HERMLE Z 36 HK. Alliance Separations Module e-2695 Waters High Performance Liquid Chromatography (HPLC) with 2487 dual detector was used for the estimation of drugs; using Empower 3 software. Field Emission scanning electron microscope (FE-SEM) from Philips were used for nanoparticle characterization. All the statistical data were analyzed and plotted using Sigma plot software. FTIR (ATIR and Thermo FTIR).

Reagents: Methanol, absolute alcohol, DMSO, acetonitrile, NaCl, Glycine, NaOH, SDS, dyes, Rhodamine123, Nile Red,

Biochemical kits: Biochemical kits were purchased from Span diagnostics and Cayman chemicals.

Software: Sigma Plot 11.0, Thermo Scientific Kinetica v5.

Methodology

Preparation of Protein Nanoparticles: Protein NP was prepared according to the previously described protocol [70]. For our study two forms of nanoparticles were prepared viz. Blank NP or Lacto-nano and drug/s loaded nanoparticles. Total four type of drugs loaded nanoparticles were prepared. Among four, two NP are single drug loaded NP and rest two are multiple drug loaded NP. Single drug loaded nanoparticles are AZT NP (AZT-lacto-nano) and EFV NP (EFV-Lacto-nano). Multiple or combination drug loaded include first line HAART drugs (AZT+EFV+3TC) loaded Lf NP and Second line HAART drugs (3TC+TNF+ATV/r) loaded Lf NP.

Preparation of mono drug loaded Lf NP

Preparation of AZT loaded Lf NP: 10mg of AZT was measured in a 0.6ml eppendorf tube. It was dissolved in 100µl of MIlli Q water. In another 2.0ml eppendorf tube one capsule (250mg) of lactoferrin was dissolved completely in 2ml of PBS of pH 7.4. From this, 320µl has been taken and transferred to the 0.6ml eppendorf containing AZT. Mixture has been incubated on ice for one hour. Then whole mixture was slowly added to a 60ml plastic container containing 25ml of ice cold olive oil followed by gentle manual vortexing. The container was kept on ice (4°C) and sonicated using the narrow titanium probe for 15minutes at an interval of 5min. After sonication the whole mixture was transferred to 50ml Oak Ridge centrifuge tube and immediately frozen into liquid nitrogen at-least for 15minutes. After 15minutes the tube was thawed on ice for four hours. The NP tube containing tube was centrifuged at 6000rpm for 10min at 4°C. Supernatant (oil) was discarded and the pellet was saved. The pellet was washed thrice with ice cold di ethyl ether to remove any oil traces. Finally the NP pellet was resuspended in PBS and used for further study or stored at 4°C for long term storage (up to 2monhts).

Preparation of EFV loaded Lf NP: EFV loaded Lf NP was prepared using the same protocol of AZT NP. Briefly, 10mg of EFV was dissolved in 100µl of methanol and mixed with varying concentration (10mg, 20mg, 30mg, 40mg and 50g) of lactoferrin dissolved in 500µl of PBS. After this same procedure has been followed as to AZT NP preparation.

The preparation protocol for blank nanoparticles is same as of drugs loaded nanoparticles, only difference is that, in this case only lactoferrin protein was used and drugs were not used.

Preparation of combination drug loaded Lf NP

Preparation of first line ARV drugs loaded Lf NP: Equal amount of 1st line ARV drugs viz. AZT (3.33mg), EFV (3.33mg) and 3TC (3.33mg) has been dissolved in 100µl of DMSO separately and varied amount of Lactoferrin (Lf) were dissolved in 500µl of 1X PBS (pH 7.4). Drugs and protein solution were incubated on ice for at least one hour, the time required for saturate binding of drug to protein. After incubation same protocol has been followed as mentioned in the section of preparation of AZT NP.

Preparation of second line ARV drugs loaded Lf NP: Second line ARV drugs such as 3.33mg 3TC, 3.33mg TNF, 3.33mg ATV and 1.11mg RTV were dissolved in 100µl of DMSO separately and mixed with 40mg of lactoferrin solution and incubated on ice for an hour. After one hour same procedure has been followed as described for preparation of AZT NP. Figure 2.1 and 2.2 shows the brief outline the steps followed in preparation of second line drugs combinations loaded nanoparticles and possible assembly for first line drugs in lactoferrin nanoparticles.

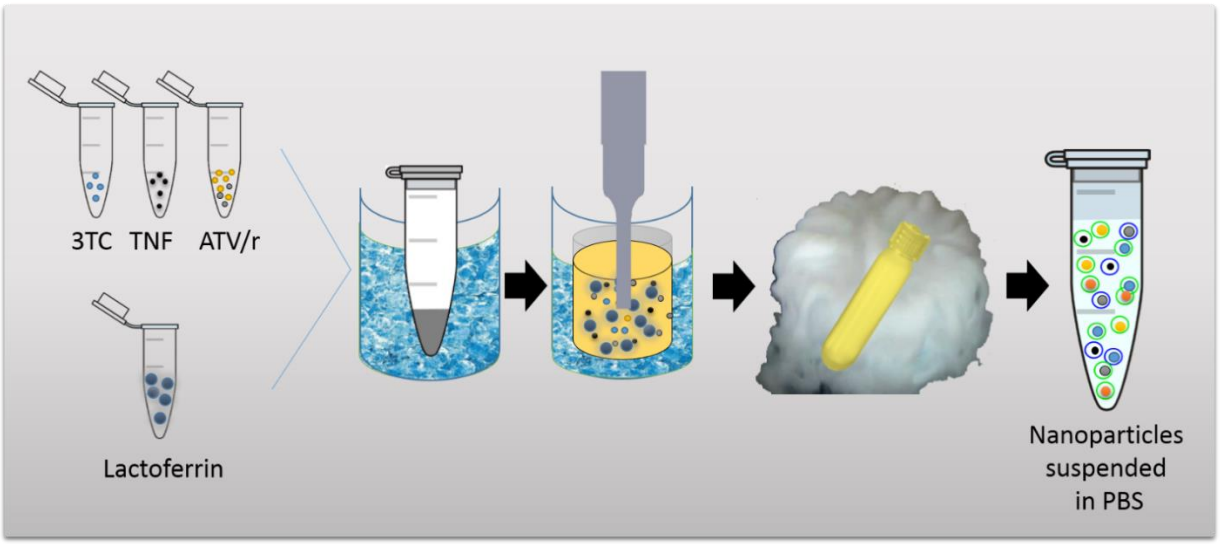

Figure 2.1: The brief outline for the preparation of second line loaded drugs lactoferrin nanoparticles.

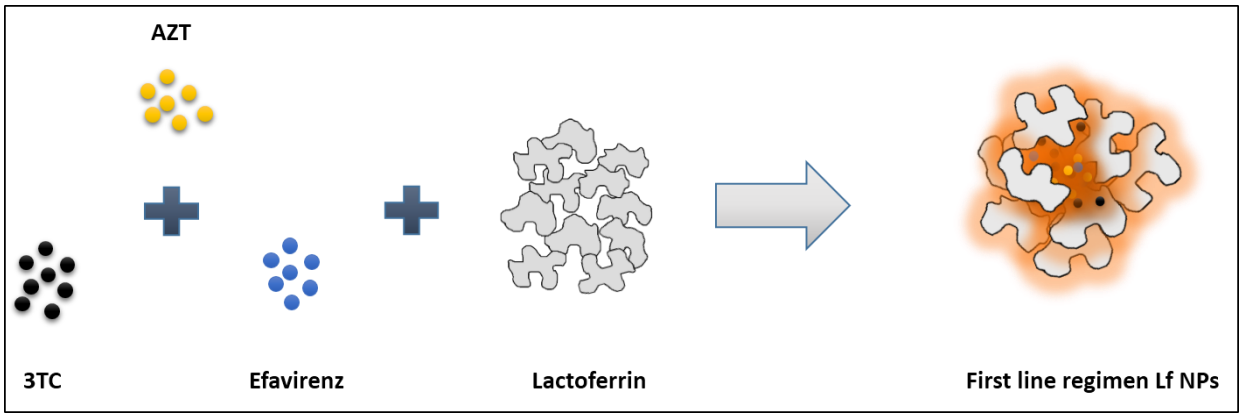

Figure 2.2: The possible assembly for first line loaded lactoferrin nanoparticles.

Characterization of nanoparticles

The NP prepared were characterized using various techniques such as FE-SEM (Field Emission-scanning electron microscope), AFM (atomic force microscopy), NanoSight, Transmission electron microscopy (TEM), DLS (dynamic light scattering) and FTIR (Fourier transform infrared spectroscopy).

FE-SEM (Field emission scanning electron microscope): FE-SEM has been performed using Philips FEI-XL 30 ESEM; FEI, Hillsboro, OR, USA) operated at 20 KV. Freshly prepared NP suspension was spread over on the 1mmx1mm square clean glass slides and kept for drying overnight. The glass slides were coated with gold before visualizing through the microscope. The images were focused and captured according to the manufacturer guidelines.

AFM (Atomic Force Microscopy): Nanoparticles were visualized through AFM (AFM; SPM-400). All samples were coated on glass slide before visualizing through microscope. All instructions were followed in accordance to manufacturer.

Particle size and size distribution – Nanoparticle tracking analysis (NTA): Nanoparticles size distribution was performed by NTA using NanoSight NS500. This instrument determines the size of nanoparticles based on the Brownian motion of particles present in the samples. Samples were diluted in Milli Q and experiments were done in triplicate. The camera setting was adjusted to minimize the background noise and video was recorded for 60s. After capturing the video, it was processed and analyzed using dedicated software (NTA analysis software version 2.0). Optimum visualization of maximum number of nanoparticles were done using manual focusing with combination of high shutter speed (600) and gain (250). Following setting has been followed during the analysis, Frames Processed: 1498 of 1498, Frames per Second: 24.98, Calibration: 141 nm/pixel, Blur: Auto, Detection Threshold: 10 Multi, Min Track Length: Auto, Min Expected Size: Auto, Temperature: 24.80°C, Viscosity: 0.89 cP.

Transmission electron microscopy (TEM): Nanoparticles were fixed on the 200mesh type-B carbon coated copper grid (TED PELLA Inc.). NP was stained with 2% Uranyl acetate prior to analysis.

DLS analysis (particles size distribution and zeta potential analysis): Size distribution and zeta potential analysis was done using Horiba Scientific (SZ-100). Nanoparticles suspension were optimally diluted in Milli Q. Sample were then transferred to 2ml quartz cuvette and analyzed for size distribution. For measurement of zeta potential 200µl of sample was transferred to specially designed cuvette with electrode.

FT-IR study of nanoparticles: The FT-IR spectral analysis was executed using kBr pellet method. The 0.1-1.0% of lyophilized nanoparticles were mixed with approximately 200mg of KBr followed by transferring of mixture to a 13mm diameter pellet forming dye under a very high pressure of 1000kg/cm^2. A transparent pallet was formed. This was then transferred to the sample holder followed by scanning in a range of 400 to 4,000 cm^{-1}. Finally the analysis of spectra was done using OMNIC series software.

***In vitro* experiments**

Encapsulation efficiency: Encapsulation efficiency (EE) is defined as the ratio of actual and initial amount of drugs encapsulated in the NP. Generally EE is measured in percentage. The procedure for calculation of EE% is as follows. Freshly prepared NP has been incubated with 1ml of PBS (pH5) at room temperature at rocking condition for 24h. After 24h, 100ul of 30% silver nitrate was added to the solution to precipitate the protein. Then drug/s was/were extracted by adding 1ml of HPLC grade methanol into it. Further the mixture was centrifuged at 12000rpm for 20min and supernatant was evaluated for the presence of drugs. All experiments were performed in triplicate. One standard curve was made using different known concentration of drug/s measured using HPLC. Finally the EE% was calculate using the below mentioned formula.

$$\textbf{Encapsulation Efficiency}\ (\%) = \frac{\mathbf{M_{total} - M_{lost}}}{\mathbf{M_{total}}} \times \mathbf{100}$$

M_{total} is the total amount of drug entrapped during preparation of NP and M_{lost} is the amount of drug unavailable after release from nanoparticles.

pH and simulatd fluid dependent drug release from NP: 600µg of freshly prepared AZT NP, EFV NP, FLART NP and SLART NP was incubated with 1ml of PBS of different values pH in the range 2-8, SIF (simulated intestinal fluid) and SGF (simulated gastric fluid) for 12hr. After incubation protein was precipitated by adding 200µl of 30% silver nitrate followed by addition of 1ml of HPLC grade methanol for extraction of drug/s. then after the samples were centrifuged at very high speed i.e at 12000rpm for 20min: supernatant were analyzed for the drugs.

Percent drug release from nanoparticles: This experiment has been performed to evaluate the time dependent release of drug from NP at two different pH. To estimate percent release, drug loaded NP was incubated for various time points such as 1, 2, 4, 6, 8, 10, 12, 16, 24h. After completion of incubation time aliquot were removed and drugs was quantified using silver nitrate method.

Erythrocytes toxicity assay (Hemolysis test): This assay was performed for the combination drugs loaded Lf NP i.e FLART NP and SLART NP. The hemolytic impact of first line drugs either in soluble or nano form on the rat erythrocytes were conducted according to previously set protocol [71]. The erythrocytes stock dispersion was prepared as follows. Initially the blood samples were collected in heparinized tubes. Blood was washed three times using 0.9% NaCl saline solution. After every wash, the cells were centrifuged for 5min at 150xg; supernatant was discarded. The final pellet dilution was done (v/v) 1:9 in 0.9% NaCl saline solution followed by dilution in Dulbecco's phosphate buffer saline (D-PBS), pH 7.0 (v/v) 1:24 [72]. The assay was started by mixing 100µl of erythrocytes stock

dispersion with 1ml of (1mg/ml or 2mg/ml) of FLART Sol, FLART NP, SLART Sol and SLART NP. The resultant mixture were incubated at 37ºC under shaking condition for various time points. Saline solution and distilled water were considered as negative (0% lysis) and positive control (100% lysis) respectively. After incubation samples were spin down for 5min at 1200 rpm to remove the debris and integral erythrocytes. Then 100µl of supernatant was mixed with 2ml of ethanol-HCl mixture (39:1; 99% ethanol [v/v], 37% hydrochloric acid [w/v]) followed by final centrifugation for 3min at 750g. The resultant supernatant were spectrophotometrically measured at 398nm. The hemolysis rate was measured using the formula; HR% = [(D1-D2)/ (D3-D2)] x 100. Here D1, D2 and D3 are the absorbance of tested samples, negative control and positive control respectively.

Cytotoxicity assay (MTT assay): MTT cell cytotoxicity assay was performed for the efavirenz either in soluble or nano form. As anti-HIV drugs mainly target T-cell and in some previous reports EFV has found to skin impairment too. Cell toxicity assay was performed using three different cell lines; Jurkat, stimulated PBMC and B16-F10 cells. Cells (100% viability) having a density of 0.2million were seeded with RPMI 1640, 10%FBS in a 96-well plate and incubated for 4h at 37degree and 5% CO_2 incubator. Cells were treated with varying concentration such as 1, 5, 10, 25, 50, 100 and 1000µm of sol EFV & Lacto-EFV-nano and incubated for 16h. After 16h the cells were pelleted down and resuspended in fresh media. To this, 20ml of 5mg/ml MTT (Sigma-Aldrich) was added and incubated for 4 h. The cells were then pelleted at 1200 rpm for 20 minutes, the medium was removed, and the precipitate was dissolved in DMSO and read in an ELISA microplate reader at 570 nm.

Cellular nanoparticles localization assay by confocal study: The localization study of NP was performed in the macrophages cell line (U-937) (Fig. 2.1). As the ART drugs were not fluorescent; the lactoferrin NP was tagged with 30µg of Rhodamine-123 green fluorescent dye. Approximately 100% viable cells with a density of 10^4 were incubated for different time such as 1, 2, 4, 6 and 8h. After completion of time points cells were collected and washed three times using PBS (pH 7.4); fixed on clean glass slide. The fluorescence was

estimated using laser confocal microscope (Carls Zeiss) by keeping the florescence setting according to rhodamine123 (Excitation – 505nm and emission – 530nm). Cells without any treatment were considered as control.

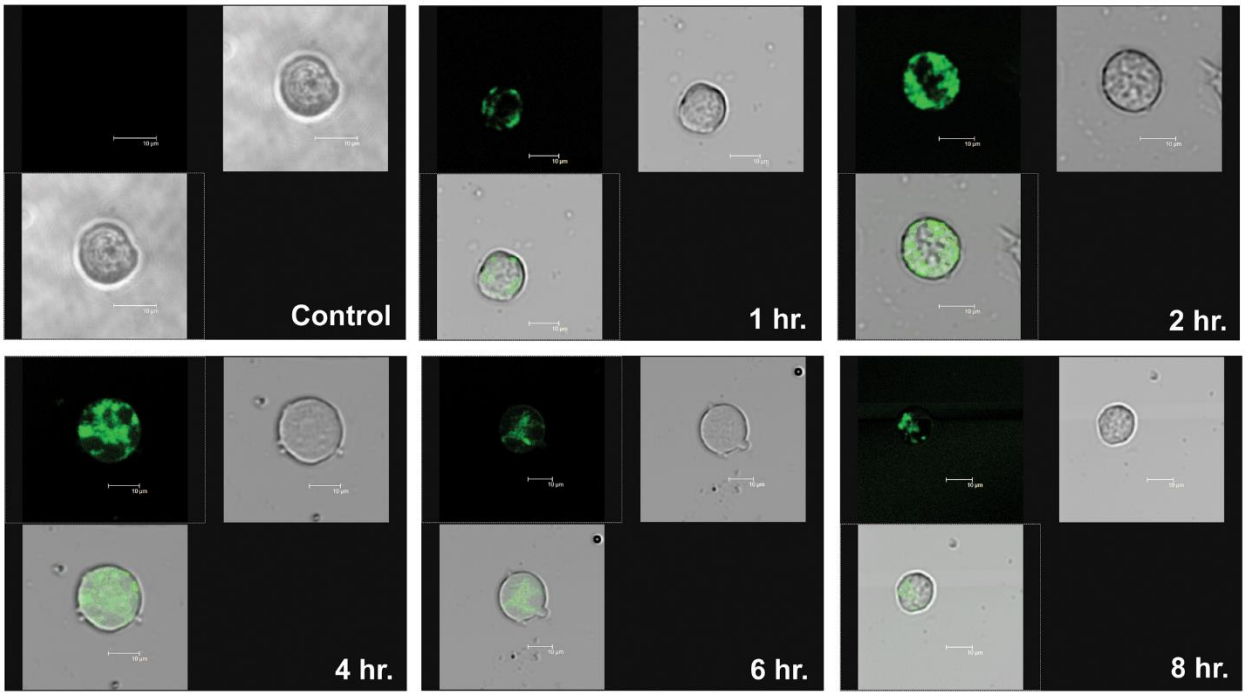

Figure 2.3: Cellular localization of Rhodamine-123 tagged lactoferrin nanoparticles: a confocal study

***In vitro* cellular drug kinetics:** This experiment was conducted to indicate the time-dependent localization of efavirenz either in soluble or nano form. Briefly, 0.1million of SupT1 cells were suspended in RPMI 1640 with 10% fetal bovine serum and seeded in a 12-well plate. Cells were incubated with 30µg of soluble EFV and Lacto-nano-EFV for different time points such as 30min, 1h, 2h, 4h, 6h and 8h. After completion of incubation, period cells were washed using 1X PBS (pH 7.4) and lysed in 500µl of PBS containing 0.1% triton X-100 under soft sonication for the 20s. Samples were mixed with 1ml of methanol and 200 µl of 30% silver nitrate; centrifuged at 12,000rpm for 10min, supernatant obtained were analyzed using HPLC.

Anti-HIV-1 assay: Antiretroviral drugs (AZT, EFV, LMV, TNF, ATV and RTV) either in soluble or nano form were evaluated for anti-HIV activity *in vitro*. Briefly, 0.1 million of SUPT1 cells with 100% viability were challenged with HIV-1_{NL4-3} virus clone for 10h. Next day cells were washed thoroughly to remove any unattached virus particles and resuspended in fresh RPMI 1640, 10% fetal bovine serum medium. Experiments were conducted at increasing concentration of sol and nanoformulation drugs. Vehicle control (Blank lactoferrin NP) and AZT were used in a concentration range of 0.1 to 15µm. AZT is considered as positive control. The cell supernatant at day 5 was collected and virus replicated was estimated in terms of p24 using p24 antigen capture assay (Advanced Bioscience Laboratories, Kensington, MD, USA, and Lot No. 11111101). The p24 level in the absence of drug was considered as 0% inhibition. The efficacy of drug was measured in terms of %Inhibition of HIV-1 replication. After evaluation of IC_{50} for individual drugs we have performed the anti-HIV for first line and second line drugs. Frist and second line drugs in the different ratio of their IC_{50} were added to the cells challenged with virus for three different time points such as 2, 8 and 12h and percent inhibition was measured using p24 ELISA assay.

HPLC analysis: Drugs concentration in blood and in various tissues were analyzed using Waters HPLC. The HPLC condition for various are indicate below in Table 2.1.

Table 2.1. HPLC conditions for all drugs.

Drugs	HPLC mobile phase condition	Flow rate	Wavelength	Ref.
AZT	acetonitrile: methanol (60:40 v/v)	1ml/min	265nm	[73]
EFV	0.1% formic acid: acetonitrile (25:75, v/v)	0.3ml/min	247nm	[74]
3TC	50 mM sodium dihydrogen phosphate: triethylamine (996:4, v/v)	1.5ml/min	278nm	[75]
TNF	Methanol: 10 mM phosphate buffer (70:30, v/v)	1ml/min	254nm	[76]
ATV	Acetonitrile: 10nM ammonium formate buffer (45:55, v/v)	0.3ml/min	210nm	[77]

***In vivo* experiments**

Animal studies and dosage schedule: All *in vivo* experiments were performed using Wistar rats. Male and female Wistar rats weighing 0.160kg to 0.250kg and approximately six month old were obtained from Sainath agency, Hyderabad. Animals were acclimatized in a hygienic, well ventilated condition at animal house facility, University of Hyderabad for at least one week prior to treatment. They were allowed freely to access the commercial rat feed pellets and clean water. Current study was carried out in strict accordance with the recommendations in the Guide for the Care and Use of Laboratory Animals of the National Institutes of Health. This study was specifically approved by the Institutional Animal Ethical Committee, University of Hyderabad.

Animals were segregated depending on the drugs. The details of animal study design is presented in Figure 2.3 and 2.4. All animals were divided into two major groups; drug treated and control. Control groups animals were injected with saline (0.9% NaCl in Milli Q). All treated groups animals were divided in to the different time points groups. All animals were injected in triplicates. A fixed dose of 10mg/kg for all the four formulations. AZT and EFV were injected with 10mg/kg body weight. First line drugs were injected in a ratio of AZT/3.33mg+EFV/3.33mg+3TC/3.33mg for soluble and equivalent to nanoformulation has been injected. For the second line 3TC/3.33mg +TDF/3.33mg +ATV/3.33mg +RTV/1.11mg was given. Time point of doses were determined according to the half-life of drugs. All dosages were administered orally with the help of 18SWG (standard wire gauze) oral bend cannula. While administration drug was suspended in PBS. After administration all the animal were monitored hourly to determine the effect of NP on their weight and behavior. There were no death reported during the treatment.

Pharmacokinetics (PK) and Tissue distribution (TD) study: After the completion of time points, all animals were euthanized using ketamine (60mg/kg) + Xylazine (10mg/kg), IP. Blood were collected through heart puncture in terminal anesthesia condition. The concentration of drugs in blood at indicated time points were evaluated using HPLC and the PK analysis was performed using Kintica.v5 software. Final sacrifice was done by

cervical dislocation. Tissues such as brain, heart, lungs, liver, esophagus, spleen, stomach, small intestine, large intestine, kidney and bone marrow were collected. All the organs except bone marrow were homogenized in 1x PBS (pH 7.4); 200µl of 30% of silver nitrate/ml of tissue suspension was added to precipitate the protein. Drugs present in the mixture was extracted by adding the HPLC grade methanol into it; centrifuged at 12000rpm for 20min at 4°C. Supernatant were filtered using 0.2micron syringe filter and quantified for the presence of drug using HPLC at respective wavelength of drugs.

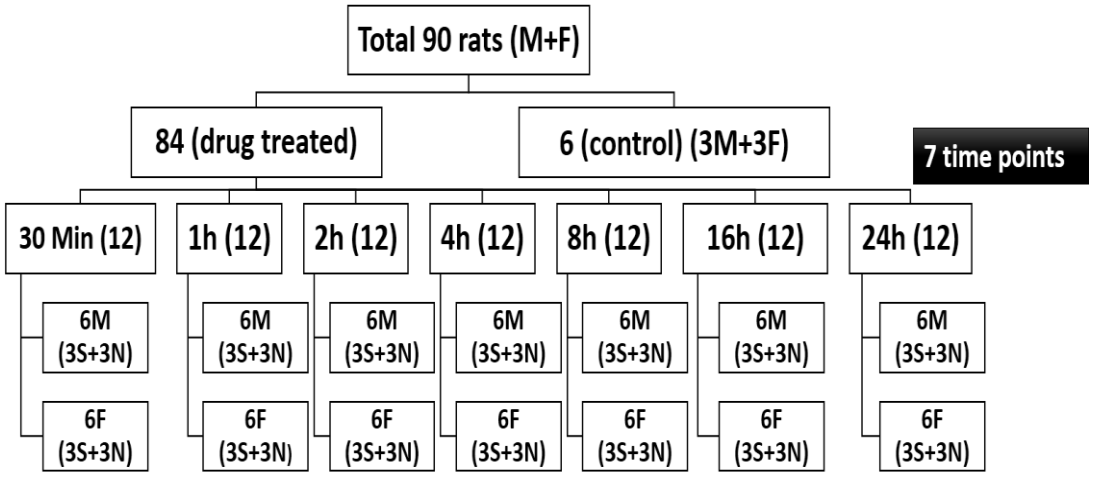

Figure 2.3: Animal Study design for AZT, First Line HAART drugs and Second line HAART drugs.

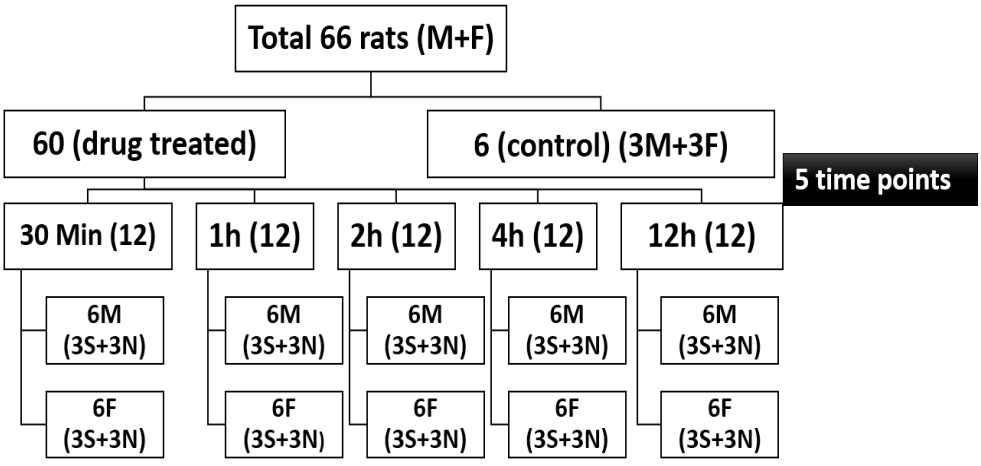

Figure 2.4: Animal Study design for EFV.

Safety analysis assay: After completion of respective time points, all animals were sacrificed under proper anesthesia; blood was collected followed by isolation of serum. For long term use small aliquot (50µl) of serum was stored in -20°C. Serum was used for the measurement of various safety parameters such as LDH, Creatinine, Urea, BUN, Lipid profile, etcetera. The safety parameters were evaluated using commercially available kits. Manufacturer instruction were followed for each kits.

Histopathology analysis: While isolating the various tissue, a small portion of same were saved in neutral buffered saline for histopathology analysis. Hematoxylin and eosin (H&E) staining were done in specialized pathology lab. The H&E images were observed under high resolution microscope for the presence of any abnormalities.

Statistical Analysis

The in-vitro and in-vivo experiments were performed in triplicates. All data were indicated as mean ± standard deviation. The significance difference between multiple groups were analyzed using one way ANOVA. Between two groups significance was evaluated using student's t test. The significance level was set to $P<0.05$.

Chapter 3

Development and characterization of AZT loaded lactoferrin nanoparticles as oral formulation.

Introduction

Zidovudine, an antiretroviral drugs also referred as azidothymidine (AZT). AZT was the first medication endorsed by FDA for clinical purpose [14]. AZT is a (Nucleoside reverse transcriptase inhibitors) NRTI class of anti-HIV drugs which inhibits HIV by inhibiting the reverse transcription reaction [78]. AZT is generally accessible as the brand name Retrovir [79]. In early days, AZT was prescribed as mono-therapy for HIV treatment. While in current scenario, AZT is recommended in combination with other ARV drugs as HAART. Combivir, the prescribed formulation for HIV treatment is the combination of lamivudine (150mg) and Zidovudine (300mg) [80]. Zidovudine is capable to inhibit a wide range of HIV isolates with an IC_{50} range of 0.003 to > 2.0 microM [81]. In-spite of its high anti-HIV activity, there are many factors that limits is usage such as, its poor pharmacokinetics profile[82], bone marrow toxicity [83], hematotoxicity [84], and mitochondrial toxicity [85]. Further, AZT is also known as a potential genotoxic compound [86, 87], which could leads to anemic condition. The aim of this study is to develop a lactoferrin based nanoparticles for Zidovudine delivery. Our laboratory has previously developed nanoformulations various anticancer drugs such as doxorubicin and carboplatin for cancer therapy [59, 61, 70, 88]. Among the various routes for drug delivery, oral administration is the best modality available for the drug delivery. The present work involves the improvement in the delivery of AZT using the lactoferrin as nanocarrier system. It is envisaged that the present nanoformulation of AZT loaded lactoferrin nanoparticles would act in a bidirectional manner, wherein the carrier itself has antiviral activity along with AZT itself. Indeed results of present work showed the improved efficacy, safety, bioavailability and pharmacokinetics of AZT encapsulated in lactoferrin nanoparticles (AZT-lactonano).

Results

Drug protein optimization time.

After incubation of equal concentration of lactoferrin protein and AZT. The fluorescence was measured at room temperature. It was observed that after 55 to 60min, there was no increase in the fluorescence intensity i.e. a saturation in the fluorescence was found (Fig.

3.1). It suggest that, an incubation time of 60min is sufficient for protein and drug before preparation of nanoparticles.

SEM microscopic analysis of AZT NP

The size of Blank NP and AZT NP were microscopically analyzed using Field Emission Scanning Electron Microscopy (FE-SEM). The size of Blank NP was found to be 27nm and after loading of drug the size was increased up to 59nm (Fig. 3.2).

AFM microscopic analysis of AZT NP

Further the surface anisotropy and size of Blank NP and AZT NP were analyzed using Atomic force microscopy (AFM). The mean diameter of blank NP was found to be 25nm whereas for AZP NP it was 61nm (Fig. 3.3).

DLS analysis of nanoparticles

DLS study reveals that the hydrodynamic radii and surface charge (zeta potential) of NP. The hydrodynamic radii for blank NP was found to be an average of 54nm, whereas for AZT-NP it was found to be approximately 106nm (Fig. 3.4). Further the zeta potential on blank NP and AZT NP were found to be -21mV and -23mV respectively.

FT-IR Analysis of AZT NP

FT-IR analysis confirmed that AZT was found to be intact after the preparation of nanoparticles. Characteristic bands found in the infrared spectra of Lactoferrin proteins (Pure and nano form) include the Amide I and Amide II (Fig. 3.5 A and B). The absorption associated with the Amide I band and Amide II band leads to stretching vibrations of the C=O bond and primarily to bending vibrations of the N—H bond respectively. Amide I bands was positioned around 1645 & 1648 cm^{-1} are usually reflected to be characteristic of alpha helices. Amide II (C-N stretching and N-H bending) and peptide N—H stretching frequency were detected at 1542 & 1539 $cm^{-1}$and 3418 & 3364 cm^{-1} correspondingly. The C-O-C stretch were observed around 1096 cm^{-1} & 1164 cm^{-1} The locations of both the Amide I and Amide II bands are sensitive to the secondary structure content of a protein. Assessment spectral analysis of Pure AZT and AZT NP (Fig. 3.5 C and D): sharp

characteristic peaks of carbonyl group (C=O) at 1682 cm^{-1} (Pure AZT) and 1685 cm^{-1} (AZT NP), Azide group (N−= N+= N−) peaks at 2117 & 2083 cm^{-1} (Pure AZT) and 2115 & 2082 cm^{-1} (AZT NP), C-O-C stretch belong to 1088 &1065 cm^{-1} (Pure AZT) and 1089 & 1065 cm^{-1} (AZT NP), -NH stretching remains at 3460 cm^{-1} (Pure AZT) and 3461 cm^{-1} (AZT NP). Our results of FT-IR spectra proved that there were only slight shifting (may be due to dipole moment of bond as a result of electrostatic interaction between AZT and Lactoferrin protein) in few stretching vibration but all the major functional group was intact in nanoformulation and didn't take part in any covalent bond formation. It confirmed that AZT is only physically associated (entrapped/adsorbed) with lactoferrin protein.

Encapsulation efficiency of AZT NP

Encapsulation efficiency of AZT NP was calculated according to the equation mentioned in materials and methods section and found to be 67%.

pH dependent release profile of AZT NP

To test the stability of AZT NP, it was subjected under different pH condition. In the starting of experiment the amount of encapsulated drugs in the nanoparticles was considered as 100%. In addition to different pH condition, nanoparticles were also treated with two different simulated fluid, i.e. simulated intestinal fluid (pH=5.4) and simulated gastric fluid (pH=3). The amount of drugs released under these pH condition were evaluated and plotted against time. The in vitro drug release profile was shown in (Fig. 3.6). Results shows that maximum release of AZT was observed at pH5, followed by pH6 and pH4. In simulated fluid condition only <30% of drugs are released, suggests the stability of NP under these conditions.

Percent release profile of AZT NP

AZT NP was subjected with two different pH for various time point. Data (Fig. 3.7) shows the percent release of AZT from AZT NP at different time points. This shows a biphasic release of AZT from NP at pH5. Approximately 60% of drugs were released (burst release) up to 4h, then a slow and sustain release until 10h followed by a limited release over 96h.

Whereas at pH7.4, a maximum of <20% drugs release was observed till the end of experiment,

In vitro Stability studies of AZT NP

The stability of AZT NP was analyzed in term of its encapsulation efficiency and its diameter. After preparation AZT NP (suspension form) was placed under observation up to 96h at two different temperature i.e. (4°C and 25°C). At specified interval of time, the diameter and EE were calculated and presented in Table 3.1. Results showed that AZT NP are found to be very stable under these condition. There is very minor shift in both parameters were observed.

Antiviral Activity of AZT Lacto Nano

Antiviral assay was done in two parts. In part I experiment, the dose dependent anti-HIV activity of sol AZT and AZT NP was performed using HIV-$1_{93IN101}$ in SupT1 cell. The IC_{50} values for Sol AZT and AZT NP was found to be 33.4nm and 20.5nm Fig. 3.8. It suggest that, AZT is more potent in nanoform as compared to its normal form. In part II experiment, the antiviral activity of lactoferrin alone and AZT loaded in nanoformulation was analyzed to determine if active form of the drug is intact. Here 80mg/ml of soluble lactoferrin and equivalent of nanoform of lactoferrin has showed 70 and 73% antiviral activity respectively. Further, the activity of AZT at one microgram concentration is similar to that of soluble AZT with more than 90% of inhibition of HIV-193IN101 replication in Sup-T1 cells. These results suggests that activity of encapsulated AZT remain stable in nanoformulation (Fig. 3.9)

Animal Study Design:

The detail animal study design is provided in methodology section (Fig. 2.3 & 2.4)

In vivo pharmacokinetics and tissue distribution of AZT NP

A single dose of 10mg/kg of sol AZT and equivalent dose of AZT NP was administered in rats orally. After completion of all time points, rats were sacrificed under standard protocol. After sacrificing all rats, blood as well as tissues were harvested and stored.

Plasma was isolated from the blood and stored in -20°C for long term use. After homogenization of all tissue, concentration of AZT was measured using HPLC. The drug concentrations in various tissue were plotted versus time (Fig. 3.10A & B). The blood concentration of sol AZT and AZT NP was found to be 10µg and 50µg after 2h of drug administration. For PK analysis, AZT concentration was estimated in blood at different time points. The PK parameters were calculated using Kinetica V 5.0 software (Table 3.2). The overall PK parameters were found to be improved in nanoformulation treated rats compared to that with soluble drug. In detail, the AUC (area under curve) was increased by >4 fold in both male and female rats when treated with AZT NP. In AZT NP treated rats, the AUMC was also found to be increase by >9 fold in both genders. The peak plasma concentration (C_{max}) was also improved by >30% in case of nanoformulation. The T_{max} and $t_{1/2}$ and were also improved by 2fold.

Safety analysis of AZT NP

After collection of serum, various safety parameters such as AST, urea, bilirubin and creatinine were estimated at various time point and plotted against time (Fig. 3.11). There was no significant change was observed in the serum AST level in case of sol or nano AZT treated rats. The serum urea concentration was elevated at 1h and 2h in case of sol AZT treated animals as compared to AZT NP treated. Results suggests low kidney toxicity in case of nanoformulation. The low bilirubin level was observed in nano treated rats as compared to it soluble formulation. Creatinine level directly relates with the kidney toxicity, results has shown the elevated level of creatinine was lowered down when treated with AZT NP.

Histopathology analysis

The histopathology analysis was done for all the major tissue. Result showed that most of the tissues such as, heart, kidney, stomach, small intestine and large intestine did don't show any inflammation or damages, either in sol or nano treated rats. Whereas, some inflammation or lesions were observed in liver and spleen, as indicated with the arrow head (Fig. 3.12A & B)

Bone marrow micronucleus Assay

Barrow marrow cells were stained with Giemsa followed by microscopic analysis. The smear slides were observed for any abnormalities. In each slide approximately 1000 cells were observed for the presence of any micronucleus (Fig. 3.13A). The maximum number of MN-PCE was observed at 8h in sol AZT treated rats, where as in nano treated rats, MN-PCE number is equal to control (Fig. 3.13B). MN is generally characterized by the presences of small darkly stained nucleus.

Discussion

Various formulations have been employed previously to improve the oral bioavailability of AZT. These include controlled [89] and extended [90, 91] release matrices, microspheres [92], nanoparticles [93] and liposomes [94], which have been proposed for the delivery of AZT. Even though various routes like intranasal, intravenous and transdermal routes have been tried for AZT delivery. Peroral route of administration is the most preferred one because of frequent dosage and patient compliance. Absorption of AZT is reported to be quick and rapid when administered orally and undergoes first pass metabolism before giving an average systemic bioavailability of more than 60% [95]. Based on physiochemical characteristics, the aqueous solubility, pKa and LogP of AZT was reported as 29.3 g/l, 9.68 and 0.06 respectively [96]. Zidovudine typically exhibits a 1-compartment model in plasma during its oral administration followed by an elimination phase that is biexponential. It is relatively a lipophilic molecule where 25% of it binds to albumin [97] and gets metabolized in the body mainly by hepatic 5'-glucouronidation forming a stable metabolite which gets excreted in the urine. In order to maintain the required therapeutic concentration of AZT, frequent doses have to be given which may lead to elevation to toxic levels in the blood resulting in severe side effects like granulocytopenia and anemia. Greater focus has been given for targeting AZT to lymphoid and reticuloendothelial cells in previous formulations since the delivery to these cells is utmost important as they constitute major viral reservoirs and a sterilizing cure for AIDS is impossible unless and until these are eliminated completely.

Since the encapsulation mechanism involves a process of partition of lipophilic-lyophilic AZT and lactoferrin in water and oil phases. Such phase transitions may induce

protein-protein associations that entrap drug in intermolecular core as well as intramolecular cavities of proteins. This lead to a defined percent of drug (67%) associated with the protein nanoparticles based on the log P value of the drug, viz., AZT (log P, 0.06). This can be supported by the observation that AZT is released in biphasic kinetics with burst (60%) when protein surface of particles exposed to pH 5, which could be due to change in orientation of protein monomers, this may follow a release of drug molecules localized at various cavities in the protein over time (to the extent of 20%). In spite of biphasic release, 80% of loaded drug was released within 10 hours, making the availability of active drug for inhibiting target enzyme, revise transcriptase activities. Furthermore, oral absorption of nanoparticles at low pH (<3.0) and circulatory pH7.4, allow particles intact with the loaded drug. When these particles reached the target cells (lymphocytes etc.), they enter through receptor-mediated endocytosis followed by fusion to endosome, a transient pH change to 5.5 in endosome will allow significant drug release in target cell and make effective concentrations of drug reaching at the site of action. Thus, stability of particles at pH below 3.0 and at 7.4 make these particles attractive for oral delivery in vivo. In vivo studies showed that the AZT-lactonano showed has improved pharmacokinetic profile with more than 4-fold increase in mean serum AUC and AUMC in both male and female rats. The serum Cmax for AZT-lactonano was increased by 30% whereas more than 2-fold increase was observed in Tmax and t1/2 for both male and females. It suggests that the AZT in the nanoparticles gets released slowly leading to this significant increase in the pharmacokinetic parameters. At the same time, this nanoformulation has not shown any abnormal concentrations in different organs leading to toxicity. The safety profile of nano and Sol AZT was compared and the results show no significant change in serum AST in nano versus soluble form, while bilirubin was lower in case of nano when compared to soluble form in female rats.Serum urea was significantly low when AZT-lactonano was administered compared to soluble

AZT suggesting low kidney toxicity when nanoformulation was used. AZT-lactonano showed no apparent differences in creatinine levels compared to soluble form suggesting low kidney toxicity. In addition H&E staining of all the tissue sections has not revealed any abnormal morphology for both of the formulations employed. Bone marrow suppression is the main reason to discontinue AZT based therapy [98] because the hematopoietic

progenitor cells are heavily damaged. Micronucleus (MN) test is very reliable and fast in vivo assay to determine any marrow cells alteration [99]. MN are minute extra-nuclear bodies formed during anaphase stage [100]. Generally two forms of MN are found in RBCs, polychromatic erythrocytes (PCE) and Normochromatic Erythrocytes (NCEs) [101]. Our results show that AZT-lactonano is not involved in any MN formation but at the same time Sol-AZT is two-time more genotoxic. As the free drug is reported to have lower penetration into the infected cells, the above formulation selectively targets and delivers AZT to cells that express lactoferrin receptors on their surface through receptor-mediated endocytosis by which the therapeutic index of AZT can be improved. The amphiphilic nature of AZT results in low entrapment and significant leakage when packed in conventional liposomal vesicles as it gets partitioned between lipid bilayers and the core aqueous environment. The lesser size of the nanoparticles with up to 67% encapsulation of AZT makes the current formulation to overcome the above problem. Currently, oral dosed HIV nanoformulation was not available for patients. The quality of patient's life can be improved by simplifying the AZT dosage schedule by less frequent administration of a sustained- release formulation since HAART regimens that combine multiple agents lead to severe side effects. The advantage in employing lactoferrin as a carrier is its ability to interfere with virus binding to DC-SIGN of dendritic cells by its interaction with the V3 loop of gp120 and co-receptors [102]. Further, the same formulation can be employed to improve the brain delivery of AZT since the lactoferrin is reported to cross the blood-brain barrier [103].

Conclusion

The Present study shows the applicability of protein-based nanoparticles formulation of AZT through oral delivery. The nanoparticles were prepared using sol-oil protocol. AZT-lactonano showed a biphasic drug release profile and releases its maximum payload at pH 5. In vivo studies concludes that the physical encapsulation of AZT in lactoferrin nanoparticles makes the formulation safer and efficacious. Nano-formulation enhances the various pharmacokinetics profile like AUC, AUMC, Cmax and t1/2 while keeping the antiviral activity of AZT intact. Further AZT-lactonano is found to be two times less genotoxic as compared to sol-AZT.

Figure 3.1 Drug (AZT) – Protein Saturation study.

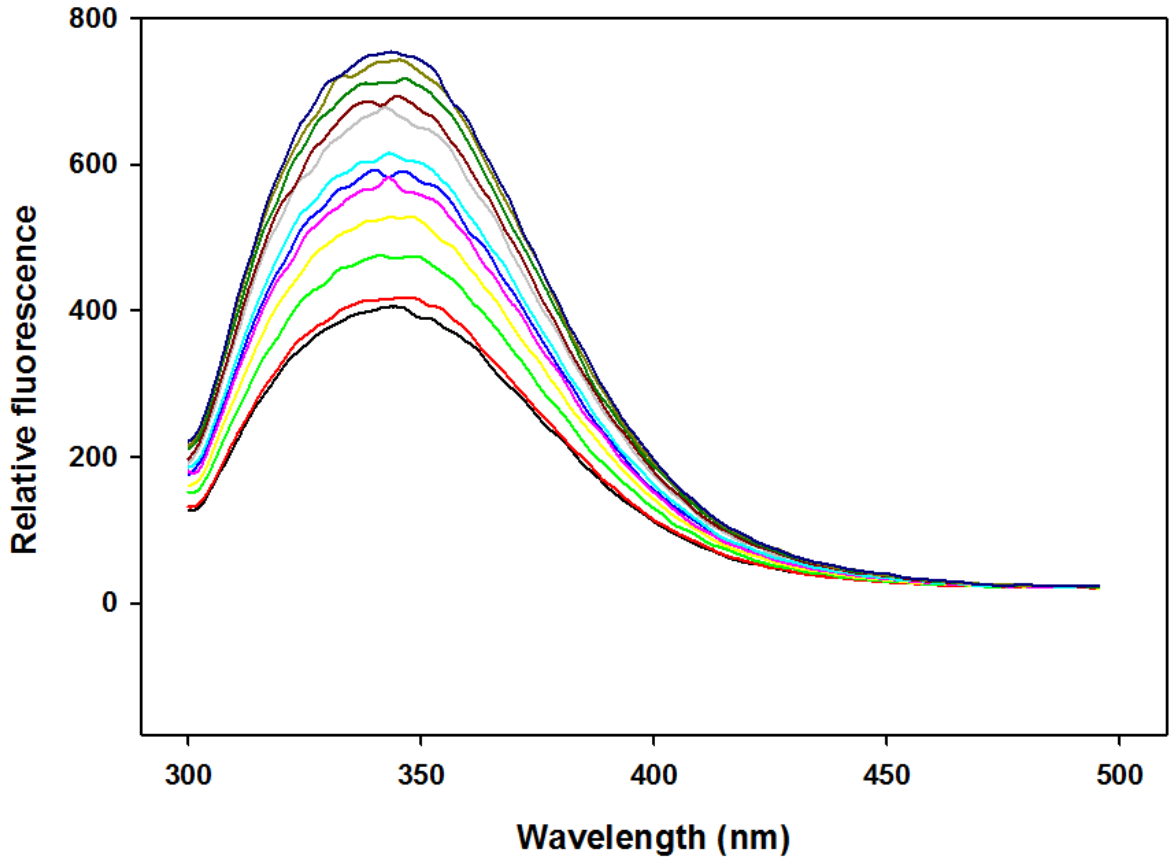

Equal concentration of lactoferrin protein and AZT were incubated up to 60minutes. The flourscence was observed at an intervel of 5minutes up to 60minutes. After 55 to 60 minutes the flourscence intensity became saturated.

Figure 3.2 FE-SEM analysis of nanoparticles.

The blank lactoferrin nanoaprticles (lacto-nano) and AZT loaded lactoferrin nanoparticles were prepared using the protocol described in methods section. The nanoparticles were analysed using FE-SEM. The mean diamtere of Blank NP was found to be 27nm. The size of particle were increased upto 59nm after the loading of AZT.

Figure 3.2 FE-SEM analysis of nanoparticles.

A. Blank Nanoaprticles (Lacto-nano)

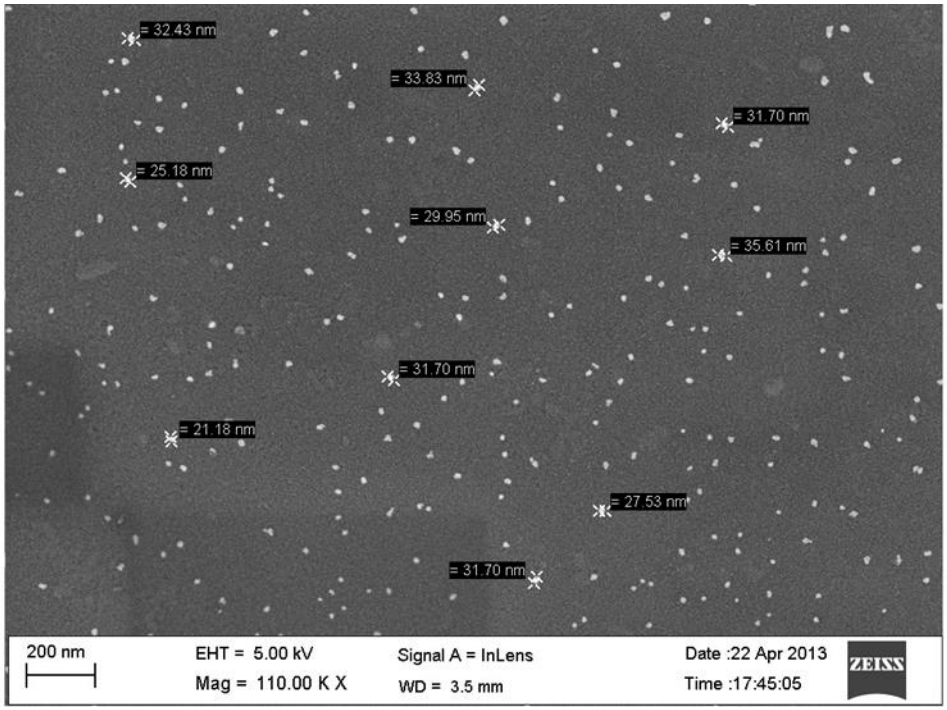

B. AZT nanoparticles (Lacto-AZT-nano)

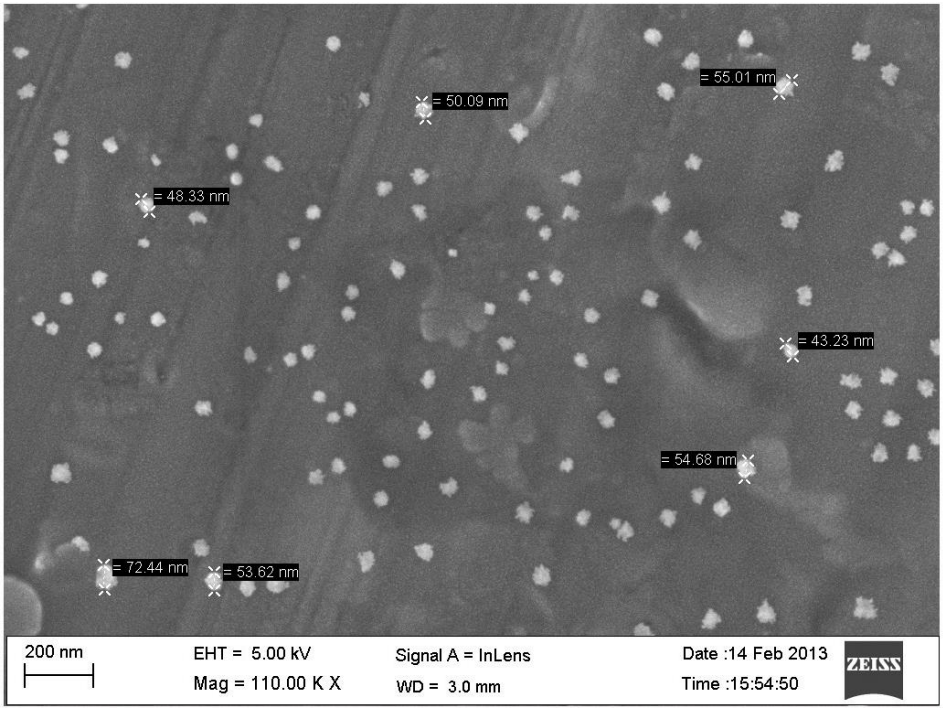

Figure 3.3 AFM analysis of nanoparticles.

A. Blank Nanoaprticles (Lacto-nano)

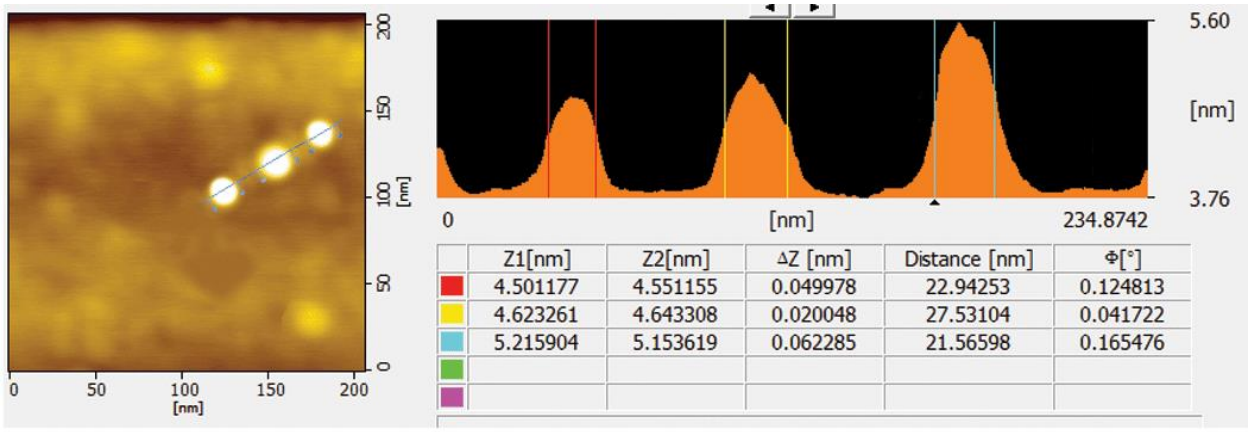

	Z1[nm]	Z2[nm]	ΔZ [nm]	Distance [nm]	Φ[°]
	4.501177	4.551155	0.049978	22.94253	0.124813
	4.623261	4.643308	0.020048	27.53104	0.041722
	5.215904	5.153619	0.062285	21.56598	0.165476

B. AZT nanoparticles (Lacto-AZT-nano)

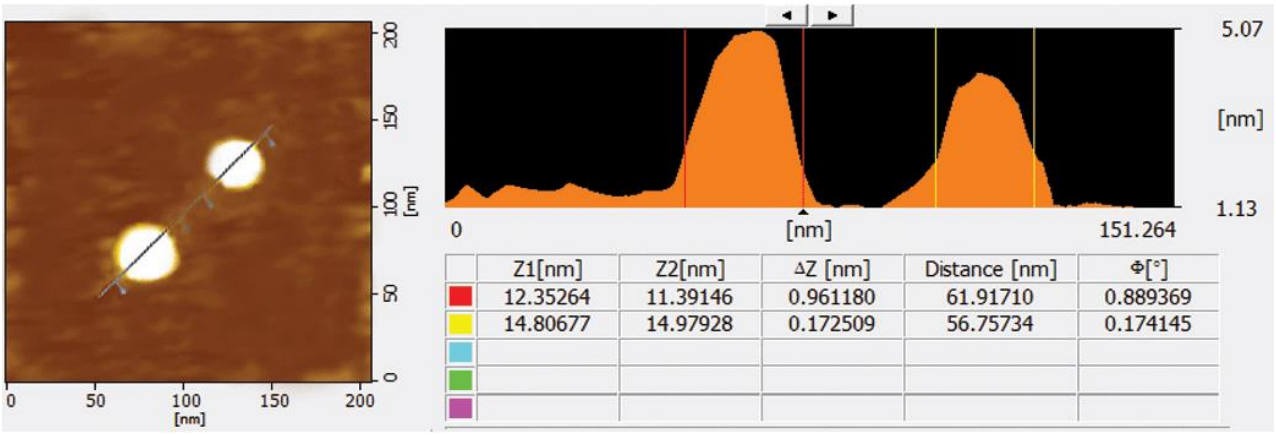

	Z1[nm]	Z2[nm]	ΔZ [nm]	Distance [nm]	Φ[°]
	12.35264	11.39146	0.961180	61.91710	0.889369
	14.80677	14.97928	0.172509	56.75734	0.174145

Blank lactoferrin nanoaprticles and AZT loaded lactoferrin nanoparticles were characterized using atomic force micrscopy. The average of blank nanoaprticles and AZT NP were found to be apprx 25nm. The average size for AZT nanoparticles was 61nm.

Figure 3.4 Dynamic Light Scattering analysis of nanoparticles.

A. Blank nanoparticles (Lacto-nano).

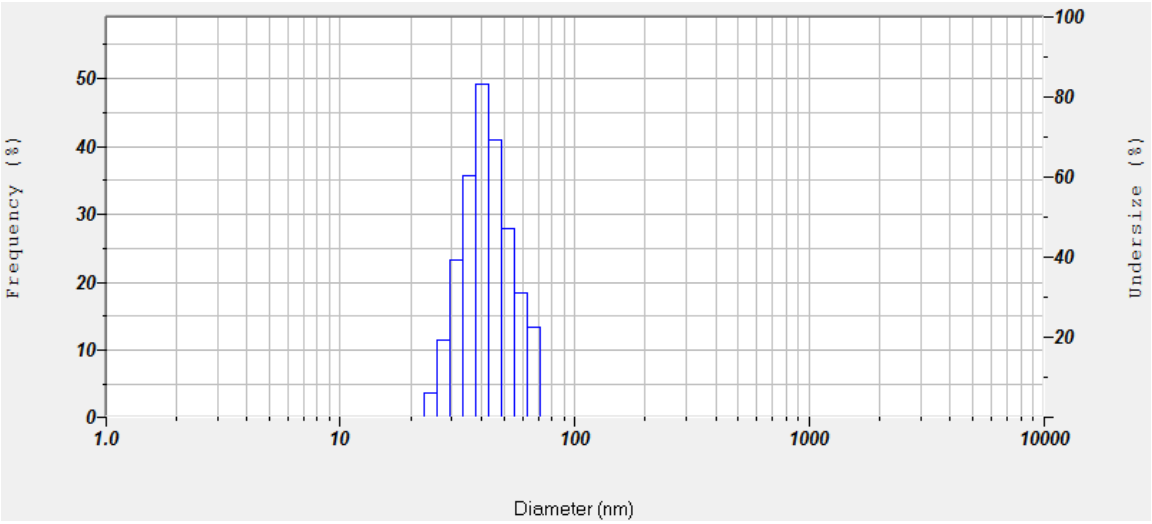

B. AZT nanoparticles (Lacto-AZT-nano).

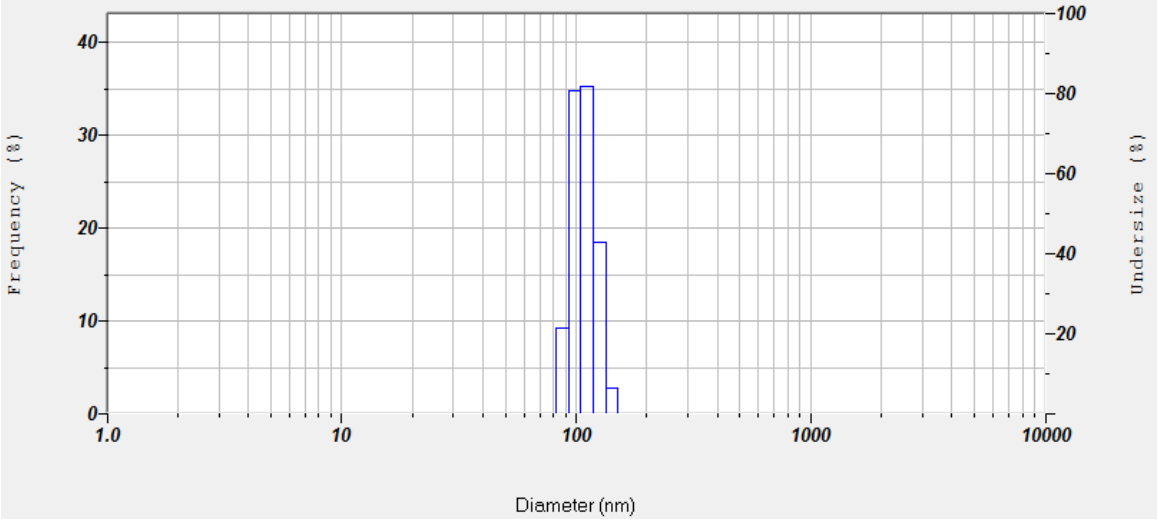

The Hydrodynamic radii was calculated using nanopartica nanoparticle analyzer, SZ-100 (Horiba Scientific). The mean size of Blank NP and AZT NP was found to be 54nm and 106nm respectively.

Figure 3.5 FT-IR spectra

A and B. FT-IR of sol Lacto and Lacto –nano

The FT-IR spectra of lactoferrin in soluble form and lactoferrin nanoparticles was presented here. The major functional groups such as, Amide I, Amide II and C-O-C was found to be intact in nanoformulaiton. Only little shift in the positions of band were observed.

The comparsion of major functional group in sol lactoferrin and Blank NP.

Functional groups	**Sol Lactoferrin**	**Blank NP**
Amide I (C=O)	1645 cm^{-1}	1648 cm^{-1}
Amide II (C-N stretching and N-H bending)	1542 & 3418 cm^{-1}	1539 & 3364 cm^{-1}
C-O-C	1096 cm^{-1}	1164 cm^{-1}

Figure 3.5A and B. FT-IR spectra.

A. Pure Lactoferrin.

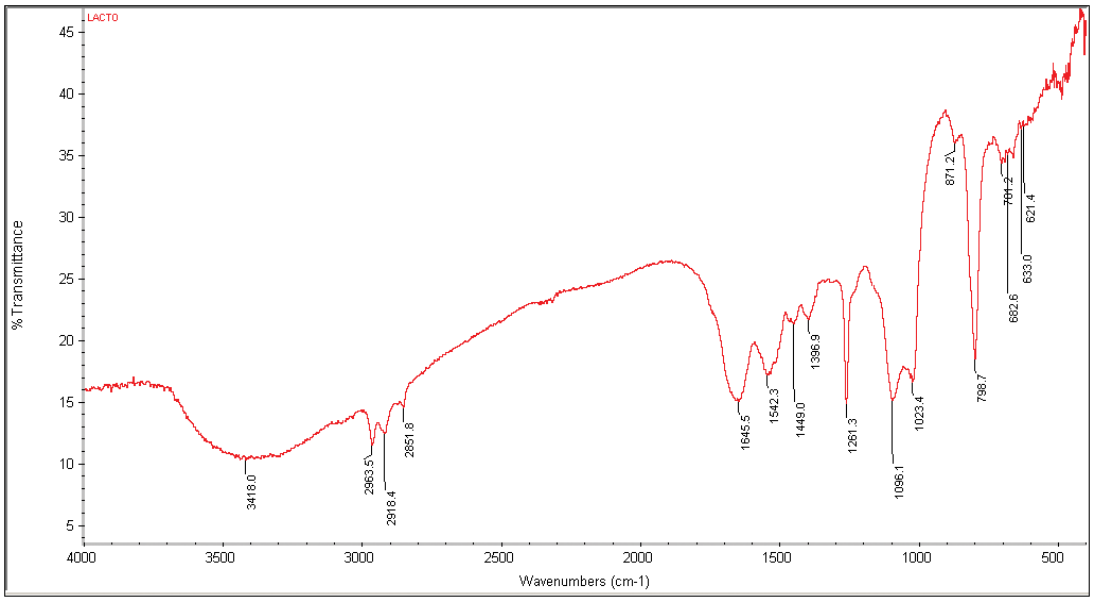

B. Blank nanoparticles (Lacto-nano)

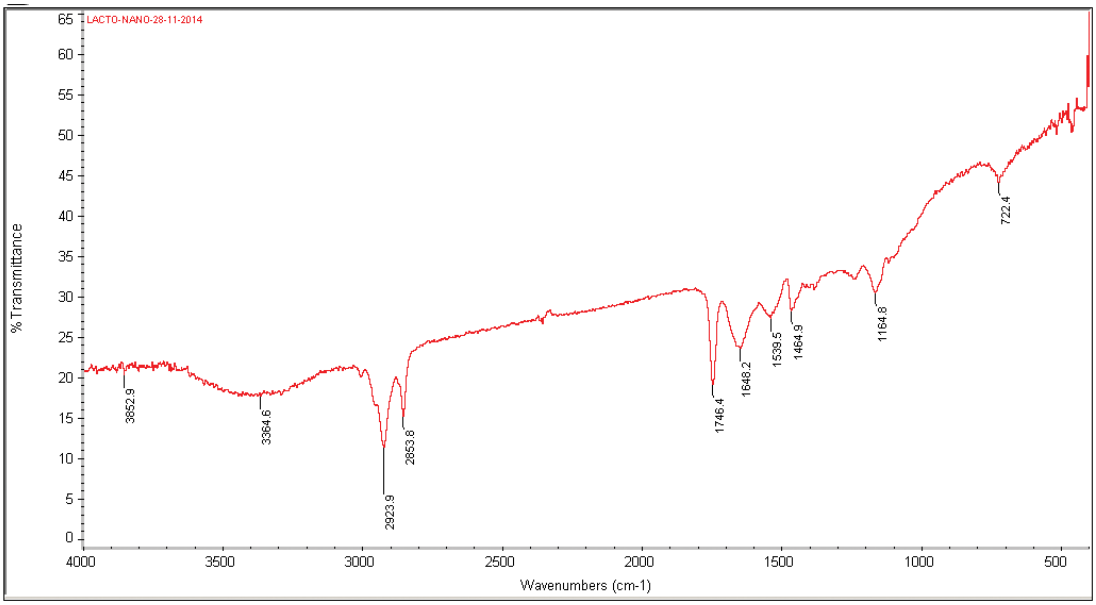

Figure 3.5 FT-IR spectra.

C and D. FT-IR of Sol AZT (Pure AZT) and AZT NP

Sol AZT and AZT NP were analyzed using FT-IR. The positond of featured functional grouops were analysed and presented below.

The comparsion of major functional group in sol AZT and AZT NP.

Functional groups	**Sol AZT**	**AZT NP**
carbonyl group (C=O)	1682 cm^{-1}	1685 cm^{-1}
Azide group ($N^{-}=N^{+}=N^{-}$)	2117 & 2083 cm^{-1}	2115 & 2082 cm^{-1}
C-O-C	1088 & 1065 cm^{-1}	1089 & 1065 cm^{-1}
-NH	3460 cm^{-1}	3461 cm^{-1}

Figure 3.5C and D. FT-IR spectra.

C. Pure AZT.

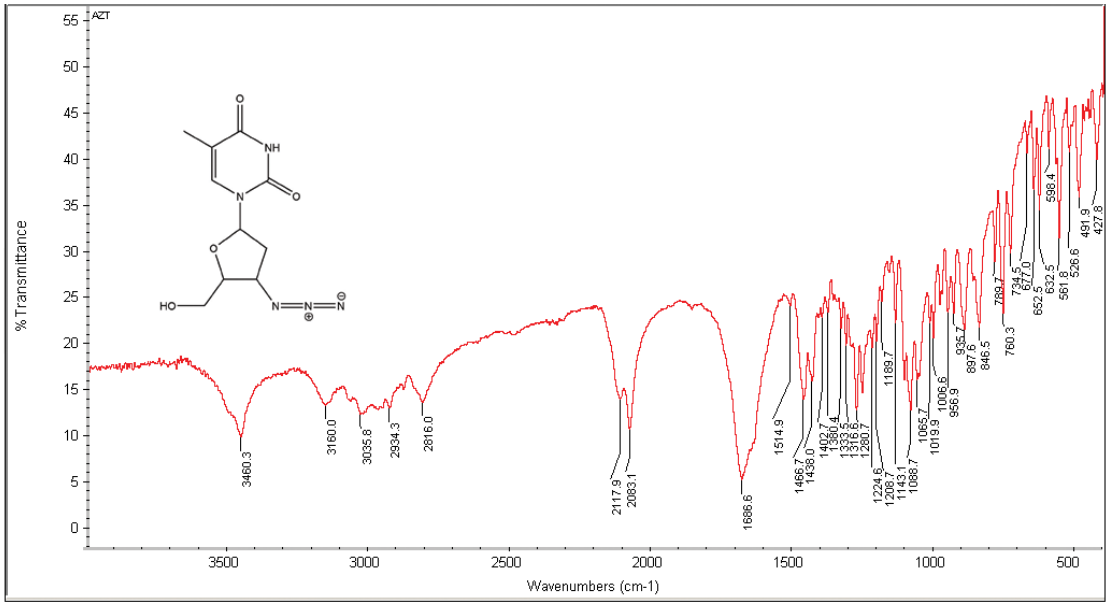

D. AZT nanoparticles (AZT-Lacto-nano).

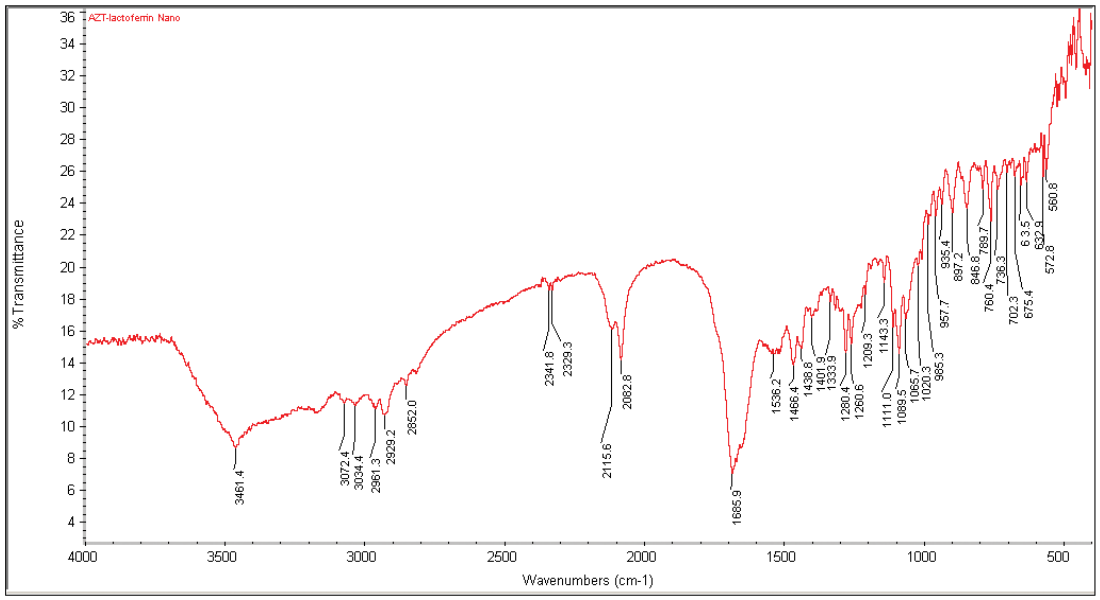

Figure 3.6 pH dependent release of nanoparticles.

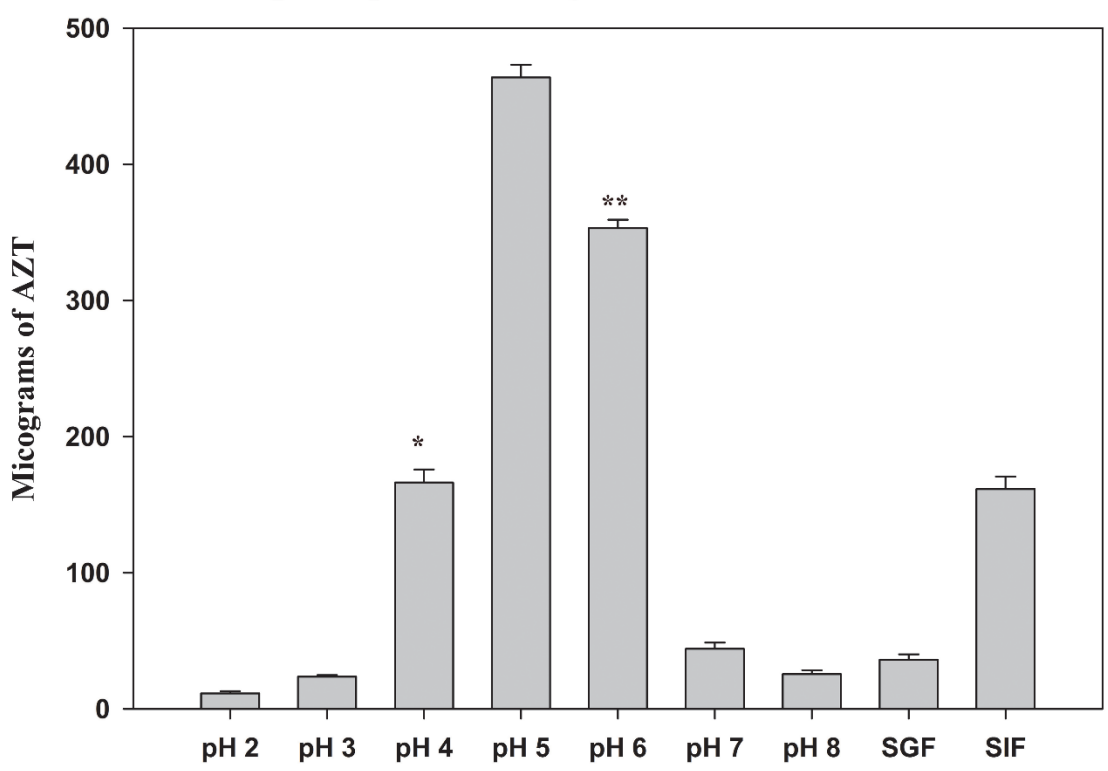

600µg of AZT loaded lactoferrin nanoparticles was incubated in the buffers of different pH (pH 2 to 8), SGF (Simulated Gastric Fluid) and SIF (Simulated Intestinal Fluid) for 12h. The maximum release of AZT was observed at pH5 followed by pH 6 and 4. <30% of drug release was observed at other pH condtion, SGF and SIF.

Figure 3.7 Percent release of drug from nanoparticles.

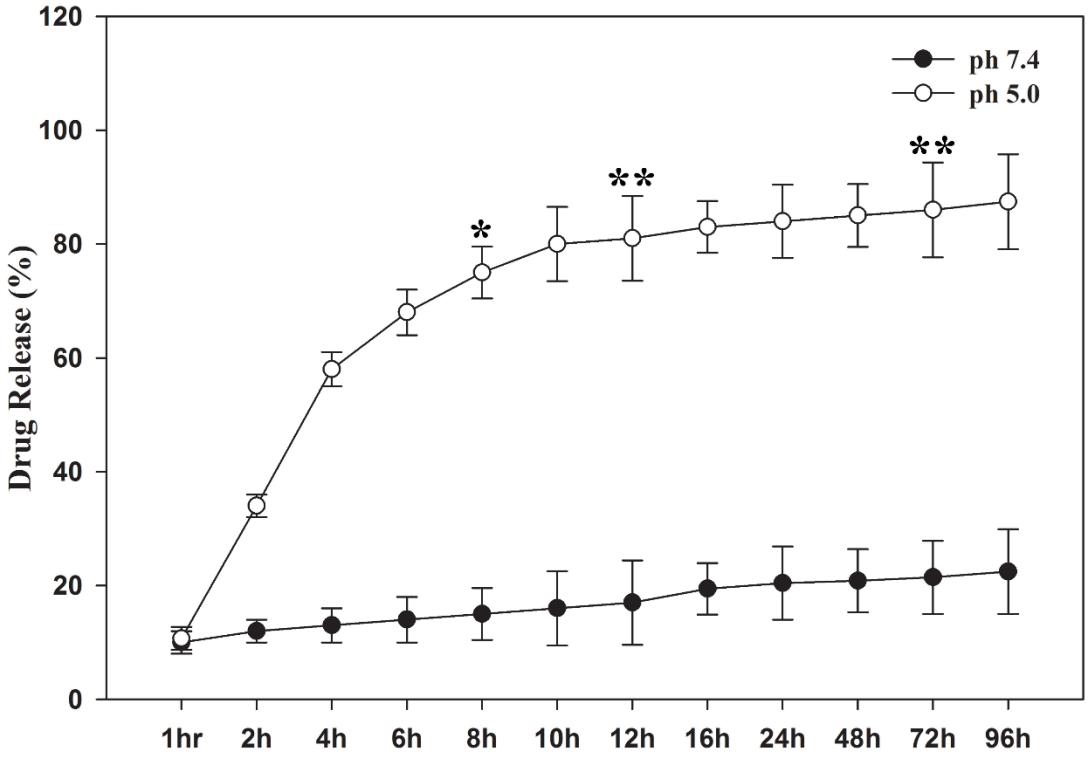

600µg of AZT nanoparticles were incubated with PBS of pH 7.4 and 5.0 with indicated time points. The cumulative percent release of drugs was calcualted and plotted. At pH5.0, the drug release was observed in bi-phasic manner; approx. 60% of drugs was reelased up to 4h followed by a constant release upto 96. At pH7.4, <20% of drug release was observed throughout the study period.

Figure 3.8 Antiviral assay.

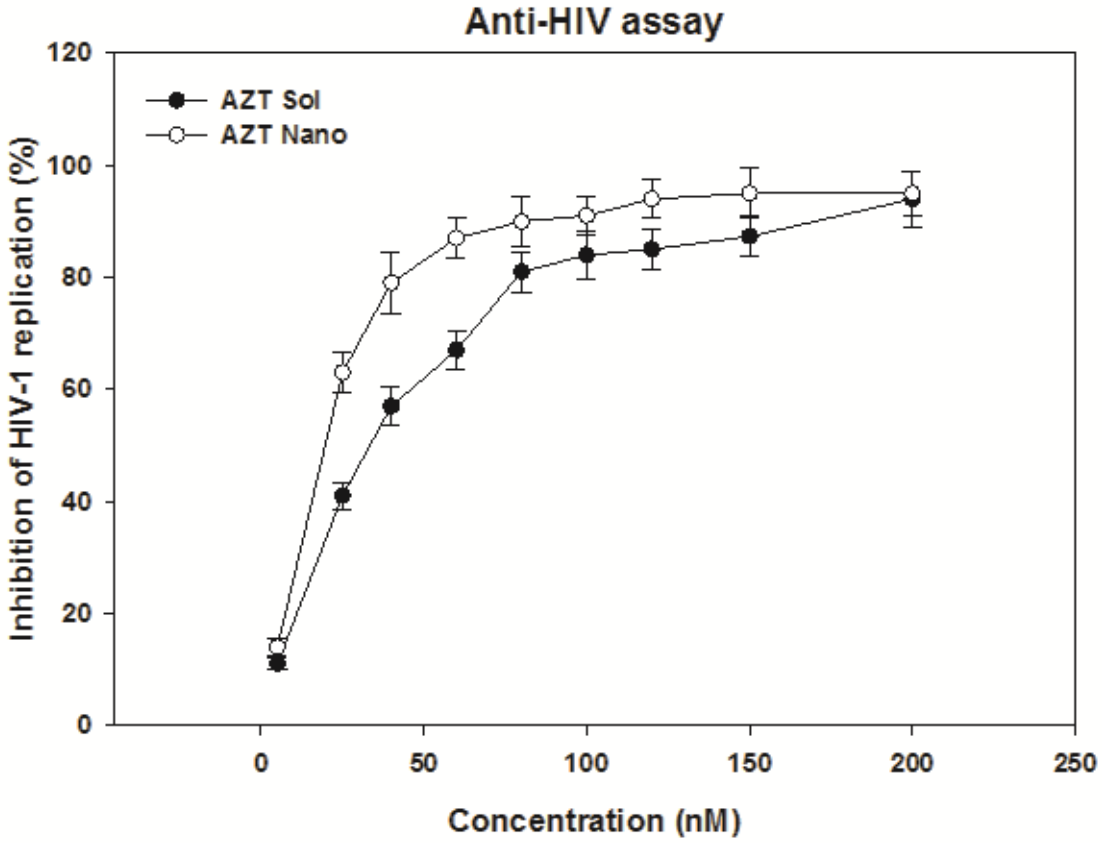

A dose dependent antiviral assay was performed using Sol AZT and AZT nano. Various increasing concentration of Sol AZT and AZT nano were used for the antiviral assay. Antiviral assay was perofmed according to the protocol mentioned in methods sections. The IC_{50} vlause for Sol AZT and AZT nano was found to be as follows.

	Sol IC_{50}	**Nano IC_{50}**
AZT	**33.4 nM**	**20.5 nM**

Figure 3.9 Antiviral assay.

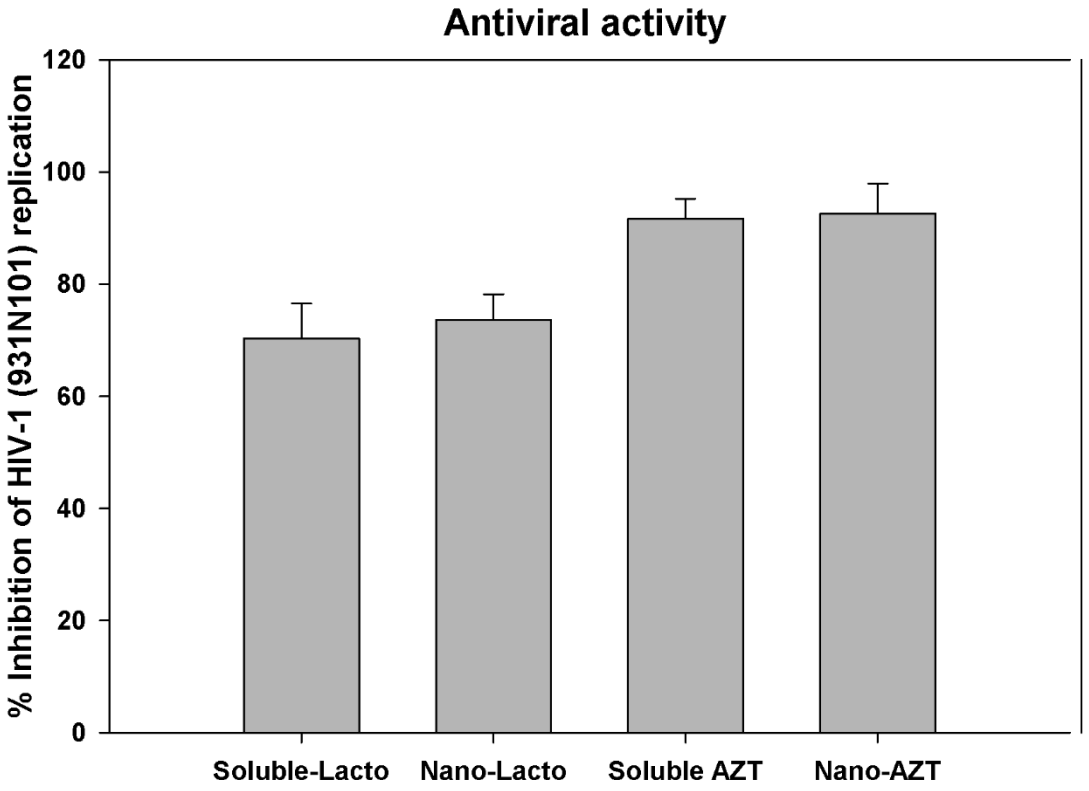

To evaluate the anti-HIV activity of AZT and Lactoferrin in the naoform, a fixed dose antiviral assay was conducted. AZT (1µg) and lactoferrin (80mg/ml) was used for the antiviral assay. Soluble and nano lactoferrin have showed 70 and 73% antiviral activity respectively. Further, the activity of AZT at one microgram concentration is similar to that of soluble AZT with more than 90% of inhibition of HIV-$1_{93IN101}$ replication in Sup-T1 cells. It suggests that activity of encapsulated AZT remain stable in nanoformulation.

Figure 3.10 A. Tissue distributin.

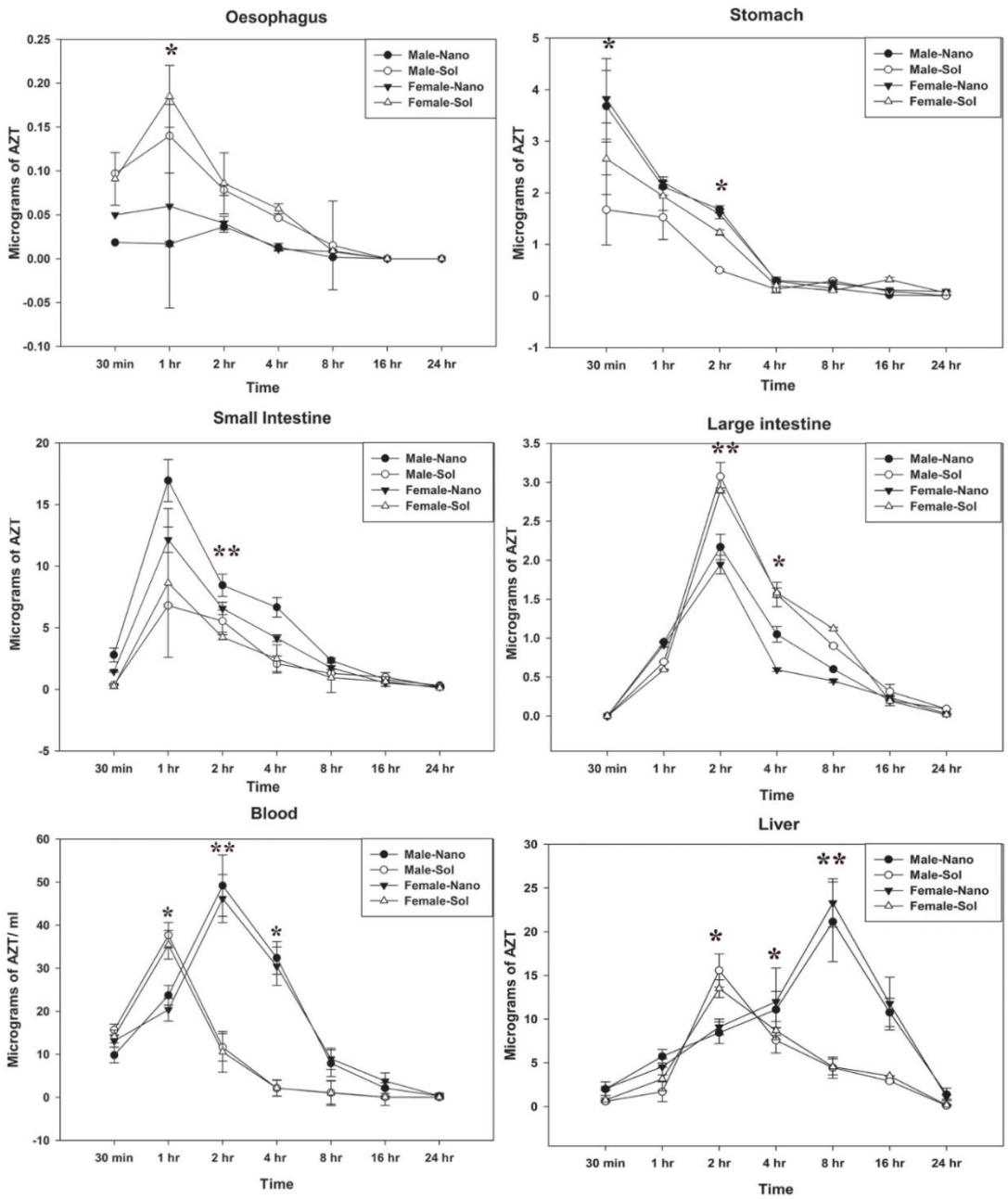

A fixed dose, 10mg/kg of soluble AZT and equivalent anount of AZT NP weas administered orally to the rats. After completion of tme points, major tissues were harvested and drugs was extracted. It was found that, after oral administration of drugs, the soluble form reaches to blood circulation early followed by a rapid decrease. On the other side the nanoformulation reaches to the circulation late and retains for the longer time, as indicated by improved half life in case of nano-formulation. Further, the GI absorption pattern for soluble and nano behave similarly in terms of kinetics.

Figure 3.10 B. Tissue distributin.

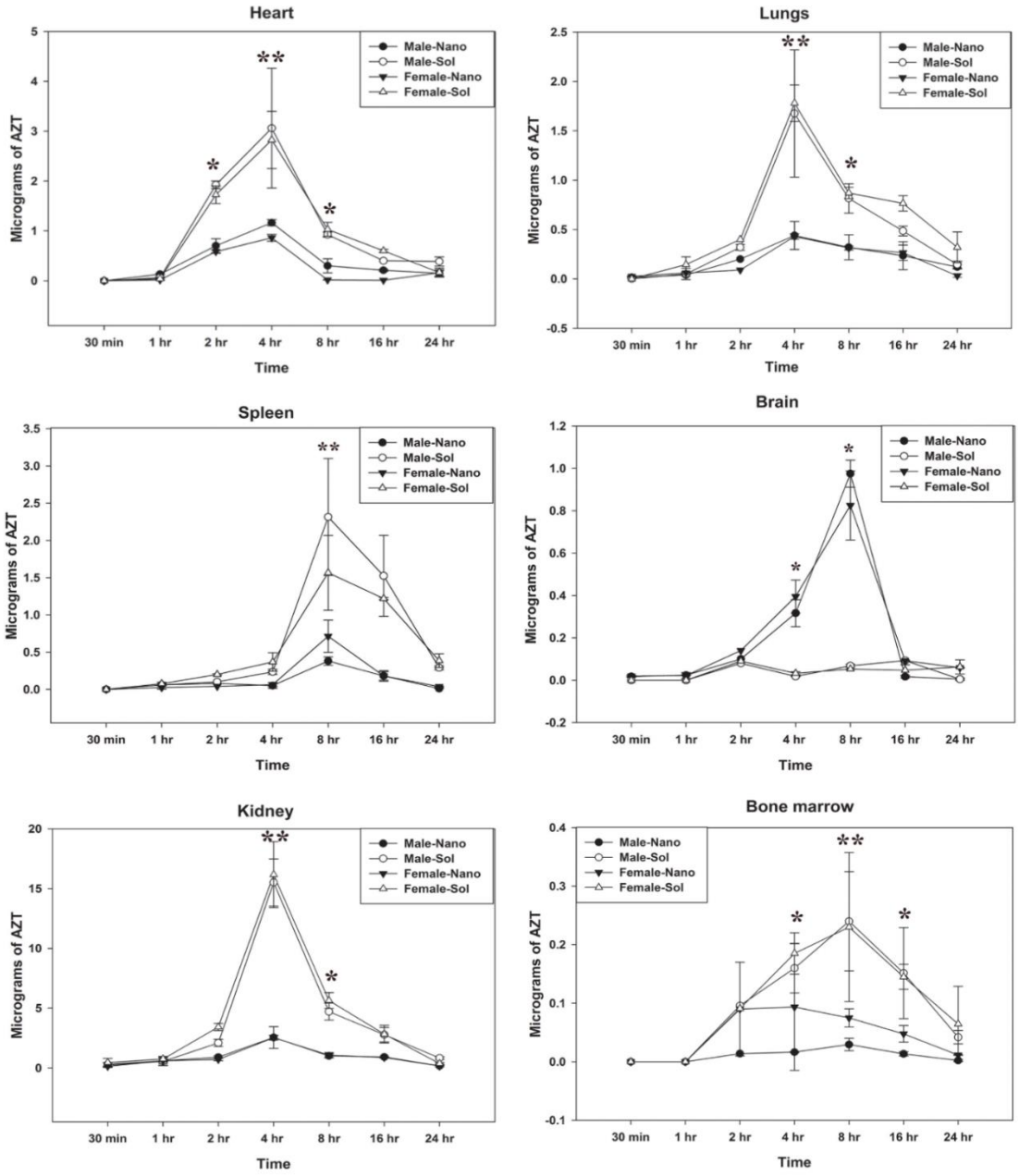

A fixed dose, 10mg/kg of soluble AZT and equivalent anount of AZT NP weas administered orally to the rats. After completion of tme points, major tissues were harvested and drugs was extracted. Result shows the distribution of druhgs in heart, lungs, speleen, brain, kidney and bone marrow. Kidney biodistribution shows the fast clearance of soluble AZT as compred to AZT NP. In bone marrow at 4h, 8h and 16h there were more accumulation of soluble AZT as caomrped to AZT NP, leads to bone marrow toxicity.

Figure 3.11 Safety analysis.

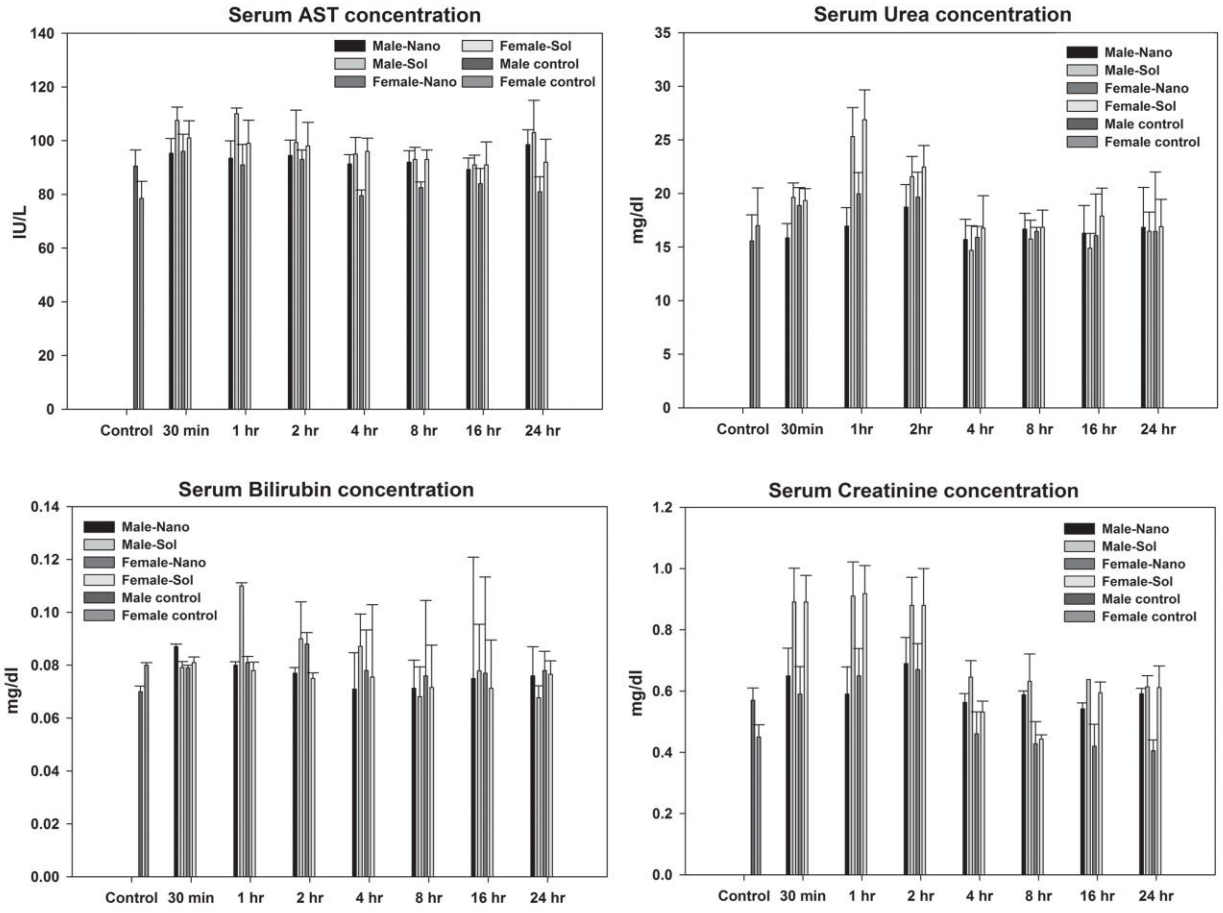

Biochemical safety analysis profile. Safety analysis was done using biochemical kits after oral administration of nano and soluble AZT (10mg/kg) in both male and female rats. Liver damage was estimated by Bilirubin and AST level whereas Kidney toxicity was checked by Urea and creatinine level. AZTlactonano showed no toxicity to both liver and kidneys on the other hand it exhibited minimal urea levels when compared to the soluble AZT.

Figure 3.12 A. Histopathological analysis of tissues.

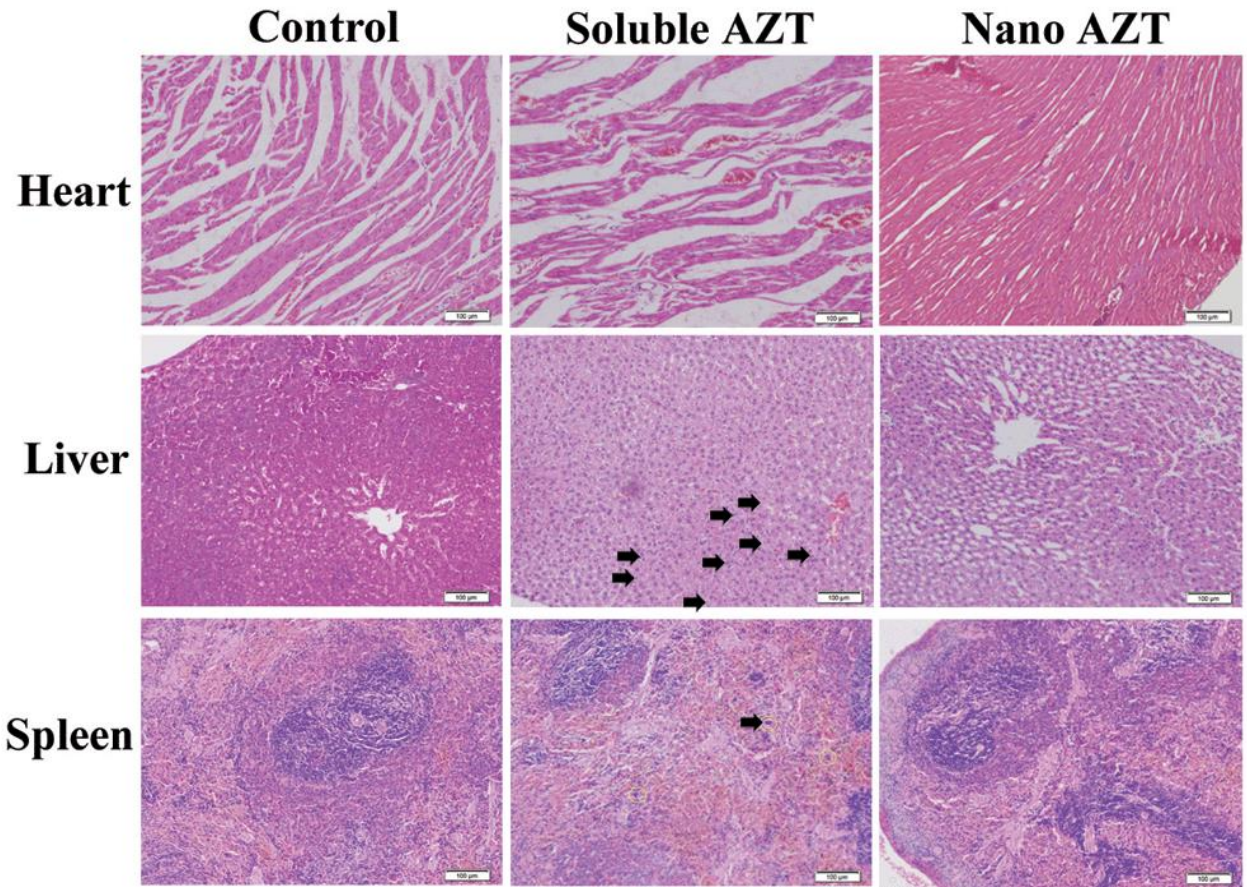

Rats were orally administered with sol AZT and AZTlactonano (10mg/kg body weight), after completion of 24hr time point, organs were removed and processed for cryo-sectioning followed by Hematoxylin and Eosin (H&E) staining. Liver and Spleen has shown some inflamamtion or leasion as indicated by printed arrow. Scale bar is equal to 100µm.

Figure 3.12 B. Hematoxylin and Eosin staining.

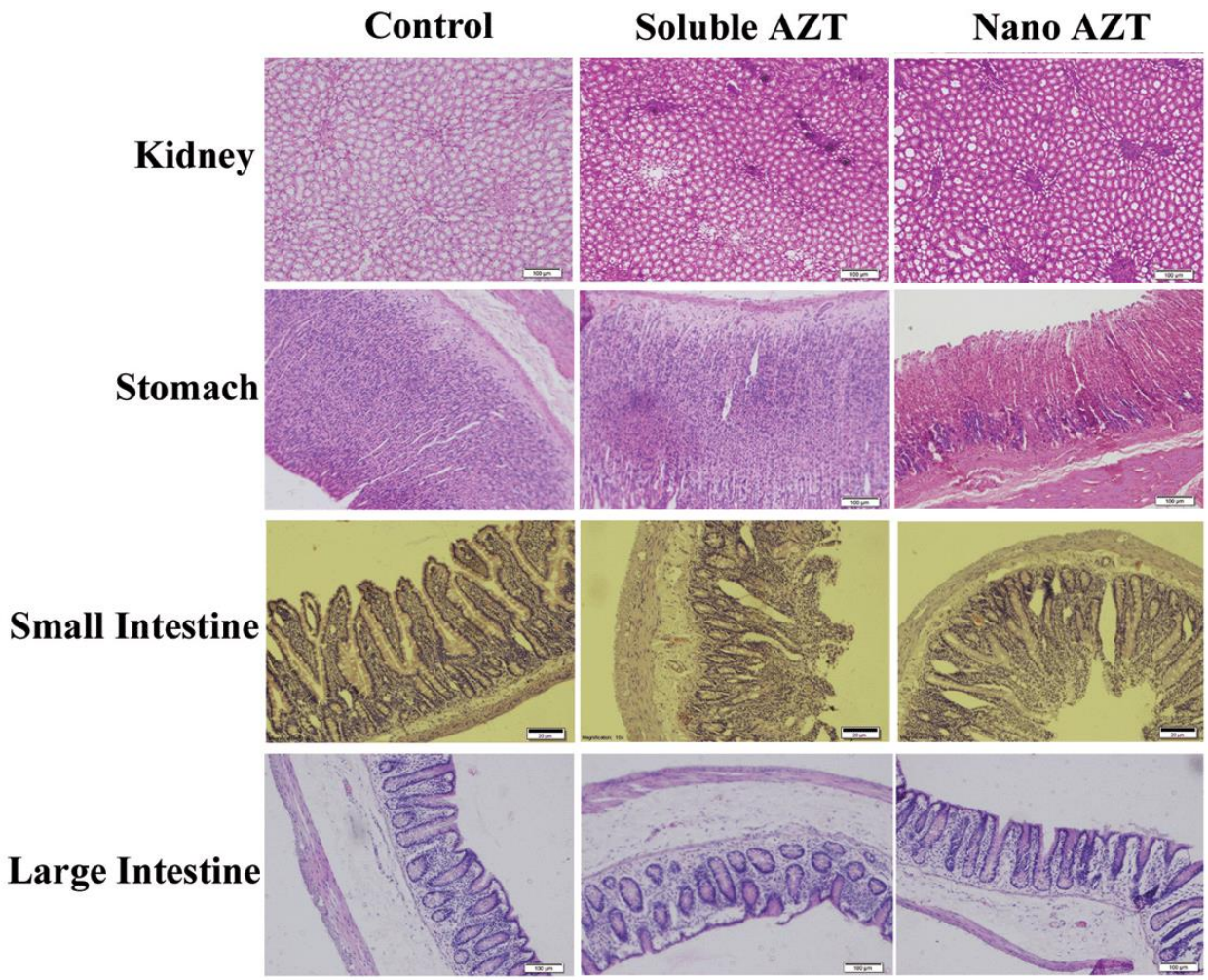

After oral administation of 10mg/kg of Sol AZT and Nano AZT, H & E staining were done for kidney, stomach, small intestine and large intestine. All the above mentioned oragns didn't show any inflamattion. Scale bar is equal to 100µm.

Figure 3.13 Bone marrow micronucleus Assay

A. Bone marrow smear

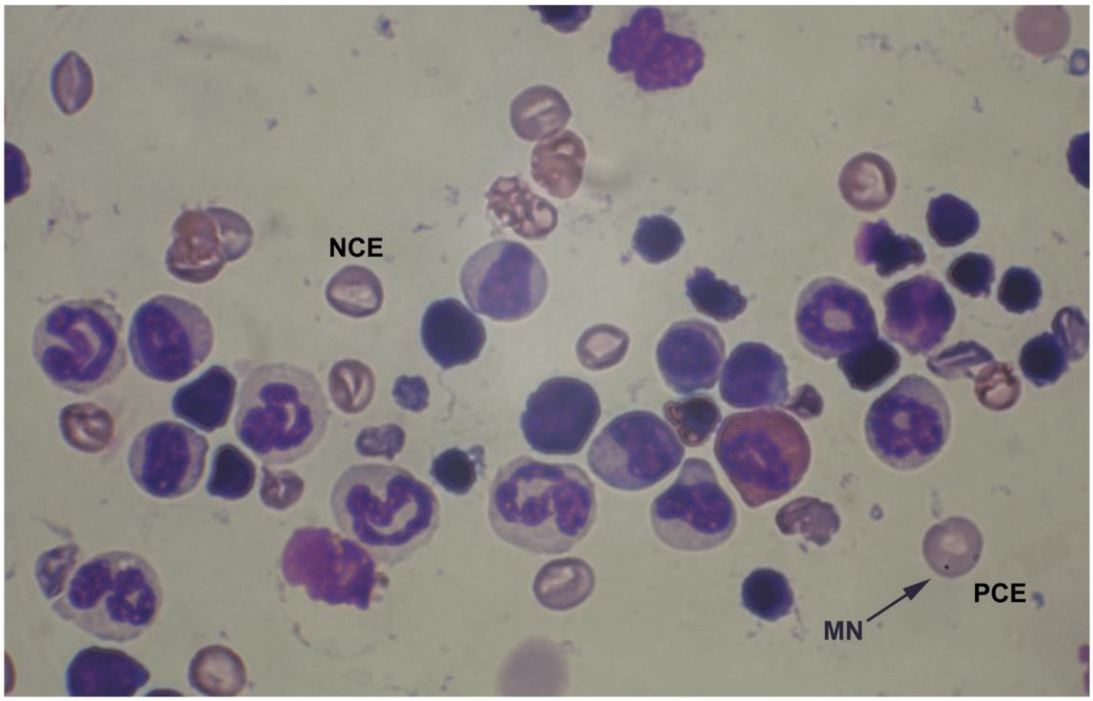

Bone marrow cells (after 8h of treatment) showing the presence of enucleated Normochromatic erythrocyte (NCE) and nucleated polychromatic erythrocyte (PCE) cells. One PCE holds a micronucleus (MN); indicated by arrow. This images was captured at 100x under oil immersion objective.

Figure. 3. 13 Bone marrow micronucleus Assay

B. Statistics of PCE in bone marrow.

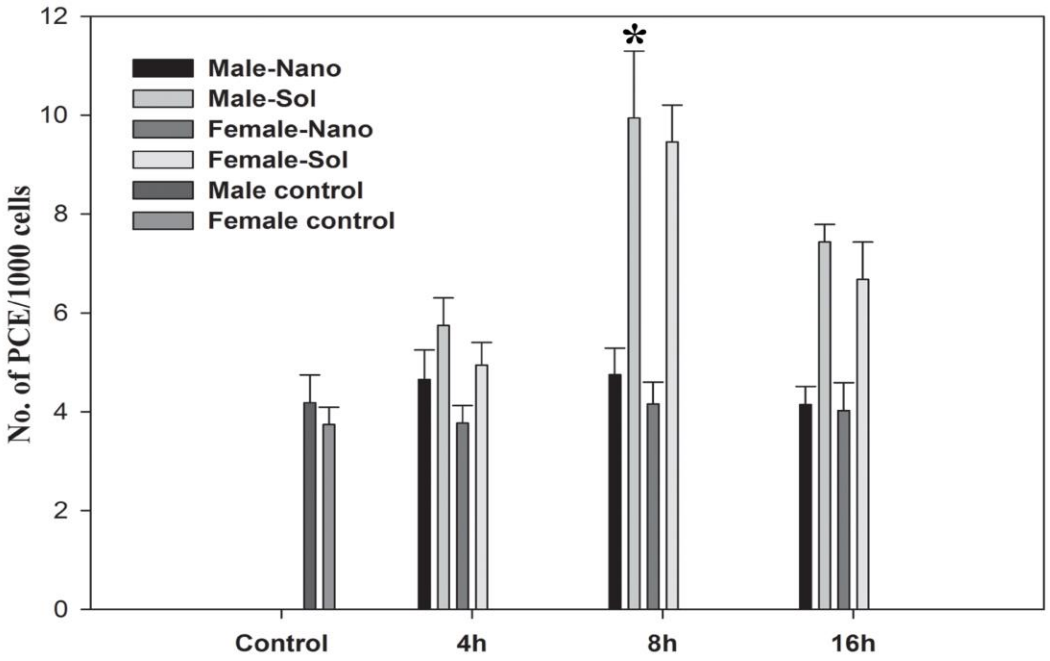

It shows the frequency of polychromatic erythrocyte (PCE) in bone marrow cells after oral administration of sol AZT and AZT-lactonano at 4, 8 and 16h. Data were presented as Mean ± SD. Value of significance, **P < 0.005, *P < 0.05.

Table 3.1: *In vitro* stability of nanoparticles

Hours	Diameter of the nanoparticles (nm)		AZT present in mg (%) #	
	4°C	Room temp*	4°C	Room temp*
0	55.67± 4.54	53.23± 3.56	6.75 ± 0.69 (100.00)	6.71 ± 0.19 (100.00)
1	54.5 ± 4.30	54.5 ± 2.68	6.49 ± 0.96 (96.15)	6.57 ± 0.82 (97.91)
2	58.6 ± 3.36	59.7 ± 5.13	6.68 ± 0.85 (98.96)	6.66 ± 0.28 (99.25)
4	53.1 ± 4.19	53.6 ± 4.35	6.71 ± 0.52 (99.41)	6.47 ± 0.18 (96.42)
6	52.3 ± 3.63	55.5 ± 4.72	6.58 ± 0.78 (97.48)	6.53 ± 0.36 (97.31)
8	54.7 ± 4.73	57.6 ± 3.81	6.37 ± 0.67 (94.37)	6.54 ± 0.49 (97.46)
10	58.3 ± 6.63	58.7 ± 4.34	6.66 ± 0.78 (98.66)	6.30 ± 0.84 (93.89)
12	53.6 ± 5.13	56.8 ± 3.92	6.48 ± 0.82 (96.00)	6.52 ± 0.92 (97.16)
16	60.2 ± 5.39	54.1 ± 4.77	6.52 ± 0.19 (96.59)	6.50 ± 0.14 (96.87)
24	58.7 ± 4.73	59.4 ± 4.65	6.64 ± 0.35 (98.37)	6.68 ± 0.49 (99.55)
48	55.6 ± 4.73	57.1 ± 2.91	6.51 ± 0.73 (96.44)	6.63 ± 0.19 (98.81)
72	56.7± 5.94	56.7 ± 2.65	6.54 ± 0.37 (96.88)	6.58 ± 0.27 (98.06)
96	60.8 ± 5.76	58.4 ± 4.39	6.65 ± 0.39 (98.52)	6.35 ± 0.38 (94.63)

All the data (n=3) were presented as mean ± standard deviation.

Drug present in the particles was estimated by using HPLC, in milligrams. The amount of drug present initially at zero hour at 4°C and room temperature are considered as 100% drug present.

* Room temperature: The temperature used here was an average equal to 23°C.

Tables 3.2: Pharmacokinetics profile of AZT-lactonano in male and female rats.

Parameters		Male		Female	
		Nano	Soluble	Nano	Soluble
AUC	(h)*(µg/ml)	251.57	63.48	254.974	58.74
AUMC	(h)^2*(µg/ml)	1270.3	139.73	1485.24	126.737
C_{max}	µg/mL	49.198	37.67	46.17	35.45
T_{max}	Hours	2	1	2	1
$t_{1/2}$	Hours	3.07	1.759	3.27	1.92

Values in the parenthesis designates the concentration of AZT in micrograms per ml of blood.

Pharmacokinetic parameters.

AUC: The integral of the concentration-time curve (after a single dose or in steady state).

AUMC: Partial area under the moment curve between t start and t end.

C_{max}: The peak plasma concentration of a drug after oral administration.

T_{max}: Time to reach C_{max}.

$t_{1/2}$: The time required for the concentration of the drug to reach half of its original value.

Chapter 4

Development and characterization of Efavirenz loaded lactoferrin nanoparticles as oral formulation.

Introduction

According to current epidemiological data sheet, approximately 35 million of World's population are living with Human immunodeficiency virus/ Acquired immune deficiency syndrome (HIV/AIDS) [104]. Progression to AIDS is done primarily on the basis of a low CD4 count, which may finally leads to immunological failure [105, 106]. Food and Drug Administration (FDA), USA has approved six classes of drugs for the treatment of HIV infection and these are (I) non–nucleoside reverse transcriptase inhibitors (NNRTIs), (II) nucleoside-analog reverse transcriptase inhibitors (NRTIs), (III) integrase inhibitors, (IV) protease inhibitors (PIs), (V) fusion inhibitors, and (VI) co-receptor antagonists [13]. Treatment for AIDS started with mono-drug therapy during late nineties, which has subsequently shifted to combination therapy with double drug and then currently to triple drug combination therapy. The triple drug combination HAART therapy includes two NRTI plus one NNRTI [13, 107, 108]. Efavirenz (EFV) is highly lipophilic [109] having very poor aqueous solubility (8.3μg/mL) [110]. It is a very commonly prescribed combination drug in the first line antiretroviral regimen for AIDS treatment [111]. EFV exhibits having very high plasma protein binding (more than 99 %) [112], that results in very low bioavailability (log P = 5.4, 40-45%), thus requiring administration of very high dose [113]. The pharmacological activity of drug is mainly dependent on unbound fraction of drug in the blood plasma. For improving the pharmacokinetic behavior of poor bioavailable drugs, various attempts have been made to deploy nanotechnology based delivery systems using nanoparticles and nano-suspension [113-115]. Amongst these nanoparticles based system is one of the most promising drug delivery systems [89]. To deliver the drug in controlled and sustained manner at the site of action and to maintain the desired therapeutic concentration for long time, various biodegradable polymers have been used as nano carriers. Our study is concerned with the development of a lactoferrin based nano delivery system. Lactoferrin (Lf) is an iron binding protein present in external secretions such as tears, nasal fluid, saliva, pancreatic, gastro intestinal, urine and reproductive tissue secretions [116-118]. It is a biodegradable multifunctional protein having various properties such as anti-inflammatory, virucidal and anti-microbial. These properties make it an efficient and safe drug delivery system as compared to systems based on other

molecules [117]. Moreover it is easily available, cost effective and is an ideal material for the development of nanoparticles.

Thus, the present study aims at developing a highly stable lactoferrin based oral nano formulation for delivery of efavirenz with sustained optimum release of drug along with reduced toxicity, improved pharmacological properties and anti-HIV activity.

Results

Nanoparticles preparation

Drug protein saturation studies: Our results of drug protein saturation studies have shown that EFV molecules (1μM) have fluorescence and with the increasing time, fluorescence intensity concentrations were increased till 1hr with 5mins interval gap. After 1hr, the fluorescence intensity was not changed. It suggest that, 1hr incubation period is sufficient for drug loading onto the protein while preparing nanoparticles (Fig. 4.1).

Estimation of Encapsulation efficiency of nanoparticles: Encapsulation efficiency (EE) of Lacto-EFV-nano was estimated in five different protein concentrations, while keeping the concentration of drug constant. The EE for different combination ratio has been shown in Table 4.1. The results presented in Table 1 show that the Encapsulation Efficiency was maximum in loading of drug in formulation code F3 (59 ± 1.3) at 1:3 molar ratio of EFV and Lf. Hence drug and protein ratio as per F3 has been used throughout the study until otherwise stated

Characterizations of nanoparticles

Field Emission – Scanning Electron Microscope analysis of EFV NP: Freshly prepared nanoparticles (lacto-nano or Blank NP and Lacto-EFV-nano or EFV NP) were

analyzed using FE-SEM (Fig. 4.2). The diameter or blank and drug loaded NP were found to be approximately 19-35nm and 45-60nm respectively.

Atomic Force Microscope analysis of EFV NP: The 3D characterization of nanoparticles were performed using AFM (Fig. 4.3). A mean diameter of approximately 29nm were found for blank NP i.e. without loading of any drug. The EFV loaded Lf NP bears a diameter size of approximately 63nm with surface projections.

Size distribution, PDI and zeta potential of NP

DLS analysis of nanoparticles: The nanoparticles were analyzed using dynamic light scattering. The suspension form of nanoparticles were analyzed for size distribution and colloidal study. DLS results (Fig. 4.4) shows the size distribution of blank and drug loaded NP. The hydrodynamic radii of blank and drug loaded NP was found to be 72±3.4nm and 103±5.3nm respectively. The size measured by DLS was found to be apparently larger than the size measured using FE-SEM. The larger size was caused by water shell present around the NP. A negative Zeta potential of -19mV was found on the Lacto-EFV-nano (Fig. 4.5). The polydispersity index of Lacto-EFV-nano was found to be less than 0.341.

FT-IR Analysis of EFV NP: The surface modification, if any was analyzed using FT-IR study. The FT-IR spectra of sol EFV and lacto-EFV-nano were performed and shown in Fig. 4.6. The comparative evaluation between sol EFV and Lacto-nano-EFV are as follows. The first value (in cm^{-1}) corresponds to sol EFV and later to lacto-nano-EFV. The peak of C-O at 1073.9/1092.6, C=O band at 1749.49/1746.5, N-H strong stretch at 3316.8/3320.3, C-F at 1385.5/1378.6, CH_2 at 1216. 8/1238.7 and the featured alkyne band at 2250.01/2268.8. Data shows that major peaks remain conserved, only slight shift in some band were observed that may be due to dipole moment of bond as the interaction between drug and protein may be electrostatic.

Differential Scanning Calorimetry studies: Differential scanning calorimetry (DSC) of pure EFV and Lacto-EFV-nano was performed. Fig. 4.7 corresponds to the thermogram of Pure EFV in which a sharp endothermic peak was obtained at approximately 138˚C (melting of efavirenz). Degradation of efavirenz was found at or above 260˚C but in case of

lacto-EFV-nano the above mentioned degradation peak was completely absent. There was slight change in the endothermic peak related to Lacto-EFV-nano when compared with pure efavirenz. Very negligible peak broadening was found at approximately 139◦C in case of Lacto-EFV-nano. DSC study concludes that there was no complex formation or interaction between the drug and protein, as the endothermic peak in both the cases remained unchanged. Thus, drug may be physically associated with the protein with no chemical interaction.

pH dependent *in vitro* drug release of EFV-lacto-nano

The results of *in vitro* drug release experiment showed that, at pH-5 highest drug release was observed, which followed by pH 4 & 6 (Fig. 4.8). It was observed that very less approximately <25% was released in case of simulated gastric fluid and simulated intestinal fluid. It indicates that drug loaded nanoparticles were stable and intact while transported through GI environment. Thus suggesting intact nanoparticle are absorbed in oral route.

Cellular drug localization kinetics of EFV-lacto-nano

Analysis of cellular uptake of Lacto-EFV-nano shows a bi-phasic localization of drug with significant increase from 0.5h to 4.5h linearly followed constant release up to 12h, then a vertical drop up to 12h (Fig. 4.9). While sol EFV uptake was increased up to 2h followed by steady decline up to 12h. Thus, Lacto-EFV-nano exhibit two-fold longer and 1.6 fold higher cellular localization of drug compared to soluble form.

***In vitro* Stability of nanoparticles**

All NP was evaluated up to four month for different physical measurements. There were no significant changes were found in all the parameters (Table 4.2).

Anti-HIV-1 activity of nanoparticles

Anti-HIV-1 activity of sol EFV and Lacto-EFV-nano was evaluated in SUPT1 cells infected with HIV-1_{NL4-3} (Fig. 4.10 A). The increasing concentrations of sol EFV and Lacto-EFV-nano

were added separately. The p24 level at a different concentrations of drug was measured and presented as % inhibition of HIV-1 replication. The Lacto-EFV-nano showed a dose-dependent activity in inhibition of HIV-1 replication with 50% inhibitory concentration (IC50) of 1.1nM, while that of soluble EFV it was found to be 2.56nM. Furthermore, Lacto-EFV-nano showed improved-dose dependent profile. In addition, lactoferrin nanoparticle (without drug) also showed a dose-dependent anti-HIV-1 activity, with IC50 <4 μM. Thus suggesting that Lacto-EFV-nano exhibits anti-HIV-1 activity both due to EFV and lactoferrin. Thus this formulation works bi-directionally against HIV-1 infection in a dual mode of action. AZT was included as positive control (Fig.4.10 B).

MTT assay

Toxicity of efavirenz in soluble and nano form were studied in various cell lines. The results shows that efavirenz either in sol or nano form was non-toxic at very low concentrations (Fig. 4.11). In Jurkat cells, 50% growth inhibition (GI50) for sol efavirenz and nano efavirenz was found to be 27.3μm and 58.50μm respectively. In case of PHA-stimulated PBMC it was found to be 24.4μm (sol EFV) and 55.30μm (nano efavirenz). The GI50 in B16-F10 cells was found to be 57.4μm (Sol EFV) and 91.20μm (Lacto-EFV-nano). These results suggest that Lacto-EFV-nano possesses lower toxicity compared to soluble EFV.

Animal Study Design

Healthy male and female animals were used throughout the study period. the details of aimla study design is provided in the methods section. (Fig. 2.4).

***In vivo* studies**

Oral pharmacokinetics study

As described in study design, a single dose of Lacto-EFV-nano and soluble form of EFV (10mg/kg) were administered orally to rats. Rats were sacrificed at indicated time point under anesthesia and plasma was collected. Efavirenz was extracted by silver nitrate method and estimated using HPLC as described in method sections. Efavirenz delivered through Lacto-EFV-nano was found to have higher localization at 2 and 4h of post

administration as compared to sol form. All pharmacokinetic (PK) parameters were computed by Kinetica v 5.0 software are shown in Table 4.3. An improved PK profile in terms of 3-4 fold increase in plasma AUC and 6-7 fold increase in AUMC was observed in Lacto-EFV-nano treated rats. Further, Lacto-EFV-nano treated rats showed enhancement by 30% in C_{max} and 100% in T_{max} and $t_{1/2}$. These results suggest that, the nanoformulation provide higher bioavailability along with improved PK profile.

Tissue distribution

After administration of indicated dose; rats were sacrificed, all the organs were homogenized and quantified for the presence of drugs. Distribution of efavirenz, administered via sol or nano form has been estimated in various tissues and plotted against time (Fig. 4.12A & B). The gut tissue such as esophagus, stomach and small intestine shows higher localization of drug-loaded nanoparticles at the initial phase of administration. Maximum drug-loaded nanoparticle were observed at 1 hour in esophagus, then reaches stomach and small intestine at 2 hours and reaches large intestine at 4 hours. Thus suggesting that nanoparticle enters through esophagus followed by stomach, small intestine and large intestine. Further, results shows maximum localization of drugs (delivered via NP) at 2h in plasma and liver, while it was 4 hours to reach maximum concentration in kidney, spleen, bone marrow, brain, lungs and heart which deliberately gets cleared by 12h. Thus suggesting nanoparticles are first absorbed through liver, enter plasma followed by transport to other tissues. As compared from sol EFV, Lacto-EFV-nano offers significant localization of drugs in plasma. Further, concentrations of drug was 600ng in liver followed by plasma with ten-fold less concentrations in other tissues viz. lungs, brain, bone marrow, spleen, heart and kidney. In addition, nano form localizes less drug compared to soluble form in lungs, brain, bone marrow, spleen, heart and kidney.

.

Histopathology analysis

Tissue sections of Brain, heart, liver, spleen, kidney and G.I tract have shown that there were no toxicities in those tissues when Lacto-EFV-nano was administered (Fig 4.13A & B). Furthermore, Lacto-EFV-nano exhibit no drug-related toxicity in all tissue, while there

were some toxicity exhibited by soluble EFV as assessed by H & E staining images, which shows a minor damage (indicated by printed arrow) in liver or brain tissue.

Safety analysis of nanoformulation

The safety analysis of Lacto-EFV-nano was studied in rats, the results show no significant change in plasma AST and ALT in Lacto-EFV-nano compared to soluble EFV, plasma urea and creatinine levels were significantly low in both males and female rats, thus suggesting that Lacto-EFV-nano exhibits low kidney and liver toxicity. Lipid profile and LDH levels also maintained low in Lacto-EFV-nano than soluble EFV (Fig. 4.14).

Discussion

Efavirenz is a non-nucleoside reverse transcriptase inhibitor (NNRTI). It is used as a main component of highly active antiretroviral therapy (HAART) for HIV/AIDS treatment. Efavirenz is characterized by a partition coefficient of 5.3 in lipophilic solvents indicating its lipophilicity [119]. However as inferred from its restricted aqueous solubility, it has variable bioavailability. In the present study, we investigated the efficacy of Lacto-EFV-nano as a therapeutic agent for treatment of HIV/AIDS. Lacto-EFV-nano was prepared using sol-oil chemistry, which yield particles bearing an average size of 45-60nm with 59% encapsulation efficiency. Our NP preparation procedure is simple and fast, which does not cause any chemical modification either to the protein or to the drug. Our procedure has the advantage over other existing chitosan based NP, in that, the later uses glutaraldehyde during preparation that may affect the cell viability and chemical forms of the components [120]. A recent quantum dots based study [121] has shown that, for renal clearance, the cutoff particles size should be approximately 5.5nm, which means any particle having size less than 5.5nm may get excreted from kidney rapidly. Our NP is usually of larger size that causes slow renal clearance that facilitates extended blood circulation and enhanced therapeutics index [121]. The DLS based analysis of hydrodynamic size of blank-NP (72±3.4nm) and Lacto-EFV-nano (103±5.3nm) were found to be larger than their FE-SEM sizes. DLS measures the NP size in suspension form and in this case particles size could be affected by the interaction between water shell and NP surface charge, which leads to increase in the overall size. A negative surface charge of -23±1.2mV was found on the NP and exhibits its stability in the colloidal state. In addition, Lacto-EFV-nano possesses a PDI of <0.341, suggesting that the

particle population are homogenous in nature with a narrow particles size distribution. During Lacto-EFV-nano preparation, protein and drugs are incubated together. The presence of aromatic groups in protein such as tyrosine, phenylalanine and tryptophan are responsible for the fluorescence. Fluorescence was found increasing with increased loading of the drug in the protein and saturates in 60 min (Suppl. Fig. S1). FT-IR analysis of drug suggest that drug incorporated in the nanoparticles was intact, as reflected by the peaks related to major functional groups. Lacto-EFV-nano was found to be very stable even at higher temperature as shown by DSC thermogram (Suppl. Fig. S2). EFV NP is found to release the maximum of its payload at pH5; corresponding to endosomal pH. Exposure of Lacto-EFV-nano to the endosomal pH condition could lead to a change in the orientation of protein monomer, so that drugs present in the cavities of protein are released. In addition to this, Lacto-EFV-nano is found to be stable at gastric condition, whereas other oral formulation derived from chitosan NP disintegrates that may limit the drug delivery potential of formulation [122]. Further, approximately <10% of the drugs are released in circulatory pH (pH 7.4) condition, thus supporting the mechanism of receptor-mediated Lacto-EFV-nano entry followed by localization of Lacto-EFV-nano in endosomes. These results are consisted with our earlier studies on oral and intravenous delivery of doxorubicin and AZT though Apo-transferrin and Lactoferrin nanoparticles [33, 123]. Cellular drug kinetics data shows a sustained and long lasting release of drug from Lacto-EFV-nano Fig_). This property makes the Lacto-EFV-nano superior to other solid lipid NP which show much faster, burst like release (100% drugs in <5min) [124]. The concentration of soluble EFV attains its maximum at 2h followed by a constant decrease up to 12h. In our study we showed that Lacto-EFV-nano is at least 50% less toxic to a variety of cell lines; supported by in vitro cell toxicity data (Suppl. Fig. S3). Toxicity is one of the important factors to be considered and it has indeed been reported that EFV therapy was suspended due to its harsh skin-related toxicity [125]. Our results demonstrate that Lacto-EFV-nano is 1.5fold safer than sol EFV in the case of skin hypersensitivity. This may be seen from Suppl. Fig. S3, which shows that B16-F10 (skin epithelial cell line) possess a GI_{50} of 57.4µM and 91.2µM for Lacto-EFV-nano and sol EFV respectively (Suppl. Fig. S3). Lacto-EFV-nano with a 50% inhibitory concentration (IC_{50}=1.1nM) were found to be more effective as compared to its soluble form (IC_{50}=2.56nM) in blocking the HIV-1 replication (Fig. 3a). Lactoferrin blank-nanoparticles has been found to inhibit the 50% viral replication at a concentration of <4µM. Anti-HIV-1 activity of Lacto-EFV-

nano is a cumulative effect of activity due to EFV and Lactoferrin in nano forms. *In vivo* study was performed on rats belong to both the sexes, since PK study profoundly depends on the gender. The drug mechanism and its action also depend on various parameters such as body weight, hormonal status, cardiac output and body composition [126].Generally women experience more adverse events than men as per the reports of Food and Administration department [127]. The nanoformulation developed in our study has helped in achieving an overall improvement in the PK profile when given orally to the rats. A highly significant improvement of PK profile was observed in terms of AUC (4 fold) and AUMC (7 fold) in the case of nano form of drugs as compared to its soluble form both for male and female rats rats and this is also relatively better than that reported for other nanoformulation which showed improvement of AUC by only 2.2 fold [128]. A comparison of male versus female PK profiles showed that the peak values of plasma concentration (C_{max}) of Lacto-EFV-nano are higher in female rats (>47%) as compared to male rats (>28%). Further the drug exposure of Lacto-EFV-nano to the body is higher in female as compared to male, as seen from the relative increase in the AUC_{tot} value for females compared to males (female >4fold and male >3fold). Higher AUC_{tot} directly is related to the systematic bioavailability of the drug, hence facilitates reduction in the dose frequency to the patient. In addition to this, other PK parameters such as $AUMC_{tot}$, T_{max} and $t_{1/2}$ are also found to be significantly improved in nanoformulation treated rats. A 100% increment in T_{max} and $t_{1/2}$ have been found in NP-treated rats (female and male); suggesting slow and sustained release of drugs through Lacto-EFV-nano. In-spite of accumulation of more nano drug in the liver, less liver toxicity was observed as depicted in histopathology images. While earlier reports have demonstrated that efavirenz treatment leads to liver debilitation and neurocognitive reaction, such as anxiety [129]. Low hepatotoxicity of Lacto-EFV-nano could be due to protection of EFV by lactoferrin protein nanoshell, further drug may not be released in liver, this free is no available for conferring drug-related toxicity. The biochemical safety profiles of nano and Soluble EFV were compared and results show a significant difference in plasma AST and ALT between nano and soluble form in both male and female rats. Creatinine and blood urea nitrogen (BUN) showed significant increase ($p<0.001$) suggesting low kidney toxicity when nanoformulation was used (Suppl. Fig. S4). Further, the treatment of Lacto-EFV-nano did not show apparent differences in lipid profile of male and female rats. Any novel drug formulation could not be accomplished until it full fill the expectation related to stability at

various physical and environmental factors. The Lacto-EFV-nano, developed in the present study is found to be highly stable, effective and has an improved PK profile, as compared to the soluble form of EFV when administered orally.

Conclusion

The present study shows the applicability of protein based formulation in increasing the absorption of lipophilic drugs. In this study, stable EFV loaded lactoferrin nanoparticles were formulated using appropriate proportions of protein and drug. This formulation has shown optimally stable physicochemical parameters with higher bioavailability in terms values of value of $C_{max,}$ $t_{1/2}$ and AUC. Further, nano-form enhances anti-HIV-1 activity and decreases the toxicity due to EFV.

Figure 4.1 Drug (Efavirenz) – Protein Saturation study.

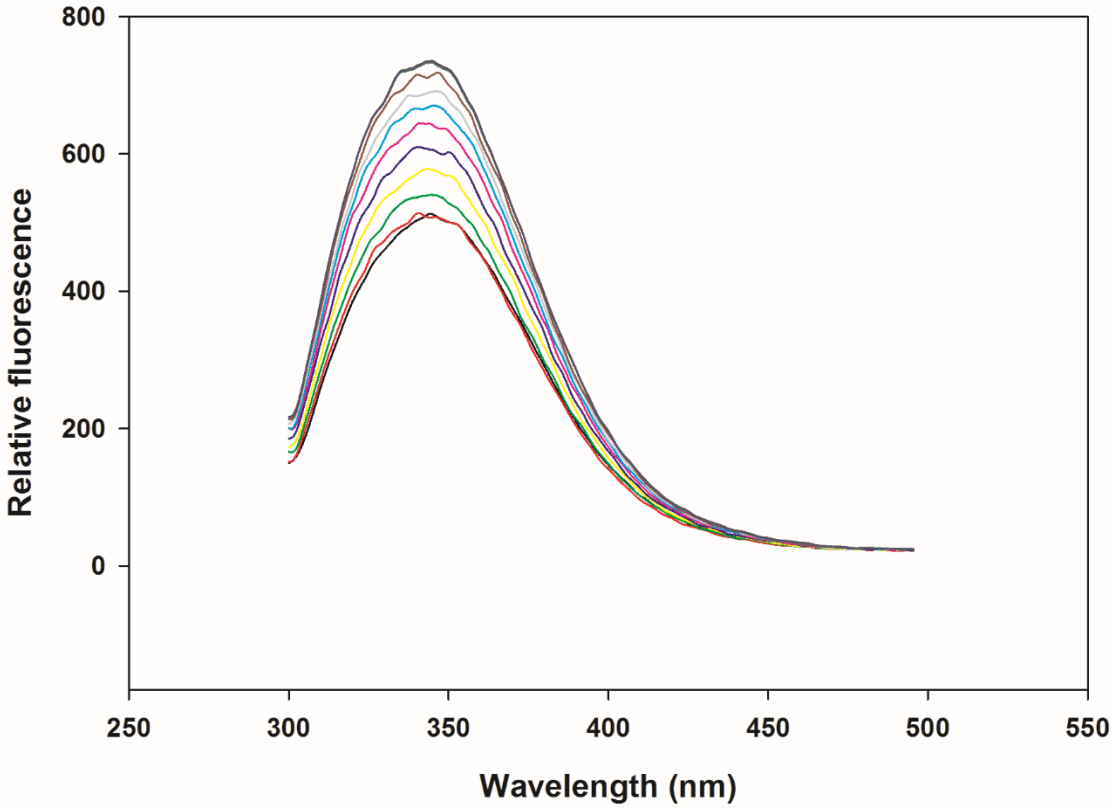

Protein (Lactoferrin) and drug (EFV) interaction saturation study. The equal molar concentration of lactoferrin and efavirenz were incubated at an interval of 5min up to 1h, before preparation of nanoparticles. Fluorescence emission spectra at room temperature were recorded using Perkin-Elmer LS55 fluorescence spectroscopy. For emission and excitation, the slit width was set to 5nm. Experiments were conducted in triplicate and similar spectra were obtained each time.

Figure 4.2 FE-SEM analysis of nanoparticles.

C. Blank Nanoaprticles (Lacto-nano). **B. EFV nanoparticles (Lacto-EFV-nano)**

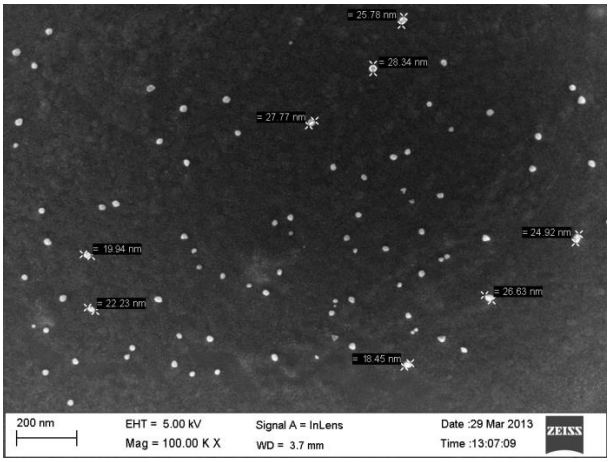

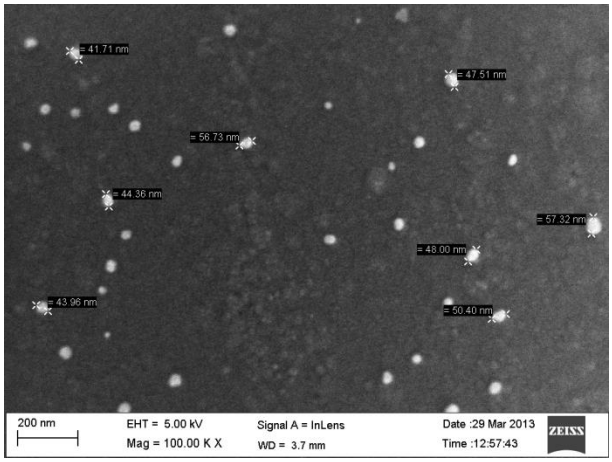

Blank NP and EFV loaded Lactoferrin nanoparticles were using The Field Emission Scanning Electron Microscope. The average diameter for Blank NP was found to be 19-35nm and for EFV loaded Lactoferrin nanoparticles it was found to be 45-60nm.

Figure 4.3 AFM analysis of nanoparticles.

C. Blank Nanoaprticles (Lacto-nano)

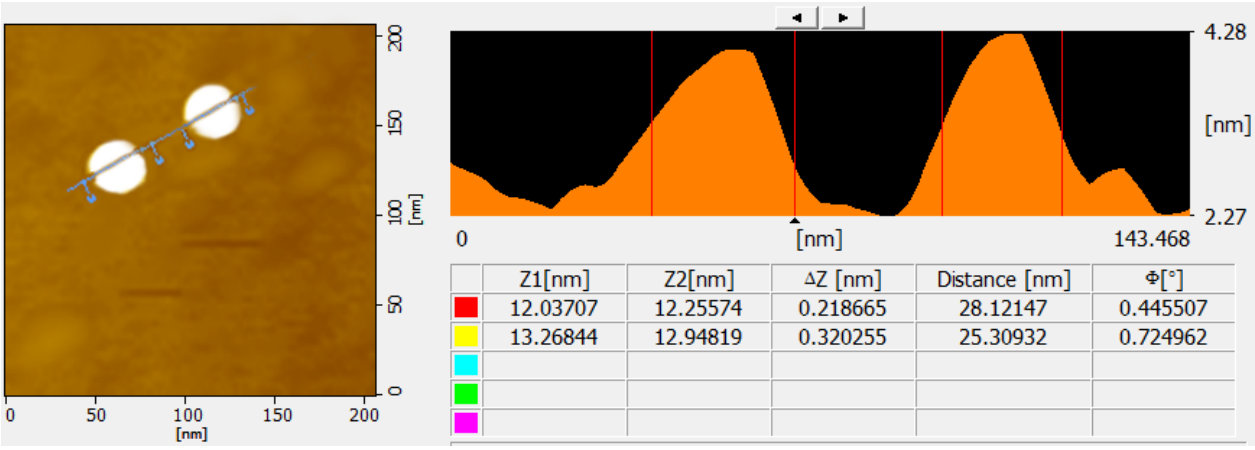

	Z1[nm]	Z2[nm]	ΔZ [nm]	Distance [nm]	Φ[°]
	12.03707	12.25574	0.218665	28.12147	0.445507
	13.26844	12.94819	0.320255	25.30932	0.724962

D. EFV nanoparticles (Lacto-EFV-nano)

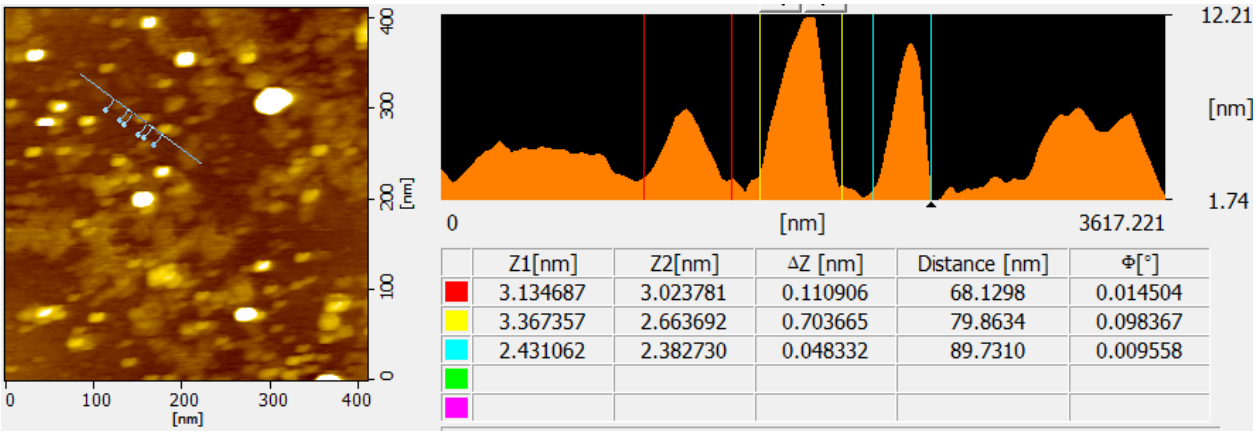

	Z1[nm]	Z2[nm]	ΔZ [nm]	Distance [nm]	Φ[°]
	3.134687	3.023781	0.110906	68.1298	0.014504
	3.367357	2.663692	0.703665	79.8634	0.098367
	2.431062	2.382730	0.048332	89.7310	0.009558

Atomic Force Microscopy was performed for Blank NP and efavirenz loaded lactoferrin nanoparticles. The average size for Blank and drug loaded nanoaprticles were found to be appriximately 27nm and 59nm.

Figure 4.4 Dynamic Light Scattering analysis of nanoparticles.

A. Blank nanoparticles (Lacto-nano).

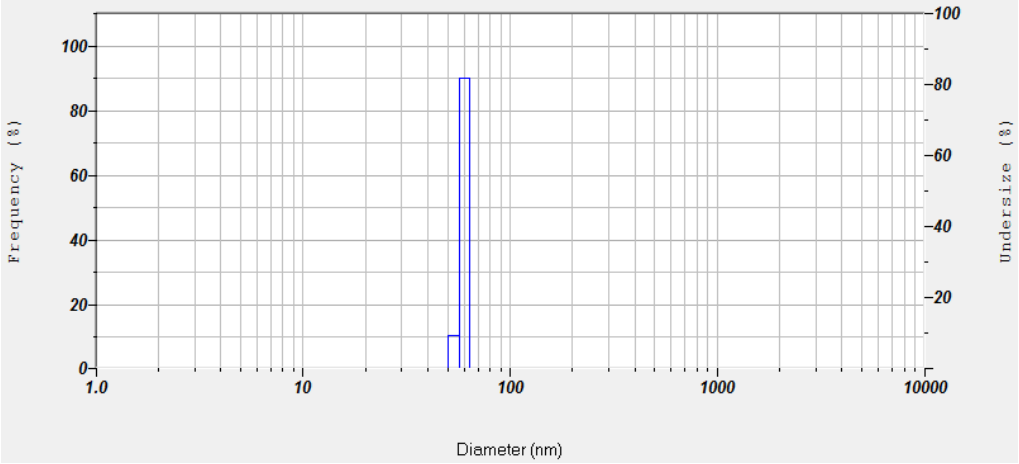

B. EFV nanoparticles (Lacto-EFV-nano).

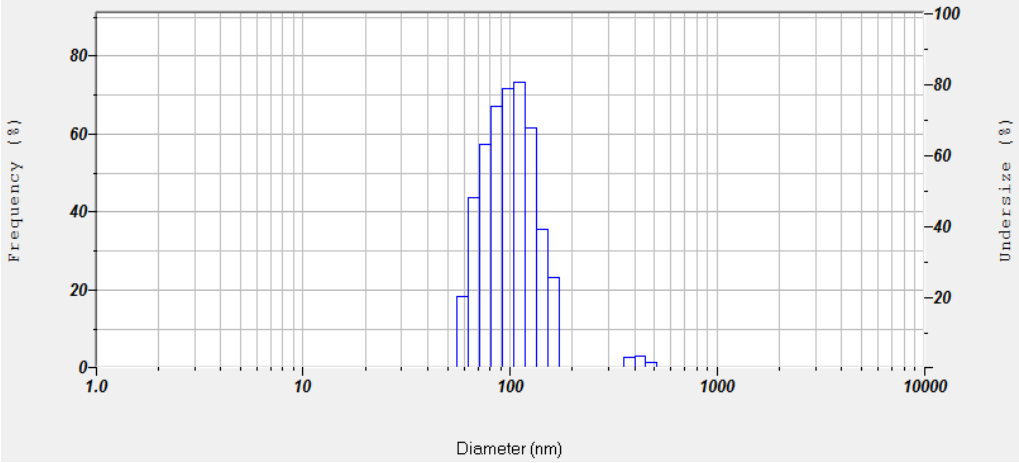

DLS analysis was performed for the measurement of hydrodynamic radii. A mean size of 72±3.4nm for Lacto-nano and 103±5.3nm for Lacto-EFV-nano was observed.

Figure 4.5 Zeta potential analysis of nanoparticles.

A. Blank nanoparticles (Lacto-nano).

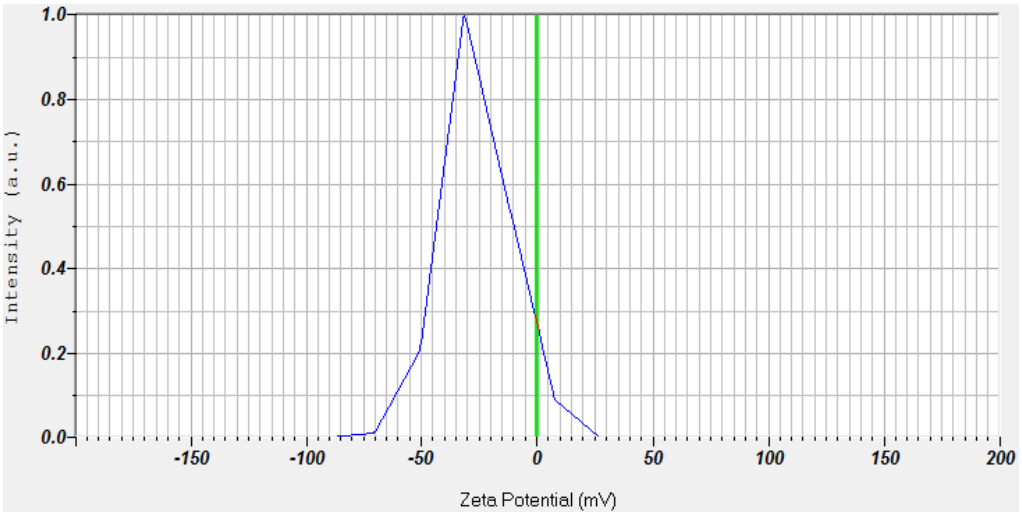

B. EFV nanoparticles (Lacto-EFV-nano).

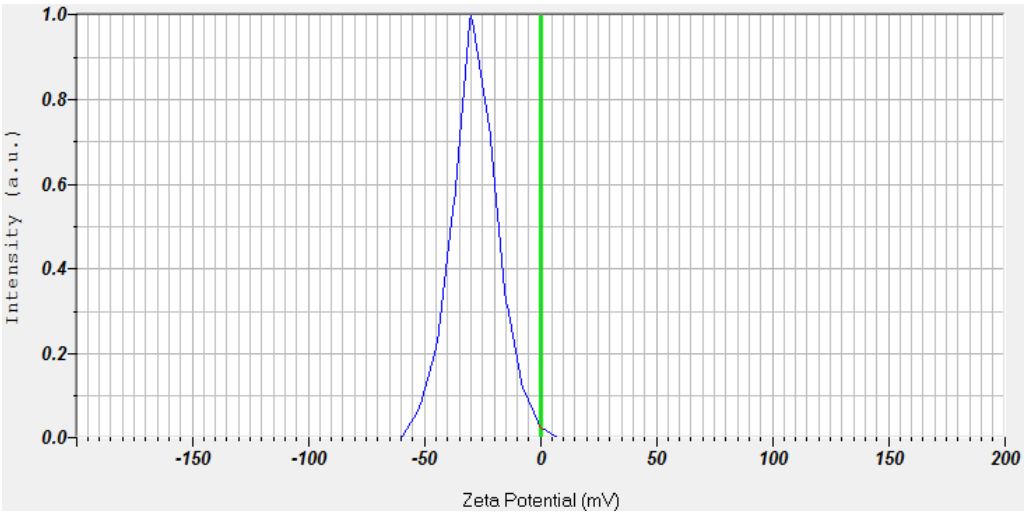

Zeta Potential or surafce changre was analysed using Zeta Sizer. A negative surface charge of -21mV for Blank NP and -19 for Lacto-EFV-nano were evaluated.

Figure 4.6 FT-IR spectra

A. FT-IR of sol efavirenz

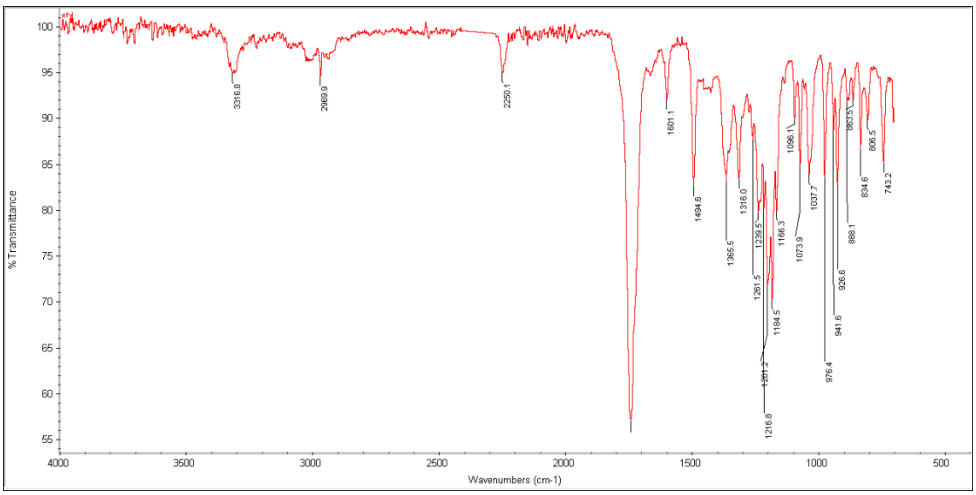

A. FT-IR of efavirenz loaded lactoferrin nanoaprticles (EFV NP)

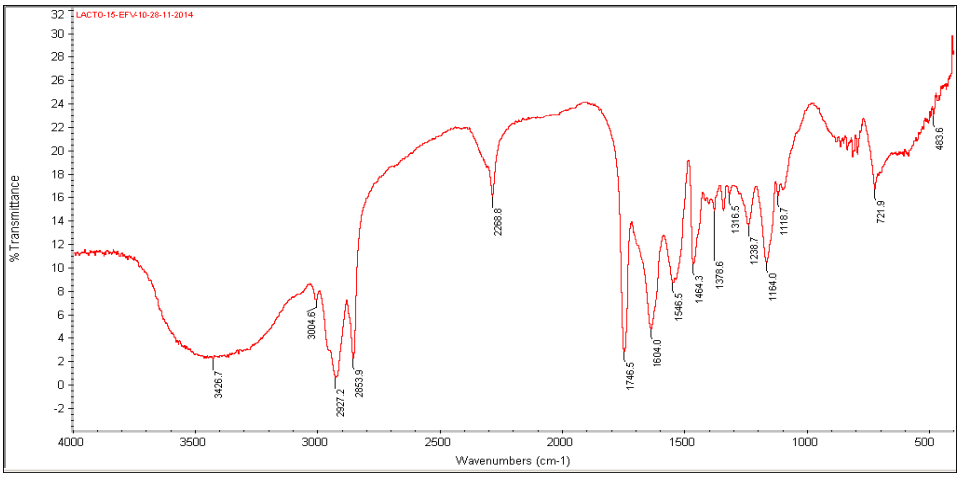

The comparision between the sol EFV and EFV NP

Functional groups	Sol EFV	EFV NP
C-O	1073.9 cm^{-1}	1092.6 cm^{-1}
C=O	1749.49 cm^{-1}	1746.5 cm^{-1}
N-H	3316.8 cm^{-1}	3320.3 cm^{-1}
C-F	1385.5 cm^{-1}	1378.6 cm^{-1}
CH2	1216. 8 cm^{-1}	1238.7 cm^{-1}
Alkyne	2250.01 cm^{-1}	2268.8 cm^{-1}

Figure 4.7 DSC (Differential Scanning Calorimetry) thermogram

A. Soluble Efavirenz

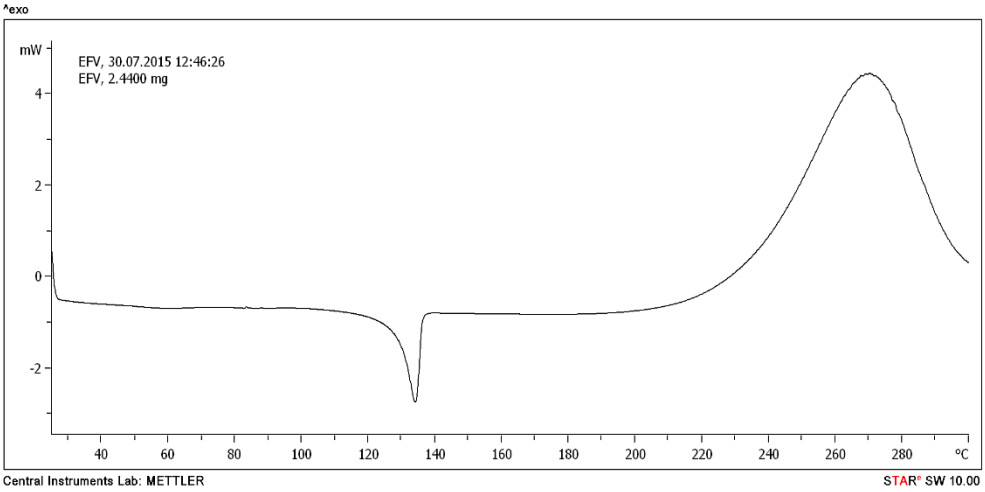

B. Lacto-EFV-nano (EFV NP)

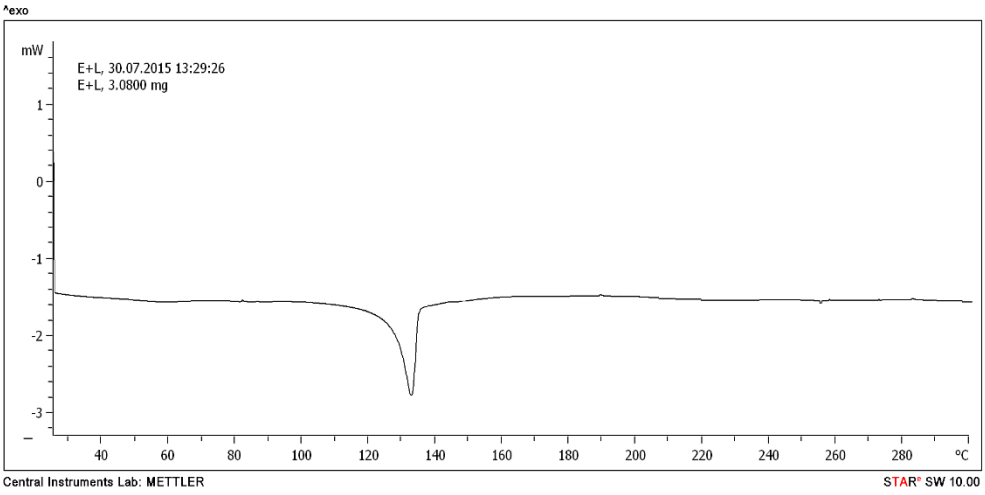

Differential scanning calorimetry (DSC) thermogram of Sol EFV (a) and Lacto-nano-EFV (b). All samples were lyophilized using lyophilizer before DSC

Figure 4.8 pH dependent release of nanoparticles.

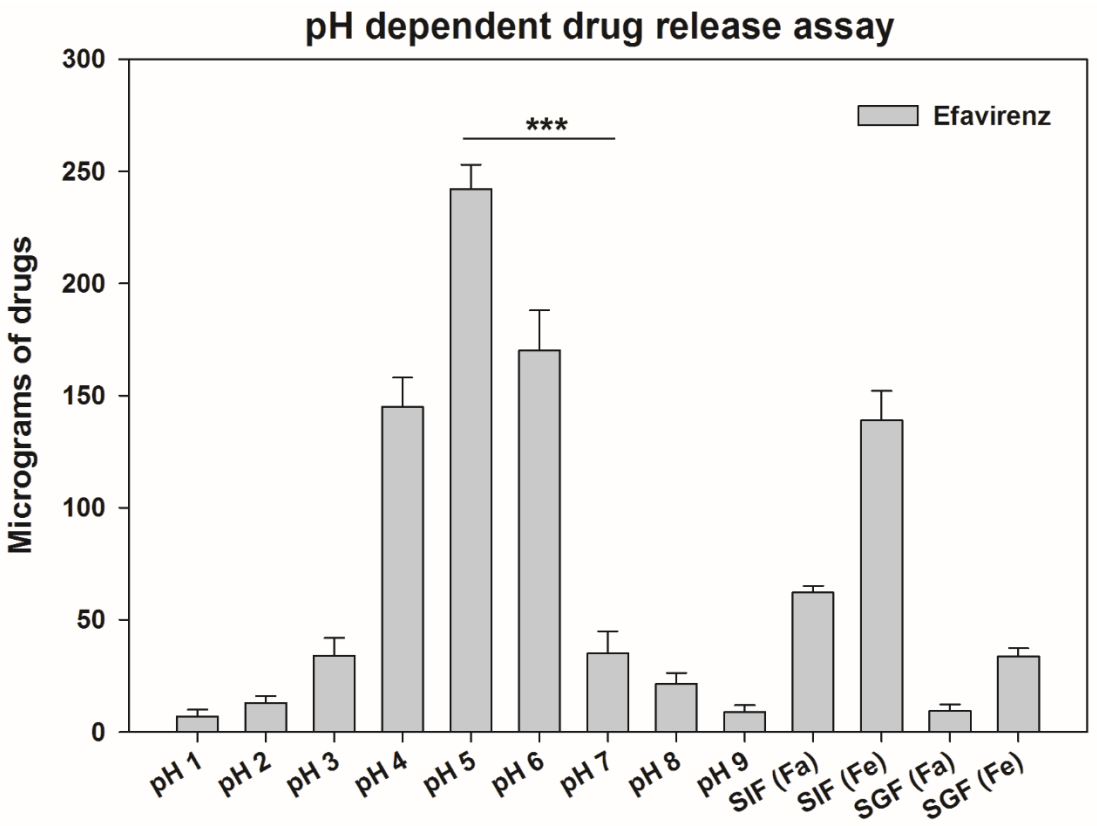

pH dependent release assay of efavirenz from Lacto-EFV-nano. 300µg of particles were incubated in the buffers of different pH, and simulated fluid. The release of EFV was found to be maximum at pH-5. This is followed by pH-6 and pH-4.The release was between <30% with the remaining fluids. **Abbreviations -** SIF (Fa): Fasted state Simulated Intestinal Fluid, SIF (Fe): feed state SIF, SGF (Fa): Fasted state Simulated Gastric Fluid, SGF (Fe): Feed state SGF.

Figure 4.9 Cellular drug kinetics

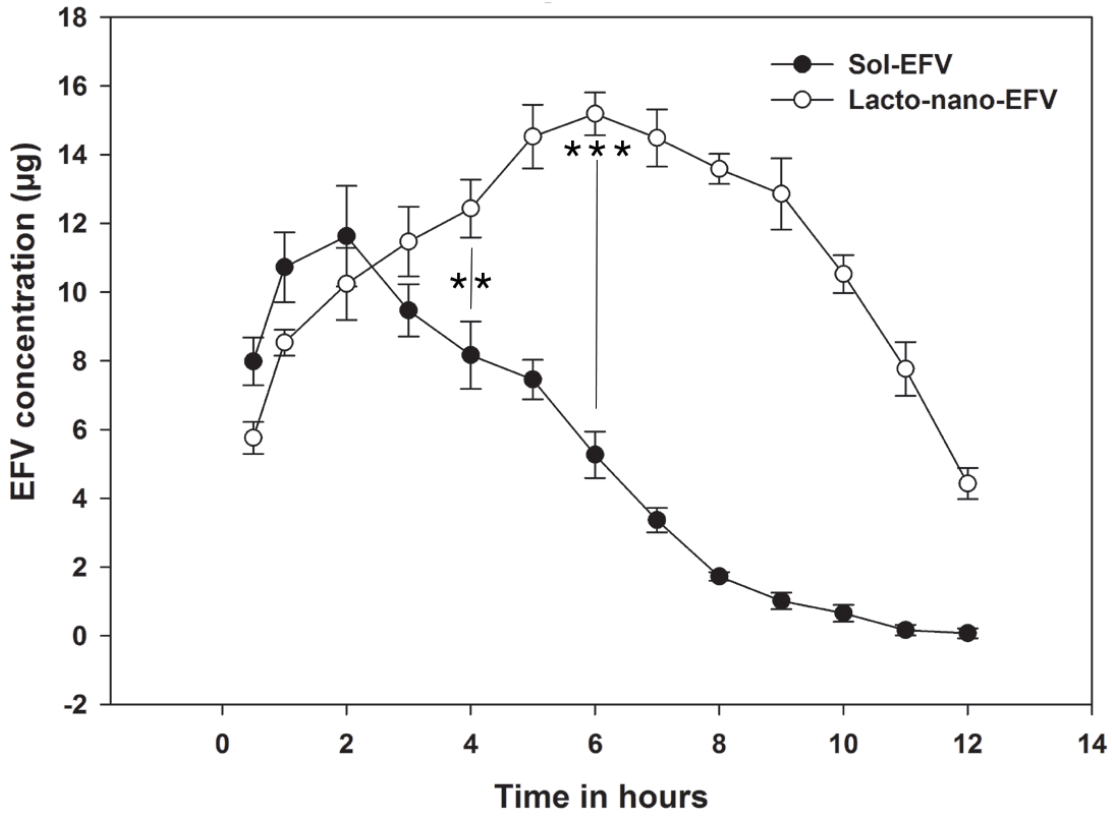

In vitro drug kinetics (cellular uptake) assay of EFV, either in sol form or loaded with lactoferrin nanoparticles. Efavirenz were estimated by HPLC at 247nm. All data points were measured in triplicate and denoted as mean ± standard deviation.

Figure 4.10 Antiviral assay.

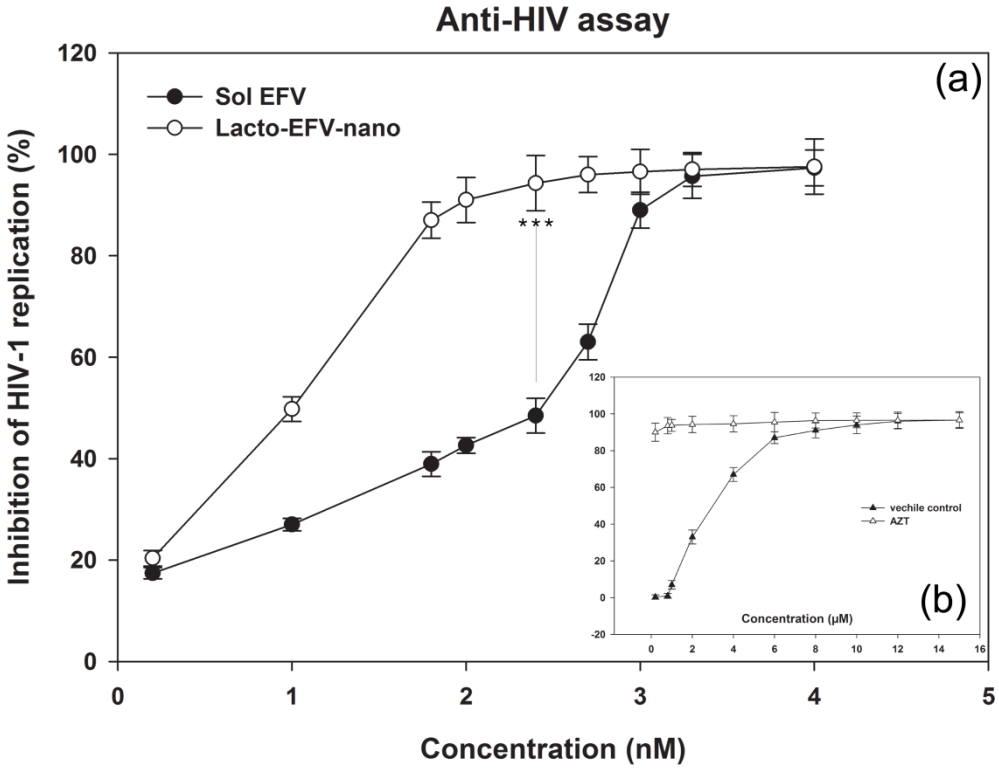

Anti-HIV-1 assay. The comparative anti-HIV-1 activity of efavirenz in sol form and nano form. SUPT1 cells infected with HIV-1_{NL4-3} were incubated with increasing concentration (0.2 – 4nM) of sol EFV and Lacto-EFV-nano. Vehicle control (Lacto-nano) and AZT (negative control) were used in a concentration of 0.2 – 15μM. On the 5^{th} days of post-infection, p24 level was measured using ELISA. p24 level in the absence of drugs was considered as 0%inhibition. Data were presented mean and standard deviation. The level of significance is **$p<0.01$ and ***$p<0.001$ compared to Lacto-EFV-nano.

Figure 4.11 MTT assay

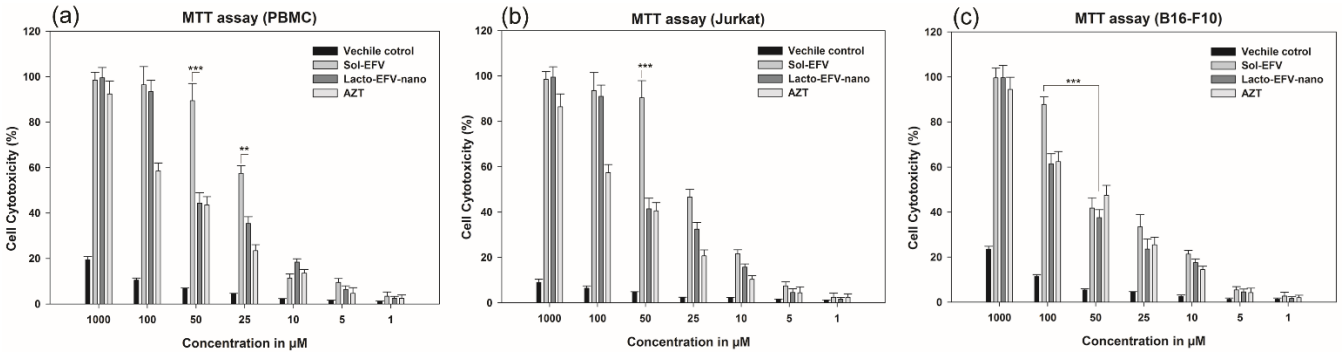

Cell cytotoxicity (MTT) assay. Stimulated PBMC (Panel a), Jurkat (Panel b) and B16-F10 (Panel c) were treated with increasing concentration (1, 5, 10, 25, 50, 100 and 1000µM) of sol EFV, Lacto-EFV-nano for 16h. Blank-NP and AZT were defined as vehicle control and positive control respectively. PBMCs were cultured with IL-2 (20IU/ml). The effects were characterized by measuring the dose to kill 50% of cells (GI_{50}). Data were presented as mean ± standard deviation. The level of significance is **p<0.01 and ***p<0.001 compared to Lacto-EFV-nano.

Figure 4.12 A. Tissue distributin.

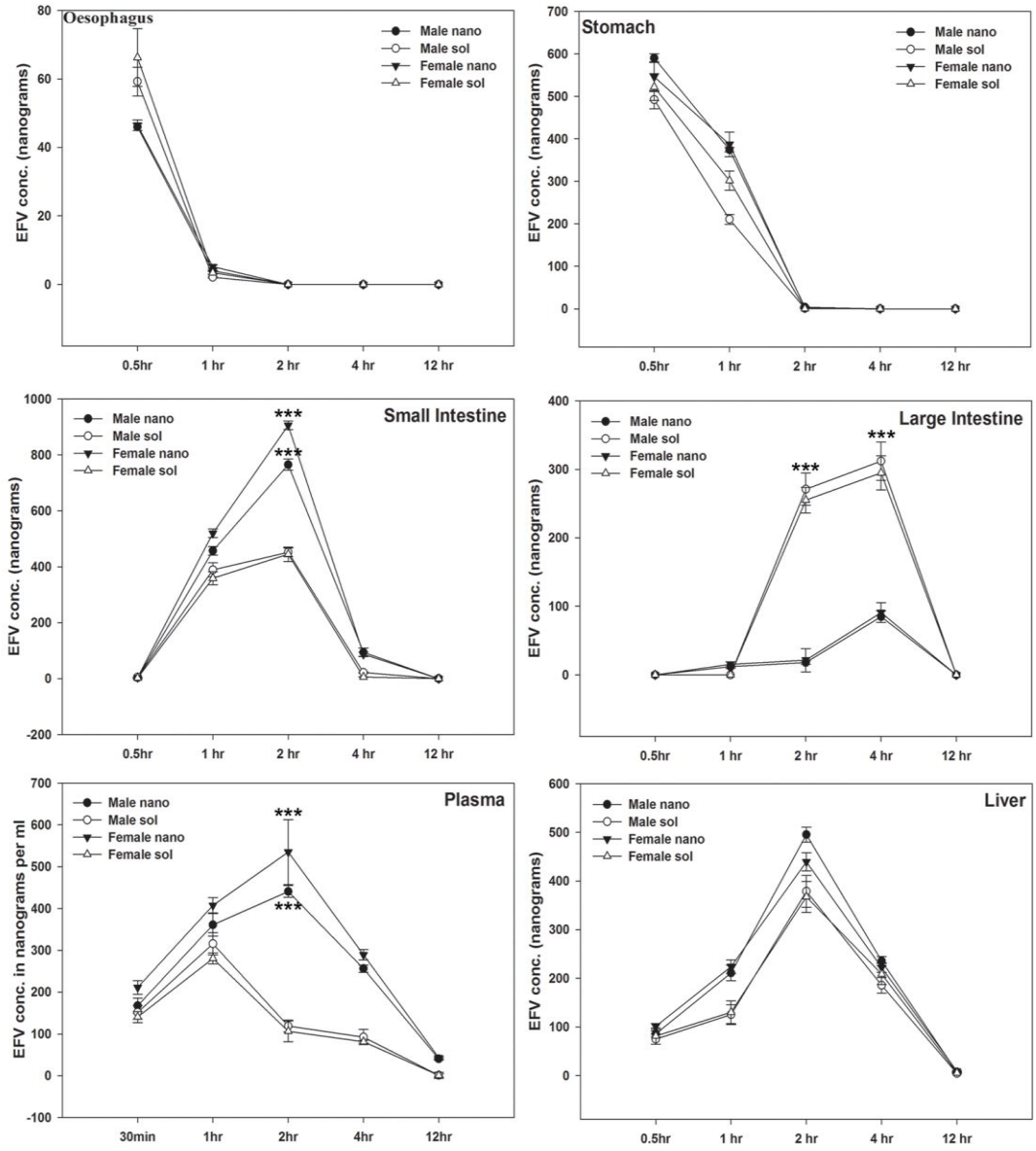

EFV Tissue distribution in Rats. Oral administration of sol EFV and Lacto-EFV-nano (10mg/kg body weight) was done and the tissues were collected at the indicated time points followed by quantification of EFV by using HPLC. It shows the drugs distribution in esophagus, stomach, small intestine, large intestine, plasma and liver. **Abbreviation:** Male sol and Female sol defines the concentration of EFV delivered via sol EFV in male and female rats respectively. Male nano and female nano defines EFV concentration delivered via lacto-EFV-nano in male and female rats. The difference between groups was calculated using one-way ANOVA; **p<0.01 and ***p<0.001.

Figure 4.12 B. Tissue distributin.

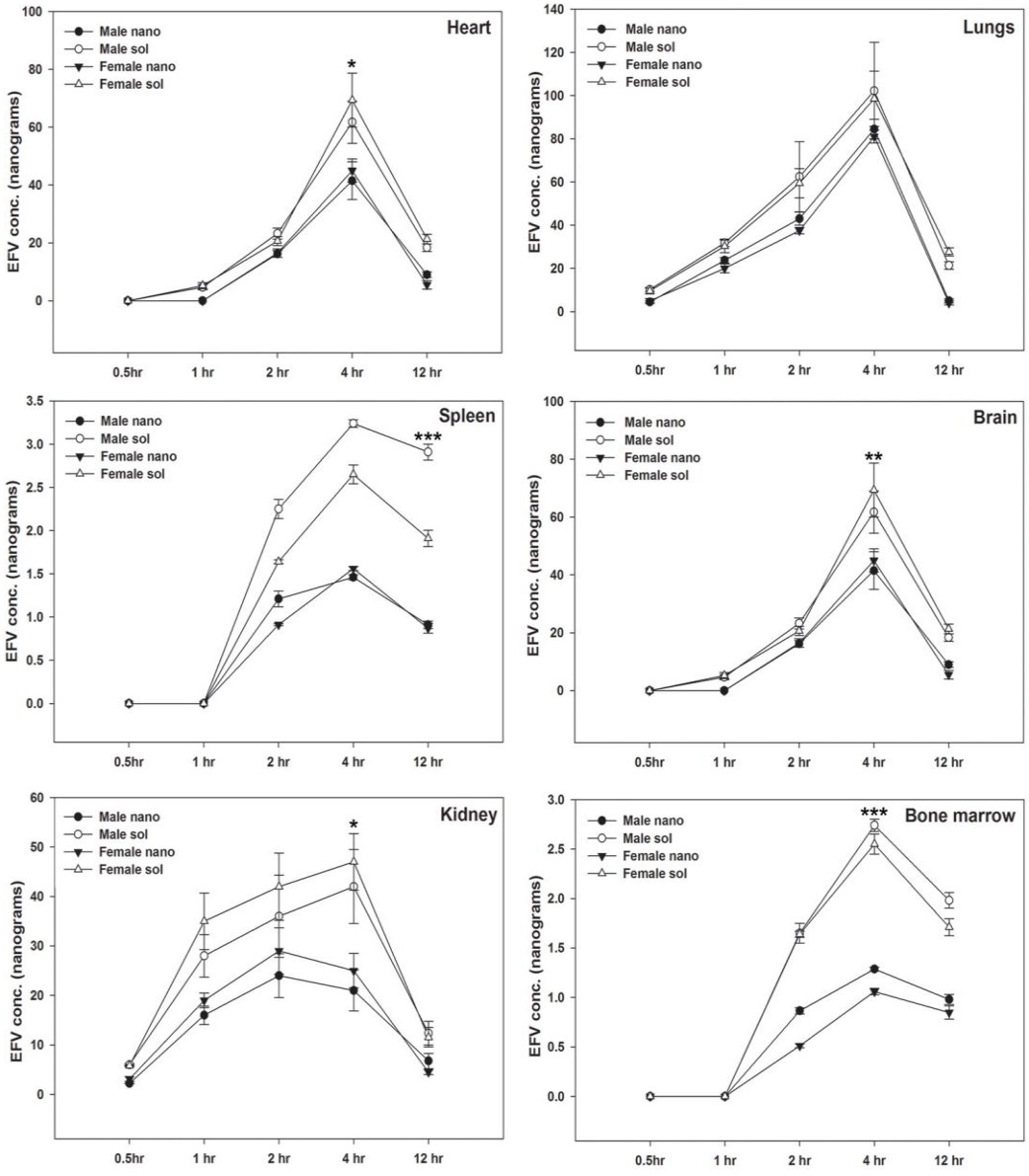

EFV Tissue distribution in Rats. Oral administration of sol EFV and Lacto-EFV-nano (10mg/kg body weight) was done and the tissues were collected at the indicated time points followed by quantification of EFV by using HPLC. It shows the drugs distribution in heart, lungs, spleen, brain, kidney, and bone marrow. **Abbreviation:** Male sol and Female sol defines the concentration of EFV delivered via sol EFV in male and female rats respectively. Male nano and female nano defines EFV concentration delivered via lacto-EFV-nano in male and female rats. The difference between groups was calculated using one-way ANOVA; **$p<0.01$ and ***$p<0.001$.

Figure 4.13 A. Histopathological analysis of tissues.

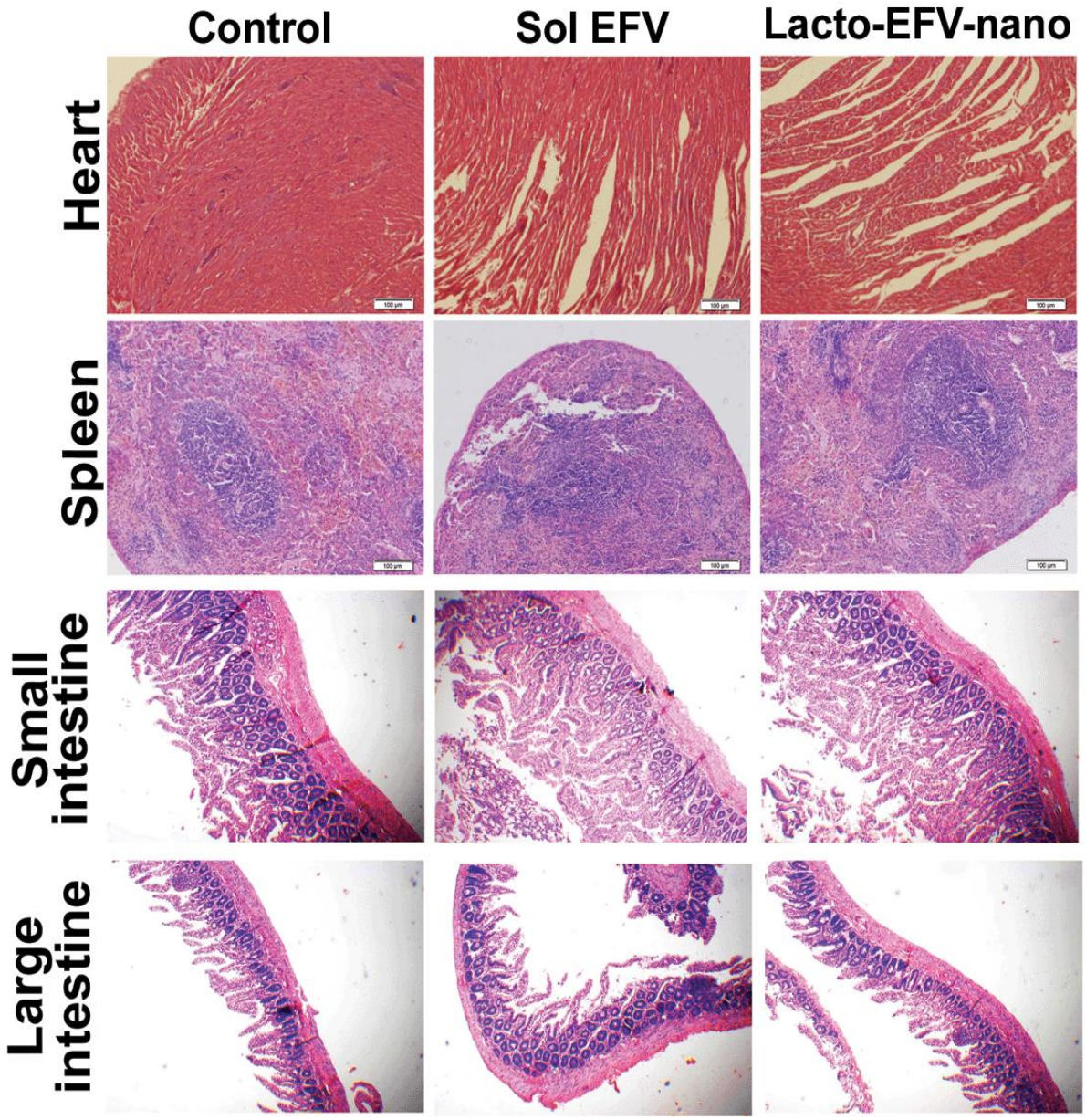

Histopathological analysis of tissues. Hematoxylin and Eosin (H&E) staining images of Heart, Spleen, small intestine, and large intestine. Scale bar is equal to 100µM or 40X otherwise stated.

Figure 4.13 B. Hematoxylin and Eosin staining.

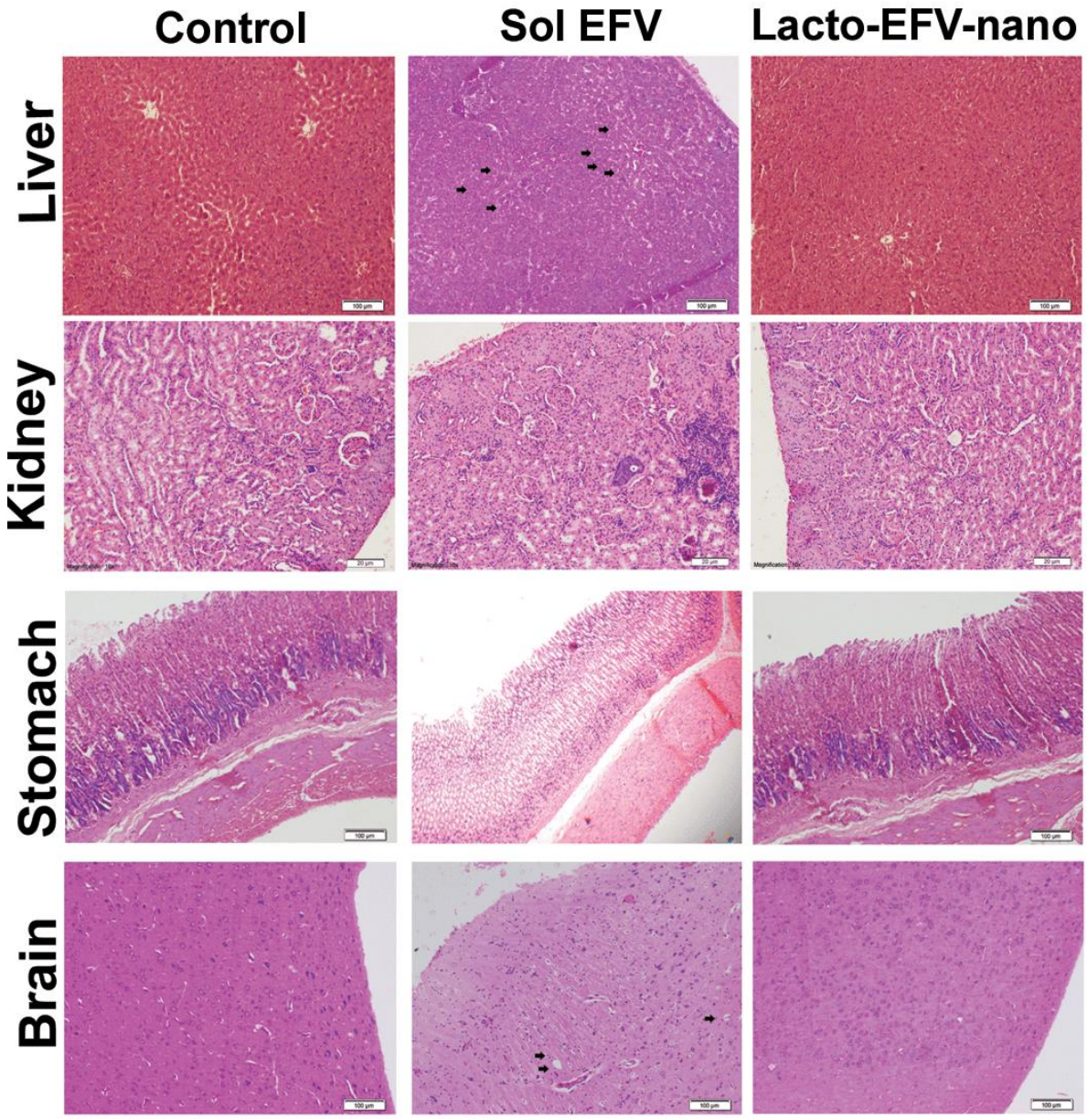

Histopathological analysis of tissues. Hematoxylin and Eosin (H&E) staining of liver, kidney, stomach and brain. It revealed that few abnormal morphology for the sol formulations compares to nano formulations employed majorly in Brain, Liver, Spleen followed other organs. Scale bar is equal to 100µM or 40X otherwise stated.

Figure 4.14 Safety analysis.

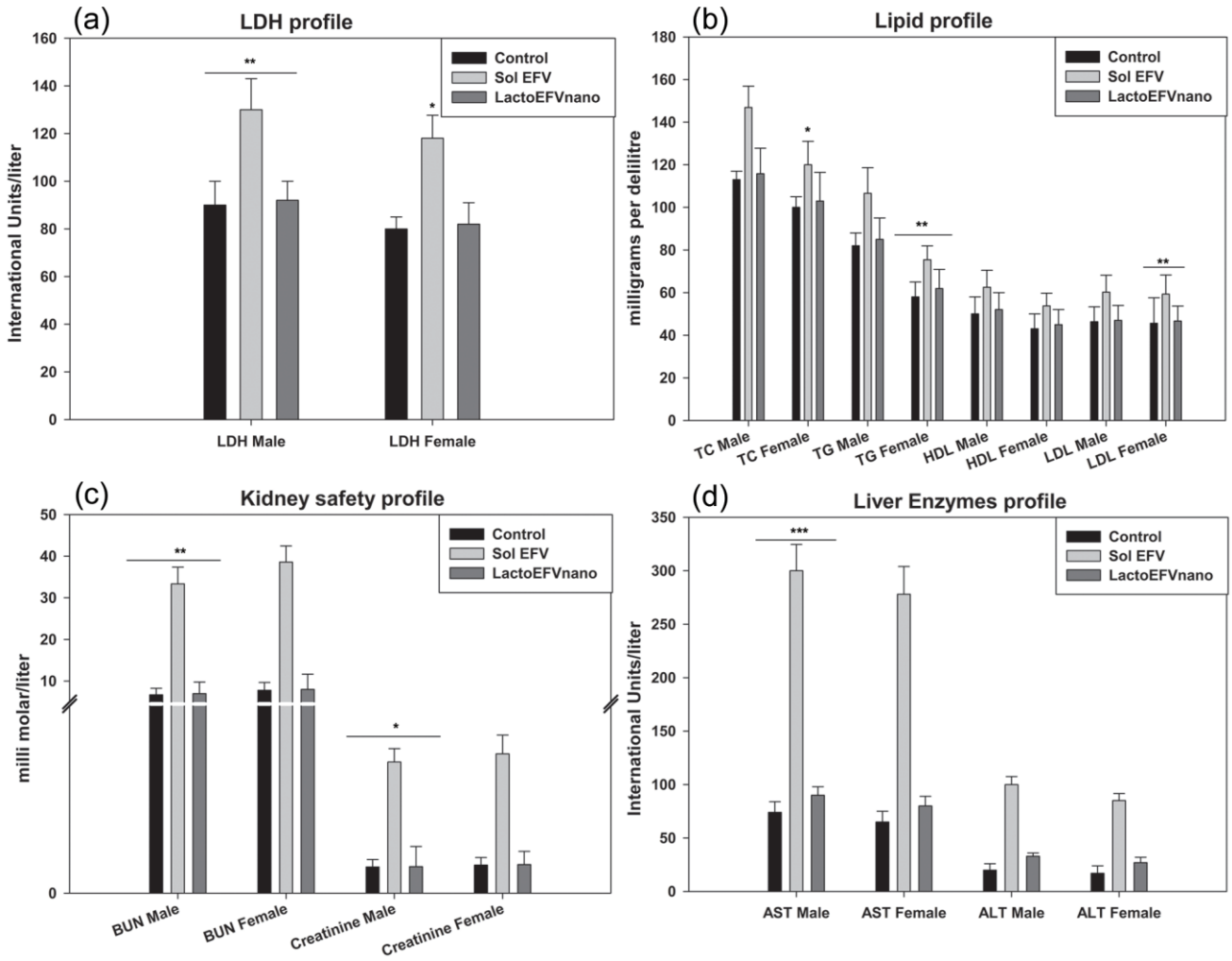

Biochemical safety analysis profile. Safety analysis was done using biochemical kits after oral administration of nano and soluble EFV in both male and female rats. Liver damage was estimated by ALT and AST level whereas Kidney toxicity was checked by Urea and creatinine level, LDH level and Lipid profile for Heart toxicity were analyzed. EFV-lacto-nano showed no toxicity to liver, kidneys and Heart. All samples were repeated thrice, error bars represent standard deviation. **Abbreviation:** control – data obtained from rats treated with saline, sol EFV and Lacto-nano-EFV – data obtained from rats treated with sol EFV and EFV loaded Lf NP respectively, LDH – Lactate dehydrogenase, TC – total cholesterol, TG – Triglyceride, HDL – high-density lipoprotein, LDL – low-density lipoprotein, BUN – blood urea nitrogen, AST – Aspartate aminotransferase, ALT - Alanine transaminase.

Tables

Table 4.1: Encapsulation efficiency optimization of efavirenz loaded lactoferrin nanoparticles.

Formulation code	EFV(mg):Lf(mg)	EFV EE (%)
F1	**10:10**	**47** ± 1.2
F2	**10:20**	**42** ± 2.3
F3	**10:30**	**59** ± 1.3
F4	**10:40**	**55** ± 1.7
F5	**10:50**	**51** ± 2.6

Table 4.2: *In vitro* stability profile of nanoparticles

Temperature	Parameter	Observation (month)			
		1	2	3	4
4°C	**Physical appearance**	White, granular	No change	No change	No change
	Average Particle size* **(nm)**	57.54	63.54	61.65	62.73
	EE%#	60 ± 3.2	58 ± 2.6	59 ± 1.8	58 ± 2.8
	DC% (w/w)$	15.0	14.5	14.75	14.5
Room temperature (25°C)	**Physical appearance**	White, granular	No change	No change	No change
	Average Particle size* **(nm)**	63.18	57.53	61.54	63.54
	EE%#	59 ± 1.64	61 ± 1.7	60 ± 2.6	59 ± 3.1
	DC% (w/w)$	14.75	15.25	15.0	14.75

* Size of NP was measured using FE-SEM in nm (nano meter).

The EE was calculated using the formula given in methods section. All experiments were repeated thrice. Data were presented as mean and standard deviation.

$ The average value of drug content was evaluated using the formula stated in methods section.

Table 4.3: Pharmacokinetic Profile for Efavirenz:

Parameters	Unit	Male		Female	
		Nano	Soluble	Nano	Soluble
AUC(tot)	(h)*(ng/mL)	2401.43	764.336	2739.81	684.856
AUMC(tot)	(h)^2*(ng/mL)	11879.8	1944.54	13035.3	1741.96
C_{max}	ng/mL	440.683	315.62	535.12	280.5
T_{max}	hr.	2	1	2	1
$t_{1/2}$	hr.	2.927	1.336	2.79	1.359

Values in the parenthesis designate the concentration of EFV in nano-grams per ml of blood.

Pharmacokinetic parameters:

AUC (Area under the Curve): The integral of the concentration-time curve (after a single dose or in steady state).

AUMC (Area Under the first Moment curve): Partial area under the moment curve between t start and t end.

C_{max}: The peak plasma concentration of a drug after oral administration.

T_{max}: Time to reach C_{max}.

$t_{1/2}$: The time required for the concentration of the drug to reach half of its original value.

Chapter 5

Development and characterization of First line regimen (AZT + EFV + 3TC) loaded lactoferrin nanoparticles as oral formulation.

Introduction

An estimated 15.8 million population were on ART treatment in June 2015 [130]. An effective and uninterrupted antiretroviral (ARV) treatment can control the viremia in infected persons, further with reduce risk in frequency of virus transmission of HIV with improved quality of life [13]. In current scenario there are no vaccine available for HIV prevention, all the candidates being studied are in the initial stage of their development [131]. In early 1990s the HIV treatment was started as monotherapy then shifted to dual drug regimen, followed by three-layered drugs combination treatment. When virus multiplies, the new copies formed contain mutation, hence progenies are slightly different from original virus; further virus can develop resistance if only one or two ARV drugs were used. This necessitates the requirement of therapy which combines drugs having different mode of action against HIV [13, 107, 108]. There are 26 drugs approved by US Food and Drug Administration (FDA); the highly active antiretroviral therapy (HAART) has improvised the health of infected individuals and lowered the morbidity and mortality [132]. Generally combination of ARV drugs are used during the HAART treatment. Each type antiretroviral (ARV) drug-targeting to specific site in virus replication providing multi-mode of action against HIV. The recommended HAART first line treatment is a combination of one NNRTI (Non-Nucleoside Reverse Transcriptase Inhibitors) plus two NRTI (Nucleoside/Nucleotide Reverse Transcriptase Inhibitors) [133]. A combination of Zidovudine (AZT), Efavirenz (EFV) and Lamivudine (3TC) is one of the frequently used fist line regimen. Long term of use of the combination of ARV drugs reported various toxicity, cardio-toxicity and erythrocyte toxicity is being frequently limit their use [134]. The most important hurdle in the ARV treatment is that, patient has to take the medication on daily basis, it may lead to various side effects and other health complications [135]. As nanoparticles (NP) are the system that deliver the drugs in a sustain manner and possess long drug retention time inside body; directly relates to reduction in the dosage schedule as well as other side effects. NP have proven as an effective drug delivery system for a wide ranges of disease complications such as cancer [136], AIDS [137, 138], Parkinson's disease [139] and many more. NP possess a varieties of properties such as biodegradable [140], sustain drug release [141] and improve efficacy of poor bioavailable drugs [142] etc. The

pharmacokinetic behavior and tissue distribution of NP is dependent mostly on its size and it surface properties [143]. Lactoferrin is a pleotropic molecule having a broad spectrum functional activities viz. anti-HIV, anti-bacterial, microbicidal etc. [144, 145]. Our previous studies showed that lactoferrin can serve as an effective delivery vehicle for cancer [61]. Indeed AZT loaded lactoferrin nanoparticle showed higher bioavailability of drug with improved safety [33]. The primary objective of present study is the preparation of a novel targeted drug delivery system composed of a triple drug (AZT, 3TC, EFV) loaded lactoferrin nanoparticle. While secondary objectives are evaluation the advantage of the nanoformulation for improved *in vivo* pharmacokinetics profile as well as with reduced side effects, when compared to the free drugs. This will provide a formulation with enhanced therapeutic utility in terms of reduced dose of drugs, minimum health complications with increased therapeutic index.

Results

Nanoparticles preparation

Drug (Lamivudine) protein saturation studies: The emission spectra shown in Fig. 5.1 reveals that, incubation period of approximately 25minutes is appropriate for the nanoparticle preparation. But on account of AZT and EFV, these drugs shown the saturation of fluorescence enhancement at 60minutes. Hence, preparation of combination drugs loaded nanoparticles, the maximum time at which the saturation binding for all 3 drugs, 60 min, is considered (Fig. 5.1).

Surface morphology (SEM and AFM) of nanoparticles

The nanoparticles (blank NP or drugs loaded) were prepared using sol-oil chemistry methods. The SEM and AFM analysis was performed to obtain the information about the particles size and surface morphology. FE-SEM analysis showed an average particles size of 27-35nm for blank LF-NP and 70-90nm for drugs loaded NP (Fig. 5.2), while nanoparticle

of individual nanoparticles of AZT was 60 to 80 nm, EFV was 60 to 70 nm and 3TC was 60 to 70, while combination of 3 drugs together is the range of 70 to 90 nm, suggesting that the 3 drugs are cooperatively loading to the lactoferrin nanoparticle in this methodology thus not contributing to significant increase in particle size, AFM data showed surface morphology of nanoparticles of particular type of projection or depression suggesting intact structural features those promote recognition and binding to the receptor present on the target cell surface.

TEM analysis of nanoparticles

The results of TEM analysis is presented in Fig. 5.3. It shows an average size of 26nm for Blank NP or Lacto-nano. Whereas after loading first line drugs (AZT+EFV+3TC), the size was found to be 60nm.

Particles size distribution studies of nanoparticles

Size distribution of blank NP and drug loaded NP was measured using NTA method. NTA accurately determine the broad range of NP population ratios. Results suggests that broad range of blank NP seize belongs to 27nm and 90nm for drugs loaded nanoparticles (Fig. 5.4).

Assembly of nanoparticles and FT-IR spectroscopic study

Fig. 5.5A and B denotes the FT-IR spectra of pure lactoferrin and Lacto-nano respectively. Fig. 5.5C and D represent the spectra of AZT+EFV+3TC in physical mixture and in loaded with lactoferrin NP respectively. The FT-IR data of FLART NP shows that all the important functional groups corresponding to each drugs and lactoferrin protein are remain intact. The slight shifting of the peaks may be observed in the nanoparticles, it may be due to the dipole moment as the bond characteristics is electrostatic.

Drugs loading (DL %) and Encapsulation efficiency (EE %)

NP were prepared by varieties of drug to protein ratios, resulted to a different EE for equal ratio of respective drugs (Table 5.1). The formulation X3 have shown the maximum EE, hence this ratio of formulation have been used throughout the experiments. The drug

loading and encapsulation efficiency for each drugs, AZT, EFV and 3TC were calculated separately according to the already developed formula [REF]. The DL % was found to be approximately 5% for each drugs (Units) and encapsulation efficiency was found to be in a range of 58 to 71% (Fig. 5.6A)

***In vitro* pH dependent drug release and percent release from nanoparticles**

FLART NP were subjected to various pH condition starting from pH 1 to 9, SIF and SGF. It was found that maximum amount of drugs were released at pH5 and 6 (Fig. 5.6B). The percent drugs release was performed at two different pH condition i.e pH 5.0 and 7.4 for various time points such as 1, 2, 4, 6, 8, 10, 12, 16 and 24h. It was found that pH7.4 leads to the release of only 20% of encapsulated drugs up to 24h. While pH5 shows the biphasic drug release; approximately 60% of the drugs were released up to 5h and rest of 40% drugs were constantly released up to 24h. (Fig. 5.6C). All three drugs are released together with similar kinetics suggesting they follow similar mode of drug loading.

Anti-HIV activity of nanoparticles

The *in vitro* anti-HIV activity of soluble lamivudine and lamivudine lactoferrin nanoparticles were shown in Figure 5.7A. The IC_{50} for soluble lamivudine and lamivudine nanoparticles are found to be 42.57nM and 23.18nM respectively. Further, the anti-HIV activity of various combination of the IC_{50} values of soluble and nanoformulation was performed (Fig. 5.7B). The 1^{st} line nanoformulation HAART has been found to be improved over its soluble formulation

Hemolytic effect of FLART NP

Fig. 5.8 shows the percentage of erythrocytes damage under the influence of first line anti-HIV drug in soluble or nano form. A hemolysis percentage of <5% is generally considered as non-toxic. The hemolysis rate (HR %) were found to be less than 2.0% at higher concentration, which could be considered as non-toxic.

In vivo pharmacokinetics and tissue distribution analysis

All the animals were given a single oral dose of 10mg (AZT/3.33mg+EFV/3.33mg +3TC/3.33mg) of drugs. Serum was isolated from blood followed by estimation of AZT, EFV and 3TC individually using HPLC. Drug concentrations were calculated and compartmental pharmacokinetics analysis was done using Kinetica software and the PK parameters were given in Table 5.2. Comparable pharmacokinetic profile was observed in both males and females. When pharmacokinetic parameters in rats treated with nano formulation versus soluble form are compared, the results show that C_{max} increased by 2.5 fold of AZT, 1.6 fold of EFV and 2.23 fold of LMV with the mean resident time of EFV being higher by a factor of at 2.41 fold, while it was 1.2 and 1.29 fold enhancement for AZT and LMV when nanoformulation is employed. Nanoformulation further increased T_{max} by 2 hours for all the three drugs (Table 5.2). Collected tissues were homogenized and quantified for the drugs available in it. The tissue distribution analysis data were plotted for various tissues and shown in Figure5.9A and B. Based on kinetics of nanoparticle absorption, NP first enters esophagus, stomach followed by absorption through small intestine. Then enters blood followed by liver, heart, lungs, spleen, brain, kidney then bone marrow. Nanoformulation shows high blood concentration and low clearance as compared to its soluble complement. Further strikingly nanoformulation shows enhanced absorption of nano-LMV as compared to its soluble form in all tissues and blood.

Safety and histopathology analysis

The isolated serum was quantified for the presence of creatinine, urea, AST, LDH and bilirubin (Figure 5.10). Enhanced level of blood creatinine and urea related to the kidney impairment when treated with soluble drug combination, which were found to be significantly reduced when nano formulation is employed. Further, increased AST and bilirubin implies the moderate liver damage when treated with soluble combination of drugs at 2-4h of post-treatment period, is found to be significantly reduced when treated with the nano formulation. These results are further confirmed by the histopathological analysis of tissue sections (Figure 5.11A and B) that show minor damage in the liver, heart or lungs tissue sections (indicated by black arrow), while such damage was not detected in these tissue sections when treated with nanoparticle formulation.

Discussion

The first line ARV treatment regimen is the starting treatment strategy for HIV infected person. World Health Organization (WHO) recommends a fixed dose combination regimen which include one NNRTI with two NRTI. In case of the failure of treatment outcome, it is recommended to change in line of therapy to second line regimen; which includes ritonavir boosted protease inhibitor plus two NRTI (that is not included in first line treatment) [146]. Which also exhibits several short comings. For effective pharmacokinetic behavior of any drug, the size of a particle should be in a range of 5.5nm to 100nm; show sustained blood circulation and effective target tissue drug delivery and a comparatively low mononuclear phagocyte system (MPS) uptake, as shown by recent quantum dot study [121, 147]. Results shows that drug loaded NP exhibit a size distribution of approximately 70nm in dry form and hydrodynamic size of 103 nm with enhanced vivo pharmacokinetics profile. The AFM microcopy images show a characteristic surface projection/depressions retaining structural features that participate in recognition and binding the receptor in the target tissue. In-spite of having different solubility properties, all the three drugs exhibit a drug loading capacity of approximately 60-65%. EFV has shown comparatively less EE because of its high lipophilicity ($\log P = 5.4$) [119]. Current lactoferrin NP has found to improve the drug loading capacity in contrast the solid lipid nanoparticles had shown very poor drug loading capacity [35]. To make the formulation more efficacious, it is important to deliver the drug to the target tissue. Non-targeted drug delivery leads to undesirable accumulation of drug inside body that results in the tissue toxicity. Localization of nanoparticles were studied in macrophages (U937 cells). The results show that localization of lactoferrin nanoparticles increased exponentially and reaches a maximum at 4 hours, followed by a significant decrease over the period of 12 hours, thus suggesting that the lactoferrin nanoparticles after release of its payload undergo exocytosis and get secreted out from cells. Thus delivery vehicle would not become burden to the cells. This inference is supported by the results of the pH dependent release assay and percent release assay, where at physiological pH (pH 7.4) only 10-20% of drugs get released while at endosomal pH (pH 5.0) approximately 80-90% of drugs release was observed from NP. After oral delivery, it is important that NP should not be able to release the drug in extracellular

condition. pH-dependent drug release assay data shows that in SIF (simulated intestinal fluid) and SGF (simulated gastric fluid) only negligible amount of drug release was observed and maximum of the drugs are targeted towards the endosomal (pH 5) intracellular delivery. Our current formulation is more superior to other formulation such as chitosan nanoparticles which is found to be unstable at gastric and intestinal condition [148]. The drugs could be encapsulated in the core of NP with a non-covalent interaction (electrostatic attraction); supported by FT-IR data as major functional groups are intact. A pH (pH 5) change triggers the protein entities present in NP to change its conformation thus leading to release of drugs from inside of the core. Earlier report suggested that Zidovudine treatment causes severe anemia that leads to cessation of HIV treatment [149]. Antiviral data suggest that, the individual drug nanoformulation is found to be more efficacious than its soluble counterpart as indicated by the reduced IC_{50} value. As HAART include all the three drugs in combination; the percent HIV-1 inhibition is found to be equal or improved in case on nanoformulation as compared to soluble drug combination, even though its dose has reduced to ½ or $1/4^{th}$ of their original concentration. Our data suggested that FLART NP is very less toxic to the erythrocytes (<2%) even at high concentration. The *in vivo* data suggest that after loading of drugs together to the NP, an outstanding improvement in the PK profile is found. We have also detected a prolonged exposure of drug in the blood circulation, as the AUC value was found to be increased by approximately 4-fold. The AUMC (tot) has been increased by 4-10 fold for nanoformulation as compared to the soluble drug combination. The T_{max} and $t_{1/2}$ have improved by 2-fold. It has been reported that AZT and 3TC the protein binding capacities are 34-38% and 16-34% respectively, while for EFV it is >99%, thus pointing out to differences in bioavailability in different tissues. The observed increase of serum biochemical profile for creatinine, urea, AST and bilirubin shows that liver and kidney impairment In the case of soluble drug combination treatment. This data has also been supported by the Histopathological study.

Conclusion

In conclusion, we have successfully encapsulated three anti-HIV drugs (Zidovudine, efavirenz and lamivudine) together in the nanoparticles. These first line loaded drugs nanoparticles were well dispersed stable colloidal solution. These protein based nanoparticles are easy to prepare, long lasting, biodegradable and non-toxic to erythrocytes. The *in-vitro* data suggest that our nanoparticles is able to release drugs intracellularly in controlled and sustained manner. Drugs loaded nanoparticles have improved the pharmacokinetics profile for each drugs without causing any toxicity to the major organs. So we can conclude that our nanoformulation provide a deep insight in the area of novel drug delivery system.

Figure 5.1 Drug (Lamivudine) – Protein Saturation study.

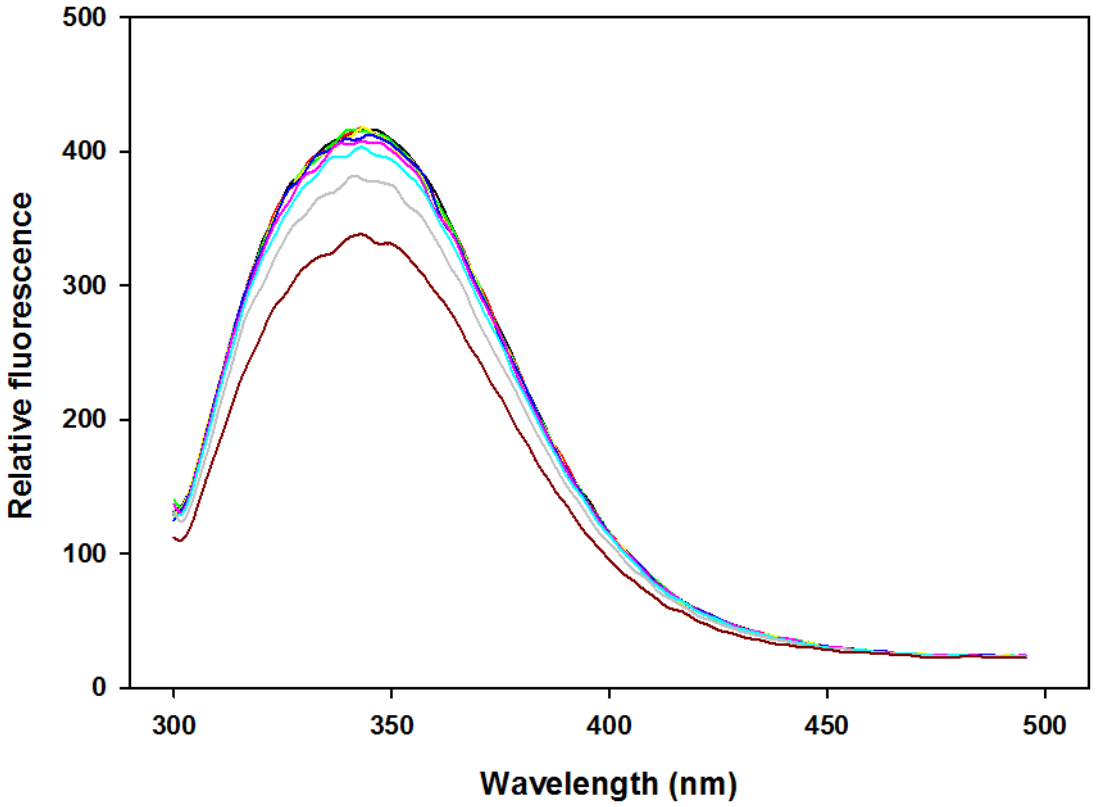

1μM of lactoferrin and 1μM of lamivudine was incubated together for various time points at an interval of 5min up to 60. The fluorescence was measured after each time interval. It was found that after 20-25 min, the fluorescence intensity became constant.

Figure 5.2 FE-SEM and AFM analysis of nanoparticles.

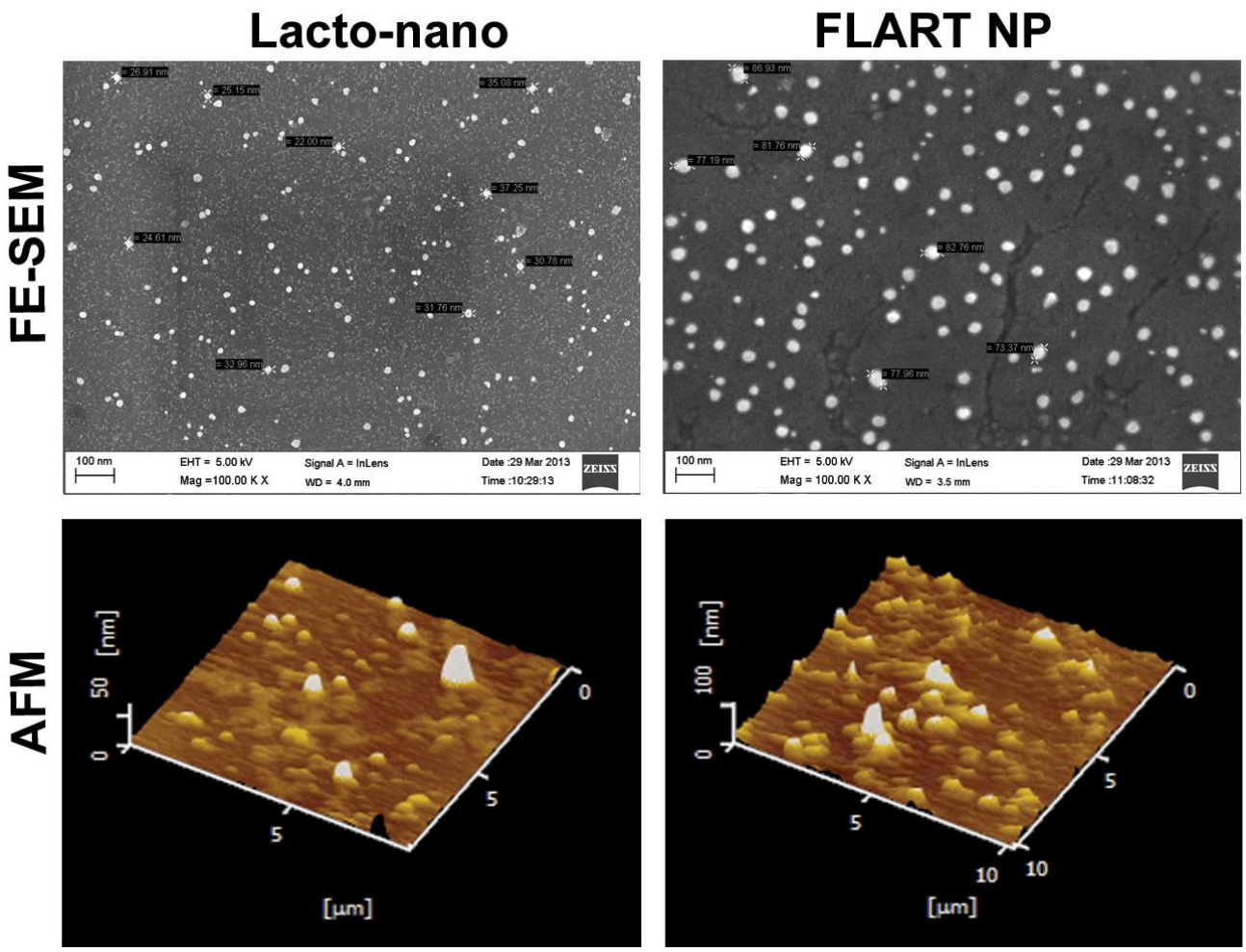

FE-SEM and AFM analysis of nanoparticles. Upper panel represent the FE-SEM images of blank Lf NP (Lacto-nano) and first line ART loaded Lf NP (FLART NP). Lower panel shows the AFM images of lacto-nano and FLART NP respectively. Size of NP has been increased up on loading of drugs.

Figure 5.3 TEM (Transmission electron microscope) analysis of nanoparticles.

C. Blank nanoparticles (Lacto-nano) **B. FLART nanoparticles**

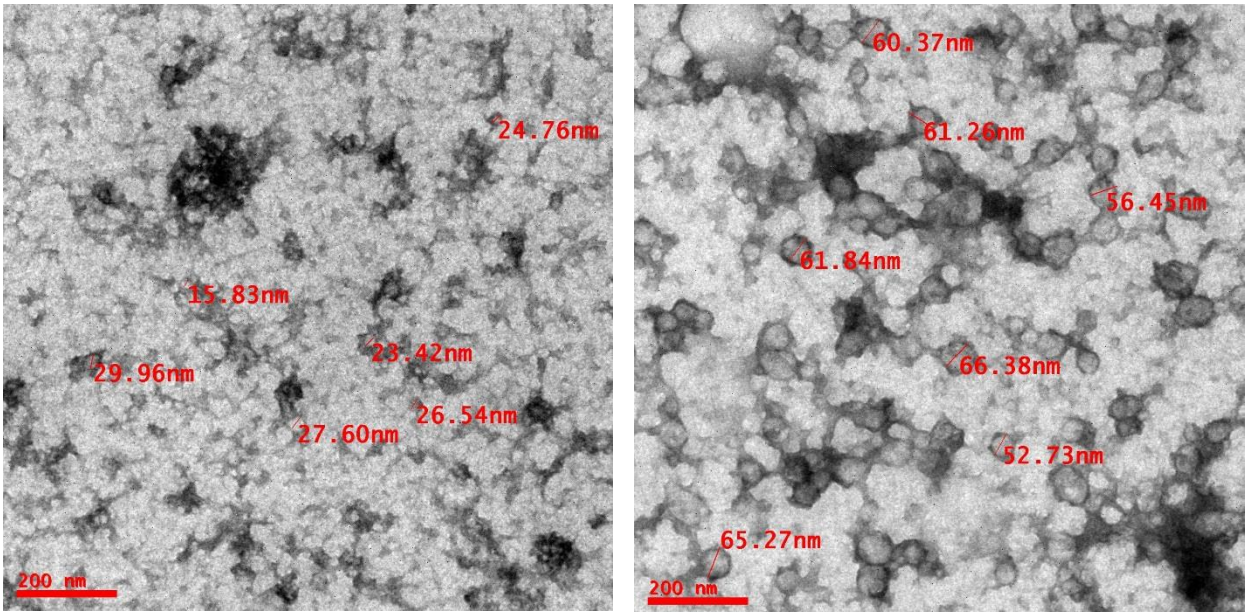

TEM analysis of nanoparticles. Blank and first line loaded drugs nanoparticles were subjected for TEM analysis. The samples were prepared according to the protocol mentioned in methods section. The diamater of Blank NP or Lacto-nano was found to be an average of 26nm. The diameter of nanoparticles after loading of AZT+EFV+3TC was recored as approximetely 60nm.

Figure 5.4 Nanosight analysis of nanoparticles.

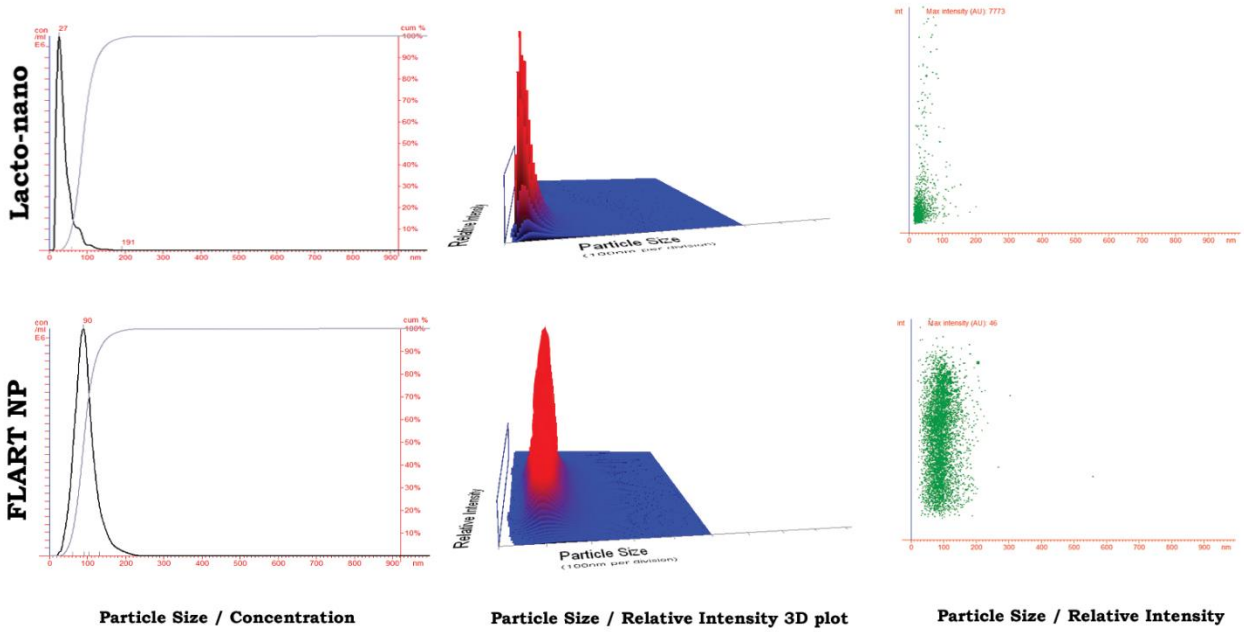

Nanoparticles size distribution analysis: (Nanoparticle tracking analysis) NTA has been performed using Nanosight NS500. Upper and lower panel images represent the lacto-nano and FLART NP respectively. Graph has been plotted between particles size verses concentration/relative intensity 3D plot/relative intensity 2D. Lacto-nano and FLART NP shows a size distribution of approximately 27nm and 90nm respectively.

Figure 5.5 FT-IR spectra

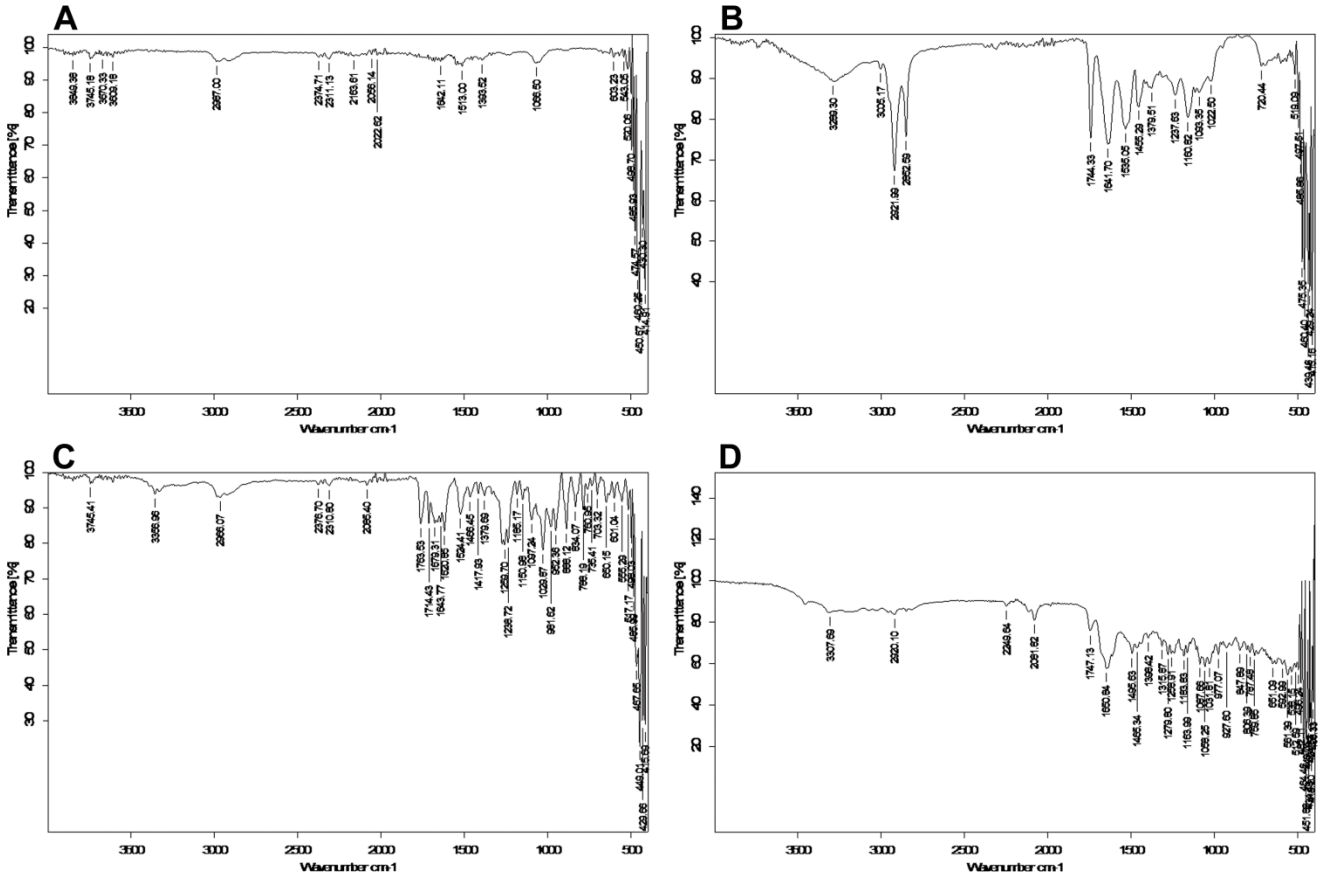

FT-IR spectra of pure lactoferrin (A), lacto-nano (blank Lf NP without loading of drug) (B), physical mixture of AZT+EFV+3TC (C) and FLART NP (first line ART drugs loaded NP (D).

Comparision of presence of featured groups in sol and naoform.

Functional groups	**Sol 1st line**	**1st line NP**
Azide group ($N^{-}=N^{+}=N^{-}$)(AZT)	2117 & 2085.4 cm^{-1}	2115 & 2081.82 cm^{-1}
CH2 (EFV)	1238.72	1242.2 cm^{-1}
C-O-C stretching(3TC)	1150 cm^{-1}	1164 cm^{-1}

Figure 5.6 Drug loading, Encapsulation pH dependent release of nanoparticles.

A. Drug loading and Enacapsulation efficicency. **B. pH dependent release**

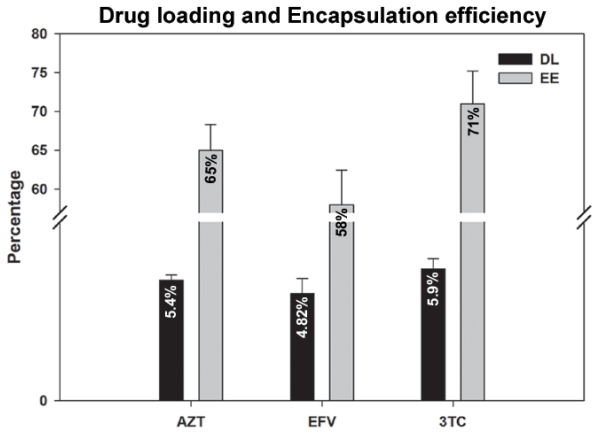

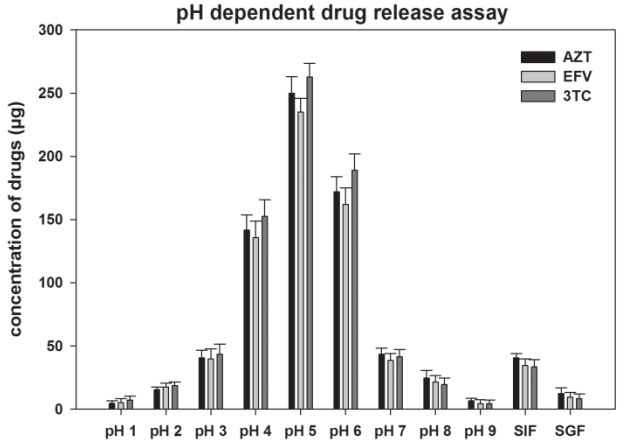

C. Percent Release

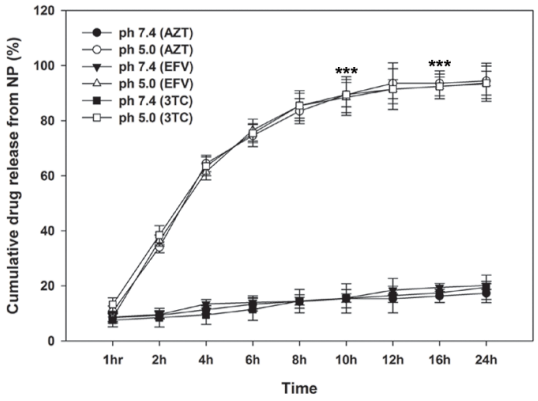

(A) Drug loading and Encapsulation efficiency of first line loaded drugs nanoparticles. **(B) pH and simulated fluid dependent drug release from Nanoparticles**: 900µg (300µgAZT + 300µgEFV + 300µg3TC) of first line regimen NP were incubated in the buffers of different pH, SIF (simulated intestinal fluid) and SGF (simulated gastric fluid). The release of all the drugs was maximum at pH-5 and this is followed by pH-6 and pH-4. **(C) Percent cumulative Drug release**: 900µg (300µgAZT+300µgEFV +300µg3TC) of first line regimen NP were incubated with pH5.0 and pH7.4. The cumulative percentage release profile of each drugs were calculated.

Figure 5.7 Antiviral assay.

A. Antiviral assay for LMV.

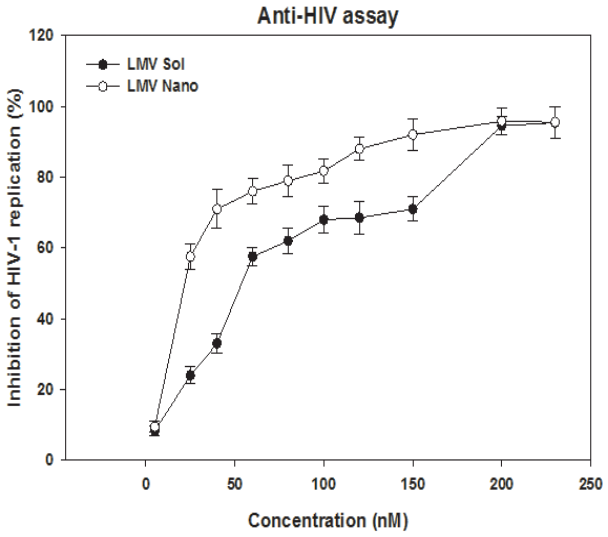

B. Combination drugs antiviral assay.

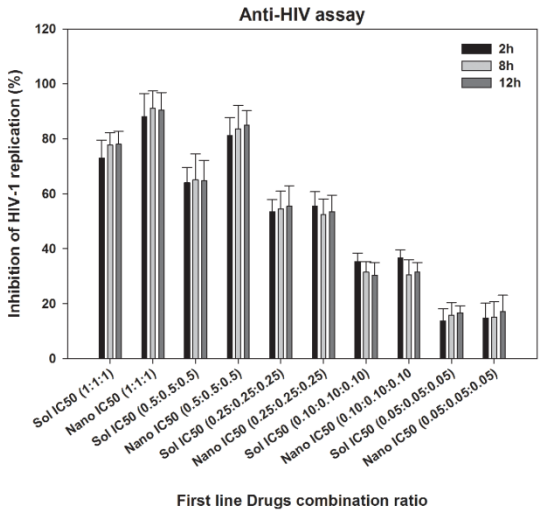

(A) The increasing concentration of lamivudine either in soluble or nanoformulation has been estimated for anti-HIV activity *in-vitro* as, described in method section. (B) After calculation of IC_{50} for AZT, EFV and 3TC; the various combination of IC_{50} for all three drugs either in soluble or nanoformulation has been analyzed for its antiviral activity. Data were presented as mean and standard deviation.

Figure 5.8 Hemolysis assay.

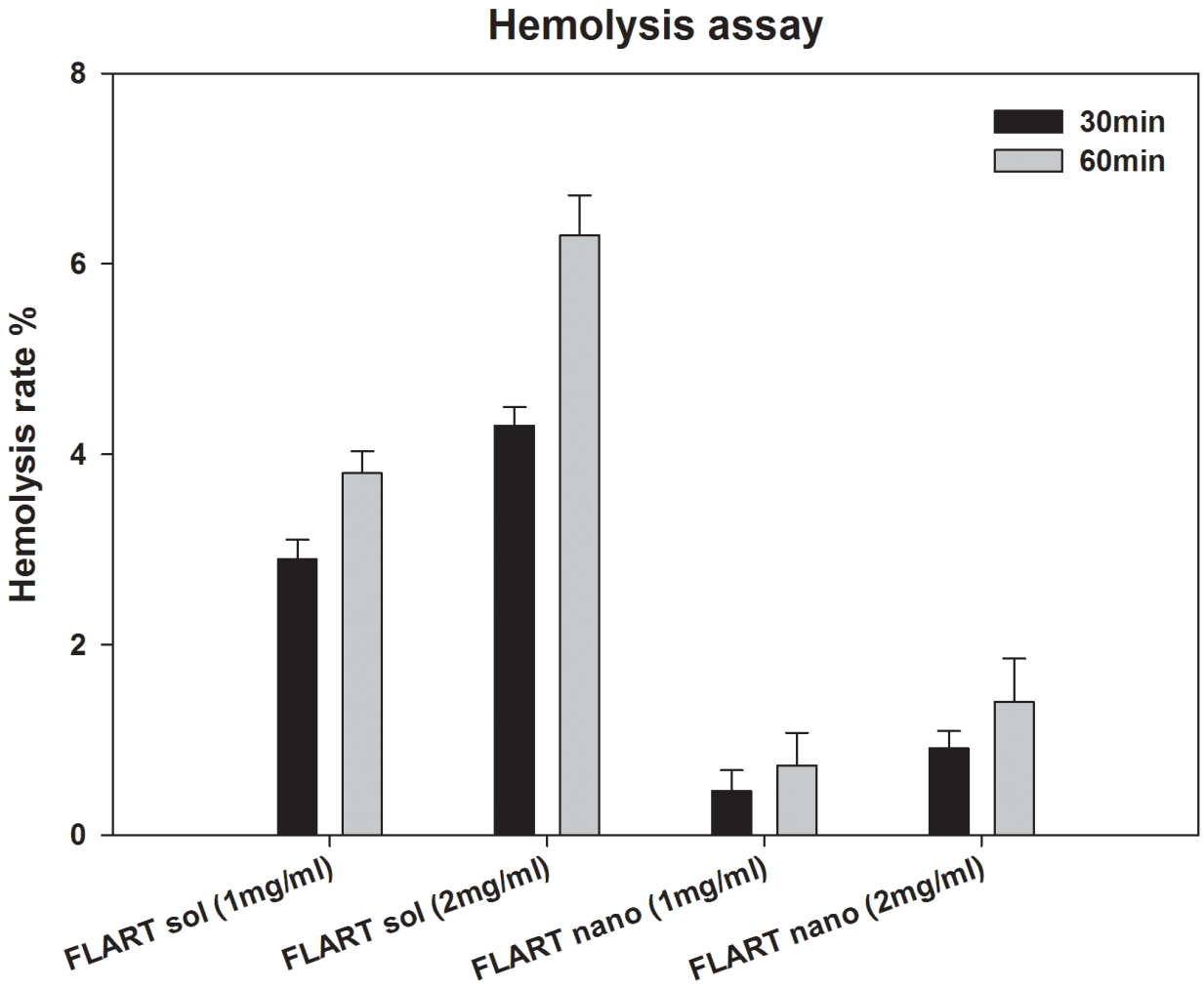

Hemolysis assay: Erythrocytes incubated with 1 or 2mg/ml or AZT+EFV+3TC in soluble or nanoform for 30 or 60min. HR% (Hemolysis rate) has been calculated and plotted. Data points were taken in triplicate and presented as Mean ± SD. Value of significance, **P < 0.005, *P < 0.05.

Figure 5.9 A. Tissue distributin.

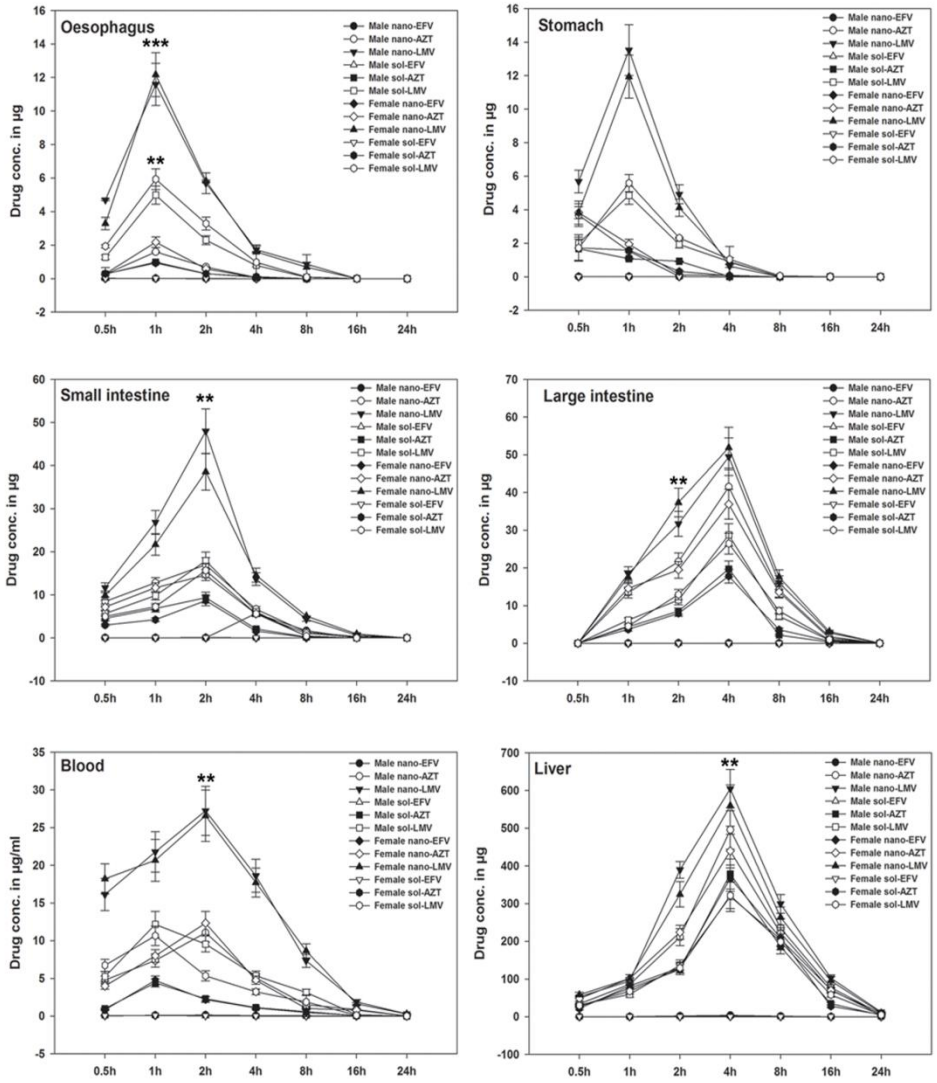

Tissue distribution of First line regimen (AZT+EFV+3TC) loaded lactoferrin nanoparticles: Rats were orally given 10mg/kg body weight of sol 1st line regimen (3.3 mg AZT+3.3 mg EFV+ 3.3 mg 3TC) and equivalent of its nanoformulation. Figure shows the drugs distribution in esophagus, stomach, small intestine, large intestine, blood, and liver. Each data points were taken in triplicate and presented as Mean ± SD. Value of significance, **P < 0.005, *P < 0.05. **Abbreviation:** Male-nano-EFV and Male-sol-EFV: - Concentration of EFV measured separately in male rats, when delivered via nano (AZT+EFV+3TC) combination and sol (AZT+EFV+3TC) combination respectively. Same nomenclature have been followed for other groups.

Figure 5.9 B. Tissue distributin.

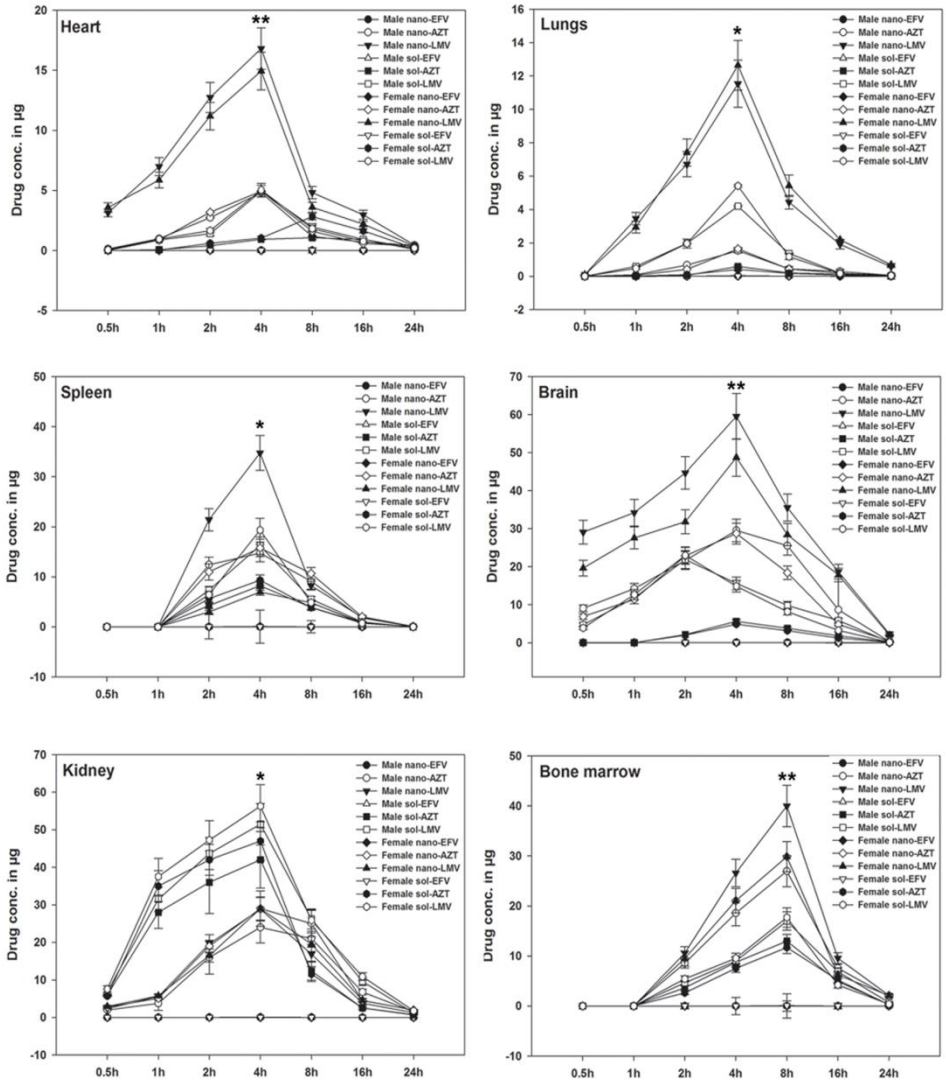

Tissue distribution of First line regimen (AZT+EFV+3TC) loaded lactoferrin nanoparticles: Rats were orally given 10mg/kg body weight of sol 1st line regimen (3.3 mg AZT+3.3 mg EFV+ 3.3 mg 3TC) and equivalent of its nanoformulation Figure shows the drugs distribution in heart, lungs, spleen, brain, kidney, and bone marrow. Each data points were taken in triplicate and presented as Mean ± SD. Value of significance, **P < 0.005, *P < 0.05. **Abbreviation:** Male-nano-EFV and Male-sol-EFV: - Concentration of EFV measured separately in male rats, when delivered via nano (AZT+EFV+3TC) combination and sol (AZT+EFV+3TC) combination respectively. Same nomenclature have been followed for other groups.

Figure 5.10 Safety analysis.

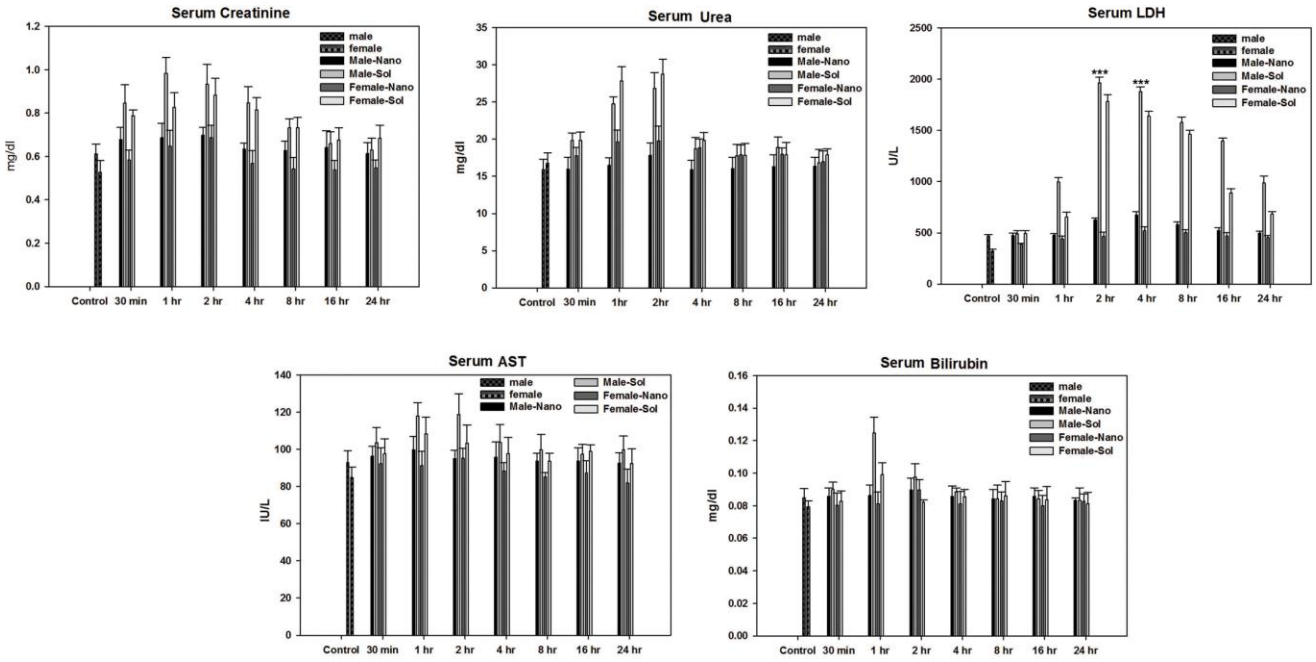

Safety analysis of First line regimen NP: Safety analysis was done using biochemical kits after oral administration of soluble first line (AZT+EFV+3TC) (10mg/kg) and equivalent of Nano form, in both male and female rats. Liver damage was estimated by Bilirubin and (Aspartate aminotransferase) AST level whereas Kidney toxicity was checked by Urea and creatinine level. General tissue damage was checked by LDH (lactate dehydrogenase) level. Nano-form has showed no toxicity to both liver and kidneys on the other hand it exhibited minimal urea levels when compared to the soluble form.

Figure 5.11 A. Histopathological analysis of tissues.

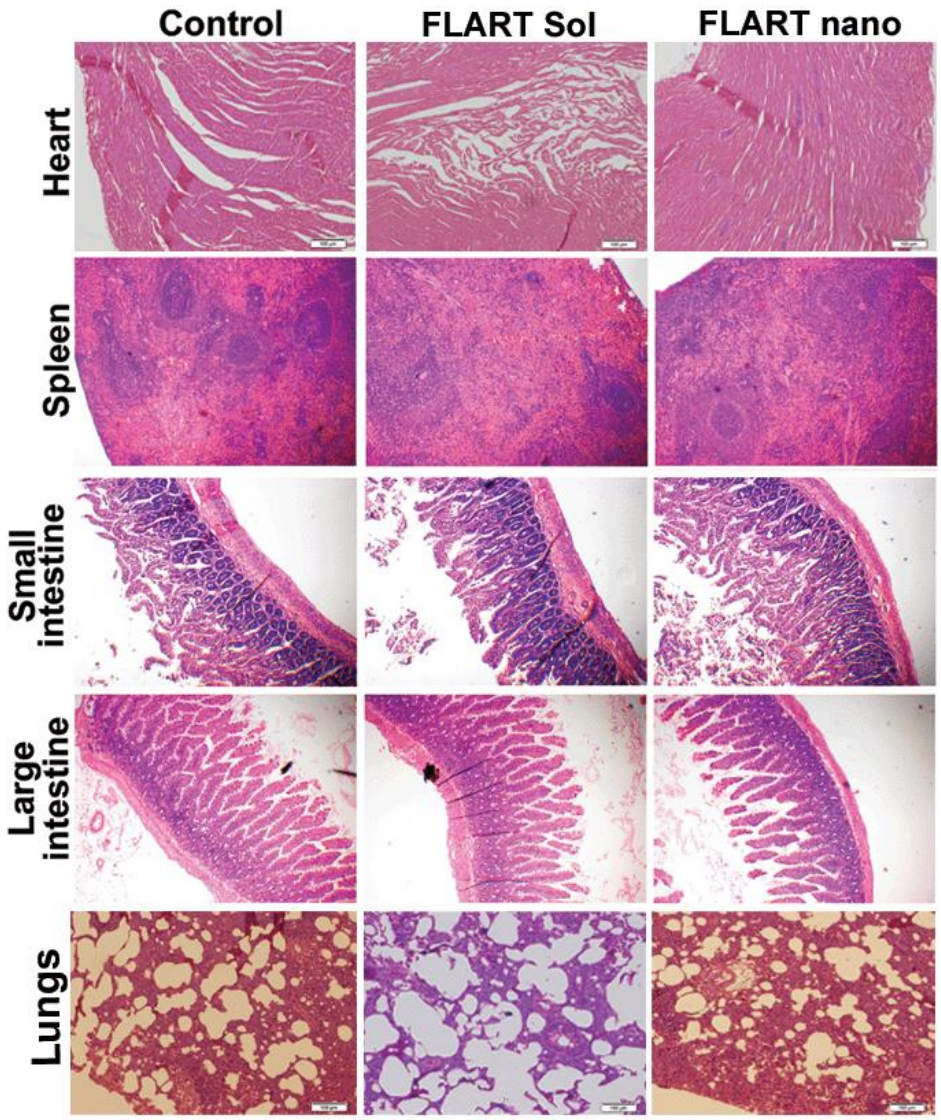

Histopathology of tissue treated with 1st line regimen: Rats were orally administered with FLART sol and FLART nano (10mg/kg body weight), after completion of 24hr time point, organs were removed and processed for cryo-sectioning followed by Hematoxylin and Eosin (H&E) staining. Figure shows the H&E images of heart, spleen, small intestine, large intestine and lungs.

Figure 5.11 B. Hematoxylin and Eosin staining.

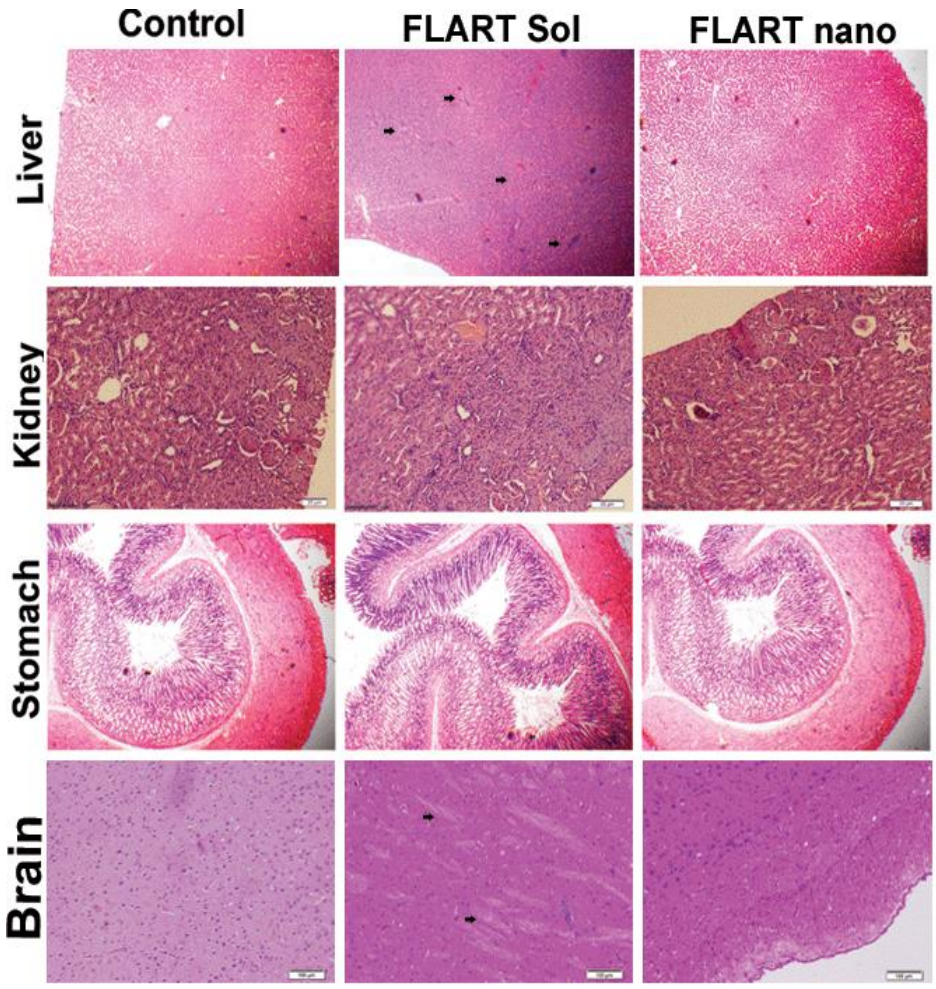

Histopathology of tissue treated with 1st line regimen: Rats were orally administered with FLART sol and FLART nano (10mg/kg body weight), after completion of 24hr time point, organs were removed and processed for cryo-sectioning followed by Hematoxylin and Eosin (H&E) staining. Figure shows the H&E images of liver, kidney, stomach and brain.

Tables

Table 5.1

Encapsulation efficiency (EE %) of first line regimen drugs (AZT+EFV+3TC) loaded lactoferrin nanoparticles under four different drug to protein combination:

Formulation code	Lactoferrin (mg)	Drugs (mg)			Encapsulation efficiency (%)		
		AZT	EFV	3TC	AZT	EFV	3TC
X1	10	3.33	3.33	3.33	56	49	54
X2	20	3.33	3.33	3.33	61	53	68
X3	30	3.33	3.33	3.33	65	58	71
X4	40	3.33	3.33	3.33	62	52	63

.

Table 5.2

PK profile for first line regimen (AZT+EFV+3TC) therapy. The blood were collected from the treated animals and PK parameter were calculated separately for AZT, EFV and 3TC.

Parameters	Units	AZT Male Nano	Soluble	Female Nano	Soluble
AUC	**(h)*(µg/ml)**	52.6876	13.7756	49.3596	13.1428
AUMC	**(h)^2*(µg/ml)**	265.396	57.5006	227.85	53.8528
C_{max}	**µg/mL**	11.05	4.41	12.331	4.73
T_{max}	**hr**	2	1	2	1
$t_{1/2}$	**hr**	2.39876	1.67061	2.31774	1.56536
MRT	**hr**	5.037	4.17	4.616	4.0975
		Efavirenz			
AUC	**(h)*(ng/ml)**	853.186	187.846	860.715	198.352
AUMC	**(h)^2*(ng/ml)**	4995.41	456.019	4971.22	522.148
C_{max}	**ng/mL**	136.91	85.33	139.71	89.92
T_{max}	**hr**	2	1	2	1
$t_{1/2}$	**hr**	2.63244	1.32146	2.49558	1.33783
MRT	**hr**	5.855	2.427	5.775	2.632
		Lamivudine			
AUC(tot)	**(h)*(µg/mL)**	176.338	57.368	177.633	38.766
AUMC(tot)	**(h)^2*(µg/mL)**	989.087	248.871	984.89	150.492
C_{max}	**µg/mL**	27.219	12.161	26.57	10.652
T_{max}	**hr**	2	1	2	1
$t_{1/2}$	**hr**	3.43024	1.35356	3.21595	1.40685
MRT	**hr**	5.60	4.33	5.54	3.88

Pharmacokinetic parameters abbreviations:

AUC (Area under the Curve): The integral of the concentration-time curve (after a single dose or in steady state).

AUMC (Area Under the first Moment curve): Partial area under the moment curve between t start and t end.

C_{max}: The peak plasma concentration of a drug after oral administration.

T_{max}: Time to reach C_{max}.

$t_{1/2}$: The time required for the concentration of the drug to reach half of its original value.

MRT: Mean Residence Times**.**

Chapter 6

Development and characterization of Second line regimen (3TC+TNF+ATV/r) loaded lactoferrin nanoparticles as oral formulation.

Introduction

The world health organization recommend the combination of antiretroviral drugs for HIV/AIDS treatment. Generally two types of combination HAART therapy is suggested for the treatment. The HAART therapy has significantly reduce the mortality and morbidity of HIV infected patients [150]. If there was a treatment failure with the first line HAART therapy, it is recommended to switchover to second line therapy. The base of second line therapy is mainly on boosted protease inhibitor, ritonavir (RTV or r). Second line HAART is recommended with a combination of two NRTI plus one protease inhibitor boosted with ritonavir. If Zidovudine or AZT (NRTI) was already used in first line drugs, then it is not recommended to use again AZT as NRTI in second line. Instead of AZT, tenofovir in combination with lamivudine (3TC). Few report suggested that, the use of lamivudine in second line regimen didn't significantly affect the viral load in patient [151]. In some cases, tenofovir is used in first line as NRTI, in that case if there is a switch to second line, it is suggested to use AZT as NRTI in second line. The importance of second line HAART is the presence of PI boosted with ritonavir. Boosted dose is recommended in a ratio of 3:1 for PI:r. In some cases lopinavir boosted ritonavir is used in combination with two NRTI. Mostly it is found that, HIV infected person is co-infected with Hepatitis B, in that case tenofovir + lamivudine is carried out for treatment of HBV and the second line regimen shall include some anti-HIV drugs [152].

Results

Drug – protein interaction study: fluorescence measurement.

Second line drugs include a combination of lamivudine, tenofovir, atazanavir and ritonavir. For optimizing the time for nanoparticles preparation, 1μM of drugs (tenofovir and atazanavir) was incubated with 1μM of lactoferrin protein. The spectra were measured as described in methods sections. Spectra shows that, for tenefovir the saturation period is approximately 40minutes (Fig. 6.1A), whereas for atazanavir it is approximately 45minutes

(Fig. 6.1B). In previous objective we have shown that, for lamivudine the saturation period was found to be approx. 25minutes. In account of this, we have incubated the drug to protein for approx. 45 minutes.

TEM, FE-SEM and DLS characterization of second line drugs loaded nanoparticles.

The diameter and surface morphology of the second line loaded lactoferrin nanoparticles were evaluated using TEM and FE-SEM using the procedure mentioned in the methods section. For FE-SEM and TEM the particles used were in dried form. The average size of SLART NP measured using TEM and FE-SEM were found to be 23nm (Lacto-nano- TEM), 60nm (SLART NP- TEM), 70nm (SLART NP- FE-SEM) (Fig. 6.2A, B and C).

DLS analysis (Hydrodynamic size, zeta potential and PDI)

The hydrodynamic size, surface charge and PDI of nanoparticles were estimated using DLS. The hydrodynamic radii of the second line loaded lactoferrin nanoparticles (in suspension form) was found to be approx. 113nm (Fig. 6.2D). The zeta potential and PDI were found to be -27mv and 0.39 respectively.

Assembly of nanoparticles and FT-IR spectroscopic study

FT-IR study was done to evaluate the stability of drugs in nanoparticles. FT-IR analysis of physical mixture of 3TC, TNF, ATV plus RTV and the SLART NP (lyophilized form) were performed and shown in Fig. 6.3A and B. The FT-IR graphs have been analyzed critically and it was found that, the featured peaks related to major functional groups were intact in case of nanoformulation. A slight variation in the peaks were observed, which may be due to dipole moment of electrostatic bond present in nanoparticles.

Drugs loading (DL %) and Encapsulation efficiency (EE %)

The drug loading (drug content) percentage and encapsulation efficiency percentage were calculated using the formula mentioned in the method section. The estimated drug loading % and encapsulation efficiency% was presented in Table 6.1.

pH and simulated fluid drugs release from second line loaded nanoparticles.

Nanoparticles equivalent to 300µg was subjected under various pH condition and two type of simulated body fluid (SIF and SGF). The drugs release profile was found to be same as of individual and first line loaded drugs as mentioned in earlier objectives. In this study, maximum amount of drug release was observed at pH 5 (Fig. 6.4A). Out of three drugs, lamivudine release was found to be maximum.

***In vitro* percent release from nanoparticles**

The cumulative percent release of drugs from nanoparticles were performed at pH5.0 and pH7.4. Only trace amount (<15%) of drugs was released at circulatory pH7.4. Exposure to pH5.0 leads to the more and sustain release of drugs from nanoparticles as compared to pH7.4 (Fig. 6.4B). All three drugs, 3TC, TNF and ATV were found to release from nanoparticles in a biphasic manner; up to 60% of drugs were released within first 4h, followed by a sustain release. Out of three drugs, lamivudine was found to release bit early as compared to other two drugs. Thus suggesting that its interaction with lactoferrin while formation of nanoparticles slightly different from other drugs.

Anti-HIV activity of nanoparticles

A dose dependent anti-HIV assay was done for tenefovir, atazanavir and ritonavir to evaluate the IC_{50} value for the soluble as well as their nano counterparts (Fig. 6.5A, B and C). The anti-HIV assay was done using the p24 ELISA capture assay, as mentioned in methods section. The IC50 value was found to be 28.31nM for Sol TNF, 12.14nM for nano TNF, 6.43nM for Sol ATV, 4.34nM for nano ATV, 19.71nM for RTV and 7.23nM for nano RTV. After estimating the IC_{50} for individual drugs, a various proportion of combination of IC_{50} values of drugs was again evaluated for the anti-HIV activity (Fig. 6.5D). The results shows that 50% of concentrations of drugs in combination nanoparticles is adequate in inhibition of HIV-1 replication, thus enhancing the efficacy of combination drugs by 2-fold.

Hemolytic effect of FLART NP

The Rat's erythrocytes were subjected to lysis under soluble combination of second lines drugs and nanoformulation. Two different concentration (1mg/ml and 2mg/ml) of soluble

and nano drugs were incubated with erythrocytes as described in methods sections for 30min and 60min. The hemolysis rate was calculated using the formula mentioned in method sections and it was found that there was <3% of hemolysis rates was observed (Fig. 6.6).

In vivo pharmacokinetics study

A single dose of soluble second line drugs and equivalent of its nanoformulation was administered orally to the rats. After completion of indicated time points, concentration of drugs at various time points were estimated and pharmacokinetics parameters were evaluated (Table 6.2). The PK profile was found to be improved both in male as well as female rats.

Drugs tissue distribution study

After sacrificing the rats, tissues were isolated and processed. The concentration of all the three drugs were estimated using HPLC. The drugs tissue distribution was plotted in Fig. 6.7A&B.

Biochemical safety analysis

Various safety parameters such as urea, AST, creatinine and bilirubin were estimated in blood and plotted (Fig. 6.8). A significant elevation in the level of urea and bilirubin were found at 2h and 4h when treated with soluble combination of drugs, whereas the same has been decreased when treated with the nanoformulation. AST and creatinine levels were found to be raised throughout the study period, but the maximum increase was observed in 1, 2 and 4h. The higher level of AST and creatinine was lowered down after treatment by nanoformulation.

Histopathology analysis

The histopathology analysis was done for all the major tissue. The tissue sections images indicates the presence of any inflammation in any organs. Fig. 6.9A and B showed that there was no sign of any inflammation or lesion when treated with either soluble or nanoformulation.

Discussion

After the treatment failure of first line drugs, the second line drugs therapy is recommended. Generally second line drugs includes in combination of two NRTI plus one protease boosted ritonavir. Our current study is focused on the development of second line combination drugs loaded lactoferrin nanoparticles. The nanoparticles were developed using the protocol mentioned in methods section. The superiority of our protocol is that, it is simple, fast and it does not involve any harmful chemicals that may affect the cellular integrity. This nanoformulation is highly stable and biodegradable. The second line drugs combination used in this study includes lamivudine + tenefovir + atazanavir boosted ritonavir. The encapsulation efficiency for all the drugs were found to be >55% for all. The microscopic and DLS characterization revealed a significant increase in the size of nanoparticles after loading of drugs. The in vitro release and percent release results confirmed the stability of particles at adverse pH condition and particles are found to be stable at circulatory pH. The drug release was <15% in case of pH7.4, revealed the stability of formulation in circulatory condition as well as release of drugs under intracellular condition. The anti-HIV activity of nano formulated drugs were improved as compared to the soluble counterpart. The oral PK study reveals an outstanding improvement in PK profile, when treated with nanoformulations. PK profile was significantly improved in terms of 4-6 fold increase in AUC and the half-life of all drugs were improved by at-least 2fold in Nano formulated drugs. Further the nanoformulation doesn't leads to any tissue related toxicity as revealed by histopathology and safety analysis study. In conclusion the second line drugs loaded lactoferrin nanoparticle could serve as better alternate formulation for HIV therapy.

Conclusion

The current objective deals with the preparation and detailed characterization of second line HAART drugs loaded lactoferrin nanoparticles. *In vitro* and *in vivo* studies suggest the, superiority of nanoformulation over the soluble combination of drugs. The nanoparticles are very well dispersed and in arrange of 113nm as assessed using DLS. The in vitro anti-

HIV activity of individual drug nanoformulation and in combination are found to be more efficacious than its soluble form. Further the pharmacokinetics study on rats shows, the improved pharmacokinetics profile of nanoformulation over soluble drugs with decreased tissues related toxicity.

Figure 6.1 Drug – Protein Saturation study.

A. TNF- Lf interaction. **B. ATV-Lf interaction**

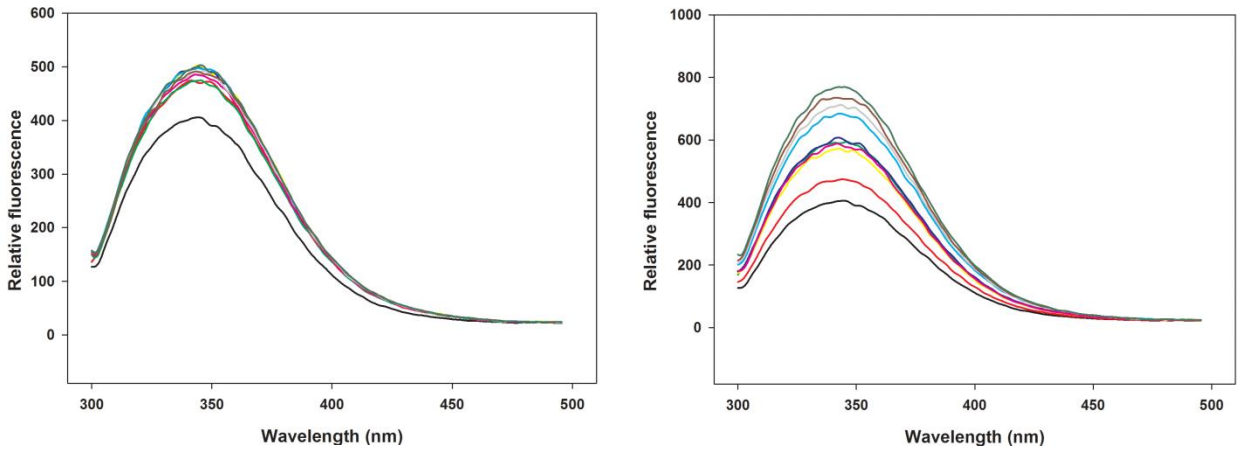

The flourscence spectra obatined after the incubation of one micrmolar of tenefovir or atazaanvir with same concentration of lactoferrin. The specra were recorded at room temperature at an intervel of five minutes up to 60minutes.

Figure 6.2 TEM, FE-SEM, and DLS analysis of second line nanoparticles.

D. Blank nanoparticles (Lacto-nano)

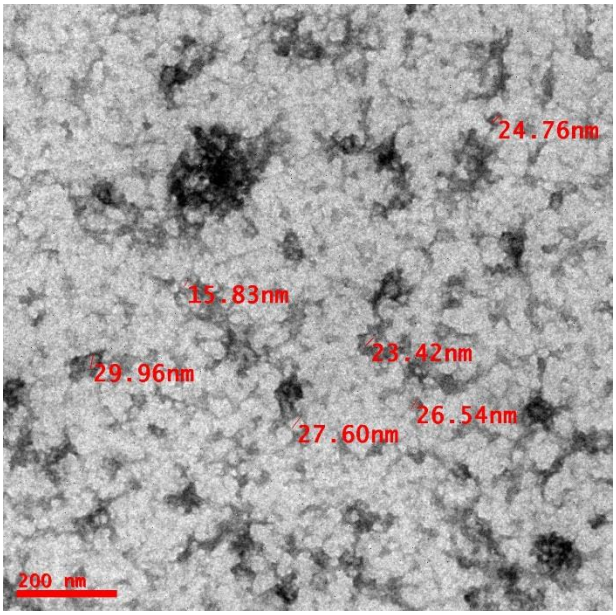

B. SLART nanoparticles

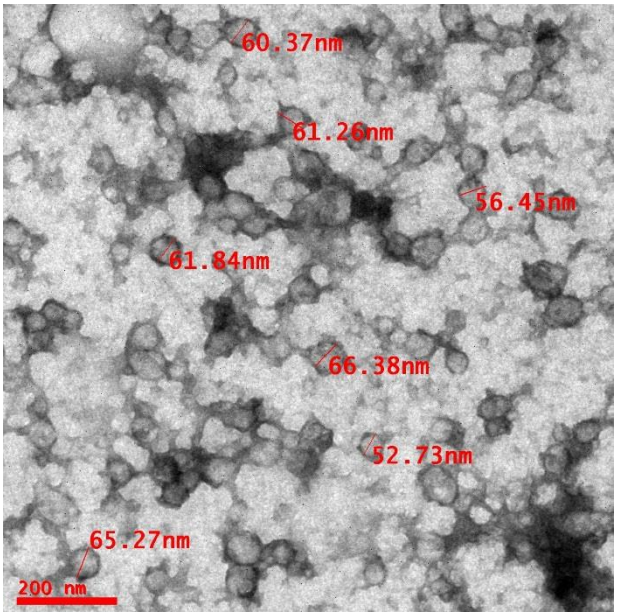

C. FE-SEM (SLART NP)

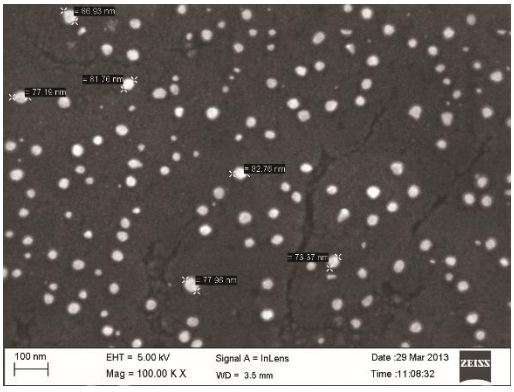

D. DLS (SLART NP)

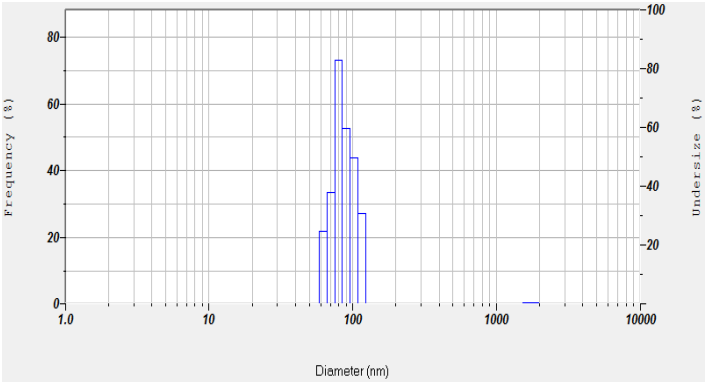

(A) TEM image of Blank NP reveals the size of approximately 23nm. **(B)** The TEM size for nanoparticles loaded with second line of drugs was approximately 60nm. **(C)** FE-SEM image of SLART NP shows the average diameter equal to 70nm. **(D)** The hydrodynamic radii of SLART NP was found to be in a range of 113nm.

Figure 6.3 FT-IR spectra

A. Second line sol

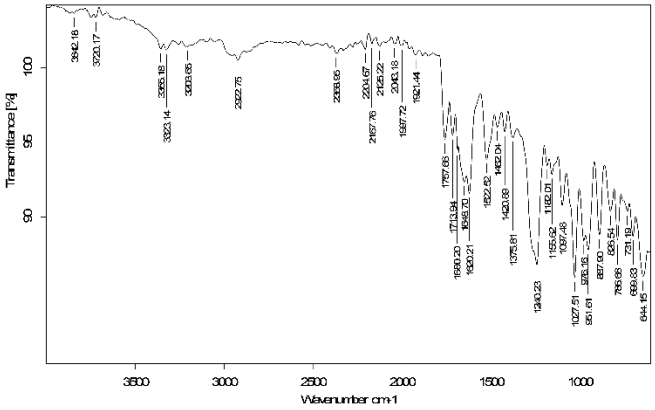

B. Second line nano

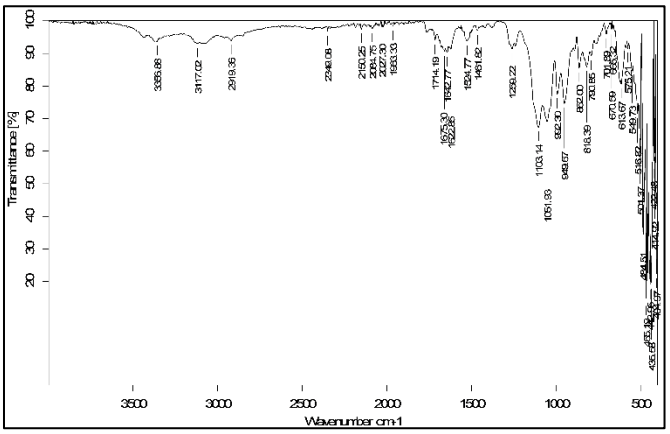

Comparision of presence of featured groups in sol and naoform.

Functional groups	Second line sol	Second line nano
P═O stretch (TNF)	1680.20 cm^{-1}	1675.30 cm^{-1}
aromatic C=C (3TC)	1462.04 cm^{-1}	1461.82 cm^{-1}
C=O stretching (RTV)	1713.94 cm^{-1}	1714.19 cm^{-1}
C=O stretching (ATV)	1620.21 cm^{-1}	1622.85 cm^{-1}

Figure 6.4 pH dependent and percent release of second line dugs loaded nanoparticles.

A. pH release. **B. Percent Release**

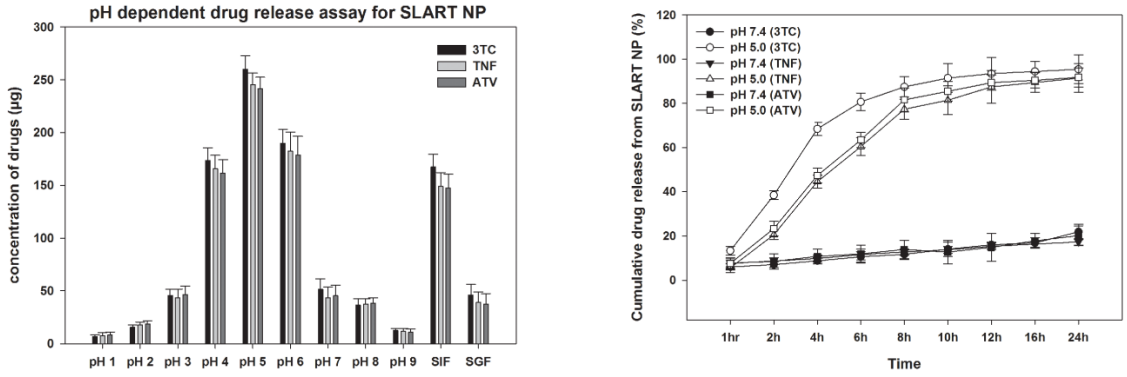

(A) In vitro pH release of SLART NP. SLART NP was challenegd to different pH condtion as well as simulated fluid. A maximum drug relase was observed at pH5. **(B)** The Percent drugs relase experiemnt was done at pH5 and pH7.4 for various time points.

Figure 6.5 Antiviral assay.

A. Antiviral assay for TNF.

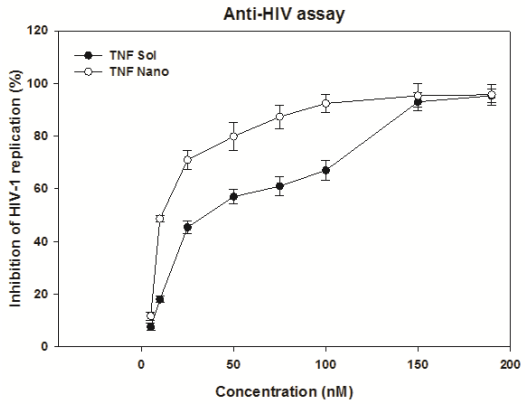

B. Antiviral assay for ATV.

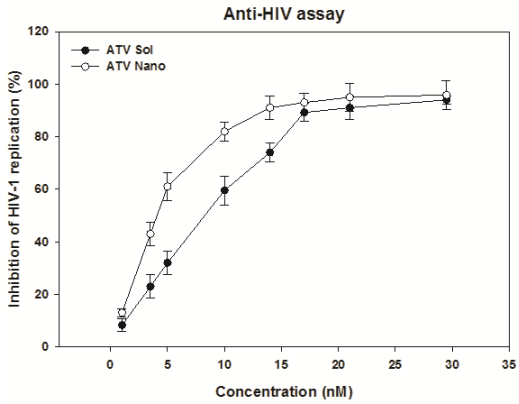

C. Antiviral assay for RTV.

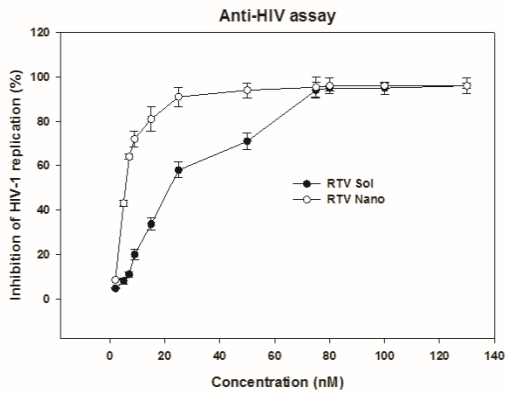

D. Combine Antiviral assay.

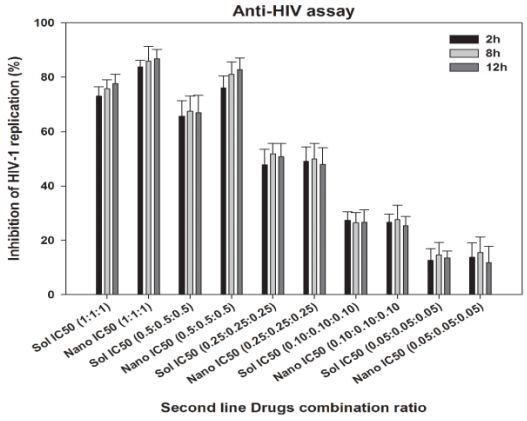

(A-C) Mono-drug antiviral assay: The dose dependent antiviral assay of tenefovir, atazanavir, and ritonavir. **(D) Combination drugs antiviral assay:** Various different IC_{50} ratio of all second line drugs were mixed in soluble and nano form. The antivral assay were performed and plotted.

Figure 6.6 Hemolysis assay.

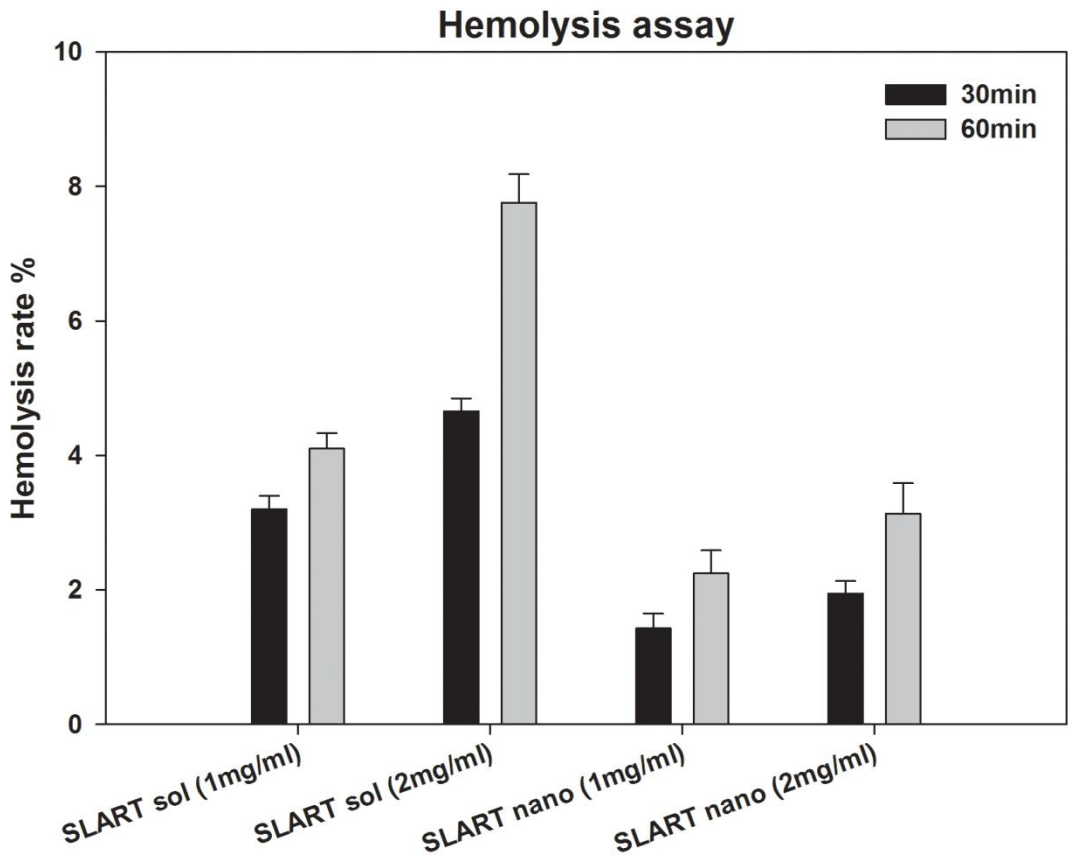

Rat's erythrocytes was chellneged with 1mg/ml or 2mg/ml of soluble second line drugs and equivalent to nanoformulatons. The rate of hemolysis was evaluetd using the formula mentioned in mehtods sections.

Figure 6.7 A. Tissue distributin.

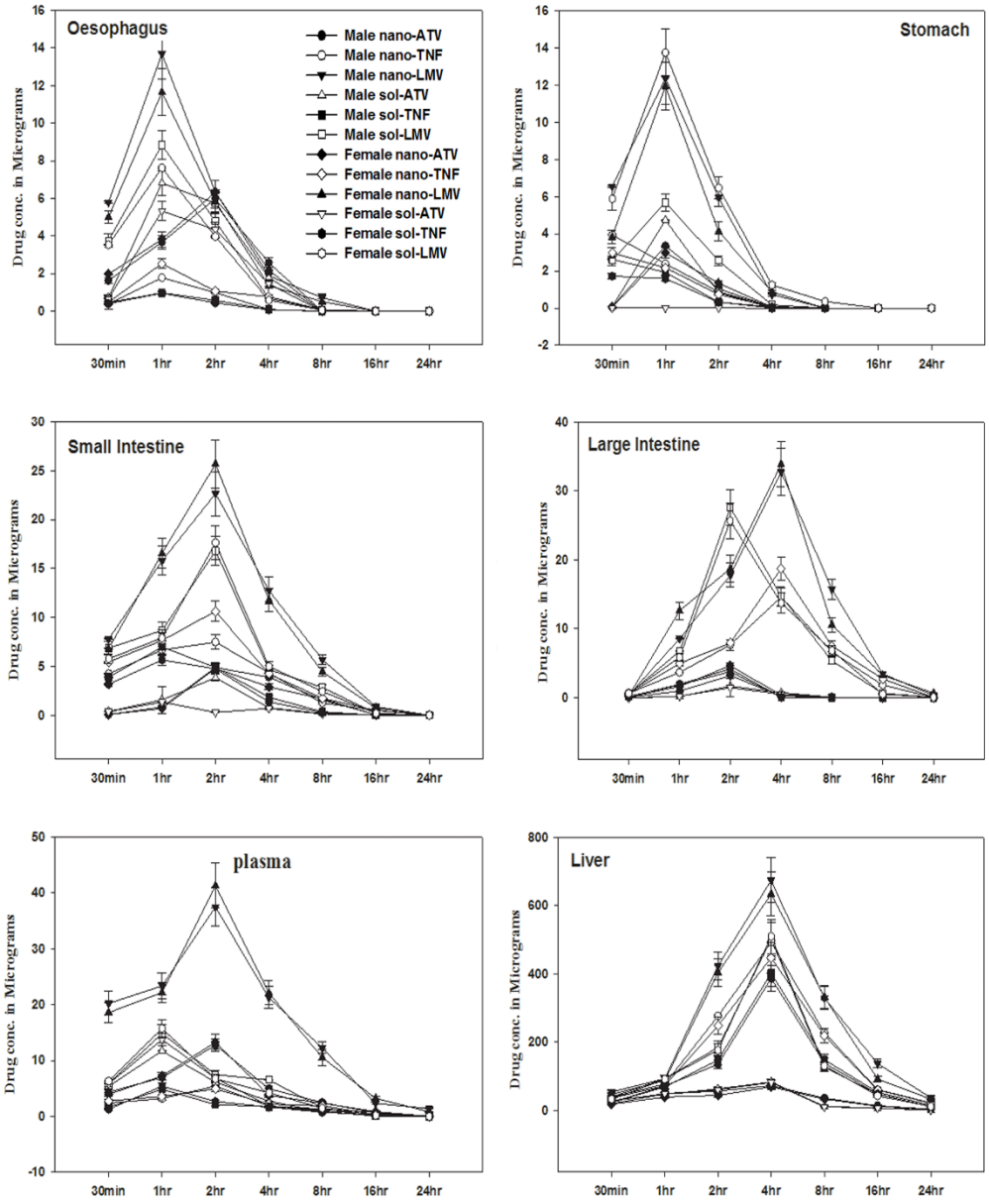

Single dose of second line HAART drugs in soluble and nanoform was administered orally. Figure shows that distribution of drugs in espophagus, stomach, small intestine, large intestine, plasma and liver.

Figure 6.7 B. Tissue distributin.

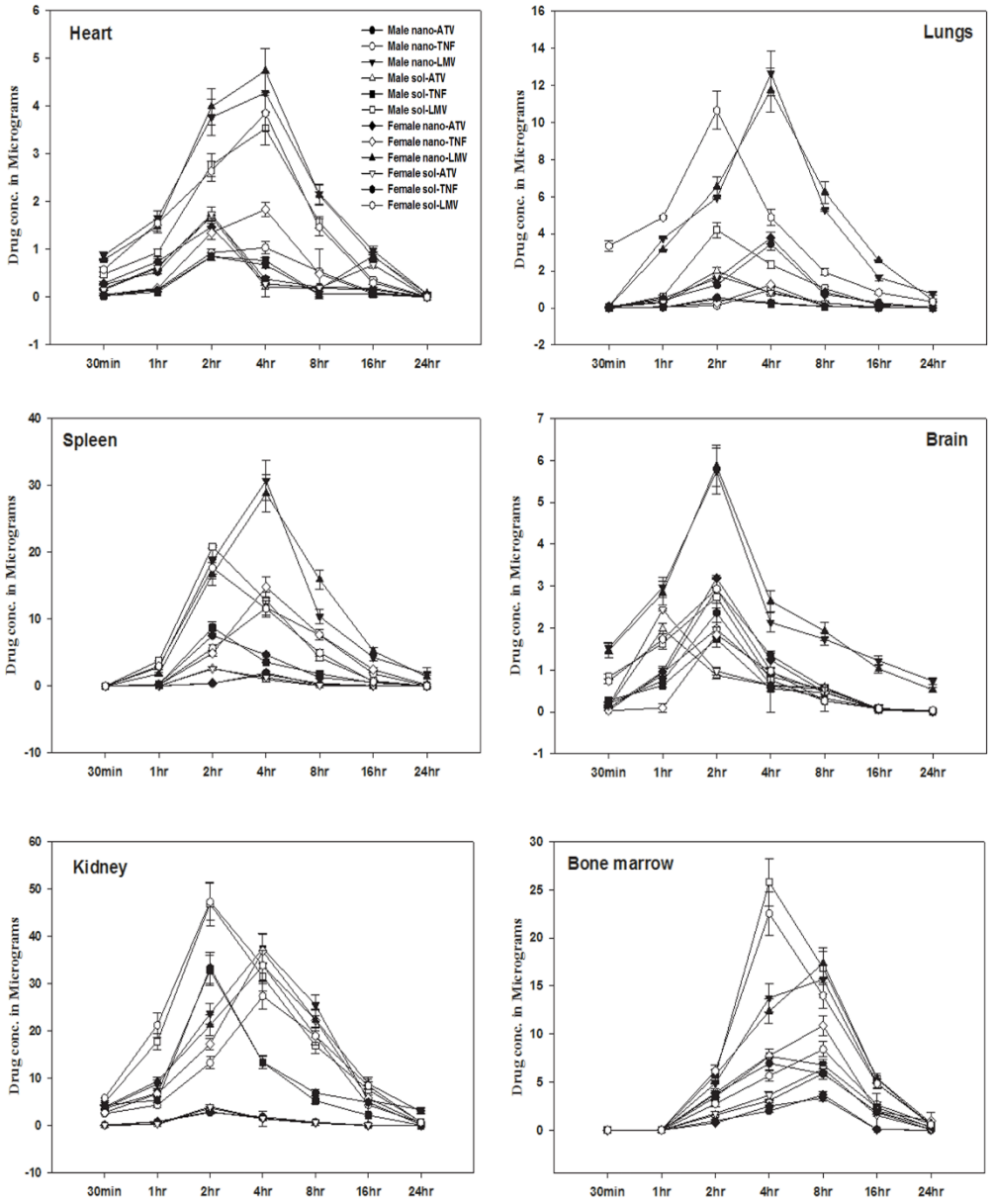

Single dose of second line HAART drugs in soluble and nanoform was administered orally. Figure shows that distribution of drugs in heart, lungs, spleen, brain, kidney and bone marrow.

Figure 6.8 Safety analysis.

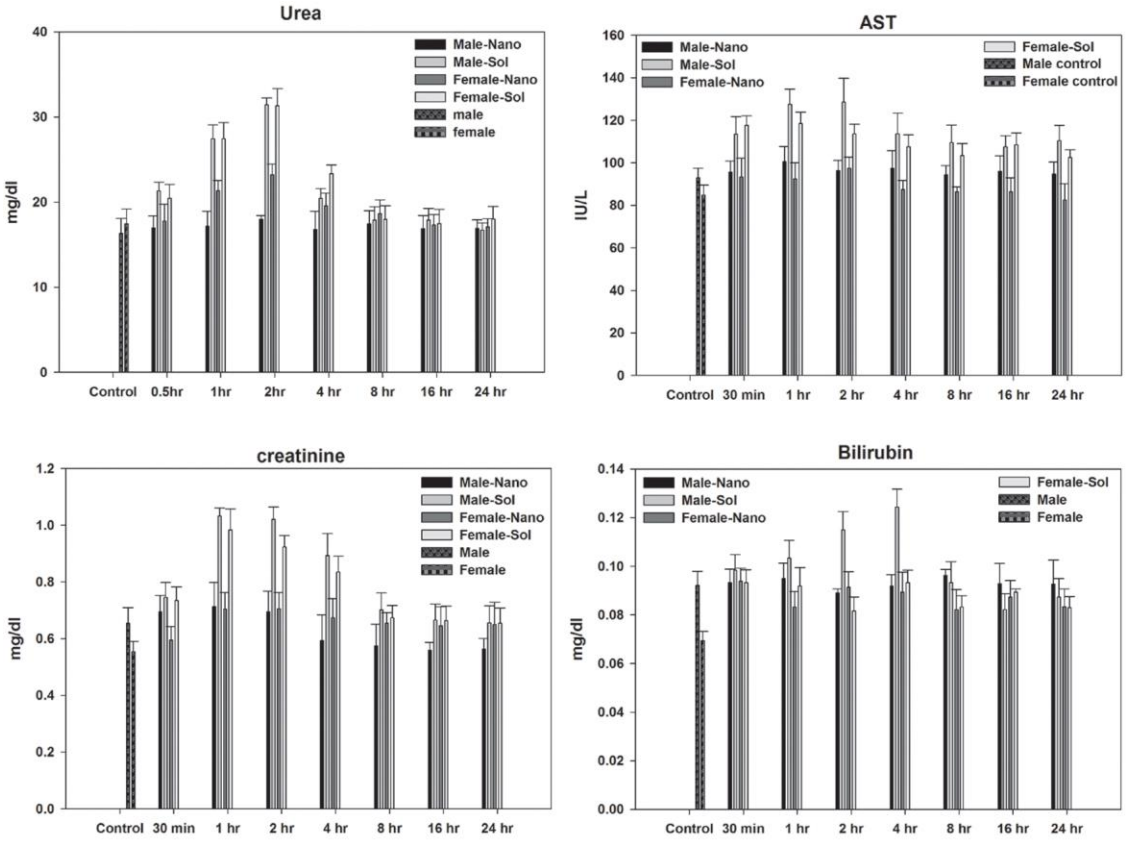

The isolated serum was subjected for various safety parameters, such as urea, AST, creatinine and Billirubin at indicated time points such as 30min, 1h, 2h, 4h, 8h, 16h, and 24h. control denotes the animal treated with saline.

Figure 6.9 A. Histopathological analysis of tissues.

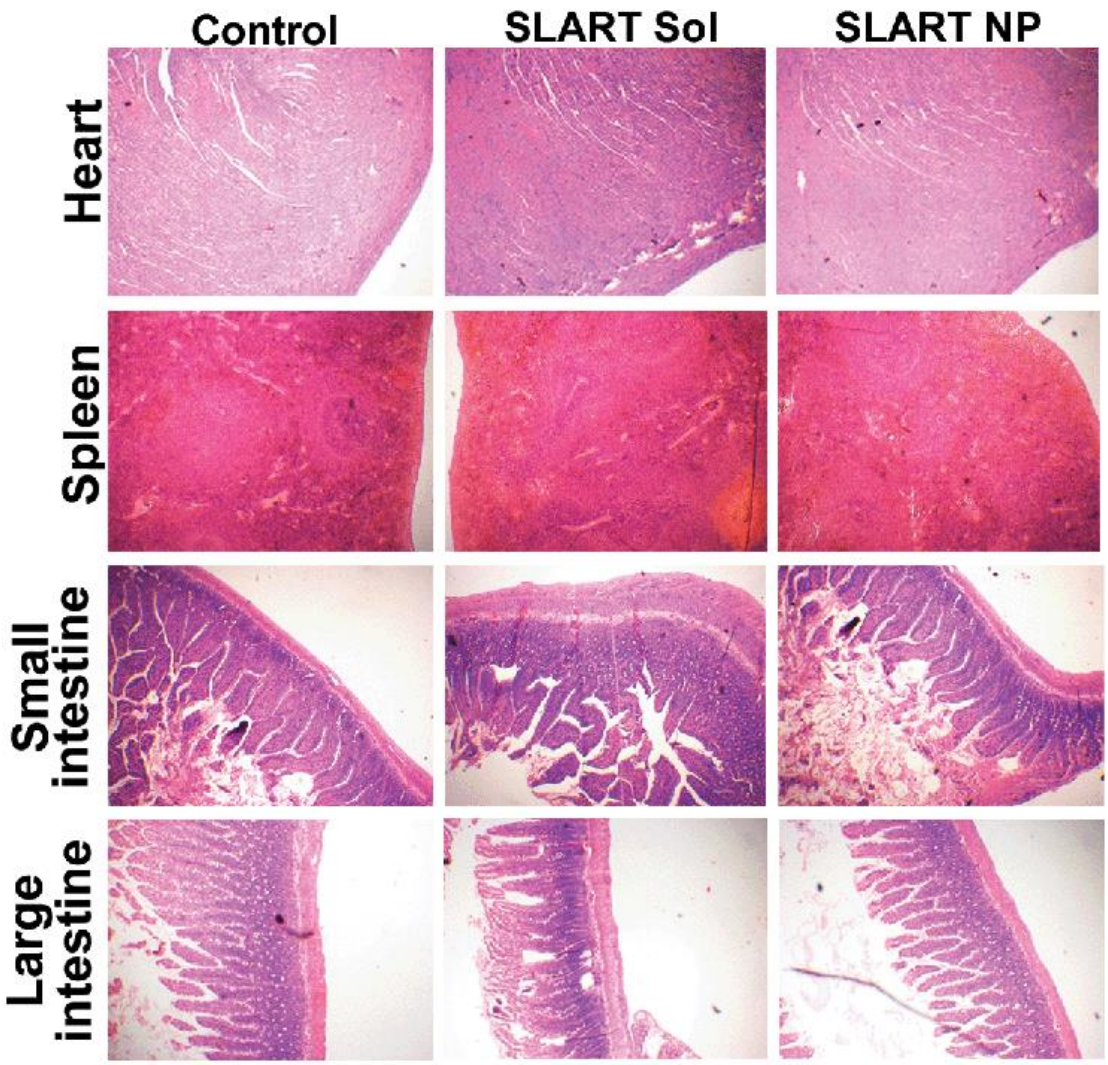

H&E images of Heart, Spleen, small intestine and large intestine.

Figure 6.9 B. Hematoxylin and Eosin staining.

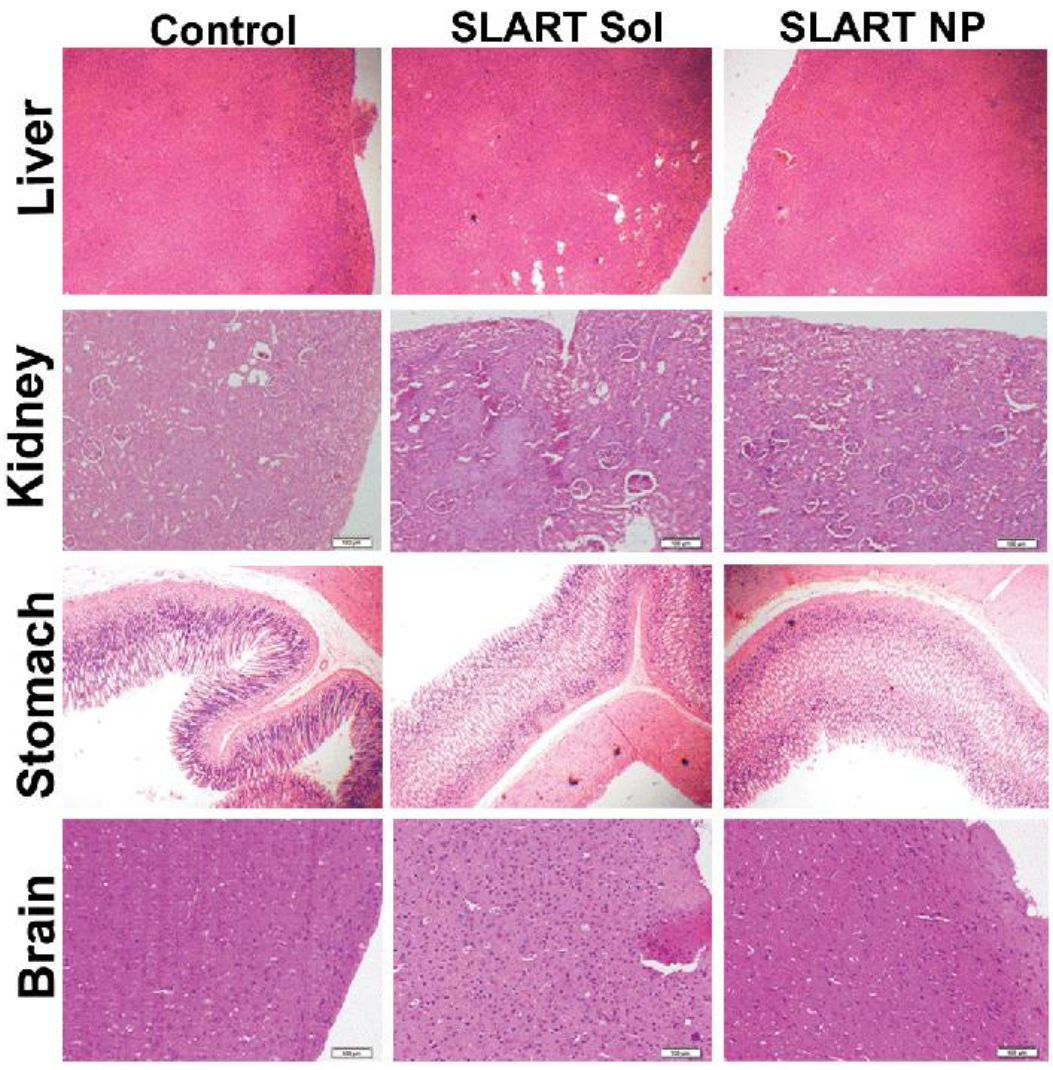

H&E images of Liver, Kidney, Stomach and Brain.

Tables

Table 6.1

DL (Drug loading percentage) and EE (Encapsulation Efficiency percentage)

Drugs	Drug loading	Encapsulation Efficiency
3TC	6.05%	73%
TNF	5.01%	62%
ATV	5.49%	68%

Table 6.2.

PK profile for second-line regimen (3TC+TNF+ATV/r) therapy. The blood were collected from the treated animals and PK parameter were calculated separately for 3TC, TNF and ATV.

		Male		Female	
Parameters	**Units**	**Nano**	**Soluble**	**Nano**	**Soluble**
		LAMIVUDINE (3TC)			
AUC	**(h)*(µg/ml)**	**243.456**	**51.5115**	**243.927**	**45.8128**
AUMC	**(h)^2*(µg/ml)**	**1628.35**	**191.137**	**1585.5**	**170.315**
C_{max}	**µg/mL**	**37.4764**	**14.8345**	**41.2647**	**15.7358**
T_{max}	**hr**	**2**	**1**	**2**	**1**
$t_{1/2}$	**hr**	**4.52772**	**1.73108**	**4.29726**	**1.76839**
		TENOFOVIR			
AUC	**(h)*(ng/ml)**	**30.4453**	**17.5858**	**30.9988**	**19.0855**
AUMC	**(h)^2*(ng/ml)**	**207.657**	**78.3823**	**189.605**	**93.9559**
C_{max}	**ng/mL**	**5.437**	**4.8753**	**4.9274**	**5.4242**
T_{max}	**hr**	**2**	**1**	**2**	**1**
$t_{1/2}$	**hr**	**3.73008**	**1.97014**	**3.4107**	**2.03589**
		ATAZANAVIR			
AUC(tot)	**(h)*(µg/mL)**	**55.8907**	**33.5643**	**55.7568**	**36.9697**
AUMC(tot)	**(h)^2*(µg/mL)**	**284.89**	**111.65**	**297.312**	**142.418**
C_{max}	**µg/mL**	**11.334**	**11.7348**	**13.2735**	**13.7457**
T_{max}	**hr**	**2**	**1**	**2**	**1**
$t_{1/2}$	**hr**	**2.20149**	**1.43037**	**2.40526**	**1.91018**

Pharmacokinetic parameters abbreviations:

AUC (Area under the Curve): The integral of the concentration-time curve (after a single dose or in steady state).

AUMC (Area Under the first Moment curve): Partial area under the moment curve between t start and t end.

C_{max}: The peak plasma concentration of a drug after oral administration.

T_{max}: Time to reach C_{max}.

$t_{1/2}$: The time required for the concentration of the drug to reach half of its original value.

MRT: Mean Residence Times**.**

Chapter 7

Conclusions

Conclusions

- In this study a total of four types drug loaded NP (AZT NP, EFV NP, 1st line HAART NP and 2nd line HAART NP) have been prepared using sol-oil chemistry. In addition to this Blank NP or Lacto-nano was also prepared using the same methodology.

- All NP have been characterized microscopically using various techniques such as FE-SEM, TEM and AFM. These studies showed the size for Blank NP in the range of 25-30nm, whereas for drug(s) loaded lactoferrin nanoparticles the diameter found to increase to 50-70nm.

- The DLS analysis to study hydrodynamic radii, zeta potential, and polydispersity index. The hydrodynamic radii and zeta potential for drug(s) loaded nanoparticles was found to be an average of 103 to 107nm and -19 to -27mV respectively. For Blank NP the same was found to be 54nm and -21mV. The PDI index for blank and drug/s loaded nanoparticles was observed in a range of 0.3 to 0.5 suggesting uniformly dispersed nanoparticles with negative surface charge for its stability.

- The DSC study showed higher temperature of phase transition for efavirenz loaded lactoferrin nanoparticles confirming the stability of nanoparticles.

- The stability of drug(s) loaded in NP has been analyzed through FT-IR study, and found that the key functional groups related to respective drugs are intact in the nanoformulation suggesting that drugs are structurally intact.

- The encapsulation efficiency e (EE %) was calculated for each type of NP and found as follows, AZT NP = 67%, EFV NP = 59%, 1st line HAART NP (AZT = 65%, EFV = 58%, 3TC = 71%) and 2nd line NP (3TC = 73%, TNF = 62%, ATV = 68%). These results suggest that our process allow cooperative loading of drugs without compromising due to drug-drug interactions.

- pH dependent drug release assay of NP shows that pH 5 is the optimum pH for drug release and at the same time NP are found to be stable in intestinal and gastric

conditions, as only 10-20% of drug(s) concentrations were released in simulated gastric and intestinal fluid.

- Percent drug release profile of NP was performed at two different pH (5.0 and 7.4). pH 5.0 showed a bi-phasic drug release; where 40-55% of drugs were released up to 4-6h followed by a constant and sustain release up to 24h.

- Antiviral properties of all ARV drugs have been found to be improved with significant decrease in IC_{50} (50% inhibitory concentration) of nano form as compared to its soluble counterpart.

Individual drug anti-viral activity.

First line regimen drugs	Soluble form IC_{50}	Nanoformulation IC_{50}
AZT	33.4 nM	20.5 nM
EFV	2.56 nM	1.1 nM
3TC	42.57 nM	23.18 nM
Second line regimen drugs		
TNF	28.31 nM	12.14 nM
ATV	6.43 nM	4.34 nM
RTV	19.71 nM	7.23 nM

- The combination therapy (First-line and Second-line HAART) are found to be more efficacious in their nano form as compared to its soluble form combination. As the percent HIV inhibition is found to be equal or improved even treated with 50% of their soluble form combination.

- The comparative *in-vivo* pharmacokinetics (PK) studies were performed on Wistar rats. Results showed a significant impartment of PK profile of drug when nanoformulation is administered (C_{max}, $t_{1/2}$ and AUC) suggesting higher bioavailability of drugs as compared to its soluble equivalents.

- The bio-tissue distribution of individual drug NP and HAART NP shows the longer retention time for nanoformulation as compared to its soluble form.
- The safety analysis studies have shown the elevated level of serum creatinine, LDH, urea, AST and ALT in rats treated with soluble formulations, whose levels were significantly decreased when treated with nanoformulation.
- The histopathology analysis for major tissues were performed after administration of soluble and Nano formulated drugs. The results shows the presence of inflammation in few tissue in soluble treated rats, whereas in nanoformulation treated rats no sign of inflammation was observed.
- The drugs associated specific toxicity (AZT- Bone marrow suppression toxicity, EFV- Skin hypersensitivity, First-line HAART & Second-line HAART- Hemolysis assay) have been reduced significantly when treated with nanoformulation.
- In summary, Lactoferrin nanoparticle formulation composed of single or multiple antiretroviral drugs is efficacious, enhanced bioavailability, PK profile and decreased toxicity.

References

1. Javaux, E.J., Extreme life on Earth--past, present and possibly beyond. Res Microbiol, 2006. 157(1): p. 37-48.
2. Lazcano, A., Historical development of origins research. Cold Spring Harb Perspect Biol, 2010. 2(11): p. a002089.
3. Pereto, J., J.L. Bada, and A. Lazcano, Charles Darwin and the origin of life. Orig Life Evol Biosph, 2009. 39(5): p. 395-406.
4. Ahmed, M. and P. Liang, Study of Modern Human Evolution via Comparative Analysis with the Neanderthal Genome. Genomics Inform, 2013. 11(4): p. 230-8.
5. Janeway CA Jr, T.P., Walport M, et al, Immunobiology: The Immune System in Health and Disease. 5th edition. 2001.
6. NIH Curriculum Supplement Series [Internet].
7. Turner, B.G. and M.F. Summers, Structural biology of HIV. J Mol Biol, 1999. 285(1): p. 1-32.
8. Engelman, A. and P. Cherepanov, The structural biology of HIV-1: mechanistic and therapeutic insights. Nat Rev Microbiol, 2012. 10(4): p. 279-90.
9. Kumar, A., L. Coquard, and G. Herbein, Targeting TNF-Alpha in HIV-1 Infection. Curr Drug Targets, 2016. 17(1): p. 15-22.
10. Fact sheet 2016. 2016.
11. Mbirimtengerenji, N.D., Is HIV/AIDS epidemic outcome of poverty in sub-saharan Africa? Croat Med J, 2007. 48(5): p. 605-17.
12. Jamieson, D. and S.E. Kellerman, The 90 90 90 strategy to end the HIV Pandemic by 2030: Can the supply chain handle it? J Int AIDS Soc, 2016. 19(1): p. 20917.
13. Arts, E.J. and D.J. Hazuda, HIV-1 antiretroviral drug therapy. Cold Spring Harb Perspect Med, 2012. 2(4): p. a007161.
14. Sperling, R., Zidovudine. Infect Dis Obstet Gynecol, 1998. 6(5): p. 197-203.
15. Barry, M., F. Mulcahy, and D.J. Back, Antiretroviral therapy for patients with HIV disease. Br J Clin Pharmacol, 1998. 45(3): p. 221-8.
16. Reust, C.E., Common adverse effects of antiretroviral therapy for HIV disease. Am Fam Physician, 2011. 83(12): p. 1443-51.
17. Montessori, V., et al., Adverse effects of antiretroviral therapy for HIV infection. CMAJ, 2004. 170(2): p. 229-38.
18. Xing, H., et al., HIV drug resistance and its impact on antiretroviral therapy in Chinese HIV-infected patients. PLoS One, 2013. 8(2): p. e54917.
19. HIV Cost-effectiveness.
20. WHO guidelines.
21. Mantri, S.S. and S.P. Mantri, The nano era in dentistry. J Nat Sci Biol Med, 2013. 4(1): p. 39-44.
22. Pal, D., C.K. Sahu, and A. Haldar, Bhasma : The ancient Indian nanomedicine. J Adv Pharm Technol Res, 2014. 5(1): p. 4-12.
23. Gonzalez-Melendi, P., et al., Nanoparticles as smart treatment-delivery systems in plants: assessment of different techniques of microscopy for their visualization in plant tissues. Ann Bot, 2008. 101(1): p. 187-95.
24. De Jong, W.H. and P.J. Borm, Drug delivery and nanoparticles:applications and hazards. Int J Nanomedicine, 2008. 3(2): p. 133-49.
25. Yu, X., et al., Targeted drug delivery in pancreatic cancer. Biochim Biophys Acta, 2010. 1805(1): p. 97-104.
26. Vela-Ramirez, J.E., et al., Safety and biocompatibility of carbohydrate-functionalized polyanhydride nanoparticles. AAPS J, 2015. 17(1): p. 256-67.
27. He, W., S.W. Horn, and M.D. Hussain, Improved bioavailability of orally administered mifepristone from PLGA nanoparticles. Int J Pharm, 2007. 334(1-2): p. 173-8.
28. Peng, Q., et al., Enhanced biostability of nanoparticle-based drug delivery systems by albumin corona. Nanomedicine (Lond), 2015. 10(2): p. 205-14.
29. Kadam, R.S., D.W. Bourne, and U.B. Kompella, Nano-advantage in enhanced drug delivery with biodegradable nanoparticles: contribution of reduced clearance. Drug Metab Dispos, 2012. 40(7): p. 1380-8.

30. Longmire, M.,P.L.Choyke, and H. Kobayashi, Clearance properties of nano-sized particles and molecules as imaging agents: considerations and caveats. Nanomedicine (Lond),2008. 3(5): p.703-17
31. Kolachala, V.L., et al., Slow-release nanoparticle-encapsulated delivery system for laryngeal injection. Laryngoscope, 2010. 120(5): p. 988-94.
32. Chu, K.S., et al., Nanoparticle drug loading as a design parameter to improve docetaxel pharmacokinetics and efficacy. Biomaterials, 2013. 34(33): p. 8424-9.
33. Kumar, P., et al., Improved Safety, Bioavailability and Pharmacokinetics of Zidovudine through Lactoferrin Nanoparticles during Oral Administration in Rats. PLoS One, 2015. 10(10): p. e0140399.
34. Padhye, S.G. and M.S. Nagarsenker, Simvastatin Solid Lipid Nanoparticles for Oral Delivery: Formulation Development and In vivo Evaluation. Indian J Pharm Sci, 2013. 75(5): p. 591-8.
35. Mukherjee, S., S. Ray, and R.S. Thakur, Solid lipid nanoparticles: a modern formulation approach in drug delivery system. Indian J Pharm Sci, 2009. 71(4): p. 349-58.
36. Naseri, N., H. Valizadeh, and P. Zakeri-Milani, Solid Lipid Nanoparticles and Nanostructured Lipid Carriers: Structure, Preparation and Application. Adv Pharm Bull, 2015. 5(3): p. 305-13.
37. Seyfoddin, A., J. Shaw, and R. Al-Kassas, Solid lipid nanoparticles for ocular drug delivery. Drug Deliv, 2010. 17(7): p. 467-89.
38. Kang, K.W., et al., Doxorubicin-loaded solid lipid nanoparticles to overcome multidrug resistance in cancer therapy. Nanomedicine, 2010. 6(2): p. 210-3.
39. Mody, V.V., et al., Introduction to metallic nanoparticles. J Pharm Bioallied Sci, 2010. 2(4): p. 282-9.
40. Monton, H., et al., The use of quantum dots for immunochemistry applications. Methods Mol Biol, 2012. 906: p. 185-92.
41. Smith, A.M. and S. Nie, Next-generation quantum dots. Nat Biotechnol, 2009. 27(8): p. 732-3.
42. A. Mazumder, J.D., V. Rangari, and M. Curry., Synthesis, Characterization, and Applications of Dendrimer-Encapsulated Zero-Valent Ni Nanoparticles as Antimicrobial Agents. International Scholarly Research Notices 2013. 2013: p. 9.
43. Malam, Y., M. Loizidou, and A.M. Seifalian, Liposomes and nanoparticles: nanosized vehicles for drug delivery in cancer. Trends Pharmacol Sci, 2009. 30(11): p. 592-9.
44. Lohcharoenkal, W., et al., Protein nanoparticles as drug delivery carriers for cancer therapy. Biomed Res Int, 2014. 2014: p. 180549.
45. Mamo, T., et al., Emerging nanotechnology approaches for HIV/AIDS treatment and prevention. Nanomedicine (Lond), 2010. 5(2): p. 269-85.
46. Zwiorek, K., et al., Gelatin nanoparticles as a new and simple gene delivery system. J Pharm Pharm Sci, 2005. 7(4): p. 22-8.
47. Elzoghby, A.O., Gelatin-based nanoparticles as drug and gene delivery systems: reviewing three decades of research. J Control Release, 2013. 172(3): p. 1075-91.
48. Kaur, A., S. Jain, and A.K. Tiwary, Mannan-coated gelatin nanoparticles for sustained and targeted delivery of didanosine: in vitro and in vivo evaluation. Acta Pharm, 2008. 58(1): p. 61-74.
49. Azimi, B., et al., Producing gelatin nanoparticles as delivery system for bovine serum albumin. Iran Biomed J, 2014. 18(1): p. 34-40.
50. Yu, Z., et al., Bovine serum albumin nanoparticles as controlled release carrier for local drug delivery to the inner ear. Nanoscale Res Lett, 2014. 9(1): p. 343.
51. Xia, X.X., et al., Hydrophobic drug-triggered self-assembly of nanoparticles from silk-elastin-like protein polymers for drug delivery. Biomacromolecules, 2014. 15(3): p. 908-14.
52. Machado, R., et al., Elastin-based nanoparticles for delivery of bone morphogenetic proteins. Methods Mol Biol, 2012. 906: p. 353-63.
53. Rishi Shukla, M.C., Zein: the industrial protein from corn. Industrial Crops and Products, 2001. 13(3)
54. Podaralla, S. and O. Perumal, Influence of formulation factors on the preparation of zein nanoparticles. AAPS PharmSciTech, 2012. 13(3): p. 919-27.
55. Xiao, C.W., Health effects of soy protein and isoflavones in humans. J Nutr, 2008. 138(6): p. 1244S-9S.
56. Teng, Z., Y. Luo, and Q. Wang, Nanoparticles synthesized from soy protein: preparation, characterization, and application for nutraceutical encapsulation. J Agric Food Chem, 2012. 60(10): p. 2712-20.

57. Mitchell, C.J., et al., Consumption of Milk Protein or Whey Protein Results in a Similar Increase in Muscle Protein Synthesis in Middle Aged Men. Nutrients, 2015. 7(10): p. 8685-99.
58. Giroux, H.J. and M. Britten, Encapsulation of hydrophobic aroma in whey protein nanoparticles. J Microencapsul, 2011. 28(5): p. 337-43.
59. Gandapu, U., et al., Curcumin-loaded apotransferrin nanoparticles provide efficient cellular uptake and effectively inhibit HIV-1 replication in vitro. PLoS One, 2011. 6(8): p. e23388.
60. Golla, K., et al., A target-specific oral formulation of Doxorubicin-protein nanoparticles: efficacy and safety in hepatocellular cancer. J Cancer, 2013. 4(8): p. 644-52.
61. Ahmed, F., M.J. Ali, and A.K. Kondapi, Carboplatin loaded protein nanoparticles exhibit improve anti-proliferative activity in retinoblastoma cells. Int J Biol Macromol, 2014. 70: p. 572-82.
62. Appelmelk, B.J., et al., Lactoferrin is a lipid A-binding protein. Infect Immun, 1994. 62(6): p. 2628-32.
63. Swart, P.J., et al., Lactoferrin. Antiviral activity of lactoferrin. Adv Exp Med Biol, 1998. 443: p. 205-13.
64. Hartog, A., et al., Anti-inflammatory effects of orally ingested lactoferrin and glycine in different zymosan-induced inflammation models: evidence for synergistic activity. Int Immunopharmacol, 2007. 7(13): p. 1784-92.
65. Rodrigues, L., et al., Lactoferrin and cancer disease prevention. Crit Rev Food Sci Nutr, 2009. 49(3): p. 203-17.
66. Actor, J.K., S.A. Hwang, and M.L. Kruzel, Lactoferrin as a natural immune modulator. Curr Pharm Des, 2009. 15(17): p. 1956-73.
67. Ramana, L.N., et al., Evaluation of chitosan nanoformulations as potent anti-HIV therapeutic systems. Biochim Biophys Acta, 2014. 1840(1): p. 476-84.
68. Shibata, A., et al., Polymeric nanoparticles containing combination antiretroviral drugs for HIV type 1 treatment. AIDS Res Hum Retroviruses, 2013. 29(5): p. 746-54.
69. Chattopadhyay, N., et al., Solid lipid nanoparticles enhance the delivery of the HIV protease inhibitor, atazanavir, by a human brain endothelial cell line. Pharm Res, 2008. 25(10): p. 2262-71.
70. Krishna, A.D., et al., An efficient targeted drug delivery through apotransferrin loaded nanoparticles. PLoS One, 2009. 4(10): p. e7240.
71. Kalaivani, T., et al., Free Radical Scavenging, Cytotoxic and Hemolytic Activities from Leaves of Acacia nilotica (L.) Wild. ex. Delile subsp. indica (Benth.) Brenan. Evid Based Complement Alternat Med, 2011. 2011: p. 274741.
72. Zhang, J., et al., Self-assembled nanoparticles based on hydrophobically modified chitosan as carriers for doxorubicin. Nanomedicine, 2007. 3(4): p. 258-65.
73. Burger, D.M., et al., Determination of 3'-amino-3'-deoxythymidine, a cytotoxic metabolite of 3'-azido-3'-deoxythymidine, in human plasma by ion-pair high-performance liquid chromatography. J Chromatogr, 1993. 622(2): p. 235-42.
74. Bienvenu, E., et al., A rapid and selective HPLC-UV method for the quantitation of efavirenz in plasma from patients on concurrent HIV/AIDS and tuberculosis treatments. Biomed Chromatogr, 2013. 27(11): p. 1554-9.
75. Alebouyeh, M. and H. Amini, Rapid determination of lamivudine in human plasma by high-performance liquid chromatography. J Chromatogr B Analyt Technol Biomed Life Sci, 2015. 975: p. 40-4.
76. Bhavsar, D.S., B.N. Patel, and C.N. Patel, RP-HPLC method for simultaneous estimation of tenofovir disoproxil fumarate, lamivudine, and efavirenz in combined tablet dosage form. Pharm Methods, 2012. 3(2): p. 73-8.
77. Muller, A.C. and I. Kanfer, An efficient HPLC method for the quantitative determination of atazanavir in human plasma suitable for bioequivalence and pharmacokinetic studies in healthy human subjects. J Pharm Biomed Anal, 2010. 53(1): p. 113-8.
78. Shah, A.N., U.K. Nihalani, and B.K. Kavina, Nucleoside reverse transcriptase inhibitors (zidovudine and stavudine) side-effects in people living with human immunodeficiency virus/acquired immunodeficiency syndrome attending the antiretroviral treatment center of B.J. Medical College and Civil Hospital at Ahmedabad, Gujarat, India. Indian J Sex Transm Dis, 2013. 34(2): p. 148-9.
79. Rachlis, A.R., Zidovudine (Retrovir) update. CMAJ, 1990. 143(11): p. 1177-85.

80. Kumar, P.N., et al., A prospective, 96-week study of the impact of Trizivir, Combivir/nelfinavir, and lamivudine/stavudine/nelfinavir on lipids, metabolic parameters and efficacy in antiretroviral-naive patients: effect of sex and ethnicity. HIV Med, 2006. 7(2): p. 85-98.
81. Campbell, T.B., et al., Inhibition of human immunodeficiency virus type 1 replication in vitro by the bisheteroarylpiperazine atevirdine (U-87201E) in combination with zidovudine or didanosine. J Infect Dis, 1993. 168(2): p. 318-26.
82. Barbier, O., et al., 3'-azido-3'-deoxythimidine (AZT) is glucuronidated by human UDP-glucuronosyltransferase 2B7 (UGT2B7). Drug Metab Dispos, 2000. 28(5): p. 497-502.
83. Balakrishnan, A., et al., Zidovudine-induced reversible pure red cell aplasia. Indian J Pharmacol, 2010. 42(3): p. 189-91.
84. Moh, R., et al., Haematological changes in adults receiving a zidovudine-containing HAART regimen in combination with cotrimoxazole in Cote d'Ivoire. Antivir Ther, 2005. 10(5): p. 615-24.
85. Scruggs, E.R. and A.J. Dirks Naylor, Mechanisms of zidovudine-induced mitochondrial toxicity and myopathy. Pharmacology, 2008. 82(2): p. 83-8.
86. Zeller, A., et al., Genotoxicity profile of azidothymidine in vitro. Toxicol Sci, 2013. 135(2): p. 317-27.
87. Guerard, M., et al., Assessment of the genotoxic potential of azidothymidine in the comet, micronucleus, and Pig-a assay. Toxicol Sci, 2013. 135(2): p. 309-16.
88. Golla, K., et al., Efficacy, safety and anticancer activity of protein nanoparticle-based delivery of doxorubicin through intravenous administration in rats. PLoS One, 2012. 7(12): p. e51960.
89. Mallipeddi, R. and L.C. Rohan, Progress in antiretroviral drug delivery using nanotechnology. Int J Nanomedicine, 2010. 5: p. 533-47.
90. Ravi, P.R., U.K. Kotreka, and R.N. Saha, Controlled release matrix tablets of zidovudine: effect of formulation variables on the in vitro drug release kinetics. AAPS PharmSciTech, 2008. 9(1): p. 302-13.
91. Kuksal, A., et al., Formulation and in vitro, in vivo evaluation of extended- release matrix tablet of zidovudine: influence of combination of hydrophilic and hydrophobic matrix formers. AAPS PharmSciTech, 2006. 7(1): p. E1.
92. Nayak, U.Y., et al., Glutaraldehyde cross-linked chitosan microspheres for controlled delivery of zidovudine. J Microencapsul, 2009. 26(3): p. 214-22.
93. Lobenberg, R., et al., Body distribution of azidothymidine bound to hexyl-cyanoacrylate nanoparticles after i.v. injection to rats. J Control Release, 1998. 50(1-3): p. 21-30.
94. Jain, S., A.K. Tiwary, and N.K. Jain, PEGylated elastic liposomal formulation for lymphatic targeting of zidovudine. Curr Drug Deliv, 2008. 5(4): p. 275-81.
95. Callender, D.P., et al., Pharmacokinetics of oral zidovudine entrapped in biodegradable nanospheres in rabbits. Antimicrob Agents Chemother, 1999. 43(4): p. 972-4.
96. Villard, A.L., et al., Phenyl phosphotriester derivatives of AZT: variations upon the SATE moiety. Bioorg Med Chem, 2008. 16(15): p. 7321-9.
97. Luzier, A. and G.D. Morse, Intravascular distribution of zidovudine: role of plasma proteins and whole blood components. Antiviral Res, 1993. 21(3): p. 267-80.
98. Zhang, R., et al., The time of administration of 3'-azido-3'-deoxythymidine (AZT) determines its host toxicity with possible relevance to AZT chemotherapy. Antimicrob Agents Chemother, 1993. 37(9): p. 1771-6.
99. Aaron, C.S., R. Sorg, and D. Zimmer, The mouse bone marrow micronucleus test: evaluation of 21 drug candidates. Mutat Res, 1989. 223(2): p. 129-40.
100. Fenech, M., et al., Molecular mechanisms of micronucleus, nucleoplasmic bridge and nuclear bud formation in mammalian and human cells. Mutagenesis, 2011. 26(1): p. 125-32.
101. Suzuki, Y., et al., The micronucleus test and erythropoiesis. Effects of erythropoietin and a mutagen on the ratio of polychromatic to normochromatic erythrocytes (P/N ratio). Mutagenesis, 1989. 4(6): p. 420-4.
102. Groot, F., et al., Lactoferrin prevents dendritic cell-mediated human immunodeficiency virus type 1 transmission by blocking the DC-SIGN--gp120 interaction. J Virol, 2005. 79(5): p. 3009-15.
103. Fillebeen, C., et al., Receptor-mediated transcytosis of lactoferrin through the blood-brain barrier. J Biol Chem, 1999. 274(11): p. 7011-7.

104. Wang, H.B., Q.H. Mo, and Z. Yang, HIV vaccine research: the challenge and the way forward. J Immunol Res, 2015. 2015: p. 503978.
105. Cloyd, M.W., et al., How does HIV cause depletion of CD4 lymphocytes? A mechanism involving virus signaling through its cellular receptors. Curr Mol Med, 2001. 1(5): p. 545-50.
106. Chinen, J. and W.T. Shearer, Molecular virology and immunology of HIV infection. J Allergy Clin Immunol, 2002. 110(2): p. 189-98.
107. Younai, F.S., Thirty years of the human immunodeficiency virus epidemic and beyond. Int J Oral Sci, 2013. 5(4): p. 191-9.
108. Nittayananta, W., et al., Effects of long-term use of HAART on oral health status of HIV-infected subjects. J Oral Pathol Med, 2010. 39(5): p. 397-406.
109. Joly, V. and P. Yeni, [Non-nucleoside reverse transcriptase inhibitors]. Ann Med Interne (Paris), 2000. 151(4): p. 260-7.
110. Avachat, A.M. and S.S. Parpani, Formulation and development of bicontinuous nanostructured liquid crystalline particles of efavirenz. Colloids Surf B Biointerfaces, 2015. 126: p. 87-97.
111. Perez-Elias, M.J., et al., Higher virological effectiveness of NNRTI-based antiretroviral regimens containing nevirapine or efavirenz compared to a triple NRTI regimen as initial therapy in HIV-1-infected adults. HIV Clin Trials, 2005. 6(6): p. 312-9.
112. Boffito, M., et al., Protein binding in antiretroviral therapies. AIDS Res Hum Retroviruses, 2003. 19(9): p. 825-35.
113. Hari, B.V., K. Dhevendaran, and N. Narayanan, Development of Efavirenz nanoparticle for enhanced efficiency of anti-retroviral therapy against HIV and AIDS. BMC Infect Dis., 2012. 12: p. P7.
114. Patel, G.V., et al., Nanosuspension of efavirenz for improved oral bioavailability: formulation optimization, in vitro, in situ and in vivo evaluation. Drug Dev Ind Pharm, 2014. 40(1): p. 80-91.
115. Tshweu, L., et al., Enhanced oral bioavailability of the antiretroviral efavirenz encapsulated in poly(epsilon-caprolactone) nanoparticles by a spray-drying method. Nanomedicine (Lond), 2014. 9(12): p. 1821-33.
116. Gonzalez-Chavez, S.A., S. Arevalo-Gallegos, and Q. Rascon-Cruz, Lactoferrin: structure, function and applications. Int J Antimicrob Agents, 2009. 33(4): p. 301 e1-8.
117. Suzuki, Y.A., et al., Expression, characterization, and biologic activity of recombinant human lactoferrin in rice. J Pediatr Gastroenterol Nutr, 2003. 36(2): p. 190-9.
118. Jiang, R., et al., Apo- and holo-lactoferrin are both internalized by lactoferrin receptor via clathrin-mediated endocytosis but differentially affect ERK-signaling and cell proliferation in Caco-2 cells. J Cell Physiol, 2011. 226(11): p. 3022-31.
119. Gaur, P.K., et al., Enhanced oral bioavailability of efavirenz by solid lipid nanoparticles: in vitro drug release and pharmacokinetics studies. Biomed Res Int, 2014. 2014: p. 363404.
120. Qi, L.F., et al., In vitro effects of chitosan nanoparticles on proliferation of human gastric carcinoma cell line MGC803 cells. World J Gastroenterol, 2005. 11(33): p. 5136-41.
121. Choi, H.S., et al., Renal clearance of quantum dots. Nat Biotechnol, 2007. 25(10): p. 1165-70.
122. Chaudhury, A. and S. Das, Recent advancement of chitosan-based nanoparticles for oral controlled delivery of insulin and other therapeutic agents. AAPS PharmSciTech, 2011. 12(1): p. 10-20.
123. Golla, K., et al., Biocompatibility, absorption and safety of protein nanoparticle-based delivery of doxorubicin through oral administration in rats. Drug Deliv, 2013. 20(3-4): p. 156-67.
124. Uner, M. and G. Yener, Importance of solid lipid nanoparticles (SLN) in various administration routes and future perspectives. Int J Nanomedicine, 2007. 2(3): p. 289-300.
125. Phillips, E.J., B. Kuriakose, and S.R. Knowles, Efavirenz-induced skin eruption and successful desensitization. Ann Pharmacother, 2002. 36(3): p. 430-2.
126. Moody, D.E., et al., Gender differences in pharmacokinetics of maintenance dosed buprenorphine. Drug Alcohol Depend, 2011. 118(2-3): p. 479-83.
127. Soldin, O.P. and D.R. Mattison, Sex differences in pharmacokinetics and pharmacodynamics. Clin Pharmacokinet, 2009. 48(3): p. 143-57.
128. Jain, S., et al., Surface stabilized efavirenz nanoparticles for oral bioavailability enhancement. J Biomed Nanotechnol, 2013. 9(11): p. 1862-74.

129. Rakhmanina, N.Y. and J.N. van den Anker, Efavirenz in the therapy of HIV infection. Expert Opin Drug Metab Toxicol, 2010. 6(1): p. 95-103.
130. Lange, J.M. and B. Schwartlander, Introduction 15 million on ART by 2015: a realistic target or just a dream. Curr Opin HIV AIDS, 2013. 8(1): p. 1-3.
131. Boyapalle, S., S. Mohapatra, and S. Mohapatra, Nanotechnology Applications to HIV Vaccines and Microbicides. J Glob Infect Dis, 2012. 4(1): p. 62-8.
132. Perno, C.F., The discovery and development of HIV therapy: the new challenges. Ann Ist Super Sanita, 2011. 47(1): p. 41-3.
133. Humphreys, E.H., L.W. Chang, and J. Harris, Antiretroviral regimens for patients with HIV who fail first-line antiretroviral therapy. Cochrane Database Syst Rev, 2010(6): p. CD006517.
134. Kebba, A., et al., Therapeutic responses to AZT + 3TC + EFV in advanced antiretroviral naive HIV type 1-infected Ugandan patients. AIDS Res Hum Retroviruses, 2002. 18(16): p. 1181-7.
135. Trotta, M.P., et al., Treatment-related factors and highly active antiretroviral therapy adherence. J Acquir Immune Defic Syndr, 2002. 31 Suppl 3: p. S128-31.
136. Sun, T., et al., Engineered nanoparticles for drug delivery in cancer therapy. Angew Chem Int Ed Engl, 2014. 53(46): p. 12320-64.
137. Freeling, J.P., et al., Anti-HIV drug-combination nanoparticles enhance plasma drug exposure duration as well as triple-drug combination levels in cells within lymph nodes and blood in primates. AIDS Res Hum Retroviruses, 2015. 31(1): p. 107-14.
138. Khalil, N.M., et al., Potential of polymeric nanoparticles in AIDS treatment and prevention. Expert Opin Drug Deliv, 2011. 8(1): p. 95-112.
139. Leyva-Gomez, G., et al., Nanoparticle technology for treatment of Parkinson's disease: the role of surface phenomena in reaching the brain. Drug Discov Today, 2015. 20(7): p. 824-37.
140. Panyam, J. and V. Labhasetwar, Biodegradable nanoparticles for drug and gene delivery to cells and tissue. Adv Drug Deliv Rev, 2003. 55(3): p. 329-47.
141. Jacobson, G.B., et al., Sustained release of drugs dispersed in polymer nanoparticles. Angew Chem Int Ed Engl, 2008. 47(41): p. 7880-2.
142. Jia, L., Nanoparticle Formulation Increases Oral Bioavailability of Poorly Soluble Drugs: Approaches Experimental Evidences and Theory. Curr Nanosci, 2005. 1(3): p. 237-243.
143. Cho, M., et al., The impact of size on tissue distribution and elimination by single intravenous injection of silica nanoparticles. Toxicol Lett, 2009. 189(3): p. 177-83.
144. Florisa, R., et al., Antibacterial and antiviral effects of milk proteins and derivatives thereof. Curr Pharm Des, 2003. 9(16): p. 1257-75.
145. Leon-Sicairos, N., et al., Microbicidal action of lactoferrin and lactoferricin and their synergistic effect with metronidazole in Entamoeba histolytica. Biochem Cell Biol, 2006. 84(3): p. 327-36.
146. Ciaffi, L., et al., Efficacy and safety of three second-line antiretroviral regimens in HIV-infected patients in Africa. AIDS, 2015. 29(12): p. 1473-81.
147. Owens, D.E., 3rd and N.A. Peppas, Opsonization, biodistribution, and pharmacokinetics of polymeric nanoparticles. Int J Pharm, 2006. 307(1): p. 93-102.
148. M.Abd Elgadir, M.S.U., Sahena Ferdosh, Aishah Adam, Ahmed Jalal Khan Chowdhury, Md.Zaidul Islam Sarker,, Impact of chitosan composites and chitosan nanoparticle composites on various drug delivery systems: A review. Journal of Food and Drug Analysis, 2014. Volume 23(Issue 4): p. 619–629.
149. Koduri, P.R. and S. Parekh, Zidovudine-related anemia with reticulocytosis. Ann Hematol, 2003. 82(3): p. 184-5.
150. Palella, F.J., Jr., et al., Declining morbidity and mortality among patients with advanced human immunodeficiency virus infection. HIV Outpatient Study Investigators. N Engl J Med, 1998. 338(13): p. 853-60.
151. Fox, Z., et al., A randomized trial to evaluate continuation versus discontinuation of lamivudine in individuals failing a lamivudine-containing regimen: the COLATE trial. Antivir Ther, 2006. 11(6): p. 761-70.
152. Antiretroviral Therapy for HIV Infection in Adults and Adolescents: Recommendations for a Public Health Approach: 2010 Revision. 2010.

Publications

PLOS ONE

RESEARCH ARTICLE

Improved Safety, Bioavailability and Pharmacokinetics of Zidovudine through Lactoferrin Nanoparticles during Oral Administration in Rats

Prashant Kumar☯, Yeruva Samrajya Lakshmi☯, Bhaskar C., Kishore Golla, Anand K. Kondapi*

Department of Biotechnology and Bioinformatics, School of Life Sciences, University of Hyderabad, Hyderabad, 500046, India

☯ These authors contributed equally to this work.
* akondapi@gmail.com

Citation: Kumar P, Lakshmi YS, C. B, Golla K, Kondapi AK (2015) Improved Safety, Bioavailability and Pharmacokinetics of Zidovudine through Lactoferrin Nanoparticles during Oral Administration in Rats. PLoS ONE 10(10): e0140399. doi:10.1371/journal.pone.0140399

Editor: Charlene S. Dezzutti, University of Pittsburgh, UNITED STATES

Received: July 3, 2015

Accepted: September 24, 2015

Published: October 13, 2015

Data Availability Statement: All relevant data are within the paper and its Supporting Information file.

Funding: Funded by the Department of Science and Technology, Government of India, through a research project under nanomission and UGC BSR FRCP one time grant.

Competing Interests: The authors have declared that no competing interests exist.

Abstract

Zidovudine (AZT) is one of the most referred antiretroviral drug. In spite of its higher bioavailability (50–75%) the most important reason of its cessation are bone marrow suppression, anemia, neutropenia and various organs related toxicities. This study aims at the improvement of oral delivery of AZT through its encapsulation in lactoferrin nanoparticles (AZT-lactonano). The nanoparticles (NPs) are of 50–60 nm in size and exhibit 67% encapsulation of the AZT. They are stable in simulated gastric and intestinal fluids. Anti-HIV-1 activity of AZT remains unaltered in nanoformulation in acute infection. The bioavailability and tissue distribution of AZT is higher in blood followed by liver and kidney. AZT-lactonano causes the improvement of pharmacokinetic profile as compared to soluble AZT; a more than 4 fold increase in AUC and AUMC in male and female rats. The serum C_{max} for AZT-lactonano was increased by 30%. Similarly there was nearly 2-fold increase in T_{max} and $t_{1/2}$. Our in vitro study confirms that, the endosomal pH is ideal for drug release from NPs and shows constant release from up to 96h. Bone marrow micronucleus assay show that nanoformulation exhibits approximately 2fold lower toxicity than soluble form. Histopathological and biochemical analysis further confirms that less or no significant organ toxicities when nanoparticles were used. AZT-lactonano has shown its higher efficacy, low organs related toxicities, improved pharmacokinetics parameter while keeping the antiviral activity intact. Thus, the nanoformulation are safe for the target specific drug delivery.

Introduction

Zidovudine is the first drug approved for the treatment of HIV infection and is still in the part of the first line regimen in Highly Active Antiretroviral Therapy (HAART) [1]. Despite of its efficacy, the factors that limit its clinical use are its toxicity, suboptimal bioavailability and

pharmacokinetics which includes bone marrow aplasia [2], inhibition of mitochondrial machinery [3], short plasma half-life [4] and high hepatic first-pass metabolism [5] etc. This will eventually lead to the increase in the frequency and dosage of the regimen resulting in the unwanted side effects that compromise in the adherence to the antiretroviral treatment. AZT (300 mg twice a day oral 1 mg per kg intravenous infusion over 1 hour every 4 hours), was the first drug approved by the Food and Drug Administration (FDA). Commercially, AZT is available in various forms such as capsules, tablets, syrup and intravenous injection. Further, FDA has approved the fixed tablet formulation of AZT for HIV naive patient in combination with other ART drugs, these includes *Combivir* (300mg AZT plus 150mg lamivudine) and *Trizivir* (300mg AZT plus 150mg lamivudine plus 300mg abacavir) [6]. This necessitates zero order and targeted delivery of AZT since excess plasma concentration occur immediately after its administration [7]. Hence, a successful treatment of HIV infection requires a uniform systemic level of the drug throughout the course of the therapy.

Apart from T-lymphocytes, reticuloendothelial cells namely monocytes and macrophages act as major reservoirs for HIV and are thought to be responsible for its distribution throughout the body and brain [8–11]. So a sterilizing cure for HIV is not possible without the access of drug regimens into macrophage system. In addition, AZT is reported to be a substrate of diverse drug efflux mechanisms present in cells of CNS, Immune system and Intestinal epithelium which is mainly mediated by ATP binding cassette (ABC) family of proteins viz., P-glycoprotein [12]. This consequently will lead to the evolution of drug resistant strains. This is one of the main reasons of the intra- and inter-patient variability and nonlinearity observed in the bioavailability of AZT [13,14]. To circumvent all of the above limitations associated with AZT delivery various methods were employed that encompasses delivery as prodrugs, encapsulation in polymeric and non-polymeric nanocarriers like nanoconjugates, micelles, surface engineered liposomes, SLNs etc. [15–18]. The various advantages in using nanoparticles as delivery vehicles are their size, surface charge, large surface area to volume ratio, stability, multifunctional and biomimetic properties [19–21].

In spite of having so much of beneficial record of AZT [22], the previous (pharmacokinetics) PK studies showed that, AZT is responsible for the bone marrow toxicity [23] which leads to bone marrow suppression [24] and finally results to various alteration related to hematopoiesis [25–27]. Further AZT has been proven as a genotoxic compound [28,29] which cause the induction of micronuclei in the mouse bone marrow cells [30].

Earlier research in our lab involved in the development of nanoformulation of doxorubicin, carboplatin and curcumin with transferrin family of proteins namely apotransferrin and lactoferrin and these were successfully applied for the treatment of hepatocellular carcinoma in rats and HIV-1 infection in cell line [31–35]. Since oral administration is the best modality available for the drug delivery, the present work involves the improvement in the delivery of AZT using the lactoferrin as nanocarrier system. So the advantage with the present nanoformulation of AZT with lactoferrin is bidirectional, where the carrier itself has antiviral activity along with AZT itself. The present work showed the improved safety, bioavailability and pharmacokinetics of AZT encapsulated in lactoferrin nanoparticles (AZT-lactonano).

Materials and Methods

Materials

Lactoferrin and olive oil used for preparation of nanoparticle were purchased from Symbiotics (USA) and Leonardo (Italy) respectively. AZT used was the pharmaceutical production of Sigma. All other reagents are of molecular biology grade. 24 well plates were from Corning (USA). For the administration of drugs 18 Standard Wire Gauge bend oral dosing/gavage

needle was used. Syringe filters were purchased from Pall, HPLC (Waters) was used for the estimation of drug. All Safety analysis experimental kits were purchased from Span diagnostics India and Cayman chemical USA. p24 ELISA kit was purchased from ABL (USA).

Animals

All the animals (Wistar rats) used in this study were approx. 6 months old and 0.160 kg to 0.250 kg weight, obtained from Sainath Agencies Hyderabad. Animals were housed in animal house facility of University of Hyderabad and all animal experiments were conducted as per the approval from Intuitional Animal Ethics Committee, University of Hyderabad.

Preparation of Lactoferrin Nanoparticles

AZT loaded lactoferrin nanoparticles were prepared through sol-oil chemistry [31]. 10 milligram of AZT was dissolved in 1000μl of Milli-Q water and was gently mixed with 40 mg of lactoferrin dissolved in 1ml of ice cold phosphate buffer saline (pH 7.4). Mixture was incubated in ice for an hr. Then it was slowly added to 25ml of olive oil with gentle vortexing. The sample was sonicated for 15 min at 4°C with the help of narrow stepped titanium probe of ultrasonic homogenizer (300V/T, Biologics Inc., Manassas, Virginia, USA). Resulting mixture was immediately transferred in liquid nitrogen for 10 min then thawed on ice for 4hr. Particles formed were centrifuged at 6000 rpm for 10 min at 4°C. Pellet formed was extensively washed twice with ice cold diethyl ether (to completely remove oil) and then dispersed in 1ml of PBS.

Nanoparticle Characterization

Nanoparticle morphology were examined through two different methods, field emission scanning electron microscope (FE-SEM, Philips FEI-XL 30 ESEM; FEI, Hillsboro, OR, USA) operated at 20 KV, and Atomic force microscope (AFM; SPM400). Gold coated Nanoparticles were used for FE-SEM and in AFM where samples were spin coated on glass slides. The characterization was done according to the protocol described as per manufacturer's instructions.

FT-IR Spectral Analysis (Drug-Nanoparticle Interaction Study)

Spectral analysis were done using KBr pellet method. All the nanoparticles were lyophilized before FT-IR analysis. 0.1 to 1.0% sample was well triturated into 200 to 250 mg of KBr in a mortar. Samples were then transferred to 13 mm-diameter pellet forming die and very high pressure (1000 kg/cm^2) was applied under vacuum; resulted to a transparent pellet. The pellet was placed on sample holder and scanned from wave number 4000 to 400. Spectral analysis was performed using FT-IR dedicated OMNIC series software on a windows 7 platform.

Encapsulation Efficiency

Encapsulation efficiency was measured by mixing 50μl of nanoparticles and 950μl of 1X PBS (pH5) and incubated for twelve hours on rocker. After incubation, 200μl of 30% Silver nitrate was added and vortexed. 1ml of methanol was added, mixed thoroughly and centrifuged at 16000rpm for 10min at 4°C. After centrifugation supernatant was collected and filtered through 0.2 micron syringe filters and then filtrate was used for estimation by HPLC (Waters) at 270 nm. Mobile phase composition used was acetonitrile: methanol (60:40 v/v) [36]. 10μl of sample was injected at the flow rate of 1ml per min. The encapsulation efficiency (EE %) was

calculated using the following formula

$$\text{Encapsulation Efficiency } (\%) = \frac{M_{total} - M_{lost}}{M_{total}} \times 100$$

Here M_{total} is the total amount of AZT entrapped during AZT-lactonano preparation and M_{lost} is the amount of AZT unavailable after release from nanoparticles.

pH Dependent Drug Release Assay and Percent Release of Drug

600μg of AZT-lactonano were incubated for 12h with 1ml of 1X PBS (pH 2 to 8), SGF (simulated gastric fluid) and SIF (simulated intestinal fluid); 200 μl of silver nitrate was added to precipitate the protein and drug was extracted by adding methanol, centrifuged and supernatant was estimated for AZT using HPLC. To measure the percent release of AZT from nanoparticles, AZT-lactonano were incubated with 1ml of PBS (pH 5.0 and 7.4). At different time interval aliquots were withdrawn, and estimated for the presence of AZT.

In Vitro Stability Study

The *in vitro* stability testing was performed for drug loaded nanoparticles (AZT-lactonano) in PBS (pH 7.4) (NP solution). The stability study was carried out in terms of quantity of drug present in the nanoparticles using HPLC and diameter. Freshly prepared nanoparticles were incubated for various time points such as 0, 1, 2, 4, 6, 8, 10, 12, 16, 24, 48, 72 and 96h at two different temperature (4°C and room temperature). Drug content was quantified using the protocol mentioned in drug release assay section. The size of above incubated nanoparticles were measured using FE-SEM.

Animal Study Design

Male and female Wistar rats of 6 months old were acclimatized for a week at animal house facility, University of Hyderabad under 12h light/dark cycle. For study, animals were divided into seven different groups according to seven time points i.e., 30min, 1h, 2h, 4h, 8h, 16h, 24h. Each group contains 3 males and 3 females and drug was administered orally to all animals. Rats were administered with 10mg/kg body weight of sol AZT and equivalent of AZT-lactonano. Each group was subjected for above mentioned time points. Animals were monitored hourly after oral administration of drugs. No death was observed during the experimentation. After completion of respective time points, animals were euthanized using sodium pentobarbital (50 mg/kg, IP) and blood was collected through heart puncture. Then, tissues such as brain, heart, esophagus, lungs, spleen, liver, stomach, small intestine, large intestine, kidney and bone marrow were collected. Serum was separated from blood by centrifugation at 4° C, 1500g for 10min. Except bone marrow, tissue from all other organs were homogenized; 30% of silver nitrate was added to precipitate the tissue protein. Extraction of AZT from tissue was done by addition of methanol followed by the centrifugation of the whole mixture at 12,000 rpm for 12 min at 4° C. After centrifugation, supernatant was filtered with 0.2 micron syringe filter and estimated by HPLC UV detector at 270nm.

Tissue Sectioning and Safety Analysis

Organs were removed and processed for histopathology. The tissues were observed under microscope for any abnormalities after the treatment with the nanoformulation. Safety analysis was done by using biochemical kits that were commercially available for serum AST, urea, bilirubin and creatinine.

Bone Marrow Micronucleus Assay

Animals were administered orally with 10mg kg^{-1} body weight of sol AZT and equivalent amount of AZT-lactonano. The test was performed using the modified protocol of Schmid [37]. Only three time points (4h, 8h, and 16h) were chosen for the test, based on drug distribution in bone marrow. After the completion of time points rats were sacrificed by cervical dislocation. Both femoral bone were dissected and the bone marrow cells were collected by flushing out with 1ml of fetal bovine serum (FBS) and mixed properly. Then cell suspension was centrifuged for 5min at 200g; supernatant were discarded. Marrow pellet was resuspended in minimal volume of FBS. One drop of cell suspension were placed on a clean dry slide and thin smear was made, air dried and then fixed with absolute methanol. Smear was stained with Giemsa stain for 20min and mounted.

Antiviral Assay

SupT1 Cells (100% viability) with a density of 0.5 million were seeded with RPMI 1640, 0.1% FBS in 24-well plates. 80mg/ml of lactoferrin was taken, and formulation with and without AZT (1μg) were added to the cells and they were challenged with HIV-193IN101 at a final concentration of virus equivalent to 20 nanograms of p24 per ml. The infected cells were incubated at 37°C and 5% CO_2 incubator for 2 h. After 2 h, the cells were pelleted at 350x g for 10 min, cells were washed twice with RPMI 1640 containing 10% fetal bovine serum. The cells were suspended in the same medium and incubated for 96 h. After 96 h supernatants had been collected and viral load was analyzed using p24 antigen capture assay kit (ABL kit). The infection in the absence of compound was considered to be 0% inhibition.

Statistical Analysis

All studies were carried out in triplicates for all groups and results are presented as mean with standard deviation. The significance of differences between treatments was analyzed by one-way ANOVA with age and treatment as factors using Sigma plot. The level of statistical significance (P) was set at $P < 0.05$.

Results

Size and EE% of AZT-Lactonano

Field Emission Scanning Electron Microscopy (FE-SEM) and Atomic force microscopy (AFM) analysis revealed that the particles were spherical and were in the range of 50-60nm diameter (Fig 1). Increase in size of AZT-lactonano (50 to 60 nm) compared to lactonano (21-35nm) suggest that drug loading enhance particle size. Encapsulation efficiency was calculated according to the equation mentioned in materials and methods section and found to be 67%.

FT-IR Analysis of AZT-Lactonano

FT-IR analysis confirmed that AZT was found to be intact after the preparation of nanoparticles (Fig 2). Characteristic bands found in the infrared spectra of Lactoferrin proteins (Pure and nano form) include the Amide I and Amide II. The absorption associated with the Amide I band and Amide II band leads to stretching vibrations of the C = O bond and primarily to bending vibrations of the N—H bond respectively. Amide I bands was positioned around 1645 & 1648 cm^{-1} are usually reflected to be characteristic of alpha helices. Amide II (C-N stretching and N-H bending) and peptide N—H stretching frequency were detected at 1542 & 1539 cm^{-1} and 3418 & 3364 cm^{-1} correspondingly. The C-O-C stretch were observed around 1096 cm^{-1} & 1164 cm^{-1} The locations of both the Amide I and Amide II bands are sensitive to the

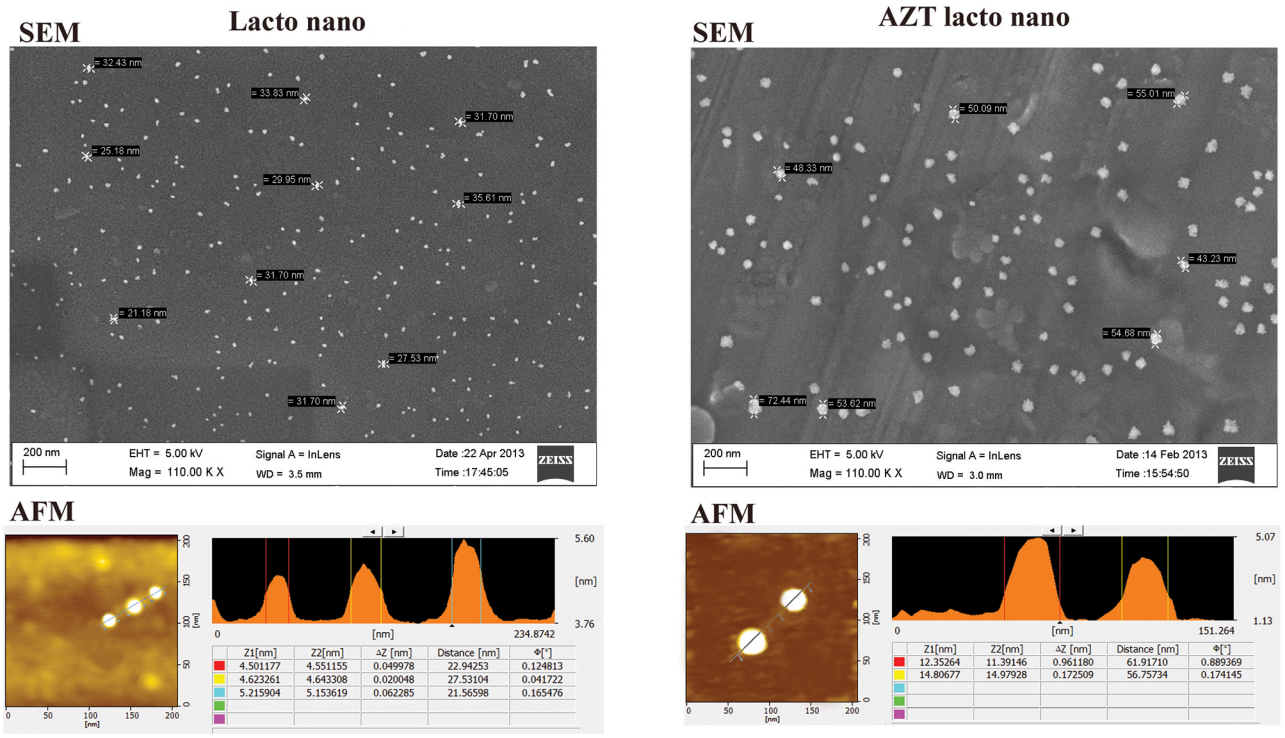

Fig 1. Size of Lactoferrin nanoparticles increases after loading of AZT. AZT containing Lactoferrin nanoparticles were prepared using sol-oil chemistry as described in methods section. The size of nanoparticles was assessed by Field emission scanning electron microscopy (top panel) and Atomic force microscopy (bottom panel). Lactonano: Lactoferrin nanoparticle without any drug loading into it, AZT Lacto nano: Lactoferrin nanoparticle loaded with AZT.

doi:10.1371/journal.pone.0140399.g001

secondary structure content of a protein. **Assessment spectral analysis of Pure AZT and AZT-Lactonano**: sharp characteristic peaks of carbonyl group (C = O) at 1682 cm^{-1} (Pure AZT) and 1685 cm^{-1} (AZT-Lactonano), Azide group ($N^- = N^+ = N^-$) peaks at 2117 & 2083 cm^{-1} (Pure AZT) and 2115 & 2082 cm^{-1} (AZT-Lactonano), C-O-C stretch belong to 1088 & 1065 cm^{-1} (Pure AZT) and 1089 & 1065 cm^{-1} (AZT-Lactonano), -NH stretching remains at 3460 cm^{-1} (Pure AZT) and 3461 cm^{-1} (AZT Lactonano). Our results of FT-IR spectra proved that there were only slight shifting (may be due to dipolemoment of bond as a result of electrostatic interaction between AZT and Lactoferrin protein) in few stretching vibration but all the major functional group was intact in nanoformulation and didn't take part in any covalent bond formation. It confirmed that AZT is only physically associated (entrapped/adsorbed) with lactoferrin protein.

AZT-Lactonano Release Assay

In case of percent drug release assay, the encapsulated drug present in nanoparticle was considered as 100% at the start of the experiment. The amount of drug released at indicated pH at different time points was estimated and presented as percent release with reference to the drug loaded in the nanoparticles. In vitro analysis of AZT release from the nanoparticles has shown that highest amount of AZT was released at pH-5 (Fig 3A) followed by pH-6 and pH-4. Its release in the presence of simulated Gastric and Intestinal fluids was lesser indicating its stability at extreme pH. Release kinetics at pH 5.0 as indicated in Fig 3B showed a biphasic release, wherein a burst release of 60% of drug within 4 hours, followed by reduced release rate until 10 hours to the extent of 80% then a limited release over 96 hours.

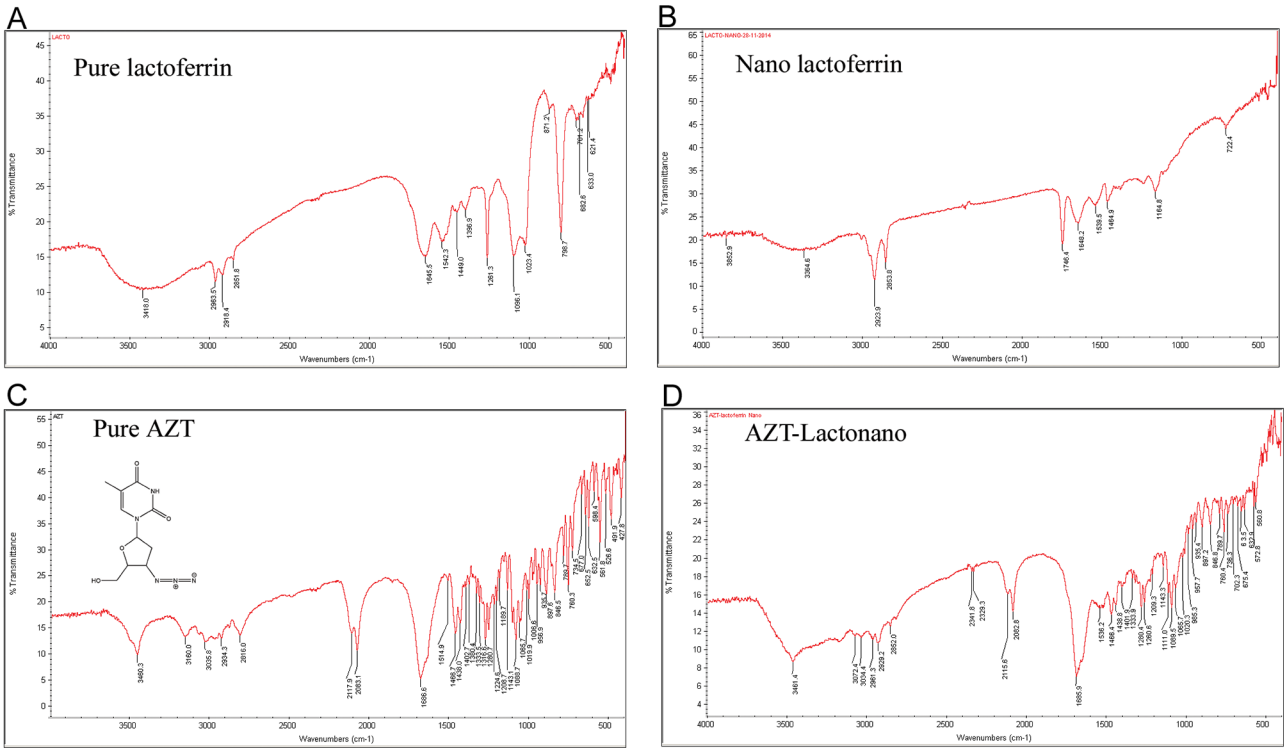

Fig 2. FT-IR spectral analysis. The FT-IR analysis of Pure Lactoferrin proteins (A), Nano Lactoferrin (Lacto nano) (B), AZT molecule (C) and AZT loaded lactoferrin nanoparticle (AZT-Lactonano) (D). It reveals that in AZT-Lactonano, AZT is physically entrapped/adsorbed with the lactoferrin nanoparticles; it didn't take part in any sort covalent interaction.

doi:10.1371/journal.pone.0140399.g002

In Vitro Stability Studies

Stability of nanoparticles suspended in PBS was analyzed at different time points at two different temperatures. Nanoparticles were found to be quite stable at both temperatures (4°C and room temperature). The drug content of nanoparticles and its diameter was found to remain same from starting to 96hr (Table 1).

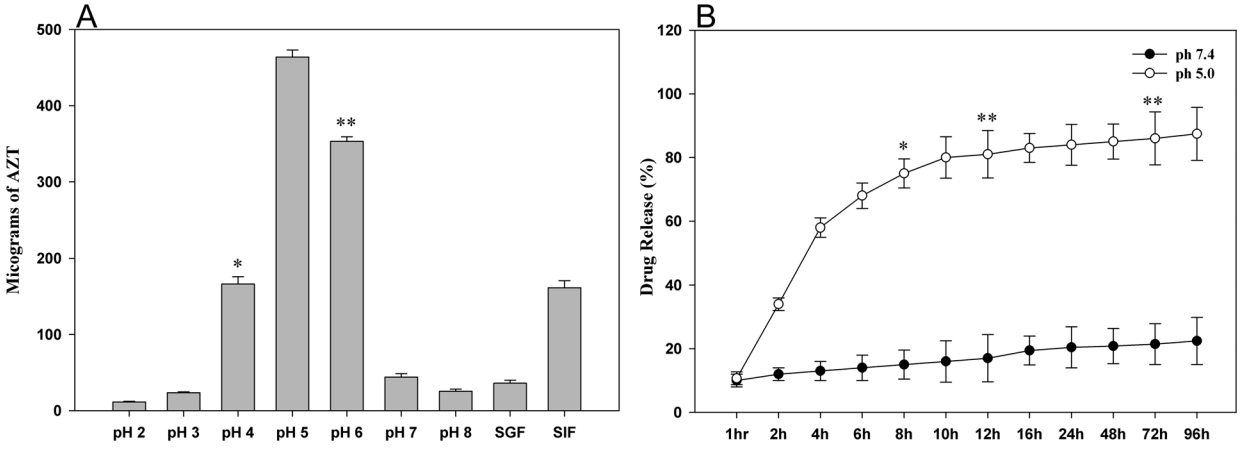

Fig 3. pH sensitivity and time dependent drug release profile of AZT-Lactonano. (A) 600μg of drug was incubated in the buffers of different pH, the release of AZT was maximum at pH-5. This is followed by pH-6 and pH-4. The release was between 1–10% with the remaining fluids. SGF: Simulated Gastric Fluid, SIF: Simulated Intestinal Fluid. (B) Cumulative percentage release profile of AZT-Lactonano at pH 5.0 and pH 7.4. Each data points were taken in triplicate and presented as Mean ± SD. Value of significance, **P < 0.005, *P < 0.05.

doi:10.1371/journal.pone.0140399.g003

Table 1. *In vitro* stability of nanoparticles.

	Diameter of the nanoparticles (nm)		AZT present in mg (%) [#]	
Hours	4°C	Room temp*	4°C	Room temp*
0	55.67± 4.54	53.23± 3.56	6.75 ± 0.69 (100.00)	6.71 ± 0.19 (100.00)
1	54.5 ± 4.30	54.5 ± 2.68	6.49 ± 0.96 (96.15)	6.57 ± 0.82 (97.91)
2	58.6 ± 3.36	59.7 ± 5.13	6.68 ± 0.85 (98.96)	6.66 ± 0.28 (99.25)
4	53.1 ± 4.19	53.6 ± 4.35	6.71 ± 0.52 (99.41)	6.47 ± 0.18 (96.42)
6	52.3 ± 3.63	55.5 ± 4.72	6.58 ± 0.78 (97.48)	6.53 ± 0.36 (97.31)
8	54.7 ± 4.73	57.6 ± 3.81	6.37 ± 0.67 (94.37)	6.54 ± 0.49 (97.46)
10	58.3 ± 6.63	58.7 ± 4.34	6.66 ± 0.78 (98.66)	6.30 ± 0.84 (93.89)
12	53.6 ± 5.13	56.8 ± 3.92	6.48 ± 0.82 (96.00)	6.52 ± 0.92 (97.16)
16	60.2 ± 5.39	54.1 ± 4.77	6.52 ± 0.19 (96.59)	6.50 ± 0.14 (96.87)
24	58.7 ± 4.73	59.4 ± 4.65	6.64 ± 0.35 (98.37)	6.68 ± 0.49 (99.55)
48	55.6 ± 4.73	57.1 ± 2.91	6.51 ± 0.73 (96.44)	6.63 ± 0.19 (98.81)
72	56.7± 5.94	56.7 ± 2.65	6.54 ± 0.37 (96.88)	6.58± 0.27 (98.06)
96	60.8 ± 5.76	58.4 ± 4.39	6.65 ± 0.39 (98.52)	6.35 ± 0.38 (94.63)

All the data (n = 3) were presented as mean ± standard deviation.

[#] Drug present in the particles was estimated by using HPLC, in milligrams. The amount of drug present initially at zero hour at 4°C and room temperature are considered as 100% drug present.

* Room temperature: The temperature used here was an average equal to 23°C.

doi:10.1371/journal.pone.0140399.t001

Pharmacokinetics and Tissue Distribution of AZT Lactonano

AZT levels in blood and other organs were located after a single dose of nanoparticles loaded with AZT (10mg/kg AZT equivalence) administered in rats orally. Drug levels were observed at seven different time point up to 24h in different tissue (Fig 4). The concentration of AZT in the blood after 2 h was determined to be around 50μg when administered with nanoformulation and around 10μg in the lack of any carrier particle. It proves the relative stability of AZT in nanoformulation against plasma clearance. Nanoformulation does not cause any organs related toxicity due to the accumulation of AZT in various organs, in contrast AZT without any carrier molecule leads to toxicity. It is followed by liver and small intestine which have shown accumulation above 5μg. Less than 5μg of the drug was found in the others remaining organs such as Kidney, Heart, Spleen, Lungs, Brain, Stomach, Esophagus, large intestine and Bone marrow. On the other side we can detect a simultaneous decrease of AZT level in serum; in liver there was an increased level of AZT when treated with AZT-lactonano at 8hr post injection. All pharmacokinetic parameters were assessed by Kinetica v 5.0 software are shown in Table 2. The AZT-lactonano showed an improvement in pharmacokinetic profile with more than 4-fold increase in AUC and AUMC in male and female rats in serum. The serum C_{max} for AZT-lactonano was increased by 30%. Similarly, there was more than 2-fold increase in T_{max} and $t_{1/2}$ (Table 2). These results show that the nanoformulation provide higher bioavailability than sol formulation.

Safety Profile of Nanoformulation

The safety profile of AZT-lactonano was compared with sol AZT and the results show no significant change in serum AST in nanoformulation versus soluble form, while bilirubin was lower in case of AZT-lactonano compared to sol AZT in female rats (Fig 5). Serum urea was significantly low when AZT-lactonano was administered suggesting low kidney toxicity when

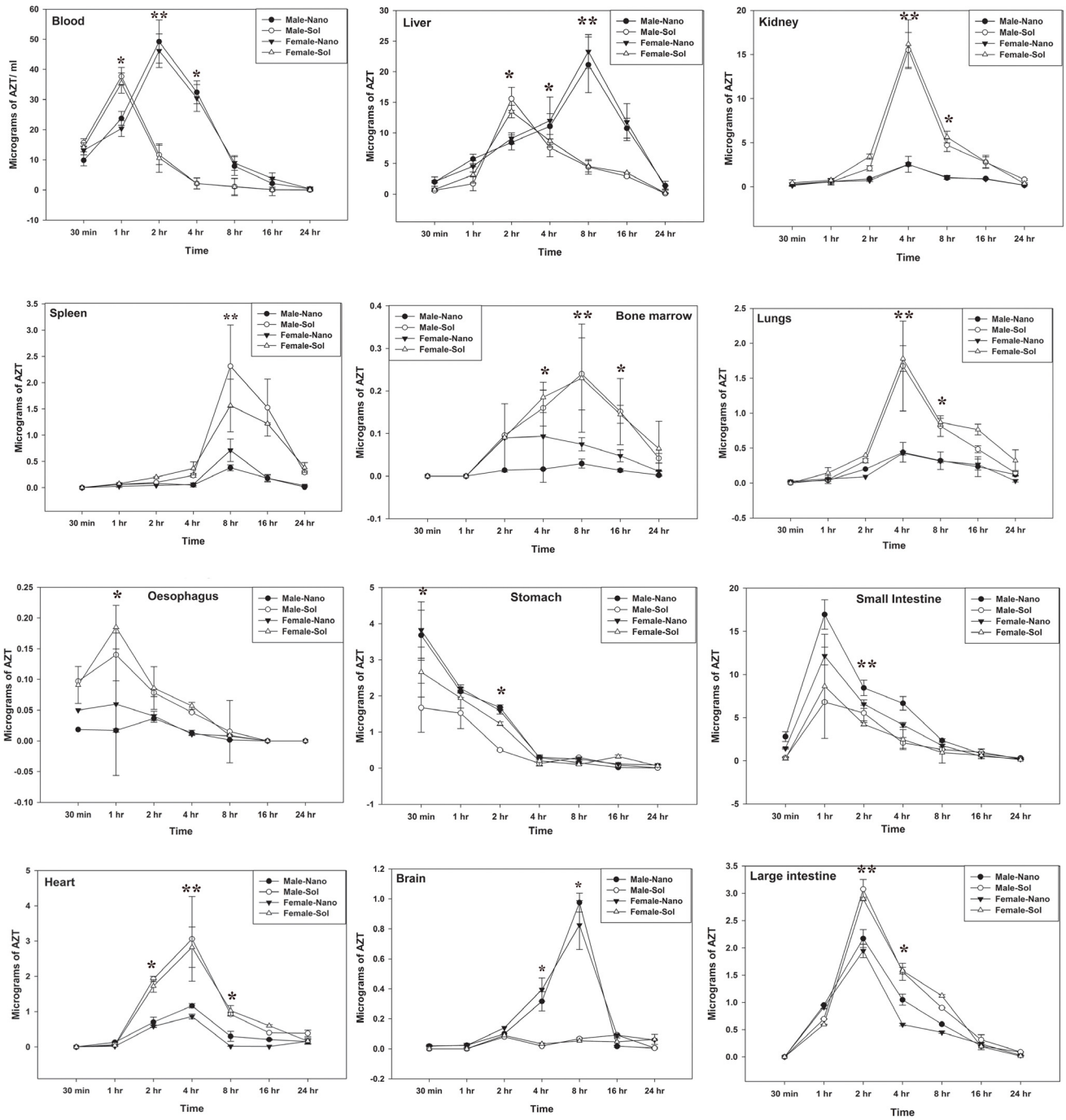

Fig 4. Tissue distribution of AZT. Single dose of sol AZT and equivalent weight of AZT-lactonano (10mg/kg body weight) was orally administered to Wistar rats. After completion of indicated time points, rats were sacrificed under proper anesthesia. AZT was extracted and estimated in blood, liver, kidney, heart, spleen, bone marrow, lungs, brain, oesophagus, stomach, small intestine and large intestine. Male-Nano and Female-Nano denotes the AZT concentration (delivered via AZT-lactonano) present in Male rats (n- = 3) and female rats (n = 3) respectively. Same nomenclature has been followed for Male-Sol and Female-Sol. Differences between groups were assessed by ANOVA. Data were presented as Mean ± SD. Value of significance, **P < 0.005, *P < 0.05.

doi:10.1371/journal.pone.0140399.g004

Table 2. Pharmacokinetics profile of AZT-lactonano in male and female rats.

AZT		Male		Female	
		Nano	Soluble	Nano	Soluble
AUC	(h)*(μg/ml)	251.57	63.48	254.974	58.74
AUMC	(h)^2*(μg/ml)	1270.3	139.73	1485.24	126.737
C_{max}	μg/mL	49.198	37.67	46.17	35.45
T_{max}	hr	2	1	2	1
$t_{1/2}$	hr	3.07	1.759	3.27	1.92

Values in the parenthesis designates the concentration of AZT in micrograms per ml of blood.

Pharmacokinetic parameters.

AUC: The integral of the concentration-time curve (after a single dose or in steady state).

AUMC: Partial area under the moment curve between t start and t end.

C_{max}: The peak plasma concentration of a drug after oral administration.

T_{max}: Time to reach C_{max}.

$t_{1/2}$: The time required for the concentration of the drug to reach half of its original value.

doi:10.1371/journal.pone.0140399.t002

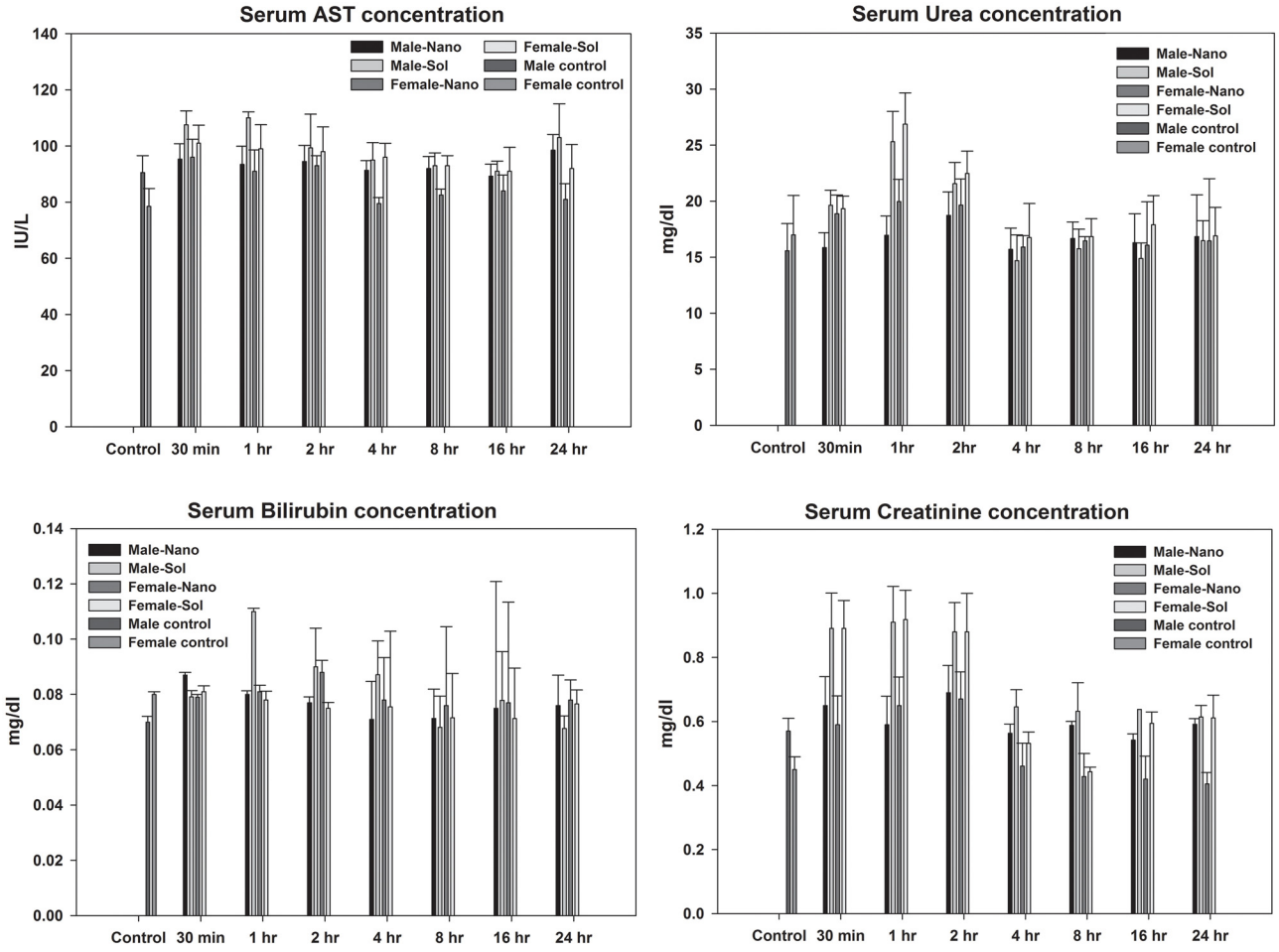

Fig 5. Biochemical safety analysis profile. Safety analysis was done using biochemical kits after oral administration of nano and soluble AZT (10mg/kg) in both male and female rats. Liver damage was estimated by Bilirubin and AST level whereas Kidney toxicity was checked by Urea and creatinine level. AZT-lactonano showed no toxicity to both liver and kidneys on the other hand it exhibited minimal urea levels when compared to the soluble AZT.

doi:10.1371/journal.pone.0140399.g005

nanoformulation was used. Nanoformulation showed improved creatinine levels compared to soluble drug form suggesting low liver toxicity. Tissue sections of heart, liver, spleen, kidney, stomach and intestines (small and large) have shown that there were no toxicities in those tissues when administered with nano forms (Fig 6).

Micronucleus Assay

Bone marrow smears were visualized using Olympus Magnus BX51 microscope under 100x magnification with oil immersion objective. Micronuclei (MN) were identified in form of RBCs (i.e., polychromatic erythrocytes as PCEs). Approximately 1000 cells were scanned per

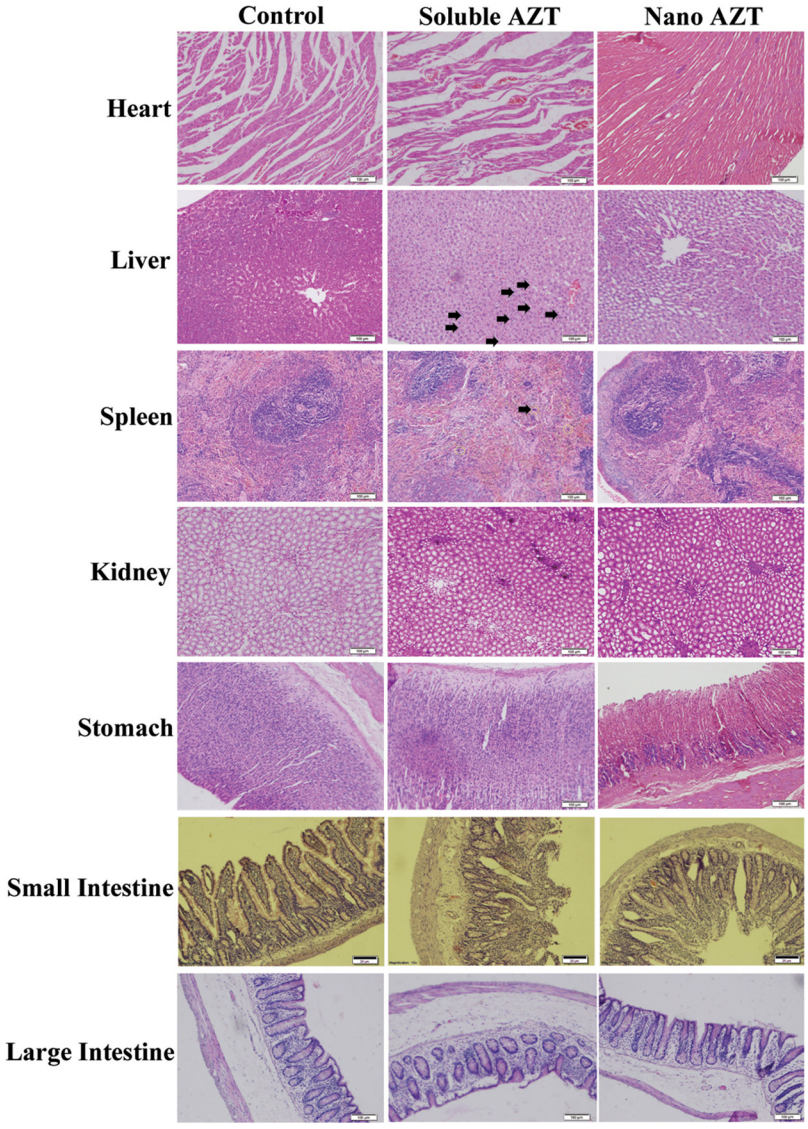

Fig 6. Histopathological analysis of tissues. Rats were orally administered with sol AZT and AZT-lactonano (10mg/kg body weight), after completion of 24hr time point, organs were removed and processed for cryo-sectioning followed by Hematoxylin and Eosin (H&E) staining. It revealed that no toxicity was found in above indicated organs, when AZT was delivered via nanoparticle form as compared to its sol form. Lesion or any abnormalities present was denoted by arrow. Scale bar is equal to 100μm.

doi:10.1371/journal.pone.0140399.g006

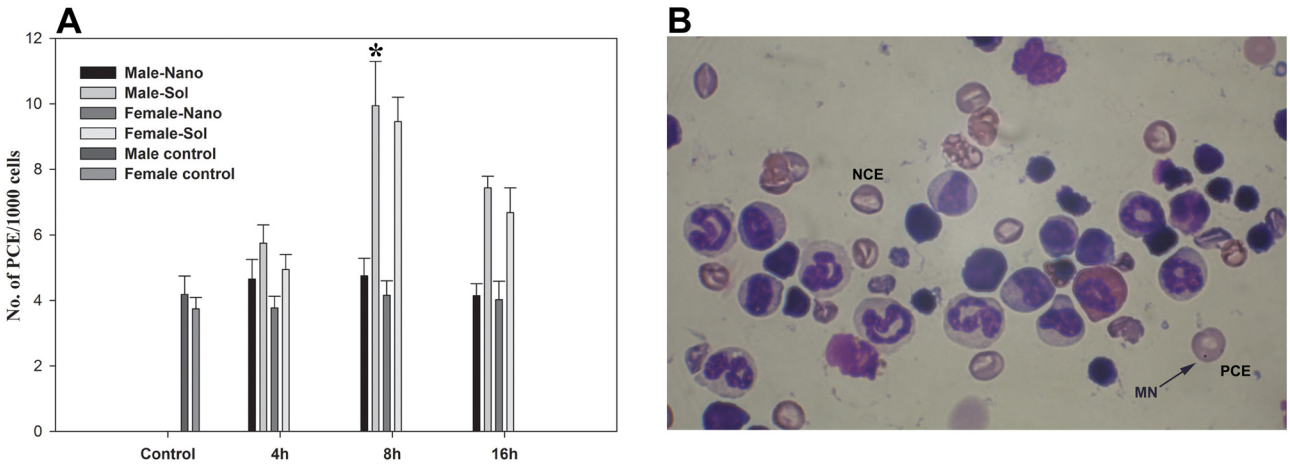

Fig 7. Bone marrow toxicity profile. (A) It shows the frequency of polychromatic erythrocyte (PCE) in bone marrow cells after oral administration of sol AZT and AZT-lactonano at 4, 8 and 16h. Data were presented as Mean ± SD. Value of significance, **P < 0.005, *P < 0.05. **(B)** Bone marrow cells (after 8h of treatment) showing the presence of enucleated Normochromatic erythrocyte (NCE) and nucleated polychromatic erythrocyte (PCE) cells. One PCE holds a micronucleus (MN); indicated by arrow. This images was captured at 100x under oil immersion objective.

doi:10.1371/journal.pone.0140399.g007

slide for the presence of micronucleus (MN) in immature PCE. Fig 7A represent that, at 8h of post application of drug a significant increase in the number of MN-PCEs was observed in case of sol AZT and at the same time AZT-lactonano showed low bone marrow toxicity. MN could be characterized as round and darkly stained (Fig 7B) nuclear fragment that indicate chromosome damage.

Antiviral Activity of AZT Lactonano

Antiviral activity of lactoferrin alone and AZT loaded in nanoformulation was analyzed to ascertain if active form of the drug is intact. Here 80mg/ml of soluble lactoferrin and equivalent of nanoform of lactoferrin has showed 70 and 73% antiviral activity respectively. Further, the activity of AZT at one microgram concentration is similar to that of soluble AZT with more than 90% of inhibition of HIV-193IN101 replication in Sup-T1 cells. It suggests that activity of encapsulated AZT remain stable in nanoformulation. (S1 Fig).

Discussion

Various formulations have been employed previously to improve the oral bioavailability of AZT. These include controlled [38] and extended [39,40] release matrices, microspheres [41], nanoparticles [42] and liposomes [43–45], which have been proposed for the delivery of AZT. Even though various routes like intranasal, intravenous and transdermal routes have been tried for AZT delivery. Peroral route of administration is the most preferred one because of frequent dosage and patient compliance. Absorption of AZT is reported to be quick and rapid when administered orally and undergoes first pass metabolism before giving an average systemic bioavailability of more than 60% [46]. Based on physiochemical characteristics, the aqueous solubility, pKa and LogP of AZT was reported as 29.3 g/l, 9.68 and 0.06 respectively [47]. Zidovudine typically exhibits a 1-compartment model in plasma during its oral administration followed by an elimination phase that is biexponential. It is relatively a lipophilic molecule where 25% of it binds to albumin [48,49] and gets metabolized in the body mainly by hepatic 5'-glucouronidation forming a stable metabolite which gets excreted in the urine. In order to maintain the required therapeutic concentration of AZT, frequent doses have to be given which may

lead to elevation to toxic levels in the blood resulting in severe side effects like granulocytopenia and anemia. Greater focus has been given for targeting AZT to lymphoid and reticuloendothelial cells in previous formulations since the delivery to these cells is utmost important as they constitute major viral reservoirs and a sterilizing cure for AIDS is impossible unless and until these are eliminated completely.

Since the encapsulation mechanism involves a process of partition of lipophilic-lyophilic AZT and lactoferrin in water and oil phases. Such phase transitions may induce protein-protein associations that entrap drug in intermolecular core as well as intramolecular cavities of proteins. This lead to a defined percent of drug (67%) associated with the protein nanoparticles based on the log P value of the drug, viz., AZT (log P, 0.06). This can be supported by the observation that AZT is released in biphasic kinetics with burst (60%) when protein surface of particles exposed to pH 5, which could be due to change in orientation of protein monomers, this may follow a release of drug molecules localized at various cavities in the protein over time (to the extent of 20%). In spite of biphasic release, 80% of loaded drug was released within 10 hours, making the availability of active drug for inhibiting target enzyme, revise transcriptase activities. Furthermore, oral absorption of nanoparticles at low pH (<3.0) and circulatory pH 7.4, allow particles intact with the loaded drug. When these particles reached the target cells (lymphocytes etc.), they enter through receptor-mediated endocytosis followed by fusion to endosome, a transient pH change to 5.5 in endosome will allow significant drug release in target cell and make effective concentrations of drug reaching at the site of action. Thus, stability of particles at pH below 3.0 and at 7.4 make these particles attractive for oral delivery in vivo.

In vivo studies showed that the AZT-lactonano showed has improved pharmacokinetic profile with more than 4-fold increase in mean serum AUC and AUMC in both male and female rats. The serum C_{max} for AZT-lactonano was increased by 30% whereas more than 2-fold increase was observed in T_{max} and $t_{1/2}$ for both male and females. It suggests that the AZT in the nanoparticles gets released slowly leading to this significant increase in the pharmacokinetic parameters. At the same time, this nanoformulation has not shown any abnormal concentrations in different organs leading to toxicity. The safety profile of nano and Sol AZT was compared and the results show no significant change in serum AST in nano versus soluble form, while bilirubin was lower in case of nano when compared to soluble form in female rats. Serum urea was significantly low when AZT-lactonano was administered compared to soluble AZT suggesting low kidney toxicity when nanoformulation was used. AZT-lactonano showed no apparent differences in creatinine levels compared to soluble form suggesting low kidney toxicity. In addition H&E staining of all the tissue sections has not revealed any abnormal morphology for both of the formulations employed.

Bone marrow suppression is the main reason to discontinue AZT based therapy [50] because the hematopoietic progenitor cells are heavily damaged. Micronucleus (MN) test is very reliable and fast in vivo assay to determine any marrow cells alteration [51]. MN are minute extra-nuclear bodies formed during anaphase stage [52]. Generally two forms of MN are found in RBCs, polychromatic erythrocytes (PCE) and Normochromatic Erythrocytes (NCEs) [53]. Our results show that AZT-lactonano is not involved in any MN formation but at the same time Sol-AZT is two-time more genotoxic.

As the free drug is reported to have lower penetration into the infected cells, the above formulation selectively targets and delivers AZT to cells that express lactoferrin receptors on their surface through receptor-mediated endocytosis by which the therapeutic index of AZT can be improved. The amphiphilic nature of AZT results in low entrapment and significant leakage when packed in conventional liposomal vesicles as it gets partitioned between lipid bilayers and the core aqueous environment. The lesser size of the nanoparticles with up to 67% encapsulation of AZT makes the current formulation to overcome the above problem. Currently,

oral dosed HIV nanoformulation was not available for patients. The quality of patient's life can be improved by simplifying the AZT dosage schedule by less frequent administration of a sustained-release formulation since HAART regimens that combine multiple agents lead to severe side effects. The advantage in employing lactoferrin as a carrier is its ability to interfere with virus binding to DC-SIGN of dendritic cells by its interaction with the V3 loop of gp120 and coreceptors [54]. Further, the same formulation can be employed to improve the brain delivery of AZT since the lactoferrin is reported to cross the blood-brain barrier [55].

Conclusion

The Present study shows the applicability of protein -based nanoparticles formulation of AZT through oral delivery. The nanoparticles were prepared using sol-oil protocol. AZT-lactonano showed a biphasic drug release profile and releases its maximum payload at pH 5. *In vivo* studies concludes that the physical encapsulation of AZT in lactoferrin nanoparticles makes the formulation safer and efficacious. Nano-formulation enhances the various pharmacokinetics profile like AUC, AUMC, C_{max} and $t_{1/2}$ while keeping the antiviral activity of AZT intact. Further AZT-lactonano is found to be two times less genotoxic as compared to sol AZT.

Supporting Information

S1 Fig. Antiviral activity of lactoferrin alone (soluble & nano) and AZT (soluble & nano). Antiviral activity of AZT was found to be intact in case of nanoformulation. The p24 level was measured as viral load. Here 80mg/ml of lactoferrin and equivalent concentration of nanoform was taken. The nano-AZT showed more than 85% antiviral activity at a final concentration of 1μg.
(TIF)

Acknowledgments

PK (orcid.org/0000-0003-1038-6149) is UGC-NET fellow, YSL is ICMR-SRF fellow. We thank the NIH-AIDS Reference and Reagents Program and reagent contributors of SUPT1 cells (Dr. James Hoxie) and HIV-1 93IN101 (Dr. Robert Bollinger and the DAIDS, NIAID) for providing the reagents.

Author Contributions

Conceived and designed the experiments: PK AKK. Performed the experiments: PK YSL. Analyzed the data: KG YSL. Contributed reagents/materials/analysis tools: KG. Wrote the paper: AKK BC.

References

1. Sturmer M, Staszewski S, Doerr HW. Quadruple nucleoside therapy with zidovudine, lamivudine, abacavir and tenofovir in the treatment of HIV. Antiviral therapy. 2007; 12(5):695–703. PMID: 17713153.
2. D'Andrea G, Brisdelli F, Bozzi A. AZT: an old drug with new perspectives. Current clinical pharmacology. 2008; 3(1):20–37. PMID: 18690875.
3. Scruggs ER, Dirks Naylor AJ. Mechanisms of zidovudine-induced mitochondrial toxicity and myopathy. Pharmacology. 2008; 82(2):83–8. doi: 10.1159/000134943 PMID: 18504416.
4. Barbier O, Turgeon D, Girard C, Green MD, Tephly TR, Hum DW, et al. 3'-azido-3'-deoxythimidine (AZT) is glucuronidated by human UDP-glucuronosyltransferase 2B7 (UGT2B7). Drug metabolism and disposition: the biological fate of chemicals. 2000; 28(5):497–502. PMID: 10772627.
5. Kieburtz KD, Seidlin M, Lambert JS, Dolin R, Reichman R, Valentine F. Extended follow-up of peripheral neuropathy in patients with AIDS and AIDS-related complex treated with dideoxyinosine. Journal of acquired immune deficiency syndromes. 1992; 5(1):60–4. PMID: 1346633.

6. Kumar PN, Rodriguez-French A, Thompson MA, Tashima KT, Averitt D, Wannamaker PG, et al. A prospective, 96-week study of the impact of Trizivir, Combivir/nelfinavir, and lamivudine/stavudine/nelfinavir on lipids, metabolic parameters and efficacy in antiretroviral-naive patients: effect of sex and ethnicity. HIV medicine. 2006; 7(2):85–98. doi: 10.1111/j.1468-1293.2006.00346.x PMID: 16420253.
7. Lobenberg R, Kreuter J. Macrophage targeting of azidothymidine: a promising strategy for AIDS therapy. AIDS research and human retroviruses. 1996; 12(18):1709–15. PMID: 8959248.
8. Gendelman HE, Orenstein JM, Baca LM, Weiser B, Burger H, Kalter DC, et al. The macrophage in the persistence and pathogenesis of HIV infection. Aids. 1989; 3(8):475–95. PMID: 2508709.
9. Roy S, Wainberg MA. Role of the mononuclear phagocyte system in the development of acquired immunodeficiency syndrome (AIDS). Journal of leukocyte biology. 1988; 43(1):91–7. PMID: 3275735.
10. von Briesen H, Andreesen R, Esser R, Brugger W, Meichsner C, Becker K, et al. Infection of monocytes/macrophages by HIV in vitro. Research in virology. 1990; 141(2):225–31. PMID: 1693221.
11. Meltzer MS, Skillman DR, Hoover DL, Hanson BD, Turpin JA, Kalter DC, et al. Macrophages and the human immunodeficiency virus. Immunology today. 1990; 11(6):217–23. PMID: 2191685.
12. Quevedo MA, Nieto LE, Brinon MC. P-glycoprotein limits the absorption of the anti-HIV drug zidovudine through rat intestinal segments. European journal of pharmaceutical sciences: official journal of the European Federation for Pharmaceutical Sciences. 2011; 43(3):151–9. doi: 10.1016/j.ejps.2011.04.007 PMID: 21540109.
13. Panhard X, Legrand M, Taburet AM, Diquet B, Goujard C, Mentre F, et al. Population pharmacokinetic analysis of lamivudine, stavudine and zidovudine in controlled HIV-infected patients on HAART. European journal of clinical pharmacology. 2007; 63(11):1019–29. doi: 10.1007/s00228-007-0337-x PMID: 17694300; PubMed Central PMCID: PMC2703659.
14. Boudinot FD, Schinazi RF, Gallo JM, McClure HM, Anderson DC, Doshi KJ, et al. 3'-Azido-2',3'-dideoxyuridine (AzddU): comparative pharmacokinetics with 3'-azido-3'-deoxythymidine (AZT) in monkeys. AIDS research and human retroviruses. 1990; 6(2):219–28. PMID: 2328158.
15. Calogeropoulou T, Detsi A, Lekkas E, Koufaki M. Strategies in the design of prodrugs of anti-HIV agents. Current topics in medicinal chemistry. 2003; 3(13):1467–95. PMID: 14529522.
16. Parang K, Wiebe LI, Knaus EE. Novel approaches for designing 5'-O-ester prodrugs of 3'-azido-2', 3'-dideoxythymidine (AZT). Current medicinal chemistry. 2000; 7(10):995–1039. PMID: 10911016.
17. Phillips NC, Skamene E, Tsoukas C. Liposomal encapsulation of 3'-azido-3'-deoxythymidine (AZT) results in decreased bone marrow toxicity and enhanced activity against murine AIDS-induced immunosuppression. Journal of acquired immune deficiency syndromes. 1991; 4(10):959–66. PMID: 1890605.
18. Kaur CD, Nahar M, Jain NK. Lymphatic targeting of zidovudine using surface-engineered liposomes. Journal of drug targeting. 2008; 16(10):798–805. doi: 10.1080/10611860802475688 PMID: 19005941.
19. Goldberg M, Langer R, Jia X. Nanostructured materials for applications in drug delivery and tissue engineering. Journal of biomaterials science Polymer edition. 2007; 18(3):241–68. PMID: 17471764; PubMed Central PMCID: PMC3017754.
20. McNeil SE. Unique benefits of nanotechnology to drug delivery and diagnostics. Methods in molecular biology. 2011; 697:3–8. doi: 10.1007/978-1-60327-198-1_1 PMID: 21116949.
21. Sanvicens N, Marco MP. Multifunctional nanoparticles—properties and prospects for their use in human medicine. Trends in biotechnology. 2008; 26(8):425–33. doi: 10.1016/j.tibtech.2008.04.005 PMID: 18514941.
22. Volberding P. Zidovudine (AZT): costs and benefits. British journal of hospital medicine. 1988; 40 (2):101. PMID: 3139119.
23. Barry M, Howe JL, Back DJ, Swart AM, Breckenridge AM, Weller IV, et al. Zidovudine pharmacokinetics in zidovudine-induced bone marrow toxicity. British journal of clinical pharmacology. 1994; 37(1):7–12. PMID: 8148221; PubMed Central PMCID: PMC1364702.
24. Balakrishnan A, Valsalan R, Sheshadri S, Pandit VR, Medep V, Agrawal RK. Zidovudine-induced reversible pure red cell aplasia. Indian journal of pharmacology. 2010; 42(3):189–91. doi: 10.4103/0253-7613.66845 PMID: 20871773; PubMed Central PMCID: PMC2937323.
25. Kurtzberg J, Carter SG. Differential toxicity of carbovir and AZT to human bone marrow hematopoietic progenitor cells in vitro. Experimental hematology. 1990; 18(10):1094–6. PMID: 2209763.
26. Scheding S, Media JE, Nakeff A. Acute toxic effects of 3'-azido-3'-deoxythymidine (AZT) on normal and regenerating murine hematopoiesis. Experimental hematology. 1994; 22(1):60–5. PMID: 8282060.
27. Moh R, Danel C, Sorho S, Sauvageot D, Anzian A, Minga A, et al. Haematological changes in adults receiving a zidovudine-containing HAART regimen in combination with cotrimoxazole in Cote d'Ivoire. Antiviral therapy. 2005; 10(5):615–24. PMID: 16152755.

28. Zeller A, Koenig J, Schmitt G, Singer T, Guerard M. Genotoxicity profile of azidothymidine in vitro. Toxicological sciences: an official journal of the Society of Toxicology. 2013; 135(2):317–27. doi: 10.1093/toxsci/kft149 PMID: 23811827.

29. Guerard M, Koenig J, Festag M, Dertinger SD, Singer T, Schmitt G, et al. Assessment of the genotoxic potential of azidothymidine in the comet, micronucleus, and Pig-a assay. Toxicological sciences: an official journal of the Society of Toxicology. 2013; 135(2):309–16. doi: 10.1093/toxsci/kft148 PMID: 23811826.

30. Phillips MD, Nascimbeni B, Tice RR, Shelby MD. Induction of micronuclei in mouse bone marrow cells: an evaluation of nucleoside analogues used in the treatment of AIDS. Environmental and molecular mutagenesis. 1991; 18(3):168–83. PMID: 1915312.

31. Krishna AD, Mandraju RK, Kishore G, Kondapi AK. An efficient targeted drug delivery through apotransferrin loaded nanoparticles. PloS one. 2009; 4(10):e7240. doi: 10.1371/journal.pone.0007240 PMID: 19806207; PubMed Central PMCID: PMC2752169.

32. Gandapu U, Chaitanya RK, Kishore G, Reddy RC, Kondapi AK. Curcumin-loaded apotransferrin nanoparticles provide efficient cellular uptake and effectively inhibit HIV-1 replication in vitro. PloS one. 2011; 6(8):e23388. doi: 10.1371/journal.pone.0023388 PMID: 21887247; PubMed Central PMCID: PMC3161739.

33. Golla K, Cherukuvada B, Ahmed F, Kondapi AK. Efficacy, safety and anticancer activity of protein nanoparticle-based delivery of doxorubicin through intravenous administration in rats. PloS one. 2012; 7(12):e51960. doi: 10.1371/journal.pone.0051960 PMID: 23284832; PubMed Central PMCID: PMC3528733.

34. Golla K, Reddy PS, Bhaskar C, Kondapi AK. Biocompatibility, absorption and safety of protein nanoparticle-based delivery of doxorubicin through oral administration in rats. Drug delivery. 2013; 20(3–4):156–67. doi: 10.3109/10717544.2013.801051 PMID: 23730724.

35. Golla K, Bhaskar C, Ahmed F, Kondapi AK. A target-specific oral formulation of Doxorubicin-protein nanoparticles: efficacy and safety in hepatocellular cancer. Journal of Cancer. 2013; 4(8):644–52. doi: 10.7150/jca.7093 PMID: 24155776; PubMed Central PMCID: PMC3805992.

36. Burger DM, Rosing H, Koopman FJ, Mennhorst PL, Mulder JW, Bult A, et al. Determination of 3'-amino-3'-deoxythymidine, a cytotoxic metabolite of 3'-azido-3'-deoxythymidine, in human plasma by ion-pair high-performance liquid chromatography. Journal of chromatography. 1993; 622(2):235–42. PMID: 8150871.

37. Schmid W. The micronucleus test. Mutation research. 1975; 31(1):9–15. PMID: 48190.

38. Mallipeddi R, Rohan LC. Progress in antiretroviral drug delivery using nanotechnology. International journal of nanomedicine. 2010; 5:533–47. PMID: 20957115; PubMed Central PMCID: PMC2950411.

39. Ravi PR, Kotreka UK, Saha RN. Controlled release matrix tablets of zidovudine: effect of formulation variables on the in vitro drug release kinetics. AAPS PharmSciTech. 2008; 9(1):302–13. doi: 10.1208/s12249-007-9030-8 PMID: 18446496; PubMed Central PMCID: PMC2976876.

40. Kuksal A, Tiwary AK, Jain NK, Jain S. Formulation and in vitro, in vivo evaluation of extended- release matrix tablet of zidovudine: influence of combination of hydrophilic and hydrophobic matrix formers. AAPS PharmSciTech. 2006; 7(1):E1. doi: 10.1208/pt070101 PMID: 16584139; PubMed Central PMCID: PMC2750708.

41. Nayak UY, Gopal S, Mutalik S, Ranjith AK, Reddy MS, Gupta P, et al. Glutaraldehyde cross-linked chitosan microspheres for controlled delivery of zidovudine. Journal of microencapsulation. 2009; 26(3):214–22. PMID: 18819029.

42. Lobenberg R, Araujo L, von Briesen H, Rodgers E, Kreuter J. Body distribution of azidothymidine bound to hexyl-cyanoacrylate nanoparticles after i.v. injection to rats. Journal of controlled release: official journal of the Controlled Release Society. 1998; 50(1–3):21–30. PMID: 9685869.

43. Jain S, Tiwary AK, Jain NK. PEGylated elastic liposomal formulation for lymphatic targeting of zidovudine. Current drug delivery. 2008; 5(4):275–81. PMID: 18855596.

44. Jin SX, Bi DZ, Wang J, Wang YZ, Hu HG, Deng YH. Pharmacokinetics and tissue distribution of zidovudine in rats following intravenous administration of zidovudine myristate loaded liposomes. Die Pharmazie. 2005; 60(11):840–3. PMID: 16320946.

45. Garg M, Jain NK. Reduced hematopoietic toxicity, enhanced cellular uptake and altered pharmacokinetics of azidothymidine loaded galactosylated liposomes. Journal of drug targeting. 2006; 14(1):1–11. doi: 10.1080/10611860500525370 PMID: 16603446.

46. Callender DP, Jayaprakash N, Bell A, Petraitis V, Petraitiene R, Candelario M, et al. Pharmacokinetics of oral zidovudine entrapped in biodegradable nanospheres in rabbits. Antimicrobial agents and chemotherapy. 1999; 43(4):972–4. PMID: 10103214; PubMed Central PMCID: PMC89240.

47. Villard AL, Coussot G, Lefebvre I, Augustijns P, Aubertin AM, Gosselin G, et al. Phenyl phosphotriester derivatives of AZT: variations upon the SATE moiety. Bioorganic & medicinal chemistry. 2008; 16 (15):7321–9. doi: 10.1016/j.bmc.2008.06.024 PMID: 18585917.

48. Luzier A, Morse GD. Intravascular distribution of zidovudine: role of plasma proteins and whole blood components. Antiviral research. 1993; 21(3):267–80. PMID: 8215300.

49. Acosta EP, Page LM, Fletcher CV. Clinical pharmacokinetics of zidovudine. An update. Clinical pharmacokinetics. 1996; 30(4):251–62. PMID: 8983858.

50. Zhang R, Lu Z, Diasio CR, Liu T, Soong SJ. The time of administration of 3'-azido-3'-deoxythymidine (AZT) determines its host toxicity with possible relevance to AZT chemotherapy. Antimicrobial agents and chemotherapy. 1993; 37(9):1771–6. PMID: 8239582; PubMed Central PMCID: PMC188068.

51. Aaron CS, Sorg R, Zimmer D. The mouse bone marrow micronucleus test: evaluation of 21 drug candidates. Mutation research. 1989; 223(2):129–40. PMID: 2525668.

52. Fenech M, Kirsch-Volders M, Natarajan AT, Surralles J, Crott JW, Parry J, et al. Molecular mechanisms of micronucleus, nucleoplasmic bridge and nuclear bud formation in mammalian and human cells. Mutagenesis. 2011; 26(1):125–32. doi: 10.1093/mutage/geq052 PMID: 21164193.

53. Suzuki Y, Nagae Y, Li J, Sakaba H, Mozawa K, Takahashi A, et al. The micronucleus test and erythropoiesis. Effects of erythropoietin and a mutagen on the ratio of polychromatic to normochromatic erythrocytes (P/N ratio). Mutagenesis. 1989; 4(6):420–4. PMID: 2516221.

54. Groot F, Geijtenbeek TB, Sanders RW, Baldwin CE, Sanchez-Hernandez M, Floris R, et al. Lactoferrin prevents dendritic cell-mediated human immunodeficiency virus type 1 transmission by blocking the DC-SIGN—gp120 interaction. Journal of virology. 2005; 79(5):3009–15. doi: 10.1128/JVI.79.5.3009-3015.2005 PMID: 15709021; PubMed Central PMCID: PMC548463.

55. Fillebeen C, Descamps L, Dehouck MP, Fenart L, Benaissa M, Spik G, et al. Receptor-mediated transcytosis of lactoferrin through the blood-brain barrier. The Journal of biological chemistry. 1999; 274 (11):7011–7. PMID: 10066755.

Antiretroviral drug loaded lactoferrin nanoparticle formulation for oral delivery

by Prashant Kumar

Antiretroviral drug loaded lactoferrin nanoparticle formulation for oral delivery

ORIGINALITY REPORT

%20	%6	%18	%3
SIMILARITY INDEX	INTERNET SOURCES	PUBLICATIONS	STUDENT PAPERS

PRIMARY SOURCES

1	Kumar, Prashant, Yeruva Samrajya Lakshmi, Bhaskar C., Kishore Golla, and Anand K. Kondapi. "Improved Safety, Bioavailability and Pharmacokinetics of Zidovudine through Lactoferrin Nanoparticles during Oral Administration in Rats", PLoS ONE, 2015. Publication	%11
2	www.science.gov Internet Source	%1
3	Submitted to King's College Student Paper	<%1
4	Upendhar Gandapu. "Curcumin-Loaded Apotransferrin Nanoparticles Provide Efficient Cellular Uptake and Effectively Inhibit HIV-1 Replication In Vitro", PLoS ONE, 08/22/2011 Publication	<%1
5	www.dovepress.com Internet Source	<%1

Bollimpelli, V. Satish, Prashant Kumar, Sonali

6	Kumari, and Anand K. Kondapi. "Neuroprotective effect of curcumin-loaded lactoferrin nano particles against rotenone induced neurotoxicity", Neurochemistry International, 2016. Publication	<%1
7	journals.plos.org Internet Source	<%1
8	www.arkat-usa.org Internet Source	<%1
9	www.landi.ufsc.br Internet Source	<%1
10	www.ncbi.nlm.nih.gov Internet Source	<%1
11	www.plosone.org Internet Source	<%1
12	Evan D. Kharasch. "Clinical Sevoflurane Metabolism and Disposition", Anesthesiology, 06/1995 Publication	<%1
13	cvi.asm.org Internet Source	<%1
14	Sahu, A.. "Synthesis of novel biodegradable and self-assembling methoxy poly(ethylene glycol)-palmitate nanocarrier for curcumin	<%1

delivery to cancer cells", Acta Biomaterialia, 200811
Publication

---

15 Rulan Jiang. "Apo- and holo-lactoferrin are both internalized by lactoferrin receptor via clathrin-mediated endocytosis but differentially affect ERK-signaling and cell proliferation in caco-2 cells", Journal of Cellular Physiology, 11/2011 <%1
Publication

---

16 Salomon, Carlos, Maria Jose Torres, Miharu Kobayashi, Katherin Scholz-Romero, Luis Sobrevia, Aneta Dobierzewska, Sebastian E. Illanes, Murray D. Mitchell, and Gregory E. Rice. "A Gestational Profile of Placental Exosomes in Maternal Plasma and Their Effects on Endothelial Cell Migration", PLoS ONE, 2014. <%1
Publication

---

17 www.ashm.org.au <%1
Internet Source

---

18 "Poster Session I (PI 1-89)Displayed 8:00 am - 3:00 pmAttended 8:00 am - 9:30 am", Clinical Pharmacology & Therapeutics, 01/16/2009 <%1
Publication

---

19 Kim, Tae-Hee, Yoonae Ko, Thierry Christophe, Jonathan Cechetto, Junwon Kim, Kyoung-Ae <%1

Kim, Annette S. Boese, Jean-Michel Garcia, Denis Fenistein, Moon Kyeong Ju, Junghwan Kim, Sung-Jun Han, Ho Jeong Kwon, Vincent Brondani, and Peter Sommer. "Identification of a Novel Sulfonamide Non-Nucleoside Reverse Transcriptase Inhibitor by a Phenotypic HIV-1 Full Replication Assay", PLoS ONE, 2013.
Publication

---

20 Adlin Jino^Nesalin, J.. "FORMULATION AND EVALUATION OF NANOPARTICLES CONTAINING FLUTAMIDE", International Journal of ChemTech Research/09744290, 20091001
Publication

<%1

---

21 www.ijppsjournal.com
Internet Source

<%1

---

22 Cronqvist, Tina, Karen Saljé, Mary Familari, Seth Guller, Henning Schneider, Chris Gardiner, Ian L. Sargent, Christopher W. Redman, Matthias Mörgelin, Bo Åkerström, Magnus Gram, and Stefan R. Hansson. "Syncytiotrophoblast Vesicles Show Altered micro-RNA and Haemoglobin Content after Ex-vivo Perfusion of Placentas with Haemoglobin to Mimic Preeclampsia", PLoS ONE, 2014.
Publication

<%1

---

23 www.researchgate.net
Internet Source

<%1

24	aseanheartjournal.org Internet Source	<%1
25	Liang, Yan, Xin Deng, Longgui Zhang, Xinyu Peng, Wenxia Gao, Jun Cao, Zhongwei Gu, and Bin He. "Terminal modification of polymeric micelles with π-conjugated moieties for efficient anticancer drug delivery", Biomaterials, 2015. Publication	<%1
26	Hari, B.N. Vedha, N. Narayanan, K. Dhevendaran, and D. Ramyadevi. "Engineered nanoparticles of Efavirenz using methacrylate co-polymer (Eudragit-E100) and its biological effects in-vivo", Materials Science and Engineering C, 2016. Publication	<%1
27	www.omicsonline.org Internet Source	<%1
28	Liu, Ya, Ming Kong, Chao Feng, Kui Kun Yang, Yang Li, Jing Su, Xiao Jie Cheng, Hyun Jin Park, and Xi Guang Chen. "Biocompatibility, cellular uptake and biodistribution of the polymeric amphiphilic nanoparticles as oral drug carriers", Colloids and Surfaces B Biointerfaces, 2013. Publication	<%1

29	Pongjanyakul, T.. "Characteristics and in vitro release of dextromethorphan resinates", Powder Technology, 20050429 Publication	<%1
30	Shende, Sudhir, Avinash P. Ingle, Aniket Gade, and Mahendra Rai. "Green synthesis of copper nanoparticles by Citrus medica Linn. (Idilimbu) juice and its antimicrobial activity", World Journal of Microbiology and Biotechnology, 2015. Publication	<%1
31	Submitted to Cranfield University Student Paper	<%1
32	Golla, Kishore, Palakolanu S. Reddy, C. Bhaskar, and Anand K. Kondapi. "Biocompatibility, absorption and safety of protein nanoparticle-based delivery of doxorubicin through oral administration in rats", Drug Delivery, 2013. Publication	<%1
33	Handbook of Nanoparticles, 2016. Publication	<%1
34	mdpi.com Internet Source	<%1
35	Submitted to University of Bristol Student Paper	<%1

36	www.actionnigeria.org Internet Source	<%1
37	pubs.rsc.org Internet Source	<%1
38	Submitted to University of Queensland Student Paper	<%1
39	Kamboj, Sunil, and Vikas Rana. "Quality-by-design based development of a self-microemulsifying drug delivery system to reduce the effect of food on Nelfinavir mesylate", International Journal of Pharmaceutics, 2016. Publication	<%1
40	Submitted to University of Newcastle upon Tyne Student Paper	<%1
41	yz-car.ci.cqvip.com Internet Source	<%1
42	Submitted to National Institute of Technology, Rourkela Student Paper	<%1
43	www.bestcompoundingpharmacyfreedelivery.com Internet Source	<%1
44	Xu, J., W. Zhu, W. Xu, W. Yao, B. Zhang, Y. Xu, S. Ji, C. Liu, J. Long, Q. Ni, and X. Yu. "Up-	<%1

Regulation of MBD1 Promotes Pancreatic Cancer Cell Epithelial-Mesenchymal Transition and Invasion by Epigenetic Down-Regulation of E-Cadherin", Current Molecular Medicine, 2013.
Publication

---

45 Sarker, Suchismita, Katherin Scholz-Romero, Alejandra Perez, Sebastian E Illanes, Murray D Mitchell, Gregory E Rice, and Carlos Salomon. "Placenta-derived exosomes continuously increase in maternal circulation over the first trimester of pregnancy", Journal of Translational Medicine, 2014.
Publication

<%1

---

46 ethesis.nitrkl.ac.in
Internet Source

<%1

---

47 Dutta, Tathagata, Hrushikesh B. Agashe, Minakshi Garg, Prahlad Balasubramanium, Madhulika Kabra, and Narendra K. Jain. "Poly (propyleneimine) dendrimer based nanocontainers for targeting of efavirenz to human monocytes/macrophages in vitro : Research Paper", Journal of Drug Targeting, 2007.
Publication

<%1

---

48 apps.elsevier.es
Internet Source

<%1

49	Ish-Shalom, D.. "Organization of chlorophyll-protein complexes of Photosystem I in Chlamydomonas reinhardii", BBA - Bioenergetics, 19830318 Publication	<%1
50	jpet.aspetjournals.org Internet Source	<%1
51	www.mdpi.com Internet Source	<%1
52	Yang, T.. "Enhanced solubility and stability of PEGylated liposomal paclitaxel: In vitro and in vivo evaluation", International Journal of Pharmaceutics, 20070629 Publication	<%1
53	angiochem.com Internet Source	<%1
54	Nanoscale Materials in Targeted Drug Delivery Theragnosis and Tissue Regeneration, 2016. Publication	<%1
55	Nanostructure Science and Technology, 2012. Publication	<%1
56	RADHA KRISHNA REDDY, M.; MURALI KRISHNA, A.; REDDY, B.S.; SRILAKSHMI, D.; NARESH KUMAR, Y. and MASTAN, S.A.. "ACCUMULATION OF ACTIVE PHARMA	<%1

INGREDIENTS IN POND RARED LABEO ROHITHA", International Journal of Pharmacy & Pharmaceutical Sciences, 2013.
Publication

57	aiche.confex.com Internet Source	<%1
58	"Patent Application Titled "Controlled Release Hydrocodone Formulations" Published Online.", Health & Medicine Week, July 17 2015 Issue Publication	<%1
59	Jorge F. Coelho. "Drug delivery systems: Advanced technologies potentially applicable in personalized treatments", The EPMA Journal, 04/10/2010 Publication	<%1
60	genesdev.cshlp.org Internet Source	<%1
61	www.microcalorimetry.com Internet Source	<%1
62	M. Delwar Hussain. "Poloxamer 407/TPGS mixed micelles for delivery of gambogic acid to breast and multidrug-resistant cancer", International Journal of Nanomedicine, 02/2012 Publication	<%1
63	Amitava Dasgupta. "Pharmacokinetic and Other Drug Interactions in Patients With AIDS	<%1

:", Therapeutic Drug Monitoring, 12/2001
Publication

---

64 Shafiee, Hadi, Erich A. Lidstone, Muntasir Jahangir, Fatih Inci, Emily Hanhauser, Timothy J. Henrich, Daniel R. Kuritzkes, Brian T. Cunningham, and Utkan Demirci. "Nanostructured Optical Photonic Crystal Biosensor for HIV Viral Load Measurement", Scientific Reports, 2014.
Publication

<%1

---

65 Alexandre Albanese. "Effect of Gold Nanoparticle Aggregation on Cell Uptake and Toxicity", ACS Nano, 07/26/2011
Publication

<%1

---

66 Teng, Zi, Yangchao Luo, and Qin Wang. "Carboxymethyl chitosan–soy protein complex nanoparticles for the encapsulation and controlled release of vitamin D3", Food Chemistry, 2013.
Publication

<%1

---

67 "Polyelectrolytes", Springer Nature, 2014
Publication

<%1

---

68 Li, Xiaoguang, Hua Qian, Fusako Miyamoto, Takeshi Naito, Kumi Kawaji, Kazumi Kajiwara, Toshio Hattori, Masao Matsuoka, Kentaro Watanabe, Shinya Oishi, Nobutaka Fujii, and Eiichi N. Kodama. "A simple, rapid, and

<%1

sensitive system for the evaluation of anti-viral drugs in rats", Biochemical and Biophysical Research Communications, 2012.
Publication

---

69 Rhee, Sangkeun White, James L.. "Investigation of structure development in polyamide 11 and polyamide 12 tubular film extrusion.", Polymer Engineering and Science, Jan 2002 Issue
Publication

<%1

---

70 "Poster Session Abstracts.(Abstracts)(Report) (Author abstract)", Indian Journal of Pharmacology, Dec 2015 Issue
Publication

<%1

---

71 abap.co.in
Internet Source

<%1

---

72 Witasp, E.. "Efficient internalization of mesoporous silica particles of different sizes by primary human macrophages without impairment of macrophage clearance of apoptotic or antibody-opsonized target cells", Toxicology and Applied Pharmacology, 20090915
Publication

<%1

---

73 Wangyang Yu. "Mannan-Modified Solid Lipid Nanoparticles for Targeted Gene Delivery to Alveolar Macrophages", Pharmaceutical

<%1

Research, 04/27/2010
Publication

74	Excipient Applications in Formulation Design and Drug Delivery, 2015. Publication	<%1
75	Khatavkar, Umesh Nandkumar, Shamkant Laxman Shimpi, K Jayaram Kumar, and Kishor Dattatraya Deo. "Development and in vivo evaluation of novel monolithic controlled release compositions of galantamine hydrobromide as against reservoir technology", Pharmaceutical Development and Technology, 2013. Publication	<%1
76	repositorium.sdum.uminho.pt Internet Source	<%1
77	www.ansaralhojah.com Internet Source	<%1
78	Submitted to Sekolah Pelita Harapan Student Paper	<%1
79	iffwww.iff.kfa-juelich.de Internet Source	<%1
80	uir.unisa.ac.za Internet Source	<%1
81	Dondi, Daniele, Daniele Merli, Luca Pretali,	<%1

Maurizio Fagnoni, Angelo Albini, and Nick Serpone. "Prebiotic chemistry: chemical evolution of organics on the primitive Earth under simulated prebiotic conditions", Photochemical & Photobiological Sciences, 2007.
Publication

---

82 Ahmed, Farhan, Mohammad Javed Ali, and Anand K. Kondapi. "Carboplatin loaded protein nanoparticles exhibit improve anti-proliferative activity in retinoblastoma cells", International Journal of Biological Macromolecules, 2014. <%1
Publication

---

83 Kalam, Mohd Abul. "Development of chitosan nanoparticles coated with hyaluronic acid for topical ocular delivery of dexamethasone", International Journal of Biological Macromolecules, 2016. <%1
Publication

---

84 Lohcharoenkal, Warangkana Wang, Liying C. "Protein nanoparticles as drug delivery carriers for cancer therapy.(Report)", BioMed Research International, Annual 2014 Issue <%1
Publication

---

85 www.clinchem.org <%1
Internet Source

---

86 Barnabas Wilson. "Design and evaluation of

chitosan nanoparticles as novel drug carrier for the delivery of rivastigmine to treat Alzheimer's disease", Therapeutic Delivery, 05/2011 <%1
Publication

87 Osinusi-Adekanmbi, O., K. Stafford, A. Ukpaka, D. Salami, S. Ajayi, N. Ndembi, A. Abimiku, C. Nwizu, B. Gilliam, R. Redfield, and A. Amoroso. "Long-Term Outcome of Second-Line Antiretroviral Therapy in Resource-Limited Settings", Journal of the International Association of Providers of AIDS Care (JIAPAC), 2014. <%1
Publication

88 Mengmeng Wang; Defranco, David; Wright, Katherine; Quazi, Shakey; Chen, Jianqing; Spencer-Pierce, Jennifer; Zaghloul, Iman; Pak, Roger; Darvair, Ramin; Krishnan, Aadithya; Perreault, Mylene; Sun, Lei; Ozer, Josef and Xin Xu. "Decreased Subcutaneous Bioavailability of an Oxyntomodulin Analog in a Controlled Release Formulation could be Caused by Skin Metabolism in Rats", Journal of Bioequivalence & Bioavailability, 2012. <%1
Publication

89 Anantharaj, Santhanaraj, and Manickam Jayakannan. "Melt polycondensation approach for reduction degradable helical polyester based on l -cystine", Journal of Polymer <%1

	Science Part A Polymer Chemistry, 2016. Publication	
90	Pham, Kevin, Diana Li, Shujie Guo, Scott Penzak, and Xiaowei Dong. "Development and in vivo evaluation of child-friendly lopinavir/ritonavir pediatric granules utilizing novel in situ self-assembly nanoparticles", Journal of Controlled Release, 2016. Publication	<%1
91	www.jnanobiotechnology.com Internet Source	<%1
92	hrcak.srce.hr Internet Source	<%1
93	www.karger.jp Internet Source	<%1
94	Zhang, L.. "Effective control of blood glucose status and toxicity in streptozotocin-induced diabetic rats by orally administration of vanadate in an herbal decoction", Food and Chemical Toxicology, 200809 Publication	<%1
95	www.spandidos-publications.com Internet Source	<%1
96	ecommons.usask.ca Internet Source	<%1

97	jcancer.org Internet Source	<%1
98	Krishnamoorthy, Balakumar, S. M. Habibur Rahman, N. Tamil selvan, R. Hari prasad, M. Rajkumar, M. Siva selvakumar, K. Vamshikrishna, Marslin Gregory, and Chellan Vijayaraghavan. "Design, formulation, in vitro, in vivo, and pharmacokinetic evaluation of nisoldipine-loaded self-nanoemulsifying drug delivery system", Journal of Nanoparticle Research, 2015. Publication	<%1
99	Yogendra Nayak, Kiran Avadhani, Srinivas Mutalik, Usha Y. Nayak. "Lymphatic Delivery of Anti-HIV Drug Nanoparticles", Recent Patents on Nanotechnology, 2016 Publication	<%1
100	www.scribd.com Internet Source	<%1
101	www.icmr.nic.in Internet Source	<%1
102	Hult, Britta, Gursharan Chana, Eliezer Masliah, and Ian Everall. "Neurobiology of HIV", International Review of Psychiatry, 2008. Publication	<%1
103	Hanna, D. B., L. S. Gupta, L. E. Jones, D. M.	

	Thompson, S. E. Kellerman, and J. E. Sackoff. "AIDS-defining opportunistic illnesses in the HAART era in New York City", AIDS Care, 2007. Publication	<%1
104	www.vitals.com Internet Source	<%1
105	edoc.ub.uni-muenchen.de Internet Source	<%1
106	Advances in Delivery Science and Technology, 2015. Publication	<%1
107	www.jtmtg.org Internet Source	<%1
108	Lange, Joep M.A., and Bernhard Schwartländer. "Introduction 15 million on ART by 2015 : a realistic target or just a dream", Current Opinion in HIV and AIDS, 2013. Publication	<%1
109	Ramana, Lakshmi Narashimhan, Shilpee Sharma, Swaminathan Sethuraman, Udaykumar Ranga, and Uma Maheswari Krishnan. "Evaluation of chitosan nanoformulations as potent anti-HIV therapeutic systems", Biochimica et Biophysica Acta (BBA) - General Subjects, 2014. Publication	<%1

110	joe.endocrinology-journals.org Internet Source	<%1
111	tdx.cat Internet Source	<%1
112	imsear.hellis.org Internet Source	<%1
113	europepmc.org Internet Source	<%1
114	www.fhi.org Internet Source	<%1
115	Kumar, Abhinav, Elif Melis Bicer, Anna Babin Morgan, Paul E. Pfeffer, Marco Monopoli, Kenneth A. Dawson, Jonny Eriksson, Katarina Edwards, Steven Lynham, Matthew Arno, Annelie F. Behndig, Anders Blomberg, Graham Somers, Dave Hassall, Lea Ann Dailey, Ben Forbes, and Ian S. Mudway. "Enrichment of immunoregulatory proteins in the biomolecular corona of nanoparticles within human respiratory tract lining fluid", Nanomedicine Nanotechnology Biology and Medicine, 2016. Publication	<%1
116	researchdirect.uws.edu.au Internet Source	<%1
117	Singh, Yuvraj, Meenakshi Singh, Jay Gopal	

	Meher, Vivek K. Pawar, and Manish K. Chourasia. "Trichotomous gastric retention of amorphous capecitabine: An attempt to overcome pharmacokinetic gap", International Journal of Pharmaceutics, 2015. Publication	<%1
118	Melis, Virginia, Iris Usach, Patricia Gandía, and José-Esteban Peris. "Inhibition of efavirenz metabolism by sertraline and nortriptyline and their effect on the efavirenz plasma concentrations.", Antimicrobial Agents and Chemotherapy, 2015. Publication	<%1
119	Simin Dadashzadeh. "9-Nitrocamptothecin polymeric nanoparticles: cytotoxicity and pharmacokinetic studies of lactone and total forms of drug in rats", Anti-Cancer Drugs, 09/2008 Publication	<%1
120	www.appconnect.in Internet Source	<%1
121	edepot.wur.nl Internet Source	<%1
122	www.mts.com Internet Source	<%1
123	www.science.ge Internet Source	<%1

124	cipladoc.com Internet Source	<%1
125	Kumar, Lalit, Shivani Verma, Deo Nandan Prasad, Ankur Bhardwaj, Bhuvaneshwar Vaidya, and Amit Kumar Jain. "Nanotechnology: A magic bullet for HIV AIDS treatment", Artificial Cells Nanomedicine and Biotechnology, 2015. Publication	<%1
126	pharmaceuticalintelligence.com Internet Source	<%1
127	Nsagha, Dickson Shey, Elroy Patrick Weledji, Nguedia Jules Clement Assob, Longdoh Anna Njunda, Elvis Asangbeng Tanue, Odette Dzemo kibu, Charlotte Wenze Ayima, and Marcelin Ngowe Ngowe. "Highly active antiretroviral therapy and dyslipidemia in people living with HIV/AIDS in Fako Division, South West Region of Cameroon", BMC Cardiovascular Disorders, 2015. Publication	<%1
128	Submitted to University of Auckland Student Paper	<%1
129	Destache, Christopher J., Subhra Mandal, Yuan Zhe, Guobin Kang, Abhijit A. Date, Wuxun Lu, Annemarie Shibata, Rachel Pham, Patrick	<%1

Bruck, Michael Rezich, You Zhou, Renuga Vivekanandan, Courtney V. Fletcher, and Qingsheng Li. "Topical Tenofovir Disoproxil Fumarate (DF) Nanoparticles Prevents HIV-1 Vaginal Transmission in the Humanized Mouse Model", Antimicrobial Agents and Chemotherapy, 2016.
Publication

---

130 Gargaud, . "Netherlands Space Office", Encyclopedia of Astrobiology, 2011. <%1
Publication

---

131 Zhang, Cheng, Guodong Li, Yihan Wang, Fuying Cui, Jien Zhang, and Qingshan Huang. "Preparation and characterization of 5-fluorouracil-loaded PLLAâ€“PEG/PEG nanoparticles by a novel supercritical CO2 technique", International Journal of Pharmaceutics, 2012. <%1
Publication

---

132 Sungkanuparph, S., W. Manosuthi, S. Kiertiburanakul, and W. Chantratita. "Reply to Vogenthaler", Clinical Infectious Diseases, 2007. <%1
Publication

---

133 Avachat, Amelia M., and Shreekrishna S. Parpani. "Formulation and development of bicontinuous nanostructured liquid crystalline <%1

particles of efavirenz", Colloids and Surfaces B Biointerfaces, 2015.
Publication

---

134 Dobrovolskaia, Marina A, and Scott E McNeil. "Opportunities and Challenges in Nanotechnology-enabled Antiretroviral Delivery", Handbook of Immunological Properties of Engineered Nanomaterials, 2016. <%1
Publication

---

135 Jingkun Jiang. "Characterization of size, surface charge, and agglomeration state of nanoparticle dispersions for toxicological studies", Journal of Nanoparticle Research, 01/2009 <%1
Publication

---

136 Zhao, Zheng, Yi Li, and Mao-Bin Xie. "Silk Fibroin-Based Nanoparticles for Drug Delivery", International Journal of Molecular Sciences, 2015. <%1
Publication

---

137 Bayomi, Eman Barakat, Ahmed El-Bassuoni,. "Cyclooxygenase-2 expression is associated with elevated aspartate aminotransferase level in hepatoce", Journal of Cancer Research and Therapeut, Oct-Dec 2015 Issue <%1
Publication

---

138 Mandal, T. K., L. A. Bostanian, R. A. Graves, S.

R. Chapman, and I. Womack. "Development of Biodegradable Microcapsules as Carrier for Oral Controlled Delivery of Amifostine", Drug Development and Industrial Pharmacy, 2002.
Publication

<%1

---

139 Lanao, José M., Elsa Briones, and Clara I. Colino. "Recent advances in delivery systems for anti-HIV1 therapy", Journal of Drug Targeting, 2007.
Publication

<%1

---

140 Bossio, O., L. G. Gomez-Mascaraque, M. Fernandez-Gutierrez, B. Vazquez-Lasa, and J. S. Roman. "Amphiphilic polysaccharide nanocarriers with antioxidant properties", Journal of Bioactive and Compatible Polymers, 2014.
Publication

<%1

---

141 Muller, Laurent, Chang-Sook Hong, Donna B. Stolz, Simon C. Watkins, and Theresa L. Whiteside. "Isolation of biologically-active exosomes from human plasma", Journal of Immunological Methods, 2014.
Publication

<%1

---

142 Boettiger, David C, Van Kinh Nguyen, Nicolas Durier, Huy Vu Bui, Benedict Lim Heng Sim, Iskandar Azwa, Matthew Law, and Kiat Ruxrungtham. "Efficacy of second-line

<%1

antiretroviral therapy among people living with HIV/AIDS in Asia : Results from the TREAT Asia HIV Observational Database", JAIDS Journal of Acquired Immune Deficiency Syndromes, 2014.
Publication

---

143 Ojewole, E.. "Exploring the use of novel drug delivery systems for antiretroviral drugs", European Journal of Pharmaceutics and Biopharmaceutics, 200811 <%1
Publication

---

144 Nadezda Apostolova. "Mitochondrial Toxicity in HAART: An Overview of In Vitro Evidence", Current Pharmaceutical Design, 07/01/2011 <%1
Publication

EXCLUDE QUOTES ON
EXCLUDE BIBLIOGRAPHY ON
EXCLUDE MATCHES < 5 WORDS